AGE RELATED CHANGES IN THE POST-CRANIAL HUMAN SKELETON AND ITS IMPLICATION FOR THE DETERMINATION OF SEX

by

Veronica L.W. Vance

Submitted in fulfillment of the requirements for the degree PhD Anatomy

In the faculty of Health Sciences

University of Pretoria

Pretoria

December 2007

Declaration

I declare that the dissertation that I am hereby submitting to the University of Pretoria for the PhD degree in Anatomy degree is my own work and that I have never before submitted it to any other tertiary institution for any degree.

Veronica L.W. Vance

1 day of December 2007

Table of Contents

List of Tables

List of Figures

Appendices

Abstract

The study of skeletal differences between males and females has rarely taken into account the physical change in hard tissue characteristics with the onset of advanced age. Anatomical change through degenerative modification may pose a challenge when diagnosing the sex of an unknown individual, especially if age is unknown. The aim of this study was to establish whether sexual dimorphism changes with age. This issue was addressed by using three types of procedural analyses. Firstly, standard measuring techniques were utilized to determine sex from 593 individuals. Visual (morphological) assessment was then performed on 608 individuals using sexually dimorphic traits in the distal humerus and pelvis. Lastly, over 300 individuals were analyzed with geometric morphometrics using four locations on the postcranial skeleton. Younger females and males (50 years of age and younger) were then compared to older individuals (over 50 years of age) to determine if sexual dimorphism was increasing or decreasing with the onset of age. Long bone measurements of the postcranial skeleton increased with the onset of age in the most osteoporotic sample (South African white females). Males exhibited an increase in size, mainly in the knee and elbow joints, and black females remained static in their measurements with age. Older white females especially can sometimes incorrectly be misclassified as males. Visual techniques indicated that all populations have similar non-metric morphology in the distal humerus and pelvis. Classification accuracies in females decreased when viewing the distal humerus, indicating a decrease in sexual dimorphism at this location. Females appeared static in their pelvic morphology with the onset of age. Males remained sexually dimorphic throughout life in the humerus and pelvis. Geometric morphometrics showed that the morphology of the distal humerus is sexually dimorphic, and does not change with age. Morphometrics also confirmed the marked sexual

dimorphism in the pelvis, and showed virtually no change in sexual dimorphism when comparing young to old groups.

Abstrak

Studies van skeletale verskille tussen mans en vrouens neem selde die fisiese veranderinge in been met toenemende ouderdom in ag. Anatomiese veranderinge as gevolg van degeneratiewe modifikasie kan problematies wees met die bepaling van geslag van 'n onbekende persoon, veral as die ouderdom nie bekend is nie. Die doel van hierdie studie was om te bepaal of seksuele dimorfisme verander met ouderdom. Hierdie probleem is aangespreek deur gebruik te maak van drie metodes van ontleding. Standaard metriese tegnieke is eerstens gebruik om die geslag van 593 individue te bepaal. Visuele (morfologiese) evaluering van seksueel dimorfiese kenmerke van die distale humerus en pelvis is daarna op 608 individue gedoen. Laastens is vier areas op die postkraniale skelet van meer as 300 individue met behulp van geometriese morfometrie ontleed. Jonger mans en vrouens (50 jaar en jonger) is vergelyk met ouer individue (ouer as 50 jaar) om te bepaal of seksuele dimorfisme toeneem of afneem met toename in ouderdom. Langbeenafmetings van die postkraniale skelet neem toe met ouderdom by die mees osteoporotiese groep (wit Suid-Afrikaanse vrouens). Mans toon 'n toename in grootte, hoofsaaklik in die knie en elmboog, en afmetings van swart vrouens was bestendig met toenemende ouderdom. Ouer wit vrouens veral kan soms verkeerdelik geklassifiseer word as mans. Visuele tegnieke dui aan dat alle groepe 'n soortgelyke nie-metriese morfologie in die distale humerus en bekken vertoon. Klassifikasie akkuraatheid in vrouens neem af in die distale humerus, wat dui op 'n afname in seksuele dimorfisme in hierdie gebied. Bekkenmorfologie van vrouens toon geen veranderinge met ouderdom nie. Die humerus en bekken van mans bly seksueel dimorfies deur hul lewe. Geometriese morfometrie wys dat die bou van die distale humerus seksueel dimorfies is, en dat dit nie verander met toename in ouderdom nie. Geometriese morfometrie bevestig ook die kenmerkende seksuele dimorfisme van die

bekken, en wys feitlik geen veranderinge wanneer jong en ouer groepe vergelyk word nie.

Acknowledgements

No scholastic endeavor such as a PhD occurs without the guidance and support of those who have paved the way beforehand. For academic counsel, technical expertise, and the persistent encouragement needed to complete this project, I thank my advisor, Professor Maryna Steyn. Professor Steyn not only served as my extremely erudite academic supervisor, but she and her family made me feel especially welcome in their lovely country. I will treasure the time we spent working and exploring together.

Dr. Ericka L'Abbé was also instrumental in the completion of this project. I thank you for your support and wisdom throughout my academic journey, as well as being a kindred American spirit in an unfamiliar setting. You made my time in South Africa a very memorable one and I will always cherish your kindness.

Marius Loots provided more technical assistance than I could have ever hoped for, and was a pillar of strength when my electronic challenges became overwhelming. All this while providing friendship, entertainment, and many well-crafted meals; thank you so much.

Several fellow students and colleagues made my scholarly experience in South Africa unforgettable. Natalie Keough, Renee Botha, Jolandie Myburgh, Yvette Schultz, Louisa Hutten, Malebo Marabene all provided guidance, support, and friendship throughout my stay in South Africa. These impressive individuals could not have been more accommodating.

My second family deserves distinct recognition and a heart-felt thank you. Dr. Johan Schutte and Lida, Jana and Retha van der Merwe offered me an emotional and intellectual foundation in which I could successfully complete my work. I honour and praise these wonderful people who truly became life-long members of my family. Your

influence and encouragement will always be paramount in my mind when I think back on the fulfillment of this degree.

I would never have started on this academic journey had it not have been for my mentor and colleague, Dr. John Lundy. Dr. John has been a consistent and positive influence in my professional endeavors, and I credit him for instilling a love of forensic anthropology that continues with every case we participate in together. Thank you for your confidence, humor and guidance throughout the years. I look forward to many more.

Finally, I applaud my family, friends and loved ones for their staunch support and confidence in me and my unique choice of careers. Dave, Ski, Greg and Kevin, you have given me the sheer strength to accomplish this- it is through your love that I am who I am today. To all my aunts and uncles, cousins, and second cousins, I truly appreciate your interest and attention to my progress throughout my studies. A special note of thanks goes to my closest friends; you've provided me with much happiness throughout our professional and personal journeys. I share this achievement with all of you.

CHAPTER 1

INTRODUCTION

The characteristic differences in the male and female skeleton, known as sexual dimorphism, are the most effective and germane traits with which to determine skeletal sex (Bass1995; Camacho *et al.* 1993; Dibennardo and Taylor 1983; Garn *et al.* 1970; McCormick and Stewart 1983; Navani *et al.* 1970; Tagaya 1989; Tarlie and Repetto 1986; White and Folkens 2000). Differences between males and females manifest themselves in numerous arrangements throughout both the axial and appendicular skeleton (Holman and Bennet 1991). Visual characteristics and osteometry both provide accepted methods for sex determination of unidentified skeletal remains. Non-metric (visual) determination is the use of morphological traits that establish whether a skeletal element is female or male, due to sexual dimorphism. For example, when researchers recover remains that include an intact cranium and pelvis, visual morphological interpretation is quite accurate for assigning a specific sex to the remains. Visual attributes of the cranium and the os coxae are the most accurate methods for determining sex from the skeleton, and continue to be the most appropriate and precise methods when these skeletal elements are available for analysis (De Villers 1968; Loth and Henneberg 1996; Phenice 1969; Steyn and Iscan 1998; Washburn 1948; Wescott and Moore-Jansen 2001). Quantitative (metric) analysis uses skeletal measurements from a known population to provide the same answer; in this case, the sex of the individual element examined (Evans 1976; Georgia *et al.* 1982; Grabiner 1989; Harper *et al.* 1984; Macho 1990; Mall *et al.* 2001; Pfeiffer and Zehr 1996; Richman *et al.* 1979; Steyn and Iscan 1999).

The ability to determine sex from long bones is important as well, and is utilized consistently when cranial and pelvic bones are absent or fragmentary (France 1998; Steele and Bramblett 1988; Woodard 1962). Because many of the

methods to determine skeletal sex are used in a medico-legal arena, (i.e., forensic anthropology), the use of proper techniques to achieve accurate results are paramount. Forensic anthropology is greatly impacted by new and more useful techniques in establishing individualizing characteristics of unknown skeletonized remains. Identification of skeletal remains is largely determined by the accuracy of the techniques used. Researchers have continually searched for more comprehensive, precise and accurate methods of sex determination to augment existing practices. Combined, the use of quantitative and qualitative analysis plays a significant role in determining skeletal sex.

Historically, numerous challenges have presented themselves as researchers continue to determine the most applicable methods to predict skeletal sex from postcranial long bones with precision and accuracy (Albanese *et al.* 2005; Allen *et al.* 1987; Bidmos 2006; Sakaue 2004; Steyn and Iscan 1997). The lack of grossly distinct sexual dimorphism in humans can make qualitative analysis difficult. Intra-population variation poses challenges which center around the principle component of size in quantitative analysis (Asala 2001; Asala *et al.* 1998; Purkait and Chandra 2004). Different populations exhibit different skeletal dimensions, to which accurate formulae must be applied. To compound the problem, fragmentary and incomplete remains are difficult to measure. Therefore, researchers have continually sought accurate methods of sexing skeletal elements when the pelvis and cranium are absent and only more robust postcranial elements remain (Case and Ross 2007; Introna *et al.* 1998; Özer *et al.* 2006; Pons 1955; Sorg and Haglund 1997). These methods are particularly desirable for long bones, which may not have distinctly different characteristics indicating sex, but tend to survive in the field quite well. So far, several methods of sex determination from skeletal elements other than the cranium and pelvis are gaining merit. The structure of the lower limb bones (femur, tibia and fibula) and their sexually dimorphic traits have been the subject of study and produced promising results (Martin and Atkinson 1977; Ruff 1987). Thus, these

sexually dimorphic characteristics would be considered extremely valuable in the realm of medico-legal death investigations, in archaeology, and in biological anthropology research.

In addition to quantitative and qualitative methods of determining sex, geometric morphometrics allows for a detailed shape analysis based on the use of comparable landmarks of certain skeletal elements (Adams 1999; Bookstein 1986, 1991, 1996; Kendall 1981; Rohlf and Marcus 1993; Siegel and Benson 1982). This relatively new method places numerical values on shapes and has been shown to be quite useful in the determination of sex using discrete areas of skeletal morphology such as the greater sciatic notch and the human orbit (Pretorius *et al.* 2006; Steyn *et al.* 2004). The lack of grossly distinct sexual dimorphism in humans can make visual assessment of skeletal elements challenging, and problems with the classification of visual traits (e.g., symmetrical, intermediate, asymmetrical) continue to be a dilemma not yet resolved (Ferson *et al.* 1985). Thus, geometric morphometric analysis appears to be at the forefront of techniques that combine the accuracy and repeatability of metrics with the form-and-contour analysis of visual assessment.

The study of skeletal differences between males and females has rarely taken into account the physical change in hard tissue characteristics with the onset of advanced age. In order to observe sexual dimorphism in the adult human skeleton, knowledge must be gained with regard to the development of these sexually dimorphic traits and the changes which they may undergo during life. Anatomical change through human developmental processes and successive degenerative modification pose a serious challenge when diagnosing the sex of an unknown individual of considerable age. Many fields (orthopaedics and geriatrics for example) have outlined the process of age changes to bone, as well as the extent and location of these changes (Grynpas 1993; Genant *et al.* 2007; Parfitt 1997; Rogers 1982; Ruff 2000; Ruff and Hayes 1982; Schnitzler *et al.* 1990; Schnitzler and Mesquita 1998; Stout and Robling 2000). No studies, however, have made diagnostic

determinations regarding how skeletal morphology of the aged affects the way osteologists and physical anthropologists use and perhaps adjust their identification techniques. The use of non-metric and metric techniques may become more accurate based on a clear increase in sexual dimorphism with age; on the contrary, if sexual dimorphism decreases with age, the standard course of analyses may lead to an erroneous conclusion regarding the sex of the individual in question. Little is known about the visual and metric transformation of hard tissue with age, let alone how this would presumably effect a researcher's determination of sex from the skeleton. Does sexual dimorphism in hard tissue, in fact, decrease or increase with advancing age?

The aim of this study is thus to establish whether sexual dimorphism changes with age. This issue would be addressed by using three levels of procedural analyses. It would firstly elucidate whether or not metric traits are altered with the advancement of age; it would also determine if visual assessments using archetypal techniques are more or less accurate as age increases; and thirdly, whether or not geometric morphometrics using homologous landmarks differ from younger to older individuals when attempting to determine sex.

CHAPTER 2

LITERATURE REVIEW

The purpose of this chapter is to discuss the development and degeneration of the skeletal system as it pertains to sexual dimorphism. Sexual dimorphism, the anatomical and morphological differences between males and females, is used consistently to draw conclusions pertaining to the eventual identification of an unknown individual. The inherent size and physical variation between males and females makes sexual dimorphism a powerful tool in assessing skeletal sex. Changes with age, and how these changes affected the characteristics of long bone morphology in males and females were the motivation for this research. However, even taking into consideration the relative size differences between males and females, difficulties can occur. Sexual dimorphism in humans can show enough variation among populations such that the determination of sex can become challenging when morphological features are ambiguous (Kennedy 1995). Therefore, a review of how sexual dimorphism develops in humans, how it manifests itself in developing and mature individuals, and how it potentially is modified in the aged indicates where most research has been concentrated, and where research has yet to accomplish comprehensive results.

Information in this chapter covers the developing skeleton and how the degree of sexual dimorphism changes as humans age, as well as studies that have been instrumental in documenting these changes. Additionally, the location of these changes, the type of bone that is modified with age, and the actual mechanisms that cause changes in bone with the advancement of age are assessed. Since this study employed three methods of determining sex from the human skeleton; metric quantitative techniques, non-metric visual techniques, and geometric morphometric techniques, these methods, and their relative success for the determination of sex

are discussed. Because this specific study only involves the postcranial skeleton, focus will be directed on hard tissue morphology as it relates to long bones and the pelvis, and not the cranium. References to skeletal material will be in the context of observing characteristics of postcranial morphology.

2.1

Manifestation of sexual dimorphism in the human skeleton

Studies in developmental changes and hard tissue growth before and after puberty have been extensive (e.g., Bushang *et al.* 1983; Buckberry and Chamberlain 2002; Cummings and Black 1995; Evans 1976a, b; Garnero and Delmas 1998; Garn 1972; Imrie and Wyburn 1958; Iscan *et al.* 1985; Lee *et al.* 1996; Meuller *et al.* 1966; Recker *et al.* 1992; Steele and Bramblett 1988; Steiger *et al.* 1992; Weaver and Chalmers 1966a, b; Young and Heath 2000). Bone development and growth occurs by the incremental replacement of cartilaginous material (endochondral ossification) or the direct replacement of mesenchyme (intramembranous ossification). Heath and Young (2000) described the long bones, vertebrae, pelvis and bones of the base of the skull as being preceded by cartilage, thus formed through endochondral ossification. Long bones are well established to have an outer matrix of cortical bone, which provides rigidity and strength, and a longitudinally located medullary cavity of thin interconnecting bone trabeculae, in which haemopoietic bone marrow is formed and stored. The shape, orientation and thickness of bone and bony elements are dependent upon the functions and stresses to which the particular bone is exposed. Weight-bearing bones (such as vertebrae and femoral necks) may exhibit numerous thick intersecting trabeculae, while very few trabeculae are found in non-weight-bearing cortex of the rib. These general characteristics of bone are homogenous between developing male and females, and originate from a common, primitive, mesenchymal cell type. Pre-adolescent males and females do not appear

to exhibit differing skeletal attributes on a microscopic or histological level (Garn 1972).

It has been established, however, that males and females begin to skeletally diverge into separate anatomical entities after birth (Bruzek and Soustal 1984; Coleman 1969; Hoppa 1992; Loth and Henneberg 2001; Miles and Bulman 1995; Reynolds 1945). Sexual dimorphism, in its most fundamental application, may begin to develop before puberty (Merchan and Ubelaker 1977; Moerman 1982 a and b, 1992; Reynolds 1947; Roche and Davila 1972; Tanner 1962; Tanner *et al*. 1976). Most of the sexually dimorphic characteristics that were the focus of this study are absent in the pre-adolescent bones of humans, and develop only as a result of the adolescent growth spurt which occurs during puberty. However, there are several indications in other skeletal locations besides the tubular long bones that may offer evidence of sexual dimorphism in the developing skeleton.

Research on the prepubescent innominate bone by Imrie and Wyburn (1958) and Schutowski (1987) suggest that morphological differences in this sex-specific skeletal element do exist, but many of these differences are either subtle or not inherently obvious until full maturation of the human skeleton. Other studies conducted on the pelvis (Humphrey 1998; Moerman 1981; Rissech and Malgosa 1997) concluded that after the metamorphosis of the pelvis to male and female forms at puberty, hard tissue in the region exhibits little change with regard to sexual dimorphism. When attempting age estimation on the auricular surface of relatively young individuals, Buckberry and Chamberlain (2002) found that rates of skeletal development, remodeling and degeneration in the pelvis (from which most methods of adult sex and age estimation are derived) could be highly variable between individuals and populations. They also found, surprisingly, that after the initial development of the adult os coxae and the primary growth surge during puberty, the bones of the pelvis remain relatively static in morphology between males and

females. In other words, a lack of systematic variation in the rate of aging between the sexes was observed.

Although this study does not involve cranial morphology, development of the cranium and its possible sexual dimorphism in children has been researched (Molleson *et al.* 1998; Newman and Meredith 1956; Scheuer and Black 2004; Schutkowski 1993; Walker 1972). Studies involving prenatal cranial development do not discern between males and females in their research, leading to the idea that differences between the two sexes are minimal in utero (Goldberg *et al.* 2005; Jeffery and Spoor 2001). Cranial bone and its properties in regard to tensile strength and bone failure rates due to trauma do not indicate a distinction between males and females, either. Studies of infant cranial bone focus primarily on the strain capacity, fusion rates for developmental purposes, and potential consequences of infant cranial trauma but again do not distinguish a difference between male and female infant cranial properties (Coats and Margulies 2006; Kriewall 1982; Margulies and Thibault 2000; Peterson and Dechow 2002, 2003; Sun *et al.* 2004;).

Continual ossification and development of all cranial elements continues after birth, and exhibits variable rates of growth and maturation. Craniofacial features are used consistently to assess sexual dimorphism in the skull of adults, and most craniofacial growth takes place before puberty (Scheuer and Black 2004). The beginnings of sexual dimorphism, then, is considered evident in this region of the cranium and may even be assessed to a certain level of accuracy in infants, but does not become inherently apparent in juveniles until after skeletal changes begin at puberty (Buschang *et al.*, 1983, 1986; Humphrey 1998; Hunter and Garn 1972; Loth and Henneberg 2001; Molleson *et al.* 1998; Newman and Meredith 1956; Schutkowski 1993; Walker and Kowalski 1972). Growth rates between boys and girls are expected to be different, and sexual dimorphism in the craniofacial region may be observed and calculated (Scheuer and Black 2004).

Males and females do not only differ in the rates in which their pelves and crania develop (and in what morphological direction, i.e. tendency towards robusticity in males or maintenance of infantile features in females), but in long bone maturation as well. Male and female rates of long bone maturation are known to be different. Cross-sectional studies performed on age and hard tissue progression towards adulthood indicated that during pubertal development, major differences between growing males and females were observed in bone mass progress according to sex and skeletal site (Bonjour *et al.* 1991). Specifically, male bone mass at different skeletal sites (lumbar vertebrae, femoral neck) continued to increase substantially between 15-18 years, but skeletal mass growth in females appeared to dramatically slow down at these same sites during the same age range. Subsequently, females showed a dramatic reduction in general bone mass growth after 15 years.

Garn (1972) investigated the relative rates of bone gain at the outer periosteal surface and the proportional rates of bone loss/ gain/ loss at the inner endosteal bone surface, which determined the gross size of the bone in addition to the amount of cortical bone within the anatomical bony element. These studies were performed throughout progressing age stages. Garn constructed the phases of bone resorption primarily at the endosteal surface of long bones and concluded that the majority of bone remodeling occurs during the 4^{th} (adolescent-to-adult) phase and 5^{th} (adult) phase of endosteal surface resorption. He also recognized a sexually dimorphic component to lifelong bone apposition at the subperiosteal surface and concluded that females exhibited a resorptive phase demonstrably larger than males that reduced skeletal mass after adolescent developmental stages were complete. This showed that dynamic processes were occurring in adolescent bones that were different between males and females, even at an early age. These dynamic processes continued to be divergent between the sexes throughout life.

Bone mass modification, remodelling, and transformation in young males and females have always shown net gains in the density of cortical bone and in the

overall density provided by active osteoblasts within both the endosteal and periosteal envelopes (Thompson 1980). Bone development in both males and females is truly a dynamic process, and the incremental addition of bone in early life can certainly play a role with regard to the way individuals change as they begin to age, skeletally, in the 3rd decade of life and beyond.

Based on the dynamic and extraordinary changes that occur in the developmental cycle of bone formation and maintenance specifically in the female skeletal system, females have been studied consistently for the last few decades, and studies on the maturation of the female skeleton have a wealth of information on which to base fundamental principles of bone gain and foundational bone density (Georgopoulos *et al.* 2001; Levine 1972; Onat and Iseri 1995; Singer and Kimura 1981; Vidulich *et al.* 2006). In general, women past the age of puberty tend to gain bone mass through the 3rd decade of life, and may even continue to gain bone if calcium supplements and exercise are introduced (Recker *et al.* 1992). In addition, specific emphasis on such features as cortical bone thickness and bone mineral density in healthy adults has provided a gauge with which to determine maturation rates and subsequent degenerative processes (Dickenson *et al.* 1981; Epker *et al.* 1965; Gotfredsen *et al.* 1987; Hui *et al.* 1985; Jowsey 1960; Matkovic *et al.* 1990; Woodard 1962).

2.2

Other factors that influence sexual dimorphism in a population

Many unique and vigorous influences on hard tissue play roles in its early development, its maturation, its variation into adulthood and its degenerative characteristics. These influences vary greatly and offer different aspects of morphological variation.

Structural characteristics in the skeleton upon maturation and its "level" of sexual dimorphism correlate often with behavioural factors (Chesnut 1993). Specifically, it has been proven that without weight bearing exercises performed consistently to strengthen hard tissue (i.e., mechanical loading or gravitational force exercises), bone mass loss will occur at axial and appendicular skeletal sites (Skedros *et al.* 2004). Weight-bearing processes that occur in the realm of occupational functions were found to strengthen muscle attachments and articular joint surfaces even to the point of modifying morphology in bone's adaptive processes. Thus, mechanical loading and behavioural stressors play a distinct role in factors influencing bone mass and structural morphology (Beck *et al.* 1992, 2000; Burr and Martin 1983; Chavassieux *et al.* 2007; Compston *et al.* 2007; Han *et al.* 1997; Maalouf *et al.* 2007; Seeman 2003; Szulc *et al.* 2006). Thus, if behavioural practices are distinctive between the sexes this can play a role in the sexually dimorphic nature of bone in males and females. Behavioural practices have been seen to be very distinct between populations and cultures. Males and females respectively play different roles in their societal environments, thus they are subjected to different physiological and biomechanical stressors. These influences have residual effects on hard tissue (Anderson 1998; Beck *et al.* 1990, 1992; Ruff *et al.* 2006; Taitz 1998).

In addition to behavioural aspects influencing bone mass and hard tissue density, environmental, nutritional and socioeconomic issues have also been shown to play a vital role in skeletal structure (Angel *et al.* 1987; Macho 1990; McVeigh *et al.* 2004; Nelson *et al.* 2004; Ruff 1987; Stini 1969; Thompson 1980). Macho (1990) determined that different living conditions and/ or nutritional availability affected bones in complex ways of which linear growth was only one aspect. As nutrition improved in the African and European populations studied, so did sexual dimorphic characteristics as well as stature. Based on this discrepancy in size and the question of stature as an indicator for living conditions, Macho concluded that relative size

variations, i.e., shape, discriminated more clearly between the sexes than did observable size when nutritional stressors were recognized as a factor. It was also concluded that when the level of nutrition improves, the amount of sexual dimorphism in stature increases (Tobias 1975; Tobias and Netscher 1977).

Other nutritional studies have focused on the rate of calcium absorption and the direct effects of reduced calcium assimilation in the body (Devine *et al.* 2004; Heaney *et al.* 1982). Heaney's study concluded that as a decrease in the intestinal calcium absorption efficiency and renal calcium conservation occurred, the medullary cavities of long bones expanded due to loss of mineral density within the endosteal-trabecular envelope. The study also determined that the average elderly person is in negative calcium balance; this fact coupled with factors such as decreased mechanical loading of the skeleton must figure prominently in age-related bone loss throughout the entire skeleton.

Behavioural and nutritional issues, among other factors, take part in skeletal differences between men and women. Perhaps two of the most important factors in sexual dimorphism are those that determine the sex of an individual itself (genetics) and those that inevitably cause maturation changes to occur (hormones). Both hormones and genetics are known to influence skeletal attributes (Ebeling *et al.* 1998; Kelly *et al.* 1990; Manning *et al.* 1992; Pollitzer and Anderson 1989).

Naturally-occurring hormones are, in fact, the basis for all bone development and maturation (Young and Heath 2000). Specifically, bone development is controlled by growth hormone, thyroid hormone, and the sex hormones. In addition, synthetic hormones used in the medical treatments of some disease processes also influence subsequent bone mass and hard tissue density. For example, the study Ebeling *et al.* performed (1998) determined that long-term inhaled or oral glucocorticoid administration for asthmatics lowered bone mineral density in both men and women. In addition to the loss of critical bone density, which acts to prevent fractures, glucocorticoids reduced bone formation in the presence of ongoing

bone resorption, which contributed directly to ultimate bone loss in asthmatics. These findings were mirrored by that of Jee *et al.* (1970), which confirmed that hormones such as corticosteroids were relevant to the decay of osseous tissues and reduced bone volume. Going further, Jee *et al.* deduced that the effect of corticosteroids was dose- and time-dependent, in which high doses of the steroid suppressed bone resorption and low doses stimulated bone resorption; corticosteroids thus act upon bone cells by directly inhibiting precursor cell proliferation.

Studies focused on genetic markers for bone loss and resorption provide significant evidence that bone turnover markers are of value in investigating the pathogenesis and treatment of bone loss in young and old (Garn *et al.* 1966; Looker *et al.* 2000). Genetics plays a significant role in the bone mass of an individual, and the genetic markers for that role can be studied and identified. These markers can lead to information with regard to specific bone gain in the developing skeleton of a young adult or subsequent bone loss and degenerative processes in the elderly. Genetic bone resorption markers appeared to be associated with increased fracture risk in elderly women, while there is less of a correlation between bone formation markers and fracture risk. Biochemical markers appeared to be valuable tools in the research of metabolic bone gain and loss, which in turn is applicable to bone density and mass.

The types of stresses that are applied to osseous tissue, which determines how dense and compact the existing trabeculae should be in a given area of stress, can also influence initial bone mass in the human skeleton. The tensile strength of osseous tissue functions as one of the main components of the mechanical properties of bone, especially as the human skeleton ages. Stresses to the tensile property of bone increase the risk of fractures, subsequent wound response, and compensatory actions by the injured and thus inherent biomechanical substitution occurs, possibly changing the anatomy of the injured element (Evans 1976). All of

these aspects determine the variance of hard tissue morphology from puberty to advanced age. Some of these changes manifest themselves in quantifiable variables, and others appear to exhibit conditions that may be best visualized other than measured.

2.3

Previous research in age-related changes in sexual dimorphism

Those interested in osteoporosis and its effects on the elderly population performed the majority of past research done in this area of skeletal anatomy (e.g., Adebajo *et al.* 1990; Aspray *et al.* 1996; Grynpas 1993; Maalouf *et al.* 2007; Ruff and Hayes 1982; Schnitzler 1993; Simmons 1985; Szulc *et al.* 2006; Wallin 1994) . Thus, different disciplines of expertise were the sources of much of the literature defined in this section. However, previous studies in these disciplines do illuminate the histological, microscopic and macroscopic modification found in bone of advanced age, thus they were considered valuable to utilize.

Bone loss and bone modification are multi-faceted processes of skeletal maturation, maintenance, and degeneration. These processes affect all types and categories of bone, from exterior cortical surfaces to the underlying matrix of the medullary cavity. Bone modification as the human skeleton ages not only affects the periosteal surface of the long bones, but also inflicts a net loss of bone mineralization within the cortical bone surface as well as the cortical endosteal surface (Epker 1965; Frost 1963; Gotfredsen *et al.* 1987; Jowsey 1960; Ruff 1987; Thompson 1980; Woodard 1962). Studies have focused primarily on the net bone loss of individuals (both male and female) of advanced age and show that this loss takes place primarily from the cortical-endosteal surface (Aloia *et al.* 1985; Deakins and Burt 1944; Evans 1976; Nilas *et al.* 1988). This type of loss was then observed to cause an expansion

of the medullary cavity while simultaneously exhibiting cortical bone thinning (Heaney *et al.* 1989; Leiel *et al.* 1988; Martin and Atkinson 1977). This type of modification typically resulted in an expansion of tubular bone circumference *within* the medullary cavity, but not necessarily in the corresponding outer cortical "shell" or envelope. Alternative studies by the Scientific Advisory Board of the National Osteoporosis Foundation (1988) discovered that age-related bone loss in the shafts of long bones is partially compensated for biomechanically by remodelling to increase the shaft diameter. This served as a response to increase resistance to bending and torsion in the limb shafts of both men and women. This compensation process was found to be at not only the long bone shafts, but also in the articular junction of joints.

Further distinctions between males and females in the compensatory reaction of thinning cortical bone and increased bone porosity were found, which contrast the results of the National Osteoporosis Foundation. Female skeletal changes occurred most dramatically at the onset and after menopause, where bone remodelling became unbalanced and resulted in bone loss at each remodelling site (i.e., articular joint surfaces). In addition, an increase in bone turnover sites resulted in an accelerated bone loss throughout the entire female skeleton (Cummings *et al.* 1990; Herd *et al.* 1992; Herrin 2001).

The location of remodelling, which represented skeletal tissue undergoing modification and therefore becoming structurally ineffective, increased in females with age and was observed in greater quantities in cancellous bone as opposed to cortical bone. These changes manifested themselves in greater microporosity, a decrease in bone mineral density, and the onset of frequent osteoporotic fractures at sites such as the femoral neck and the vertebral bodies (Cummings *et al.* 1985; Cummings *et al.* 2000; Dickenson *et al.* 1981; Evers *et al.* 1985; Hurxthal *et al.* 1969; Kanis and McCloskey 1993; Orwoll *et al.* 1996; Steiger *et al.* 1992; Thompson 1979). Riggs *et al.* (1982) categorized this bone loss further into "postmenopausal osteoporosis", characterized by excessive and disproportionate trabecular bone loss

associated mainly with vertebral fractures; and "senile osteoporosis", a more general term, which is characterized by a proportionate bone loss in both cortical and cancellous bone.

Males, conversely, showed an increase in bone porosity with age but also exhibited compensatory structural strength that did not occur in females. This mechanism indicated a physiological adaptation resulting in a difference between males and females and their varying deficit of bone surface remodelling that is independent of internal remodelling (Martin and Atkinson 1977). Age-related bone change in males was also linked explicitly to unique hormonal changes related to prostate health, including treatments for cancer and other age- and gender-related therapeutic management (Bilezikian 1999; Daniell 1997; Eastel *et al.* 1998; Finkelstein *et al.* 1987; Grasswick and Bradford 2003; Ross and Small 2002; Thiebaud *et al.* 1996; Vasireddy and Swinson 2001).

Various studies from different biological groups found throughout the world give further details about the unique characteristics in patterns of bone modification with age. Spinal density in females from Japan and India with low calcium intake decreases dramatically with age, in contrast to British and American populations (Nordin 1966). Several studies have indicated that higher bone mineral densities in African American subjects were a reasonable explanation for differential fracture rates when contrasted with American white females (Aldridge 2005; Garn *et al.* 1969; Garn 1972). Osteoporosis was seen with less frequency in African American females as well, and Trotter *et al.* (1960) determined that bone density is not only sex-specific (male osseous material is denser than female osseous material) but population-specific as well (African Americans exhibited greater bone density as did American whites). Orwoll *et al.* (1996) were forced to remove African American women from their axial bone mass and fracture study based on the low incidence of hip fractures. A Native American sample of three geographic groups were seen to parallel bone loss studies conducted on American white female samples, with overall

loss of cortical bone amounting to two to three times that of males (Ericksen 1976). Finally, mineral density levels in Eskimo tibiae were found to again follow a classic model of cortical and cancellous bone loss, with male bone density measurements exceeding those of females as age progressed and female bone mineral density declining with age (Martin *et al.* 1985). In studies to date, even when focused on specific geographical groups, bone loss is seen with advancing age in both sexes and in all biological affiliations.

Although research has focused primarily on the net periosteal and endosteal bone loss of individuals with the onset of age, others report the surprising increase of total diameter of long bones due to a periosteal bone gain, and the continued positive periosteal bone balance (indicating continued periosteal bone formation) after the age of 65 years (Jowsey 1960; Smith and Walker 1964). Smith and Walker (1964) specifically showed evidence of the mean periosteal femoral diameter increasing as cortical thickness declined. Since the cortical area was enlarged, periosteal accumulation exceeded endosteal resorption, meaning a net bone gain was found due to periosteal bone activity that superseded the endosteal bone loss. This same result was seen in humeral dimensions from Rother *et al.*'s study (1977) where quantitative overlap was found between the sexes. Subsequently, it was concluded that humeri showed a decrease in sexual dimorphism with age.

Evans (1976) reported that as age increased in the human skeleton, the incidence of fractures increased for two reasons: first, because older individuals exhibit less bone density (a quantitative difference) and because the osseous material of older individuals is structurally weaker than that of younger individuals (a qualitative difference). An increase in osteon numbers is also found in older individuals, which subsequently increased the amount of cement lines around osteons in a given area. Thompson confirmed this observation in his 1979 study of age-at-death determination by osteon count. Other researchers who study age-at-death with bone histology methods have mirrored his conclusions (Ortner 1975;

Young and Heath 2000). The increase in osteons led to an increase in structural porosity (due to increased canals, lacunae, and canaliculi) and created sites more prone to microfractures based on fracture patterns around the cement lines surrounding osteons. The 1) increase in porotic spaces of bone and 2) increased numbers of osteons per millimetre squared decreased the amount of hard tissue available for force resistance or load-bearing strength. These tensile stresses resulted in microfractures, which subsequently resulted in more active bone remodelling sites, which finally manifested in an increase in bone surface area and dimension.

Nilas *et al.* (1988) advanced this theory by reporting the increased bone width at two forearm sites in females while originally attempting to observe bone loss. In addition, Linday *et al.* (1978) determined that estrogen replacement therapy in osteoporotic women prevented further bone loss in postmenopausal women and in fact modestly increased bone mass if estrogen treatment had been delayed for several years.

Irregular bones such as the structure of the hyoid bone have been examined as well, and showed similar results in cumulative bone gain to their surfaces with age, resulting in larger bone mass and increased asymmetry (Miller *et al.* 1998). These areas of aggregate bone change appear contradictory (or in the very least, contrasting) from one study to another, and have been examined in detail to understand the total changes affected upon the skeleton. In general, females appear to be either maintaining their size or becoming larger in skeletal dimensions, which may be a reason for the reduction in sexual dimorphism with age between the sexes in any given population.

Walker (1995) provided a comprehensive study of an English population that elucidated the challenge of age-related changes in bone when studying sexual dimorphism. Because decreased bone density in women was highly correlated to the degradation of skeletal material in Walker's cemetery sample, os coxae could not

be utilized on a large scale to confirm sex classification. Disintegration of the greater sciatic notch and other pelvic features lead researchers to categorize sex from craniofacial features; these features ultimately suggested that post-menopausal females contributed to the apparent excess of males in the skeletal collection due to misclassification based on supraorbital robusticity. Walker cautioned that overlooking these age changes in female postmenopausal cranial morphology could introduce significant biases regarding the determination of sex in mortality profiles (and forensic analyses) based on poorly preserved skeletal collections or samples.

In conjunction with this was Walker's study of greater sciatic notch morphology (2005), and its determination that there was a greater tendency for male sciatic notch morphology to shift in a masculine direction with increased age, resulting in greater sexual dimorphism. Both young males and females tended to have more feminine morphology than did older individuals. This feminine morphology appeared more prevalent in young males, and thus the shift in a more "male-like" morphology with age was quite dramatic.

The extensive changes documented in past research summarized here may suggest that perhaps these modifications appear in bone concurrently. The human skeleton changes dynamically with the onset of age after puberty. These changes manifest themselves in both the negative and positive; bone is both lost and gained depending on the skeletal site, various biological factors, and sex of the individual. Anthropological analyses on skeletal material have been extensive and comprehensive in documenting morphology of the skeleton. The discipline of anthropology is also established in its extensive array of research performed on the intricacies of sexual dimorphism and how to categorize skeletal sex. While performing initial inquiries into the subject, however, all disciplines appeared to be lacking in documentation regarding how each effects each other; how hard tissue anatomy changes with the onset of advanced age, and if the differences between young and old individuals is great enough to note, and large enough to quantify. It is

this discrepancy between posing the query and finding the answer that outlines the need to understand the extent of these changes, and their physical manifestation on elements used to make scientific determinations of sex.

Sexual dimorphism is known to be apparent in the human skeleton, but a review in how anthropologists determine sex from skeletal elements may aid in determining which elements are important and which ones could be susceptible to modification with age.

2.4

Non-metric techniques for determining sex in the postcranial skeleton

Researchers historically have used quantitative analysis on postcranial elements and discovered its benefits early on; however, most agreed that nothing could take the place of a visual assessment of specific skeletal element's characteristics by a trained and experienced analyst (Stewart 1954). Most of these visual techniques historically have been used on the cranial and pelvic regions, and not long bones. Although some researchers considered measurements to be more accurate than visual techniques, they continually argued that there are inherent limitations to measurements, "...namely, that they are poor descriptive agents and are subject to various kinds of error. As is all too well known to anthropometrics, an index tells nothing but the percental relationship of two linear dimensions; it tells nothing about the shapes of the parts included within the dimensions" (Stewart 1954). Many researchers concluded that measurements were no substitute for visual assessment by an experienced analyst who can quickly and effectively diagnose the sex of a skeleton (Hill 2000; Inman *et al.* 1944; Ubelaker and Volk 2002; van Dongen 1963; Walrath *et al.* 2003; Weiss 1972). For example, Van Dongen's research on the shoulder girdle and humeral element of Australian

Aborigines showed numerous applications of visual, non-metric assessment in order to discern males from females. Most of the specimens in this sample would have been misclassified as male based on metric techniques applied to epiphyseal long bones sites and shaft diameters.

The dominant factor in quantitative analysis for all populations is nearly always size, and its relationship to males versus females. When size is "removed" from the statistical analysis of sex, only descriptors are left to reveal differences between sexes and establish clear guidelines with regard to what constitutes male and female morphology. Visual characteristics and their meaning are inherent in anthropological research. Quantitative analysis depends solely on size differences to correctly assign sex, but this method fails where the sexes over lap (i.e., a large female or a small male).

Visual assessment offers an alternative by relying on descriptive features and observer experience to interpret the distinctive variation in shapes between male and female elements, and to come ultimately to an accurate conclusion (Wanek 2002). Specifically, visual assessment of the distal and posterior humerus uses several characteristics to determine skeletal sex, a technique that was developed by Rogers (1999). Physical characteristics of olecranon fossa shape, the angle of the medial epicondyle, the absence or presence of symmetrical borders between the trochlea and the capitulum, and the position of the medial epicondyle within the trochlear profile were all sexually dimorphic. These traits, which were tested on a Caucasian sample by Rogers and subsequently tested on numerous populations by Wanek (2002), were shown to be sexually dimorphic, and again provided another non-metric technique that focused on sexual dimorphism in sex determination.

Some non-metric visual techniques have been developed and tested innumerable times with the same results. These methods hold some of the most accurate and appropriate means by which to determine sex in the adult human skeleton. Specifically, a detailed description of pelvic traits has endured throughout

decades of anthropological research and continues to fill many of the canonical texts used by students, researchers and scholars alike (Bass 1995; Krogman 1962; Steele and Bramblett 1988; White 2000). Physical characteristics of visual pelvic morphology are conventionally based on shape, contour, angle, the relative width of a feature, or a combination of several morphological traits. Common physical characteristics of the pelvis, which appear as sexually dimorphic, are the width of the greater sciatic notch, the width and robusticity of the ischio-pubic ramus, the shape and width of the subpubic angle, and the contour of the subpubic concavity. All of these features show distinct differences between males and females, and have been documented extensively in their scope of accuracy in numerous biological populations.

Because these suites of features from both the humerus and pelvis have been established as accurate ways of assessing sexual dimorphism in the human skeleton, they were employed in this study as the characteristics in which to establish sex by non-metric, visual means.

2.5

Metric techniques for determining sex in the postcranial skeleton

Metric studies were brought about by a need to quantify traits identified by visual techniques. Sexual dimorphism in a classic sense illustrates the observable, physical characteristics that make males and females anatomically distinctive from one another. Many professional osteologists, physical anthropologists and anatomists rely on these characteristics in order to determine the fundamental, individualistic information from a skeleton. The postcranial skeleton continues to be a source of information in regard to determining skeletal sex because most long bones exhibit noticeable size differences (Borgognini Tarli and Repetto 1986).

Various researchers have studied the metric differences between males and females in the long bones of the upper limb (e.g., Jantz *et al.* 1994; France 1998; Grabiner 1989; Mall *et al.* 2001; Richman *et al.* 1979; Steyn and Iscan 1999), the lower limb (King *et al.* 1998; Martin and Atkinson 1977; Thompson 1980; Woodard 1962) and the pelvis (Phenice 1969; Steyn *et al.* 2004). Many of these studies focus on the dimensions of articular joint surfaces such as the humeral or femoral head, and distal epicondylar breadth. Several provided discriminant function formulae for the determination of sex for multiple population groups (Dibennardo and Taylor 1982; Giles and Klepinger 1998; Richman *et al.* 1979; Tagaya 1989). These measurements have now become standard, such that they are easily repeatable and reproducible by researchers.

In addition to epiphyseal measurements on long bones, the length of long bones, their diaphyseal diameters, and their circumferences have been the subject of diverse studies which span from anthropology to geriatric medicine (Evans 1976; Garn 1970; Georgia *et al.* 1982; Harper *et al.* 1984; Klepinger 2001; Leiel *et al.* 1988; Macho 1990; Pfeiffer and Zehr 1996; Stewart 1963; Stini 1969; Woodard 1962). These studies and their subsequent development of sex determination techniques focus on the principal size component of long bone shaft diameter discrepancies between males and females in the appendicular skeleton (King *et al.* 1998; Martin and Atkinson 1977; Thompson 1980; Woodard 1962). As expected, all these researchers found differences between males and females, with Chesnut (1993) observing additional linear correlations between the maintenance of bone mass and the implementation of weight-bearing exercises (mechanical loading) regarding to the shoulder girdle and elbow joint. Factors such as these (i.e., size components, weight-bearing differences) and the broad-spectrum differences in male and female anatomy make sexing methods of the postcranial skeleton quite robust and accurate when utilizing a known sexually dimorphic trait or suite of traits.

Most of these studies focus on the bimodally distributed metric differences between males and females, the variation of shaft diameters with age and osteoporotic degenerative changes, and the possibility of metric overlap between populations and/ or sexes. Metric studies concluded that males, regardless of population, are larger in size than their female counterparts (Takahasi and Frost 1965; Wiredu 1999). Articular surfaces and breadths are greater, shaft diameters are larger and tubular bone lengths are consistently longer in males than females. Since men are morphologically larger than women, quantitative analysis depends solely on these size differences to correctly assign sex. Thus long bone morphology and their unique attributes at epiphyseal junctions as well as shaft and length dimensions continue to be the focus of sexual dimorphism research.

2.6

Geometric morphometric techniques for determining sex from the postcranial skeleton

Morphometrics in biology has been utilized consistently for the past twenty years for species determination, developmental transformation, and sexually dimorphic variation between males and females of a specimen group (Loy *et al.* 1999). Bookstein (1982) described morphometrics as "the biometric study of effects upon form", "form" being the intrinsic combination of size and shape. Form was determined by assigning homologous landmarks that exploited the data of curvatures, corners, or surfaces that may serve as points of net biological change or variation (Rohlf *et al.* 1985; Rohlf 2000). As biological inquiry became more quantitative, modern statistical methods within the discipline of morphometrics were employed to provide a new compilation of tools used for discrimination processes (Richtsmeier *et al.* 2002; Walker 2000). The geometry of biological form in two- or three-dimensional space and the efforts to preserve the physical integrity of form

developed into the most recent form of geometric morphometrics, a fusion of geometry and biology (Bookstein 1982, 1990; Ferson *et al.* 1985).

Because craniometry, anatomy and palaeontology had already distinguished classic anatomical definitions of biological landmarks, these could now be used to accurately obtain coordinate locations and provide researchers with homologous data points on which to base their morphometric analyses. Cranial morphology and the quantification of shape characteristics through geometric morphometrics have been studied at length by biologists to typify the varying orders of mammals and to assign crania to possible groups for more discrimination in species determination (e.g., Adams 1999; Pretorius and Scholtz 2001; Ross *et al.* 1999). Morphometric analysis followed logically by using these established landmarks in anthropological studies as well. Only in the second half of this morphometric era has anthropology gained with quantification techniques applied to the shapes and contours of the human skeleton. While anthropology has gained information in the morphometric analysis of two-dimensional and three-dimensional skeletal features, challenges in landmark assignments have also been recognized as a potential limiting factor with geometric morphometrics (von Cramon-Taubadel *et al.* 2007).

Geometric morphometrics, then, is the analysis of a set of digitized landmark coordinates, with each set recording the form of the specimen (form = shape + size). Landmarks are specific locations on biological forms and are recorded as two- or three-dimensional coordinates. These coordinates, when visualized and recorded on a collection of objects of the same biological form, are then known to be corresponding, or homologous (Richtsmeier 2002). Homologous landmarks remove the effects of variation in orientation and dimension of specimens, with the remaining distinctions representing shape variation. This approach detects shape differences with more statistical power as landmark coordinates can obtain more data regarding shape, resulting in different and perhaps enhanced visualization of the results than conventional methods (Rohlf 2003).

Morphometric methods are simply tools to help define the difference between forms via geometry. Two methods most commonly used (and those utilized in this study) are deformation methods and linear distance-based methods.

- Deformation Methods:

  Deformation methods take the area or volume of a reference form (normally a precisely symmetrical grid structure) and deform it to correspond with that of the target form. Sir D'Arcy Thompson's work (Thompson 1992) is the first and best-known instance of the use of deformation techniques for the demonstration of the difference between forms. He created "transformation grids" where a two-dimensional grid was placed over one structure (or form), and the grid was transformed to correspond to the morphology of the second structure (or form). The "transformation" in the grid described the difference in structures. Thompson's work imparted information more about outlines than to landmarks, and he did not propose any quantitative method for creating these grids.

Thin-plate splines are the modern configuration of Thompson's "transformation grid" efforts. Thin-plate splines use chosen functions to chart the relative location of points in an initial configuration to their precise locations in a corresponding target form precisely. These functions also can predict how points that lie in those areas between landmarks in an initial form are arranged on the target form. Richtsmeier *et al.* (2002) described the process as "...placing a continuous and bendable surface (or plate) over the area or volume encompassed by the landmarks. This plate is then deformed in such a way that: 1) corresponding landmarks in the two objects are mapped to one another exactly; and 2) the quantity of a specific parameter, often bending energy, within the function is minimized. This

means that only the minimal amount of energy required to bend the plate to conform to the target object is used" (pg. 79).

- Linear distance-based methods:

  These methods evaluate the linear distances that connect landmark pairs in one structure to analogous linear distances in another structure. They also provide data regarding the differences in length and magnitude of linear variations of these distances. This not only shows the amount of distance between corresponding forms, but also shows where the differences occur and in what direction they are exhibiting their modifications. These variations are considered "vector" variations.

Robust statistical tests built into analytical software have benefited from additional computer models, which allow researchers to easily visualize results in morphometric studies. James F. Rohlf developed the 'tps' series of programs that calculate statistics and provide easily created thin-plate spline grids to visualize the quantifiable changes in form (Rohlf 2000). The 'tps' series consists of a collection of programs utilized in many of the past studies performed on morphological analysis of form, and were employed in this study as well.

Geometric morphometrics can provide indications of explicit variation locations on a specific skeletal element. This means that the divergence between males and females in a specific location on a skeletal element can be shown to exist, and the direction of that variation may be observed. In addition, classification results and accuracy are comparable to traditional discriminant analysis. For example, Hennessy and Stringer (2002) provided a summary of craniofacial variation that allocated modern humans to regional geographic groups based on three-dimensional landmark analysis using classic anatomical markers already established as possible points of craniofacial diversity.

Applications of morphometrics on hard tissue to determine variances between the sexes have included both cranial and post-cranial elements (Marcus *et al.* 2000). The efficacy of morphometric analysis to determine sexual dimorphism in the skeleton has been established and utilized in numerous studies to observe the quantifiable variances between the male and female shape (e.g., Franklin *et al.* 2006; Pretorius and Steyn 2005; Pretorius *et al.* 2006). These applications have led to the possibility that size and shape are never biologically independent, but the quantification of shape and the "normalization" of size differences will assist in an attempt to reduce the influence of size on the shape of an element being studied.

Comparing the relative locations of features and how they differ in arrangement from the "mean" form of a skeletal element has been established as the greatest asset in using geometric morphometrics to determine the level of sexual dimorphism in skeletal features. Results that may be expected from geometric morphometrics on the pelvic region may include variation in the shape and contours of the subpubic concavity; the distinct robusticity or gracile nature of the ischio-pubic index; the elongation and rectangular shape of the subpubic angle in females as opposed to the relatively blunt and triangular shape of the male subpubic angle; and the width of the greater sciatic notch. Results expected from analysis of the distal and posterior humerus may include differences in olecranon fossa shape; the extension of the trochlea past the distal margin of the capitulum; and the angling or parallel nature of the medial epicondyle as it projects from the trochlear profile.

Sexual dimorphism in humans has long been the topic of research, study, and technical interpretation. Changes in bone with the onset of age (both macroscopically and microscopically) have also been subjected to consistent scrutiny. The history of research done on these topics forms the foundation of observing traits and measurements in the human postcranial skeleton that may or may not change when age increases.

CHAPTER 3

MATERIALS AND METHODS

3.1

Sample

The skeletal sample in this study originated from the Pretoria Bone Collection at the Department of Anatomy, University of Pretoria and the Raymond Dart Collection at the University of Witwatersrand. The Pretoria Bone Collection was established in partnership with the Department of Anatomy and the Medical School at the University of Pretoria, South Africa in 1987. These individuals, being both donated and unclaimed by relatives, are received as cadaver teaching specimens first, then macerated and stored in acid-free boxes for research purposes (L'Abbe *et al.*, 2005). The collection houses several biologically distinct groups of individuals, the most common being black South African males. Also represented are black South African females and white South African males and females. Bodies are acquired by either direct donation or as an unclaimed specimen.

Those wishing to donate their body may complete paperwork before death occurs; in addition, an individual's next of kin may donate a body for research and study after death has occurred. Unclaimed bodies are handled differently in the fact that they are transported directly from the hospital where the individual died to the University for study and research, without the traditional consent form required according to the Human Tissues Act (1983). In addition, age restrictions exist with tissue donation; so all individuals over the age of 65 or those who have died from specific pathological conditions are not appropriate for tissue donation. These specimens again are transported immediately to the University of Pretoria Medical School campus for embalming and subsequent teaching purposes.

Ages within the sample range from 19 to 94 years. The postcranial long bones of 404 adult males and 189 adult females were used in this study (Table 3.1). The difference between numbers of males and females reflects their disproportionate representation in the collection. The sample size varied among the various measurements, due to the fact that some skeletal elements had broken shafts or absent epiphyseal ends. These samples were not wholly excluded because of the goal sample size of 500.

The sample was divided into categories of "young" (50 years of age or younger) and "old" (over 50 years of age). Because of the abundance of specimens over the age of 50, all individuals in the young age group that were deemed appropriate for analysis were utilized in this study. The age boundary between young and old was developed based on the amount of data from scientific sources (osteoporosis journals, geriatric publications) that described bone modification occurring not only in the second and third decades of life, but well within the seventh and eighth decades. Ultimately, individuals (women) over 50 were clearly postmenopausal, and thus the discriminating boundary was 50 years of age. Skeletal elements that exhibited acute pathology or healed trauma at the measurement site were excluded. Bones with age-related pathology were not excluded due to the information they provide regarding age-related changes. Clearly defined osteophytes were not included in the measurements. The Pretoria Bone Collection was primarily used for compiling data, however where specimens in a specific group were lacking, the nearby Raymond Dart Skeletal Collection was utilized as well. The Dart Collection offered a small percentage of specimens, but was helpful in supplementing information on young white females, a population that is in short supply in the Pretoria Bone Collection.

3.2

Data Collection

A data sheet was created to record measurements and appropriate information (Appendix A). From this information, a spreadsheet was generated with appropriate box and cadaver numbers as well as the approximate sample size for each population. The spreadsheet did not list the known age or sex of the specimens, so as not to introduce bias in the assessment of characteristics. The goal was not to illuminate the differences between South African blacks and South African whites, but to determine whether men and women change morphologically with age, and to what extent. Non-metric visual traits were recorded on the data sheet first. Quantitative data was collected second so as not to bias the observer with potential morphological size information that indicated the sex of the individual.

3.2.1

Data collection of non-metric information

Collection of data from the postcranial skeleton was taken from one long bone (the humerus) and one irregular bone (the pelvis) in order to determine sex by visual methods. Non-metric morphology of long bones has not been conventionally employed to determine the sex of skeletal specimens. However, Rogers (1999) defined several traits of the distal humerus that proved sexually dimorphic on a statistically significant level. These traits were subsequently used to determine skeletal sex with numerous populations, producing accurate results as well (Wanek 2002). These results reinforced the assertion that traits from the distal humeral articular surface were, in fact, sexually dimorphic. Therefore, the humerus (the distal and posterior aspect of the humerus, specifically) was identified as one of the two skeletal elements to be used in this study to record non-metric information on sex.

Traditional visual characteristics used to determine sex from the postcranial skeleton, on most occasions, utilize the pelvis. Pelvic morphology has been

confirmed on numerous occasions as being highly sexually dimorphic and quite accurate in the determination of skeletal sex. The os coxae, therefore, was used in this study to apply classic non-metric attributes to all specimens.

Attributes from both skeletal elements and the ultimate estimated sex were recorded separately, first from the humerus and next from the pelvis. This order of documentation was used in an effort to not bias the observer with classic pelvic morphology when looking at the lesser-known traits of the humerus.

3.2.2

Data collection of non-metric information from the humerus

Four visual indicators of sex in the distal and posterior humerus were defined as "medial epicondylar symmetry", "trochlear extension", "olecranon fossa shape", and "angle of the medial epicondyle". Rogers (1999) first described these characteristics. Modification of these characteristics were subsequently made by Wanek (2002) and utilized successfully. Descriptions of the typical male and female morphology of the distal humerus are described in Table 3.2. In addition, visual representations of each characteristic are shown in Figures 3.1 to 3.8. Data on the left humeri were used for analysis.

Non-metric traits were first observed and recorded on the data sheet. A degree of "femaleness" and "maleness" of the trait was determined by assigning the most obvious male features a [1], an intermediate yet still discernable male feature a [2], an ambiguous feature a [3], an intermediate yet still obviously female feature a [4], and a clearly female feature a [5]. The combined total of the numerical values of traits were used to make an estimation of sex for the humerus as a whole. A particular humerus could therefore obtain a maximum score of 20, if it was hyperfeminine. A total score of four through 11 indicated that the specimen was a male; a score of 12 indicated an ambiguous specimen; and a total score of 13 through 20 indicated a female specimen. Finally, either a [1]/ male or [5]/ female was

recorded on the data sheet and for data input into subsequent spreadsheets for statistical analysis. "Five" was given to females under the categories of "known sex" and "estimated sex" because it best described females to those interpreting the data. The number five always illustrated an unambiguous female when used with all single variable determinations; it was logical to extend this representation of females in the "known" and "estimated" fields of the database. Just as a "five" value showed an obvious female, a "one" represents the most blatant and robust of male traits. A "one", then, was used to denote males in the same categories of "known sex" and "estimated sex" within the spreadsheet whenever applicable.

This scoring method is illustrated by the following two examples:

- Reference Number: 5569
  Box Number: 1140
  Medial epicondylar symmetry: 5
  Trochlear extension: 2
  Olecranon fossa shape: 3
  Angle of the medial epicondyle: 1
  - Final score = 11
    Final determination = [1]/ Male

(This specimen was eventually revealed as a black male, 23 years old.)

- Reference Number: 2228
  Box Number: 3069
  Medial epicondylar symmetry: 4
  Trochlear extension: 4
  Olecranon fossa shape: 5
  Medial epicondylar angle: 1
  - Final score = 14
    Final determination = [5]/ Female

(This specimen was eventually revealed as a white female, 43 years old.)

3.2.3

Data collection of non-metric information from the pelvis

Four well-defined and proven characteristics of pelvic morphology were used for the determination of sex. These traits included the length of the subpubic concavity, the width of the subpubic angle, the ischio-pubic ramus width and the width of the greater sciatic notch (Bass 1995; Steele and Bramblett 1988).

Descriptions of the typical male and female characteristics of the pelvis are given in Table 3.3.

These suites of characteristics have been tested consistently throughout the last four decades of physical anthropological research, and proved to be accurate in assisting in the determination of sex from the os coxae (Bass 1995). Visual representations of each pelvic characteristic are shown in Figures 3.9 to 3.16. Data on the left os coxa was used for analysis.

Observations of the os coxae were collected after all humerus data was recorded for each specimen. This sequence of events was established for the same reason as quantitative data was collected last, so as not to bias the observer with well-known and well-defined criteria for male and female pelvic morphology. A gradient value of 1-5 was recorded next to each of the characteristics of the os coxae of each individual. These values paralleled the grades assigned to non-metric traits of the humerus.

3.2.4

Data collection of metric information from long bones

Measurements from all six major long bones were included in this study. In all of these skeletal elements, the maximum diameters of proximal and distal articular ends, maximum midshaft diameters, and circumferences (when applicable) were collected. Twenty-three total measurements from long bones were gathered. All measurements and descriptions were based on established data collection protocols in order to be as comprehensible and unambiguous as possible (Moore-Jansen *et al.*, 1994; Bass 1995). Measurements and their descriptions of the postcranial skeleton appear in Table 3.4.

Locations of each long bone measurement were chosen based on numerous criteria. All major postcranial long bones were included to provide a comprehensive observation with regard to where metric changes were taking place, if any were

detected. The articular ends (proximal and distal) were both measured based on their importance as joint surfaces and recipients of stress throughout the various decades of life. It was determined that if changes with age were occurring, these changes may be observable in these articular joint surfaces. Maximum midshaft diameters of all long bones were collected based on past research indicating that cortical thickness changes with age, medullary cavities expand with age, and the combination of these traits possibly contributing to an increase in the diameter of long bones (Epker *et al.*; Jowsey 1960; Thompson 1980). Midshaft circumferences of tubular long bones (humerus and femur) were collected for the same reason. It is also these measurements (articular ends and midshaft circumferences) that have been shown to be most dimorphic when using metrics – e.g., in those discriminant function formulae. These locations are the sites that are most sexually dimorphic and may change with age, thus influencing the accuracy of developed formulae.

Overall, the reasoning behind the choice of long bone measurement sites was largely due to logical deductions in regard to where skeletal changes may be taking place. Past research indicated that joint surfaces might be adversely affected (with a result of net bone gain or loss) in the advancement of age in humans. The details of each long bone measurement are shown in Figures 3.17 - 3.24. Data on left bones were used for analysis.

3.3

Statistical analysis of metric and non-metric data

Statistics are defined as "a quantitative characteristic of a sample" (Slitor, 1987). Statistical analyses are ways of discriminating between and within groups or samples. If an individual is to be classified into a defined group based on certain measurements, they must be compared to a known sample and placed with a certain amount of accuracy into the most-correct group based on these variables. Basic

descriptive statistics, including means, standard deviations, and ranges were done for all metric data. Definitions of each are as follows:

Mean: the average of the data set. The mean is equal to the sum of the measurements divided by the number of measurements.

Standard deviation: a measure of variability or variation when considering all data. The standard deviation is calculated by finding the mean, calculating the deviation from the mean for each observation, squaring these deviations, averaging the squared deviations, and taking the square root of this average (Slitor, 1987). This is essentially equal to the positive square root of the variance. It is a measure of the dispersion of the frequency distribution, or a statistical measure of the spread or variability between a group of measurements.

Range: the difference between the highest and the lowest values in the data set of measurements. The range provides the extreme variation in the sample.

An analysis of variance (ANOVA) was also computed for all metric data to observe irregularity between elements of the sample. Analysis of variance is a procedure that computes the amount of variability attributed to each one of a variety of components. Specifically, it compares the means of two or more groups of subjects that vary on a single independent variable (Cronk 1999). ANOVA can also be described as the measurement of distance between individual distributions.

In this case, groups with categorized metric means were defined as "male" and "female", while the single independent variable in which they vary was the measurement provided. A one-way ANOVA comparing male metric data and female metric data was computed. A significance value (F-ratio) was provided by this analysis, and from this value an assessment of the variability between two groups (e.g., male and female) was determined. Theoretically, as the F-ratio goes up, the p-value goes down (i.e., more confidence there is a difference between the male and female means). If the F-ratio is large (much greater than 1), it suggests that a possible group effect exists.

The p-value is a probability with a value ranging from zero to one. A p-value is a measure of how much evidence there is against the null hypothesis. The smaller the p-value, the more evidence against the null hypothesis (and the larger the F-ratio). The general rule is that a small p-value is evidence against the null hypothesis, while a large p-value means little or no evidence against the null hypothesis (Kendall and Stuart 1979). Traditionally, researchers will reject the null hypothesis if the p-value is less than 0.05.

The comparison of groups followed a progression of analysis set forth to observe all possible variations in skeletal change between assemblages. All females and all males in the study sample were first compared to establish that a size component existed between the two. This is a common observation seen in all populations, in which males are metrically larger than their female counterparts.

Second, males and females were separated into population categories and compared, e.g., white males were compared to white females; black males were compared to black females. This comparison was performed to confirm that this sexually dimorphic size difference not only occurred when the populations were pooled, but when the populations were separated as well. Information on the relative size of each population was also obtained from this comparison.

Third, females were separated into the two groups ("black females" and "white females"), and their measurements were compared. This comparison was performed in an effort to possibly pool the two groups if they resembled each other metrically.

The metric means of young females (50 years of age and under) were compared to the metric means of old females (over 50 years of age) for each skeletal measurement site, and for both groups. If a statistically significant increase or decrease was observed with the onset of age at a particular skeletal measurement site, this site was compared to the equivalent metric mean for the corresponding male population. For example, if the diameter of the head of the humerus increased

significantly with the onset of age in white females, then the humeral head diameter mean for old white females would be compared to the mean humeral head diameter of old white males to determine if any metric overlap of data existed at this skeletal site.

This progression of analysis repeated itself with the male sample. Males were separated, and the metric means of young males (50 years of age and under) were compared to the metric means of old males (over 50 years of age) for each skeletal measurement site. If a statistically significant change with age occurred (either a decrease or an increase in metric size) this metric mean was compared to the corresponding female metric mean to determine if overlap existed between the sexes. These observations provided information on the increase or decrease of robusticity in the skeletal measurement location, which could be extrapolated as an increase or decrease in sexual dimorphism.

To test for intra-observer repeatability in the metric analysis, 15 male specimens and 15 female specimens were randomly selected and re-measured after all initial data was collected. The repeated metric data was statistically compared to the original data set using a one-way analysis of variance (ANOVA).

To test for inter-observer repeatability, 30 specimens were once again selected and an independent observer re-measured several long bone sites (four from the humerus) and all four pelvic measurements. The independent observer was someone not involved in the study, but who had limited experience with metric analysis. Measurement techniques were described and reviewed with the observer. This metric data collected by the observer was statistically compared to the original dataset using a one-way ANOVA.

Pearson's chi square test was performed initially on all nonparametric data of the humerus and os coxae to establish association and significance between variables. A chi square test uses nominal scale data to compare samples to theoretical distributions, and assess relationships between nominal variables. It can

also be described as a measure of agreement between the observed and expected values (Butler 2000). This statistic is more likely to establish evidence that (1) the relationship is strong (or weak), (2) the sample size is large, and/or (3) the number of values of the two associated variables is large. Statisticians commonly interpret a chi square probability of 0.05 or less as justification for rejecting the null hypothesis. This implies that the one variable is unrelated (that is, only randomly related) to another variable.

After significance between groups (males vs. females, black males vs. black females, white males vs. white females) was determined, a comparison of young and old individuals in a specific sex-population affiliation was performed to determine if a significant decline in the classification accuracy was present, i.e., if the accuracy in predicting sex from a certain skeletal feature decreased with the onset of advanced age.

3.4

Data collection for geometric morphometric analysis

The sample size used for geometric morphometric analysis was set at 50 individuals of each age, ancestry, and sex group. The ideal total sample size was 400 specimens (50 per age/ ancestry group) for a geometric morphometric examination of four sexually dimorphic features. The Pretoria Bone Collection and the Raymond Dart Skeletal collection combined provided an amalgamation of young and old individuals. The reality of both skeletal collections, however, is that they house a disproportionate amount of older individuals, whose population falls within the "black" category. The geometric morphometric analyses were performed regardless of this fact and based on the assumption that any amount of data on young individuals would make the study valuable.

When all data was collected and all digital images captured, young white females were the least represented (n=13) followed by young white males (n=24). Young black males (n=57) and young black females (n=50) supplemented the data sufficiently to provide insight regarding common morphology in young individuals.

Standardized landmarks were chosen for four two-dimensional views for geometric morphometric analyses. Two views of the humerus were used; a two-dimensional perspective of the distal and inferior humerus which documented the angle of the medial epicondyle (referred to as "EPI") and a two-dimensional perspective of the distal and posterior humerus which documented the olecranon fossa shape and trochlear extension (referred to as "OL"). Two views of the os coxae were used; a two-dimensional representation of the subpubic angle and subpubic concavity (referred to as "SUB") and a two-dimensional perspective of the greater sciatic notch (referred to as "SCI"). Each of the four perspectives was utilized in order to quantify shape and form differences observed in these features. Definitions of each feature are listed below:

- **EPI:** this view captured the distinct feature of the medial epicondylar angle from the inferior aspect of the humerus.

- **OL**: this view captured features specifically of the distal and posterior humeral aspect. It included the olecranon fossa shape and trochlear extension, thus corresponding to two non-metric visual traits.

- **SUB**: this view captured pelvic features such as the subpubic concavity and the subpubic angle, two characteristics that directly corresponded to non-metric visual traits were observed. It also provided information on the shape of the obturator foramen. Obturator foramen landmarks were chosen

because this skeletal feature's centralized location within the two-dimensional perspective, and its relationship to other landmarks that were difficult to assign without using corresponding points from the foramen.

- **SCI:** this view captured the anatomy and morphology of the greater sciatic notch.

Because each of the four views was considerably different from each other, standardization of bone positioning and landmarks will be described separately. Figures 3.25 - 3.28 depict the anatomical locations of homologous landmarks chosen for geometric morphometric analysis.

As documented in Appendix B-I (the specimens utilized for each sex and ancestry group) the number of actual digital photographs for each view varied for several reasons. The original goal of the study was to create digital images of 50 specimens per group, resulting in 400 photographs total. All specimens were chosen randomly, and not based on past knowledge of the skeletal sample. Because of this random selection of specimens from the collection, numerous individuals in the study exhibited damage, degradation, or the absence of specific element features required to capture a digital image. Thus, one specimen may have both images of the distal humerus present, but only one image of the os coxa present due to the degradation of the pubis or the absence of the ischium. Osseous elements used for geometric morphometrics must be placed in a standardized position for each digital image taken. In order to achieve a controlled position for the bone, the same specific procedure was used, depending on which perspective was being photographed.

3.4.1

Image capture of the EPI view of the humerus

The left humerus was placed on grid paper on an osteometric board with the posterior side facing upwards. The superior surface of the humeral head and greater tubercle touched the upper left-hand-corners of the osteometric board. The distal end of the humerus was then aligned along a grid paper axis to place the trochlear constriction (the indentation made between the capitulum and the trochlea) in a standardized location, 11 centimetres to the right of the left margin of the osteometric board. This was to eliminate the variation of curvature that exists in this element (which was not an important characteristic to capture). The camera lens was at a perpendicular angle to the bone surface.

Photographs were taken of the inferior "spool" feature of the distal humerus with a Cannon SureShot 95 digital camera. The camera was placed in a fixed position in front of the inferior feature, 60 centimetres from the top margin of the osteometric board. A reference number corresponding to the specimen number was placed in the image for consistency in image file maintenance. The viewfinder was focused on the middle of the bone and the image filled the frame at all times. The captured images were saved and recorded with reference numbers onto a computer, and 19 homologous landmarks were assigned to features for geometric morphometric analysis.

Landmarks were chosen to mirror the morphology observed in the visual techniques used for the non-metric portion of this study. Nineteen distinct points along the surface of the inferior humerus were chosen to best characterize the form of this skeletal element. The captured images were entered into a computer and the 19 landmarks were assigned to each humerus to use for geometric morphometric analysis. The program tpsDig allowed for the assignment of each homologous landmark chosen. The landmarks assigned were as follows (see Figure 3.25):

- Landmark 1 was the medial margin of the lateral epicondyle, on top of the ridge of bone that constitutes the posterior surface of the capitulum.

- Landmark 2 was situated halfway between Landmark 1 and Landmark 3
- Landmark 3 was the lowest portion of the posterior spool, which constituted the inferior margin of the olecranon fossa.
- Landmark 4 was halfway between Landmark 3 and Landmark 5.
- Landmark 5 was the most superior point of the medial margin/ ridge of the posterior trochlea.
- Landmark 6 was the superior "root" of the medial epicondyle; where the posterior edge of the medial epicondyle meets the vertical ridge of the trochlea.
- Landmark 7 was halfway between Landmark 6 and Landmark 8.
- Landmark 8 was halfway between Landmark 7 and Landmark 9.
- Landmark 9 was halfway between Landmark 8 and Landmark 10.
- Landmark 10 was the most medial point on the medial epicondyle.
- Landmark 11 was halfway between Landmark 10 and Landmark 12.
- Landmark 12 was halfway between Landmark 11 and Landmark 13.
- Landmark 13 was halfway between Landmark 12 and Landmark 14.
- Landmark 14 was the inferior "root" of the medial epicondyle; where the inferior edge of the medial epicondyle meets the vertical ridge of the trochlea.
- Landmark 15 was the inferior edge of trochlea. This landmark was placed where the straight vertical edge of the trochlea becomes curved again.
- Landmark16 was the most constricted point on the anterior trochlear "spool".
- Landmark 17 was the most constricted point on the anterior capitulum "spool".
- Landmark 18 was the inferior border of the capitulum. This landmark was placed on the point where the curved edge becomes a distinct ridge.
- Landmark 19 was the lateral-most point of the lateral epicondyle.

Landmarks 7 through 19 and 11 through 13 were based around Landmarks 6, 10, and 14 (the fixed, unambiguous locations on the medial epicondyle). Landmarks

7 through 9 and 11 through 13 should be an approximately equal distance from one to another. These landmarks cannot be exactly equidistant, as it is not possible to assign equidistant landmarks on a curved surface with no border except "superior" root and "inferior" root. These landmarks were assigned based on the supposition that a landmark placed consistently along the surface of the medial epicondyle would correctly record its general form and angle.

3.4.2

Image capture of the OL view of the humerus

The humerus was placed on graph paper on an osteometric board with the posterior side facing upwards. The superior surface of the humeral head and greater tubercle touched the upper left-hand-corners of the osteometric board, as in the previous perspective, "EPI". The distal end of the humerus was then aligned along a grid paper axis to place the trochlear constriction in a standardized location, 11 centimetres to the right of the left margin of the osteometric board. This ensured that the inferior edges of the trochlea and capitulum were correctly aligned with each other.

Images were captured with the Canon SureShot 95 digital camera mounted on a small tripod 30 centimetres above the surface of the bone. A reference number corresponding to the specimen number was placed in the image for consistency in image file maintenance. The image filled the frame each time an image was captured. The captured images were entered into a computer and the 15 landmarks were assigned to each humerus to use for geometric morphometric analysis. The program tpsDig allowed for the assignment of each homologous landmark chosen. These distinct points along the surface of the distal and posterior humerus were chosen to best characterize the form of this skeletal element. The landmarks assigned were as follows (see Figure 3.26):

- Landmark 1 was placed on the supra-condylar ridge, aligned with the superior margin of the olecranon fossa. The grid paper placed underneath the bone was used to assist in assigning this landmark, based on a grid line's linear progression across the bone, which most accurately showed the positioning of the upper margin of the olecranon fossa.
- Landmark 2 was the medial ridge of the humerus, placed on the supra-condylar ridge, aligned with the superior margin of the olecranon fossa.
- Landmark 3 was the most lateral point of olecranon fossa seen on the posterior surface. This landmark was not placed within the fossa itself, but on the lateral edge of the fossa.
- Landmark 4 was the most medial point of the olecranon fossa, also placed on the surface of the bone as opposed to within the fossa itself.
- Landmark 5 was the most superior point of the olecranon fossa.
- Landmark 6 was the inferior edge of olecranon fossa, directly in the middle. This landmark was placed halfway between landmark 3 and 4, and was placed on the smooth bone "ridge" that begins there.
- Landmark 7 was halfway between Landmark 3 and Landmark 5.
- Landmark 8 was halfway between Landmark 4 and Landmark 5.
- Landmark 9 was halfway between Landmark 3 and Landmark 6, on the smooth bone "ridge" that begins in this location.
- Landmark 10 was halfway between Landmark 4 and Landmark 6, where the smooth edge of bone begins in this location.
- Landmark 11 was the most lateral edge of the lateral epicondyle.
- Landmark 12 was the most medial point on the medial epicondyle.
- Landmark 13 was the inferior edge of capitulum, at the point of the where the curved edge becomes a distinct ridge.
- Landmark 14 was the most constricted point of the posterior trochlear "spool".

- Landmark 15 was the inferior edge of trochlea, at the junction where the straight ridge became curved.

3.4.3

Image capture for the SUB view of the os coxa

An osteometric board with grid paper along both the flat surface and along the short vertical surface was used to place the left os coxa into position to capture the form of the subpubic angle and subpubic concavity. The superior margin of the iliac crest was placed against the long vertical edge of the osteometric board, while the edge of the acetabulum that aligns with the pubis was placed against the short vertical edge of the osteometric board. This, in turn, placed the entire pubic region against the short vertical edge. The bone rested on the posterior inferior iliac spine and the medial surface of the ischium, as well as the posterior edge of the acetabulum.

Images were captured with the Canon SureShot 95 digital camera. The camera was placed in a fixed position in front of the pelvis, 60 centimetres from the top margin of the osteometric board. The right edge of the camera was placed 19 centimetres to the left of the long right vertical edge of the osteometric board to standardize the position of the image. A reference number corresponding to the specimen number was placed in the image for consistency in image file maintenance. The image filled the frame each time.

Twenty-eight distinct points along the surface of the pubis, ischium, and obturator foramen were chosen to best characterize the form of this skeletal element. Landmarks 1 through 13 are along the interior border of the obturator foramen. The landmarks assigned were as follows (see Figure 3.27):

- Landmark 1 was the junction where the body of the pubis meets the obturator groove. This point is indicated by a visible “overlap” of bone.

- Landmark 2 was the lowest point of the obturator foramen. A linear junction on the grid paper assisted in the assignment of this landmark.
- Landmark 3 was the highest point, or "apex" of the obturator foramen.
- Landmark 4 was the narrowest point on the superior ventral margin of the obturator foramen.
- Landmark 5 was halfway between Landmark 2 and Landmark 4.
- Landmark 6 was halfway between Landmark 1 and Landmark 2.
- Landmark 7 was halfway between Landmark 1 and Landmark 3.
- Landmark 8 was halfway between Landmark 3 and Landmark 4.
- Landmark 9 was halfway between Landmark 4 and Landmark 5.
- Landmarks 10 and 11 were two points spaced evenly between Landmarks 2 and 5, Landmark 10 placed superiorly, Landmark 11 placed inferiorly.
- Landmark 12 was halfway between Landmark 2 and Landmark 6.
- Landmark 13 was halfway between Landmark 1 and Landmark 6.
- Landmark 14 was the superior edge of the pubis, positioned at a 45-degree angle from Landmark 1.
- Landmark 15 was the superior edge of pubic symphysis.
- Landmark 16 was halfway between Landmark 14 and Landmark 15.
- Landmark 17 was halfway between Landmark 14 and Landmark 16.
- Landmark 18 was halfway between Landmark 15 and Landmark 16.
- Landmark 19 was the most inferior edge of pubis. This location may or may not be the edge of pubic symphysis.
- Landmark 20 was halfway between Landmark 15 and Landmark 19.
- Landmark 21 was the shortest distance from landmark 4 on the ischial surface. This could also be considered the thinnest portion of the ischium.
- Landmark 22 was a point directly across from landmark 2 on a horizontal plane. The placement of the vertical grid paper was used for guidance in assigning this point.

- Landmark 23 was halfway between Landmark 19 and Landmark 21.
- Landmark 24 was halfway between Landmark 21 and Landmark 22.
- Landmark 25 was halfway between Landmark 19 and Landmark 23.
- Landmark 26 was halfway between Landmark 21 and Landmark 23.
- Landmark 27 was halfway between Landmark 21 and Landmark 24.
- Landmark 28 was halfway between Landmark 22 and Landmark 24.

Eighteen of the 28 landmarks assigned to this view were based on placing these locations between each other or between two fixed landmarks used as foundational points of morphology. These landmarks cannot be exactly equidistant, as it is not possible to assign equidistant landmarks on a curved surface with no border except "most superior edge" and "most inferior edge". These landmarks were assigned based on the theory that a landmark placed consistently along the surface of the ischium would correctly record its general form and curvature.

3.4.4

Image capture of the SCI view of the os coxa

The position of the left pelvic bone did not change from the "SUB" view to the "SCI" view; only the position and angle of camera were altered to capture the features of the greater sciatic notch. Thus, the superior margin of the iliac crest was again placed against the long vertical edge of the osteometric board, while the edge of the acetabulum that aligns with the pubis was placed against the short vertical edge of the osteometric board. The bone rested on the posterior inferior iliac spine and the medial surface of the ischium, as well as the posterior edge of the acetabulum.

Images were captured with the Canon SureShot 95 digital camera, which was mounted on a small tripod 40 centimetres above the bone's surface. A reference number corresponding to the specimen number was placed in the image for

consistency in image file maintenance. The image of the greater sciatic notch filled the frame each time an image was captured.

Landmarks were chosen based on past geometric morphometric studies (Steyn *et al.* 2004), and mirrored the morphology observed in the visual techniques used for the non-metric portion of this study. The landmarks assigned were as follows (see Figure 3.28):

- Landmark 1 was the most projecting point of the spina ischiadica, or inferior ischial spine.
- Landmark 2 was the point of maximum curvature of the greater sciatic notch.
- Landmark 3 was the end of the sciatic notch before the bone curves backwards towards the auricular surface.
- Landmark 4 was halfway between Landmark 2 and Landmark 3.

Landmark 5 was halfway between Landmark 1 and Landmark 2.

3.5

Statistical analysis of geometric morphometric data

The entire dataset for each view (EPI, OL, SUB and SCI) was divided first into subgroups of two, namely males (M) and females (F) to initially provide evidence of morphological differences between the sexes. Second, the dataset was separated into four different subgroups; young females (YF), old females (OF), young males (YM), and old males (OM). This was to illuminate differences with the onset of age between members of the same sex group, i.e., young females and old females. Finally, a third set of eight subgroups was created to visualize potential changes with the onset of age between populations. These subgroups were categorized as young black females (YBF), old black females (OBF), young white females (YWF), old white females (OWF), young black males (YBM), old black males (OBM), young white males (YWM), and old white males (OWM).

The homologous landmarks for each perspective were assigned on the digitized images of the distal humerus and os coxae using the program tpsDig (defined below). Generalized least-squares Procrustes analysis was used to compute the average shape for each sample (Hennessy and Stringer 2002; Rohlf 2000; Loy *et al.* 1999). Landmarks were then used to perform geometric morphometric analyses on each of the four perspectives in a series of steps, based on the tps program **tpsDig**, (FJ Rohlf, Version 1.31), **tpsSplin** (FJ Rohlf, Version 1.14), **tpsRelw** (FJ Rohlf, Version 1.25), **CoorGen**, **CVAGen6- IMP**, and **TwoGroup6-IMP** (Sheets 2001).

- **tpsDig:**

The standardized landmarks (described above) were digitized using tpsDig. The tpsDig-program makes collection and maintenance of landmark data from digitized images simpler. The program also creates statistical results from landmark data. It is used to indicate the position of landmarks in an initial file and creates specific, discrete file names containing the images of specimens. The data is saved as tps data-files and these files are then used with the other tps-programs (e.g., tpsSplin and tpsRelw) (Slice *et al.* 2005).

In order to study the shape differences between groups, the average, or consensus configuration of landmarks for each of these two groups (males and females) was computed using tpsSplin. From this it was possible to visually assess whether any differences existed between the males and females for each view.

- **tpsSplin:**

The tpsSplin-program is used to compare the same homologous landmarks in different specimens by utilizing thin-plate spline transformations. Principal and partial warps were also created and used. A preliminary reference shape is produced; this is the average shape of the entire sample population, and is

designated by a precise perpendicular grid pattern exhibiting no deformations of 90-degree angles with the homologous landmarks included. The thin-plate splines for each specimen illustrate the deformation (or incongruence) of this grid. Deformation grids of the consensus configurations of the groups made it possible to determine where the variation was for each perspective. The consensus thin-plate splines were also viewed in "vector mode" to determine which landmarks were responsible for the greatest amount of variation. In other words, vector thin-plate splines indicate where and by how much the landmarks of two specimens in the sample group differ from each other (Scholtz 2006).

- **tpsRelw:**

Differences in shape were determined and analyzed using tpsRelw. This program facilitates the statistical analysis of geometric morphometric landmark data by showing the distribution of specimens within the groups that are to be compared to each other (e.g., young males and old males) in order to scrutinize intra-sample distinctions. This is presented in graph form to make the representation of any variation between groups in a sample population possible to visualize.

The Relative Warp Analysis (RWA) was performed in order to determine general trends in shape between the two sexes and with the onset of age. From this analysis it was possible to see whether a definite separation between the male and female dataset existed or whether there was no clear distinction between the shape of the two sexes.

- **CoordGen:**

The CoordGen-program was used to translate tps data-files to "Bookstein's Coordinates" (or BC) format which is subsequently used with other programs in the IMP package (e.g. CVAGen6 and TwoGroup). Bookstein's Coordinates are described as an arrangement of shape coordinates consisting of a compilation of

landmarks "1, 2...15" whose structures have been rescaled to a standardized scale. Thus, landmarks 1 and 2 are fixed at (0, 0) and (1, 0) respectively, in a Cartesian coordinate system (Sheets 2001). This is used for two-dimensional data.

- **CVAGen6:**

Statistically significant differences were determined between each group by a discriminant function analysis (or CVA) using CVAGen6-IMP. A Canonical Variates Analysis assesses the ability to correctly classify random, individual specimens in a dataset to groups (e.g. male or female), rather than asking if the two groups merely have a different shape. This program feature is crucial in determining the power or robusticity of the predictive power from a certain morphological feature. The program computes partial warp scores to a common reference, and determines how many CVA axes there are in the data at a p=0.05 level of significance and computes the canonical variate scores of all specimens entered (Sheets 2001).

CVAGen6 generates a plot signifying the similarities or differences in "clusters" of landmarks from specimens of different groups. Groups of specimens may either be tightly clustered together and distinct from one another when observing the CVA plot, or be dispersed exhibiting homogeneity. This clustering or dispersal is indicative of variation between groups. The program then generates a Canonical Variates Analysis-plot that shows whether any superimposition or overlay is present in the clusters of landmarks.

- **TwoGroup6:**

Determination of how each group "assembled" in a cluster of landmarks was performed using TwoGroup-program-IMP TwoGroup6. Then inter-group shape differences between the males and females were tested by these means. TwoGroup uses BC files to perform two-group comparisons in a sample population. The amount of overlap can be scrutinized to establish whether any variations are seen.

This program also uses Hotelling's T^2-test and Goodall's F-test to calculate p-values to determine the statistical significance, if any, of the morphological feature analyzed. Goodall's F-test specifically compares the Procrustes distance between the means of two samples to the amount of variation found in the samples (Scholtz 2006).

To test for intra-observer repeatability, 15 male specimens and 15 female specimens were randomly selected and re-assigned the above-described homologous landmarks for each of the four views of the humerus and os coxae. The repeated landmark data was statistically compared to the original data set using Hotelling's T^2-test and Goodall's' F-test of the TwoGroup program.

To test for inter-observer repeatability, the four views of the same 30 specimens were once again selected and an independent observer re-assigned the defined landmarks. The independent observer was someone not involved in the study, but who had experience with geometric morphometrics. The landmark data assigned by the observer was once again statistically compared to the original dataset using Hotelling's T^2-test and Goodall's F-test of the TwoGroup program.

Table 3.1: Frequency distribution of males and females in total sample size (N = 593).

Group	Male	Female
50 years old or younger("young")	151	79
Over 50 years old ("old")	253	110
Total	404	189

Table 3.2: Non-metric distal humerus characteristics for males and females.

Feature	Male	Female
Olecranon fossa shape:	The fossa appears roughly triangular	The fossa appears oval
Angle of the medial epicondyle:	The medial epicondyle extends parallel to the table (or exhibits a slight angle) placed posterior side up	The medial epicondyle clearly angles upwards away from the parallel plane of the tabletop surface when placed posterior side up
Medial epicondylar symmetry:	Medial epicondyle sits within the trochlear profile with an equal amount of trochlear bone surrounding it. Appears "symmetrical"	Medial epicondyle sits towards the posterior portion of the trochlear profile, creating asymmetry in the trochlear bone surrounding it
Trochlear extension:	Medial edge of the trochlea extends further distally than does the lateral edge	Distal extension of the medial and lateral edges of the female trochlea is almost equal; more symmetrical in shape

Table 3.3: Non-metric pelvic characteristics for males and females.

Feature	Male	Female
Length of subpubic concavity:	Short, stout curving surface with little to no distance between inferior of the pubic symphysis and beginning margin of the ischial surface	Laterally curving surface of some distance inferior to the pubic symphysis
Width of the subpubic angle:	Short and narrow, less than 90 degrees	Wide, flared and extended past a 90-degree angle
Width of the ischio-pubic ramus:	Thick and broad	Thin and narrow
Width of the greater sciatic notch:	Narrow, relatively short	Broad and wide-angled

Table 3.4: Descriptions of measurements taken on postcranial elements.

From:* Data Collection Procedures for Forensic Skeletal Material, *Moore-Jansen et al., 1994

Long bone	Measurement	Description
Humerus:	Maximum vertical diameter, head of the humerus	The direct distance between the most superior and inferior points on the border of the articular surface
	Maximum diameter of the humerus at midshaft	Measure of the midpoint of the humerus located a few millimetres below the inferior margin of the deltoid tuberosity
	Epicondylar breadth of the humerus	The distance of the most laterally protruding point on the lateral epicondyle from the corresponding projection of the medial epicondyle
	Midshaft circumference of the humerus	Circumference measurement at the same position as maximum diameter
Ulna:	Superior transverse diameter of the head of the ulna	Maximum diameter of the superior ulnar head, from the lateral margin to the outermost edge of the projection above the semilunar notch
	Medial transverse diameter of the head of the ulna	Maximum diameter of the ulnar head, from the deepest point of the semilunar notch to the deepest point on the surface of the coronoid process
	Inferior transverse diameter of the head of the ulna	Maximum diameter from the inferior margin of the radial notch to the most inferior margin of the coronoid process
	Maximum diameter of the ulna at midshaft	Maximum diameter of the ulnar diaphysis where the crest exhibits the greatest development
	Maximum distal diameter of the ulna	Maximum diameter measured along the inferior border, superior to the styloid process
	Olecranon-coronoid distance	Maximum distance from the most superior point of the anterior projection of the olecranon process to the anterior projection of the coronoid process
Radius:	Maximum diameter of the head of the radius	Maximum diameter of the circular head of the radius
	Maximum diameter of the radius at midshaft	Maximum diameter, whether measured in the sagittal plane or transversely
	Maximum distal diameter of the radius	Maximum diameter from the outermost projection of the styloid process to the outermost projection of the ulnar notch
Femur:	Maximum vertical diameter of the femoral head	Maximum diameter measured superior-to-inferior on the border of the articular surface
	Maximum diameter of the femur at midshaft	The maximum diameter, usually found as the anterio-posterior position, measured approximately at the midpoint of the diaphysis, at the highest elevation of the linea aspera. May be located at the medio-lateral margin
	Epicondylar breadth of the femur	The distance between the two most laterally projecting points on the epicondyles
	Circumference of the femur at midshaft	Circumference measured at the midshaft, same level of the sagittal and transverse diameters

Table 3.4 (continued)

Long bone	Measurement	Description
Tibia:	Maximum bicondylar breadth of the proximal tibia	The maximum distance between the two most laterally projecting points on the medial and lateral condyles of the proximal epiphysis
	Maximum diameter of the tibia at midshaft	The distance between the anterior crest and the posterior surface at the level of the nutrient foramen
	Maximum epiphyseal breadth of the distal tibia	The distance between the most medial point on the medial malleolus and the lateral surface of the distal epiphysis
Fibula:	Maximum diameter of the proximal fibula	The distance between the most lateral edge and most medial edge of the proximal epiphysis
	Maximum diameter of the fibula at midshaft	The maximum diameter at the midshaft, usually including the superior interosseous crest
	Maximum diameter of the distal fibula	The distance between the most lateral edge and the most medial edge of the distal epiphysis, usually including the edge of the lateral malleolus
Pelvis:	Maximum length of the pelvic bone	The distance between the top margin of the iliac crest and the margin of the pubic symphysis
	Maximum width of the pelvic bone	The distance between the medial and lateral edges of the iliac blades
	Ischio-pubic index	Pubis length x 100/ Ischium length. Pubis length is measured by placing spreading callipers on the superior tip of the pubic symphysis and the meeting point of the ischium and pubis within the acetabulum. This meeting point is visualized as an irregularity, a change in thickness of the bone, or a notch. Ischium length is measured by placing spreading callipers on the most inferior point of the ischial tuberosity to the convergence point within the acetabulum

Figure 3.1: Triangular olecranon fossa shape observed in males.

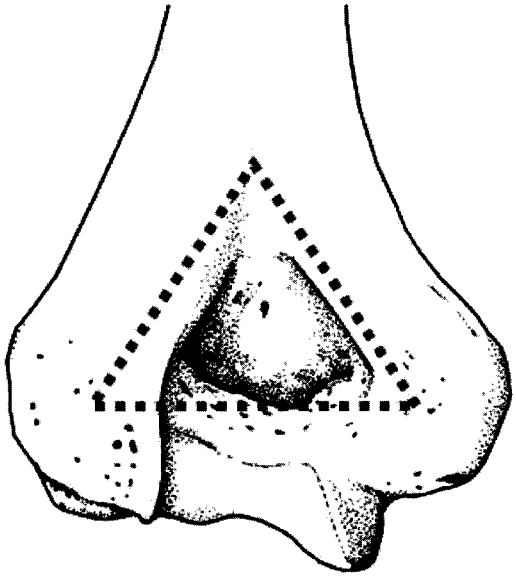

Figure 3.2: Oval olecranon fossa shape observed in females.

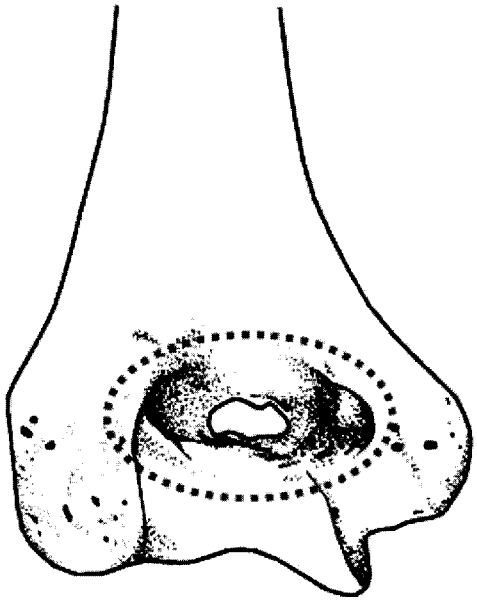

Figure 3.3: Angle of the medial epicondyle observed in males (humerus is posterior side up). The angle appears parallel to the table on which the humerus rests.

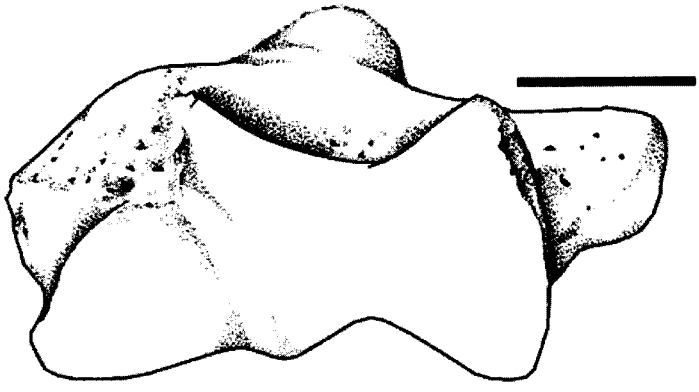

Figure 3.4: Angle of the medial epicondyle observed in females. The angle appears to project upwards from the table on which the humerus rests.

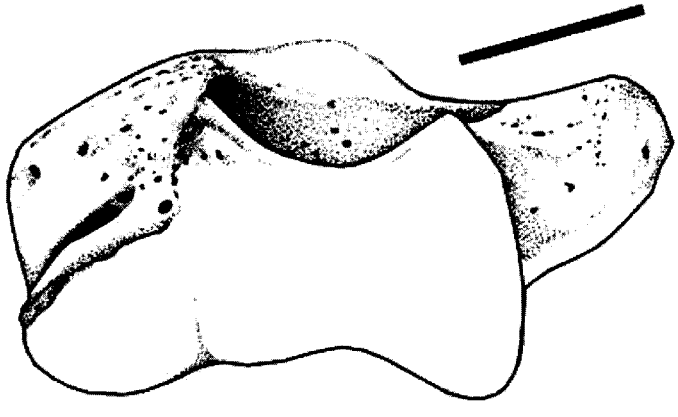

Figure 3.5: Medial epicondylar symmetry observed in males. The medial epicondyle sits centrally within the profile of the trochlea. Anterior surface is to the right.

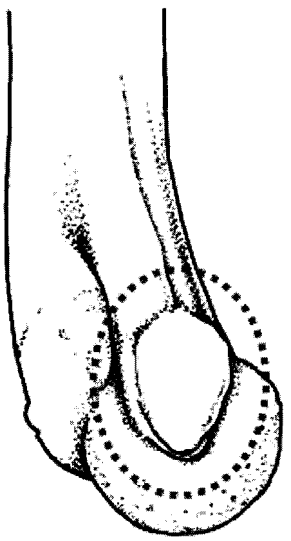

Figure 3.6: Medial epicondylar symmetry observed in females. The medial epicondyle sits posteriorly within the profile of the trochlea. Anterior surface is to the right.

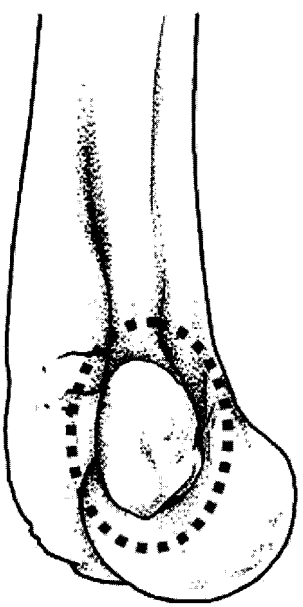

Figure 3.7: Trochlear extension observed in males. The trochlea extends well past the margin of the capitulum.

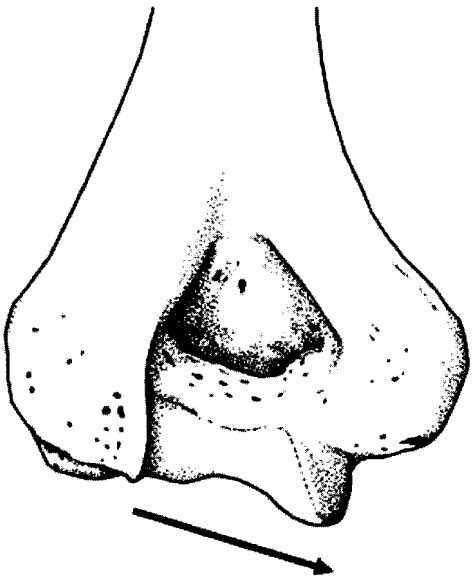

Figure 3.8: Trochlear extension/ relative symmetry observed in females. The trochlea is more symmetrical with the margin of the capitulum.

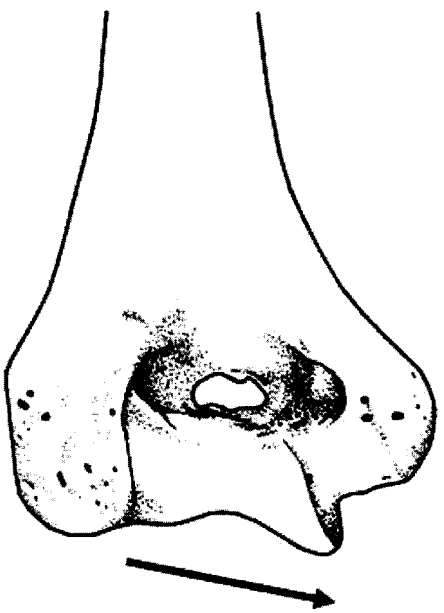

Figure 3.9: Length of the subpubic concavity as observed in males. The subpubic cavity has a short, stout curving surface.

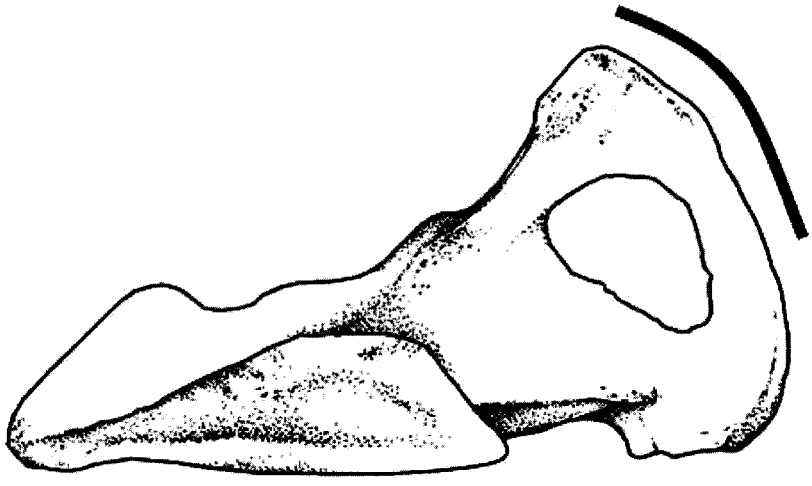

Figure 3.10: Length of the subpubic concavity as observed in females. The subpubic concavity has a long, rectangular-shaped curving surface.

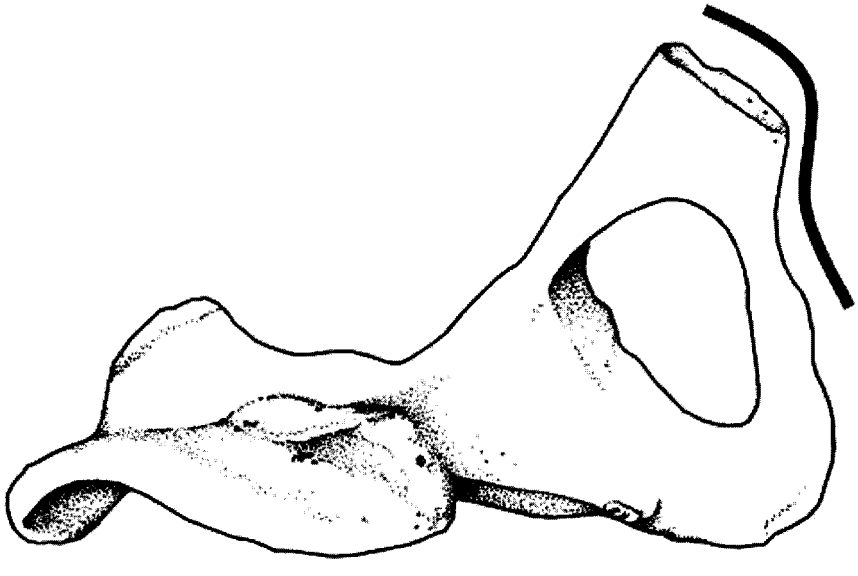

Figure 3.11: Width of the subpubic angle as seen in males. The subpubic angle is narrow.

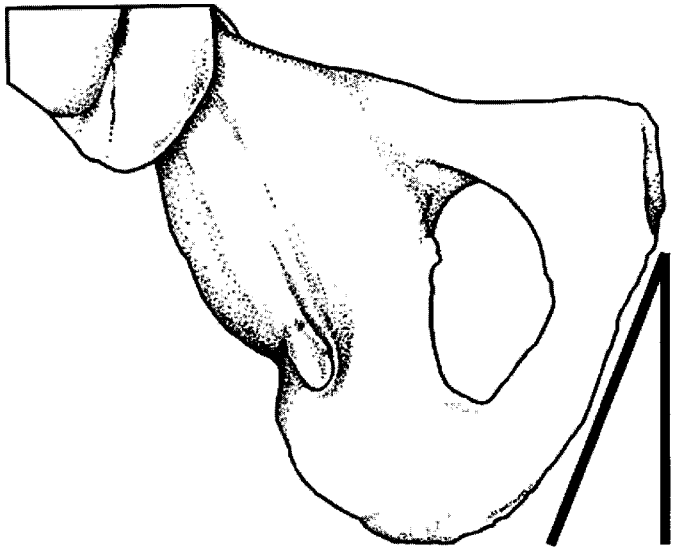

Figure 3.12: Width of the subpubic angle as seen in females. The subpubic angle is wide.

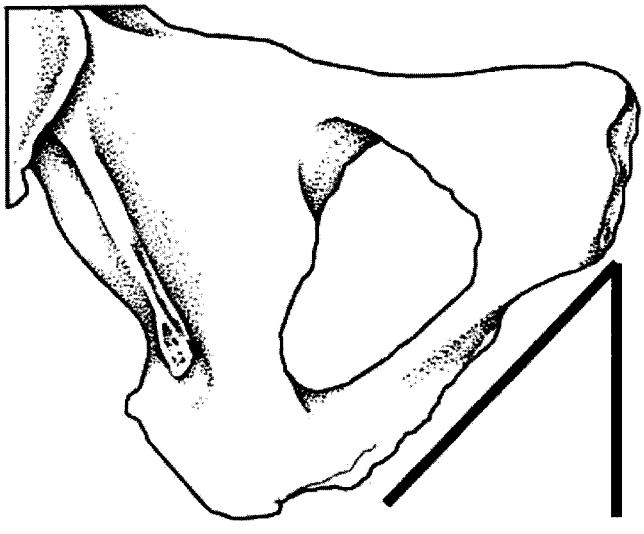

Figure 3.13: Ischiopubic ramus width as seen in males. The ramus width appears thick and broad.

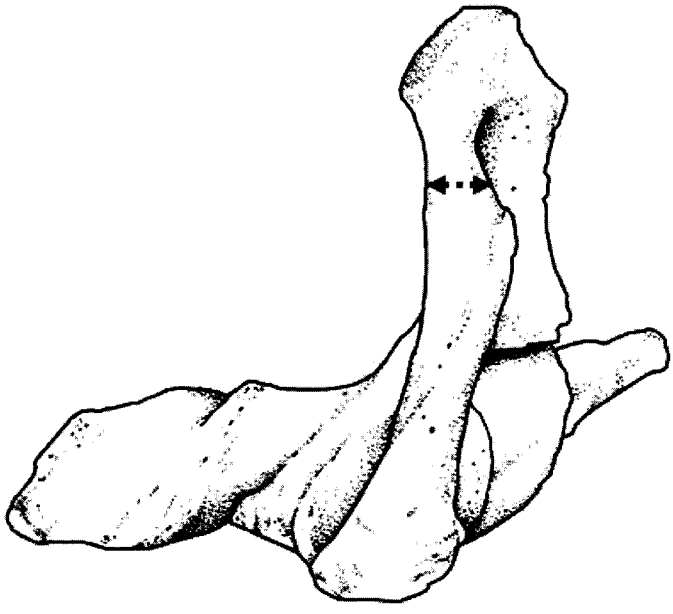

Figure 3.14: Ischiopubic ramus width as seen in females. The ramus width appears thin and gracile.

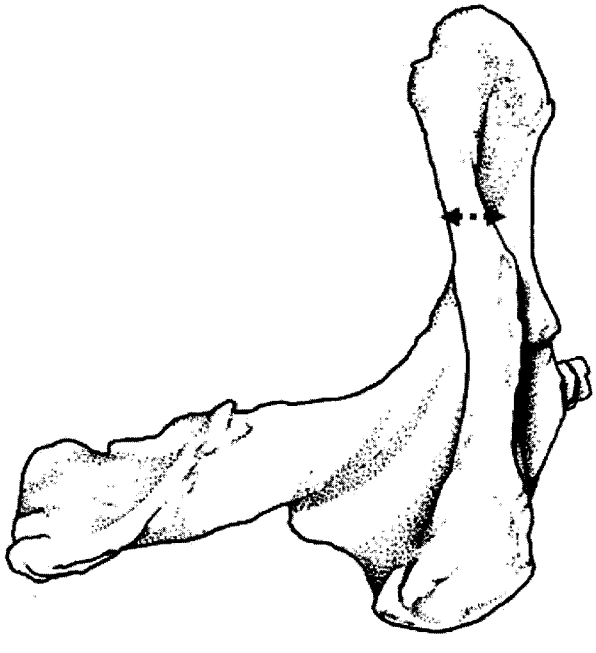

Figure 3.15: Greater sciatic notch width as seen in males. The greater sciatic notch appears narrow and compacted.

Figure 3.16: Greater sciatic notch width as seen in females. The greater sciatic notch appears wide and expansive.

Figure 3.17: Measurements of the humerus. a) maximum vertical diameter of the humeral head, b) maximum midshaft diameter, c) distal epicondylar breadth of the humerus.

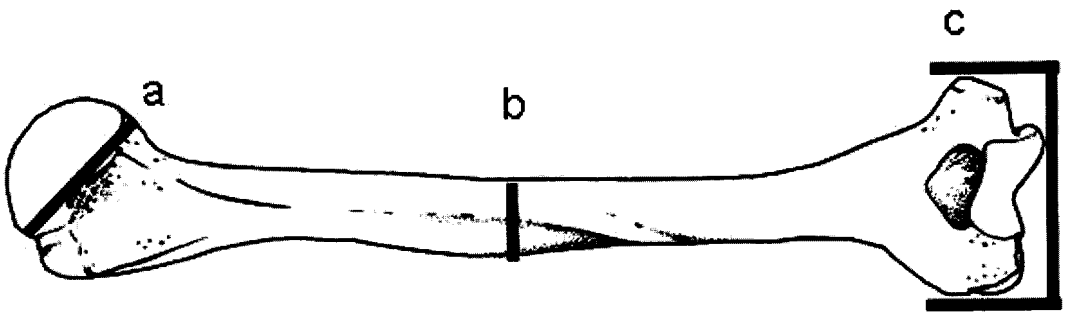

Figure 3.18: Measurements of the ulna. a) maximum superior ulnar head diameter, b) maximum medial ulnar head diameter, c) maximum inferior ulnar head diameter, d) maximum midshaft diameter, e) maximum distal diameter.

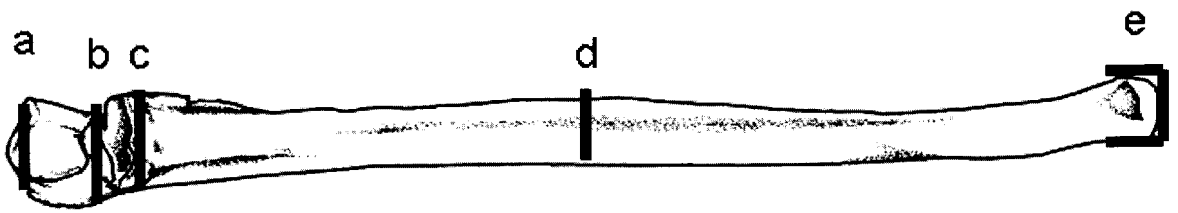

Figure 3.19: Measurements of the radius. a) maximum vertical diameter of the radial head, b) maximum midshaft diameter, c) distal breadth of the radius.

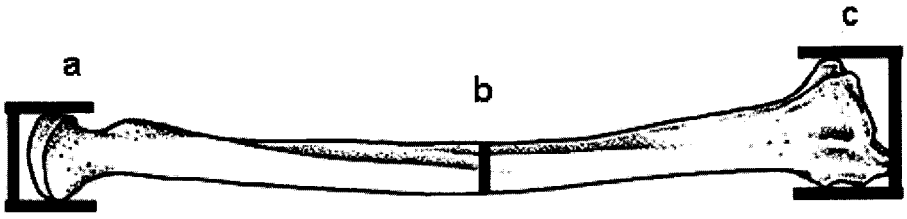

Figure 3.20: Measurements of the femur. a) maximum vertical diameter of the femoral head, b) maximum midshaft diameter, c) distal epicondylar breadth of the femur.

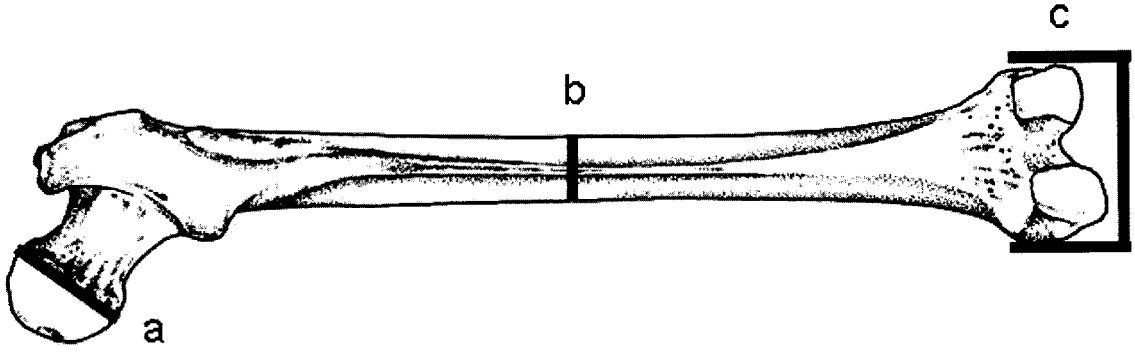

Figure 3.21: Measurements of the tibia. a) maximum bicondylar breadth of the tibia, b) maximum midshaft diameter, c) distal breadth of the tibia.

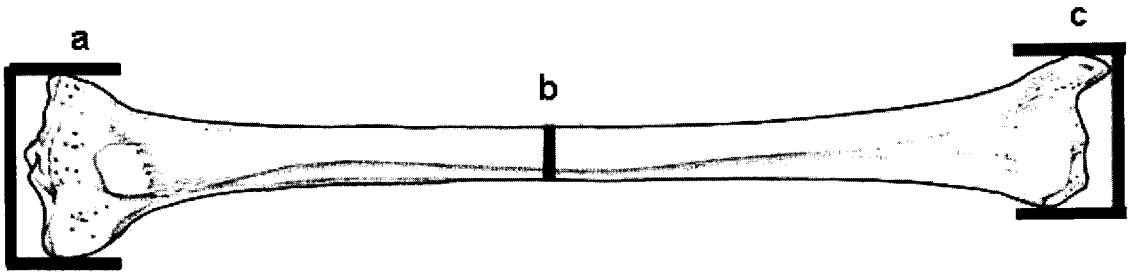

Figure 3.22: Measurements of the fibula. a) maximum diameter of the proximal fibula, b) maximum midshaft diameter, c) distal breadth of the fibula.

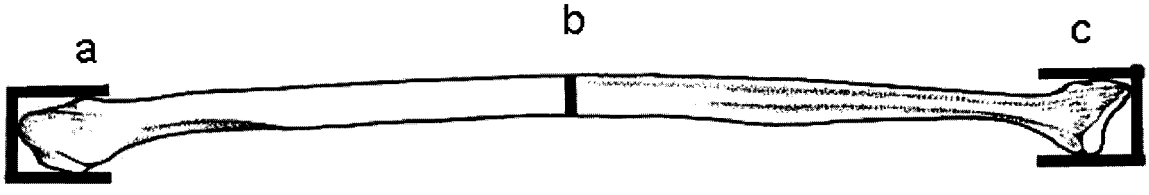

Figure 3.23: Measurements of the pelvis. a) maximum length, b) maximum breadth.

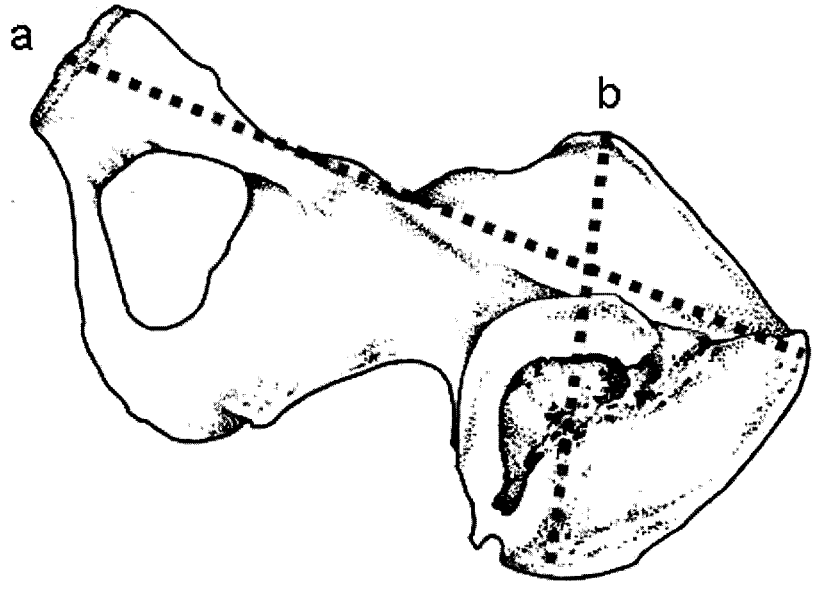

Figure 3.24: Measurements used to calculate the ischio-pubic index. a) pubis length, b) ischium length.

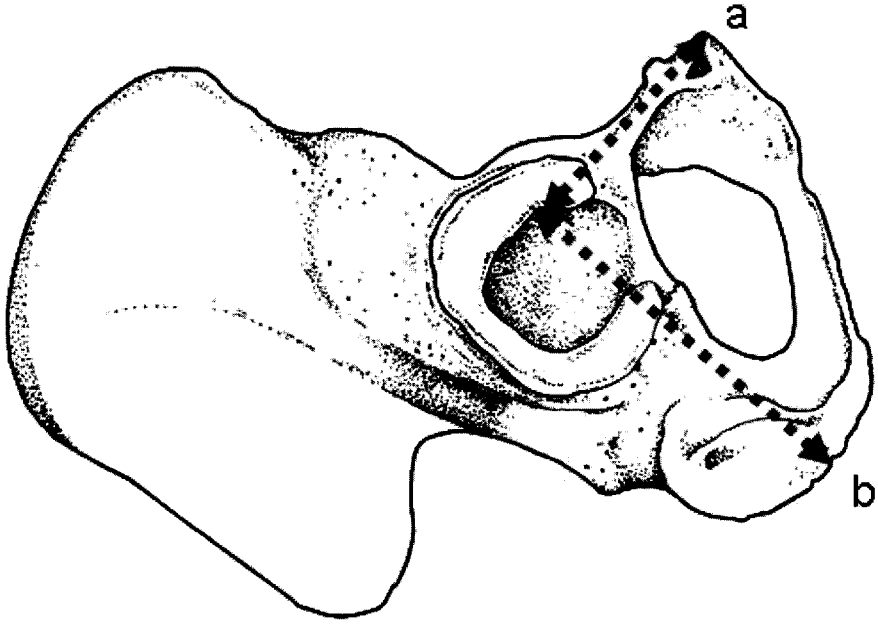

Figure 3.25: Homologous landmarks for the EPI view. See description of each landmark location in Section 3.4.1.

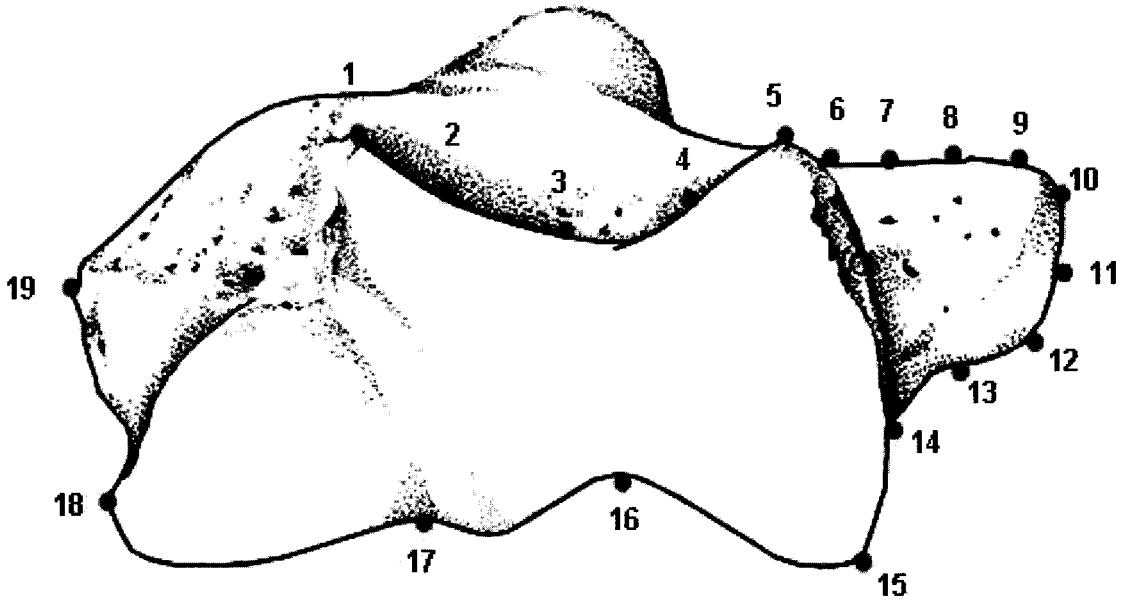

Figure 3.26: Homologous landmarks for the view OL. See description of each landmark location in Section 3.4.2.

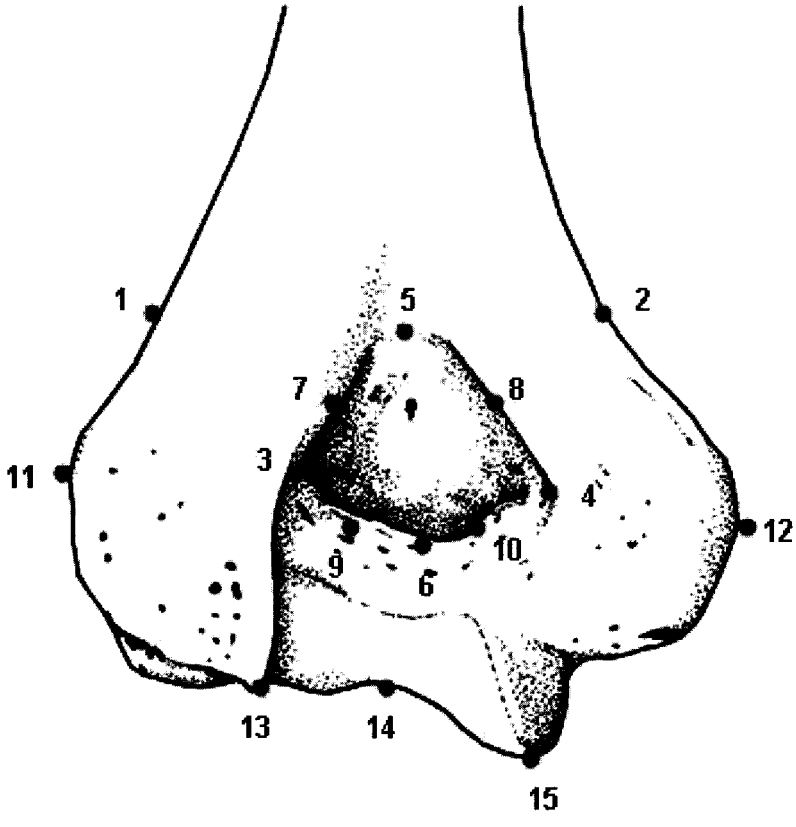

Figure 3.27: Homologous landmarks for the view SUB. See description of each landmark location in Section 3.4.3.

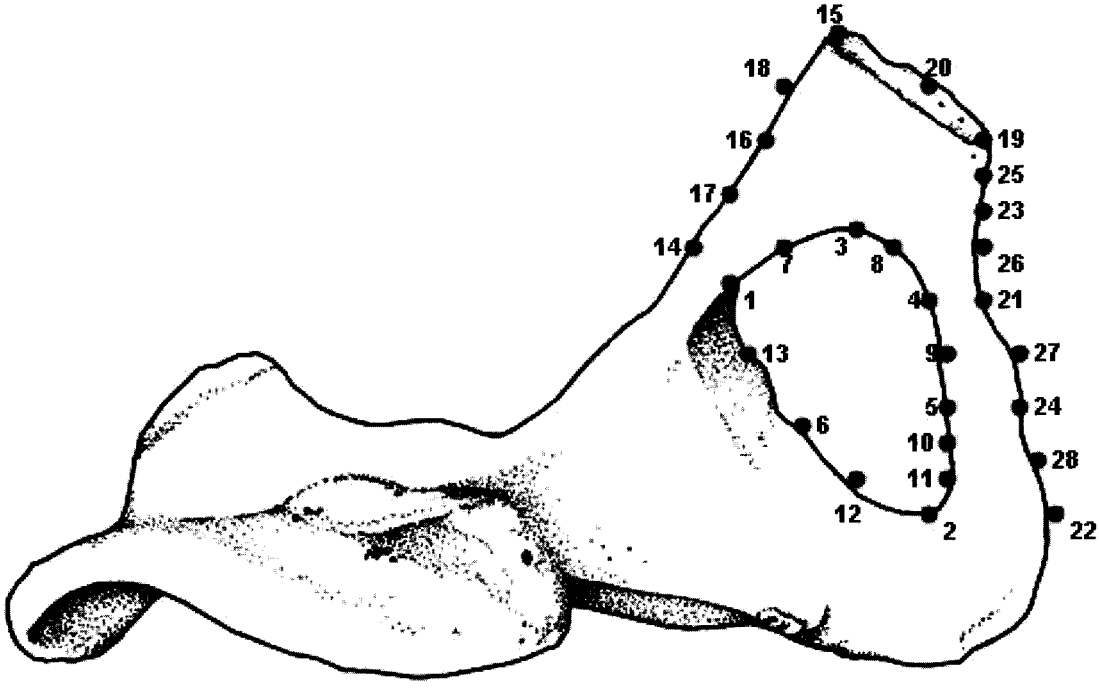

Figure 3.28: Homologous landmarks for the view SCI. See description of each landmark location in Section 3.4.4.

CHAPTER 4

RESULTS of METRIC ANALYSIS

The basis of this study was to use three distinct methodologies to test whether sexual dimorphism increases or decreases with the onset of advanced age. The first objective was to metrically compare males and females, and these metric analyses are summarized here.

Metric data was collected from 25 regions in the long bones of the postcranial skeleton and from the pelvis. One pelvic index (the ischio-pubic index) was also calculated. The dimensions were subjected to statistical analysis to determine the differences between groups. This was done in order to ascertain if significant differences do, indeed, exist among the sexes for the selected measurements. Data from the two different groups was then compared. White females were compared to black females, and white males compared to black males. If no significant differences were found, they were pooled into a "male" and "female" group. If, however, metric differences were found to be present, the two populations were kept separate for the remainder of the analysis.

Young and old individuals from the same sex were then compared. Each metric value from a skeletal trait that changed significantly from "young" to "old" was compared to the same skeletal metric value in the opposite sex. This was to clearly define the magnitude of changes that occurred at that site, and to visualize whether the male and female values were diverging upon each other. Age ranges were categorized into 10-year divisions to illuminate possible trends in size changes with the onset of incremental age.

4.1

Comparison of postcranial metric data: all populations

Descriptive statistics were first employed to determine if any difference in size was observed between males and females in the long bone measurements. The vast majority of past studies indicated that significant differences would be observed (e.g., Bass 1995; Holliday and Falsetti 1999; Holman 1991; Imrie 1958; King *et al.* 1998; Krogman 1962; Rother *et al.* 1977; White 2000). Table 4.1 summarizes the basic descriptive statistics, including standard deviation and standard error. The significance of differences between means was tested by ANOVA analysis, and were also indicated in the table. In this table, data from all males and females were pooled, regardless of their biological affiliation.

All male dimensions were larger than female dimensions. The F-value in Table 4.1 indicates the large distance between metric distributions of all males and females, which designated a clear and significant difference between the groups for all 23 measurements. All p-values, therefore, were at the level of <0.05, thus the distinct differences in size between males and females can once again be confirmed through this study. Inter-observer data exhibited virtually the same results, and statistical analyses were analogous to the original data analyses.

Intra-observer data collection exhibited similar results in measurement parameters. Representative samples of measurements were collected by an independent observer, and descriptive statistics in addition to ANOVA analysis were primarily analogous to the original data analyses. Pelvic measurements taken from the independent observer showed a smaller amount of variation between the sexes than found with the original researcher and the subsequent re-collection of measurements by the original researcher. See Appendix J for specific statistical results from the independent observer in metric analysis.

4.1.1

Comparison of postcranial metric data between sexes and populations

Males and females within different population affinities may also show marked sexual dimorphism in metric values, or may show a less distinct occurrence of sexually dimorphic metric traits, i.e., comparably similar in size dimensions. Because this study sample consisted of both black South African specimens and white South African specimens, each population was analyzed to observe the relative sexual dimorphism for each group.

Table 4.2 illustrates the differences between black South African males and females. The differences between males and females within this group are also significant on a statistically significant level. Sexual dimorphism was evident and manifested as, once again, males being metrically larger than females.

Table 4.3 illustrates the differences in measurements between white males and females for this sample population, with males appearing also to be dramatically larger than their female counterparts. Sexual dimorphism thus existed on a marked, statistically significant level in the both the black and white samples.

4.2

Comparison of female postcranial data between populations and age groups

Distinctions between populations within the categories of "male" and "female" were examined. An assessment was done in order to establish whether significant differences existed between the black and white South African populations. If not, they can be pooled, but otherwise should be kept separate in future analyses. Reiteration should be made, however, that population categories have always been regarded as a secondary consideration in this study. The division of "black female "," white female "," black male and "white male" were made only in an effort to attempt to

pool the aggregate data together, when and if they were shown to be statistically congruent with each other, i.e., the null hypothesis could be accepted and no differences existed. The metric data of black females were therefore compared to that of white females and differences noted where applicable. Comparison of the descriptive statistics (mean, standard deviation, ranges between minimum and maximum measurements) illustrated distinct differences between the population categories of "black" and "white" within the female population in certain locations of measurement, but not all.

Table 4.4 represents the differences in metric dimensions between black females and white females. As can be seen, the dimensions of the bones of white females tended to be, in general, larger than that of the black females. White females were significantly larger on a statistical level ($p<0.05$) at the vertical head diameter of the humerus, the maximum midshaft diameter of the ulna, the distal diameter of the ulna, the olecranon-coronoid distance of the ulna, the maximum midshaft diameter of the radius, the vertical head diameter of the femur, the distal epicondylar breadth of the femur, the midshaft circumference of the femur, the proximal and distal diameters of the tibia, the maximum head diameter of the fibula, and the maximum midshaft diameter of the fibula.

Humeral head measurements, as well as ulnar dimensions, a radial dimension, and lower leg dimensions appear to be the most dissimilar between the females of the two populations. Specifically, the most distinct differences appeared to be in that of the measurements regarding diaphyses, i.e., diameters at midshaft and circumferential data. The ulna, radius, and fibula diameters were statistically distinct between black and white females, while the femoral circumference was also different between the two female groups. Additionally, another noteworthy location of statistical significant differences was in the knee joint articular surfaces, i.e. distal epicondylar breadth of the femur and its counterpart, the proximal condylar breadth of the tibia. Other measurements, mostly located within the upper appendicular

skeleton of the female specimens appeared quite congruent and would not be considered significantly dissimilar from one another in absolute size. Table 4.5 demonstrates the cataloguing of metrical traits found to be statistically significantly different or similar in the female skeleton between the populations "black" and "white".

The distribution of statistically significant differences appeared to be largely random; no pattern developed except those subtle arrangements listed above and no consequential evidence led to certain element measurements as standing out as discernibly "black female" or discernibly "white female". One possible trend was seen in four measurements from the humero-radio-ulnar joint; these all appeared metrically similar between black and white females. Because the majority of measurements are of statistical significance, however, it was concluded that the female groups should remain separate for the remainder of statistical analysis for subsequent queries placed upon metric data. As it was expected that metric changes in size with age may be subtle, pooling the data would obscure these changes, especially due to the dissimilar sample sizes between the populations.

The purpose of this study was to determine if skeletal elements change with age; if so, were the changes great enough to observe and substantial enough to quantify? With the resulting black females separated from the white females, analyses were then performed on each group to determine if either population changed with age; if there were statistically significant changes as age advanced, the next step would be to interpret the changes and to interpret why these transformations were taking place. Dimensions of individuals younger than 50 were therefore compared to those of individuals older than 50 to observe differences in metric proportions.

4.2.1

Metric changes in long bone measurements with the onset of age: black females

Black females appeared to stay relatively static in their measurements of long bones with the onset of advanced age (Table 4.6). Only one skeletal site, the circumference at midshaft of the humerus, appeared to be statistically distinct between young and old individuals. The midshaft circumference of the humerus in black females showed a decrease in size with age. Young black females exhibited a mean humeral midshaft circumference of 60.35 mm (with a standard deviation of 4.27 mm) as opposed to a significantly smaller humeral midshaft diameter in the older black females of 58.15 (with a standard deviation of 4.77 mm).

As can be seen from Table 4.6, black females change very little in metric values with the advancement of age. Older individuals are approximately the same size in all measurements as their younger counterparts.

4.2.2

Metric changes in long bone measurements with the onset of age: white females

White females, in contrast to black females, appeared distinctly different in regards to their long bone metric values and thus size with the onset of age. White females were significantly different between the age groups of "50 years of age and younger" and "over 50 years of age" in several sites of the postcranial skeleton. Table 4.7 illustrates these mean-based size differences and their statistical significance.

Old white females were shown to increase in size with all postcranial measurements. Statistical significance of these findings was tested with an ANOVA statistical test. F-values demonstrated that several postcranial skeletal

measurements were significant at $p < 0.05$. In those long bone measurements, again, the change was a distinctive increase in skeletal size among midshaft circumferences, diameters, and proximal/ distal articular surface data. These results showed a clear and unmistakable trend in white females becoming metrically larger in their postcranial dimensions with age.

4.3

Comparison of male postcranial data between populations and age groups

Males and females were found to be unique from each other in their morphological size when comparing postcranial measurements. Sexual dimorphism between males and females was quite apparent, but once again it was necessary to question possible differences between black and white South Africans, in this case between males. Because the female population was further divided into separate groups, the same was attempted with males.

Measurable differences were observed between the black male population and the white male population in 18 out of 23 postcranial measurements (Table 4.8). The only sites in which both groups appeared similar were dimensions located at the ulnar head, and the midshaft dimensions of both lower leg bones, the tibia and fibula. All other skeletal sites of the male postcranium bore differences that were statistically significant. These variations between the groups manifested themselves as size differences, as was the case with the female populations; white males tended to be larger than black males in their postcranial/ long bone skeletal features.

The F-values depicted in Table 4.8 signify the distance between individual distributions and their significance level. White males, with few exceptions, were significantly larger than their black male counterparts.

The significantly larger skeletal sites of white males as compared to black males included the maximum head diameter of the humerus, radius, femur and fibula, as well as the proximal breadth of the tibia, and one proximal measurement of the ulna. Midshaft diameters of all long bones were significantly larger in white males than in black males, except for both midshaft diameters of the lower leg bones (tibia and fibula); the midshaft circumferences of both the humerus and femur were larger as well. In addition, the distal diameters of all six long bones were significantly larger in white males than in their black counterparts. Table 4.9 demonstrates the list of metrical traits found to be statistically significantly different or similar in the male skeleton between the populations "black" and "white".

Because of these statistically significant metric differences between populations, it was concluded that the groups should remain separate for the remainder of statistical analyses.

4.3.1

Metric changes in long bone measurements with the onset of age: black males

Following this, a comparison of young specimens and old specimens from each population was done, as was the case with the female sample. Data collected on black males indicated that indeed black males increased in size with age; certain sites on the skeleton, more than others, were observed as being significantly larger, producing statistically noteworthy results. As seen in Table 4.10, black males increased with age at 21 skeletal measurement sites. Seven of these differences were statistically significant when subjected to an ANOVA.

Table 4.10 illustrates that the majority of statistically significant skeletal sites in which young black males and old black males differ were the midshaft diameters of the appendicular skeleton and the elbow and knee joint locations. The midshaft diameters of the humerus, ulna, and femur in black males were the most obvious

measurements changing with the onset of age. Additionally, the proximal tibia and the proximal fibula, being an integral component of the knee joint, increased with size when young and old black males were evaluated, as well as the distal epicondylar breadth of the humerus and the superior diameter of the head of the ulna (comprising two-thirds of the bony structures of the elbow).

4.3.2

Metric changes in long bone measurements with the onset of age: white males

White males also increased in size with the onset of age, although not with any statistical significance at the majority of skeletal measurement sites (Table 4.11). The locations of the significant changes, however, parallel those seen in the black male skeleton. The white males increased in metric dimensions on a statistically significant level with one location at the elbow joint (inferior diameter of the head of the ulna), and a component of the knee joint (the proximal bicondylar breadth of the tibia). In addition, the distal diameter of the radius increased significantly with age. These locations (elbow and knee joints) are the same areas that increased in dimension with the black male skeleton.

4.4

Implications of metric changes with age between males and females: long bone measurements

When statistically significant changes with age were observed in the skeletal measurements for each biological affiliation, that particular measurement site was compared to the opposite sex and their corresponding measurement to visualize whether the male and female values were diverging upon each other. Male metric measurements were consistently larger than their female counterparts with the young

populations studied. However, females (specifically, white females) were observed to increase in size in a number of skeletal measurement sites. They were subsequently compared to their male counterparts to detect the differences between the metric values. These differences were important to note, based on the possibility of metric misclassification between males and females if measurements were seen to increase, especially in the female population. In addition, metric decreases in the postcranial skeleton were observed and compared. Age categories were determined on a ten-year incremental scale basis after the age of 20. Ages 18 to 20 were pooled for the first age category. Table 4.21 shows the age categories on which all Figures were based upon.

4.4.1

Statistically significant long bone changes in black females with age

The only site seen as statistically different with the onset of age in black females was the circumference of the humerus at midshaft. The humeral circumference of black females was then compared to that of black males in order to visualize the possible convergence of sexual dimorphism in this group (Figure 4.1). Various observations were made from Figure 4.1. No black female specimens 18-20 years of age were obtained for this study, thus the break in the line of data throughout that time period. In addition, no black females over the age of 80 were analyzed. Black males and females appeared to change in different ways through time in regard to this isolated measurement site, with males decreasing in size early in age and females increasing in size late in age (age category 6, 61-70 years of age). Based on comparison of means and classic statistical analyses, black males and females change in age but do not come close to converging to the point that misclassification would be possible.

4.4.2

Statistically significant long bone changes in white females with age

Numerous sites were seen as statistically different with the onset of age in white females. These specific measurement sites were compared to white males to visualize the changes with this group through time. White females were observed to increase in size with the onset of age at the humeral head, especially from the age of 41 through their 70s (Figure 4.2). White males increased in size during their 20s through their 40s, stayed relatively static from the age of 50 to the age of 70, and then gradually increased in size with advanced age. Metric values for white females and males appeared close in the second age category of life, but never converge with an incremental progression of age. However, old females and young males, when compared, were becoming very similar metrically.

Figure 4.3 shows the second statistically significant measurement site for white females, namely the diameter of the humerus at midshaft. Again, white females are seen to metrically become larger with age, with a slight decrease in the advanced age category of 70 years to 80 years. These changes occurred gradually. White males were statistically larger than their white female counterparts and continued to grow slightly or stay static with the onset of age. A distinct size increase was seen in the advanced age categories of white males.

The distal epicondylar breadth of the humerus was the third statistically significant measurement site in which white females increased with age. Figure 4.4 illustrates the differences between white females and white males with the advancement of age. White females were seen to gradually increase with age at the distal humerus, but never approach the metric mean of white males even with the advancement of age. White males continued to increase in size somewhat through their last decade of advanced age.

The diameter of the superior ulnar head (Figure 4.5), the diameter of the inferior ulnar head (Figure 4.6), the diameter of the ulna at midshaft (Figure 4.7), the distal diameter of the ulna (Figure 4.8) and the olecranon-coronoid distance (Figure 4.9) were statistically significant between young and old white females, and thus compared to white males to observe the magnitude of changes. White females again never approach the metric mean of white males with this skeletal measurement, since both females and males are increasing in size with age. However, the female measurement in old age is becoming very close to the male measurement mean in age category two.

The distal diameter of the ulna was shown to increase in size with age as well in both white females and white males, with white males in age category 2 being metrically close to the dimensions of white females (Figure 4.8). Males in this group increase in size dramatically throughout the 3rd category of age and continue to stay metrically larger than their white female counterparts for the duration of the age categories. Both males and females decreased slightly in size during the onset of advanced age in the distal diameter of the ulna, specifically, age categories eight and nine. However, the general increase in size for white females over time was statistically significant.

Every measurement collected from the radius resulted in statistically significant increases in size with white females. Figures 4.10, 4.11 and 4.12 show this increase in size compared to the radial measurements of white males. These sites may increase in size with the onset of age in white females, but they do not come close to diverging with the white male mean. However, the measurements of old white females were approaching those of young males.

The maximum diameter of the femoral head, the diameter of the femur at midshaft, and the distal epicondylar breadth of the femur were also sites of significant change with age in white females. The white female mean of the femoral head increased gradually, particularly through the age categories four, five, six, and seven

(40 years of age through 70 years of age, Figure 4.13). A slight decrease in femoral head size in white females was observed after 71 years of age. The mean of the femoral head diameter of white females did not, however, near the size dimensions of the white male femoral head diameter. This pattern was also seen in the femoral shaft diameter and distal epicondylar breadth, although the old females and young males are converging somewhat. Figures 4.14 and 4.15 illustrate differences seen between males and females with these two metric values.

The tibia and fibula were sites of significant size changes with the onset of advanced age in white females as well (Figures 4.16-4.19). The proximal measurement site of the tibia (the bicondylar breadth, Figure 4.16) increased in size as white females progressed through age categories 4, 5, 6, and 7 (40 years of age through 70 years of age). A slight decrease in size was noted between 71 and 80 years of age.

The diameter of the tibia at midshaft showed a definite increase in size as white females advanced through age (Figure 4.17). This increase in the metric midshaft of the tibia began at age category two (21 years of age) and continued through age category seven (70 years of age), where it then decreased slightly with advanced age. The diameter of the tibia at midshaft did not reach a size dimension close to that of white males.

The white female fibula showed signs of increased dimensions with the onset of age at both the proximal and distal measurement sites (Figures 4.18 and 4.19). The proximal fibular diameter was noticeably larger than the white male mean at the beginning of age category 2, and did diverge with the white male mean within this same age category (21 years of age until 30 years of age).

This result is also seen with the distal portion of the fibula, as the mean measurement for white females is larger than the white males at the beginning of age category 2. White male means in both skeletal locations went on to increase in size more than white female means at the same locations; white females were seen to

increase in age during the advanced age categories, but are still smaller in size than their white male counterparts.

In summary, white females show significant signs of becoming larger in size with the onset of age when observing long bone measurements. Males and females within this group were getting closer metrically. However, these measurements rarely came close to the white male mean, although some metric dimensions of old white females often approached that of young males.

4.4.3

Statistically significant long bone changes in black males with age

Black males increased in size with age in 21 skeletal sites of measurement, with seven measurement locations increasing on a statistically significant level (Table 4.10). Specifically, the midshaft diameter of the humerus, ulna, and femur increased significantly (Figures 4.20, 4.23 and 4.24) in addition to the distal epicondylar breadth of the humerus and the superior head diameter of the ulna (Figures 4.21 and 4.22, respectively). These last two measurements show that a distinct incremental size change was occurring in the elbow joint with the onset of age. This increase continued to be metrically well above the values black females exhibited in all measurements. Finally, the proximal bicondylar breadth of the tibia and the proximal diameter of the fibula exhibited a size increase in the black male skeleton (Figure 4.25 and Figure 4.26, respectively).

The diameter of the humerus at its midshaft increased in size with the onset of advanced age in the black male skeleton. Figure 4.20 illustrates the gradual increase in the element's size as age categories increase. The measurement site rarely decreases at any of the age category locations; only a gradual increase in the humeral dimension is observed. In this site, sexual dimorphism thus appeared to increase with age.

Sexual dimorphism was apparent in the articular surfaces of the elbow joint of black males, and measurements of two locations increased significantly with the onset of age. The distal articular surface of the humerus increased in size with age, but only in the late old age category. This value appeared above the black female mean and never came close to converging with female metric values (Figure 4.21). This was an expected result. In addition, black males increased in size at the superior head of the ulna (Figure 4.22). Figures 4.21 and 4.22 show parallel increases with the age, with the distal epicondylar breadth of the humerus diverging in old age. Thus, two out of three bony elements of the elbow joint were affected and manifested themselves as an increase in dimension that was statistically significant. The black male metric means for both locations were well above that of the black female mean, which eliminated any possible misclassification of this measurement if it was used in isolation to determine sex.

The diameter of the ulna (Figure 4.23) as well as the femur at midshaft increased on a statistically significant level in black males with the onset of age (Figure 4.24). This metric value was observed to far exceed that of the black female metric value, thus the possibility of misclassification from the metric value of the femoral shaft diameter is unlikely. Interestingly, the mean metric value of the diameter of the femur at midshaft decreased briefly between the early age categories of one (18-20 years of age) and two (21-30 years of age).

The bicondylar breadth of the proximal tibia became larger with age, but did appear fairly close metrically to black females in earlier age categories (Figure 4.25). Although the two values between age categories one and two began relatively close together (73.19 mm for black males and 69.22 mm for black females) the metric values for this skeletal site remained separate during the incremental increase in age.

The corresponding articular feature of the inferior knee joint, the proximal fibula, also increased significantly in size with the onset of age. Again, black males

and females were closest metrically during age categories 1 and 2, with males becoming significantly larger than females through time (Figure 4.26). The two metric values for the diameter of the fibular head in black males and females never came close to converging after age category 2.

In summary, the measurements between males and females in this population remain largely parallel to one another (with the black male value being significantly above that of the black female mean). Each actually increases with the incremental progression of age. Males and females do not converge in dimension with one another when compared; this reduces the chance of misclassification through metric means, even with the onset of age and the increase in size.

4.4.4

Statistically significant long bone changes in white males with age

White males increased in size with age at three skeletal measurement sites. The diameter of the inferior head of the ulna became larger in white males through time, but appeared close metrically to that of white females throughout the duration of each age category. The two groups paralleled each other in their direction and magnitude of change, both gradually becoming larger with age (Figure 4.27). The diameter of the old female, however, approached that of the young male sample. Dimensions of the distal radius also increased in size with the onset of age in white males (Figure 4.28). This metric value always appeared above the white female mean, which indicated significant sexual dimorphism in this site and its continuation during advanced age categories.

Finally, another articular joint location was seen as increasing significantly in white males with the onset of age (Figure 4.29). The maximum bicondylar breadth of the tibia became larger with age, but did appear close metrically to white females in age category 2. This result is similar to those seen in black males with the proximal tibia; both male groups increased significantly in at least one metric measurement of

the knee joint. White males in this skeletal location increase most dramatically in the last age category of life. This could possibly be due to arthritic changes.

4.4.5

Summary

It is apparent that males and females stayed metrically separate in their sexual dimorphism when comparing long bone measurements, even when an increase in size was observed at numerous skeletal sites for the females. Metric means of the old female sample came closer to the young male metric means. Midshaft diameters/ circumferences of long bones were the most common measurement to increase, especially in males. The humero-radial-ulnar joint and its articulated surfaces also showed increased size with age in both males and females, as did the tibia-fibular articular surfaces. This indicated that structural modification was occurring at these well-used and weight-bearing skeletal sites with the onset of age. Results also indicated that females do not collectively decrease in their skeletal dimensions with age, even though bone mineral density may very well be decreasing. Skeletal remodelling and aggregate bone gain in various forms was observed in all skeletal samples, manifesting itself in an increase in skeletal dimensions. The female skeleton (especially the white population) exhibited the most remarkable changes.

4.5

Comparison of pelvic metric data between sexes

Four pelvic measurements (coxal length, coxal breadth, pubis length and ischium length) were taken for males and females. The ischio-pubic index was calculated as well. Descriptive statistics can be seen in Table 4.12, and includes the combination of the two ancestry groups. The significance of differences between means was tested by ANOVA analysis, and is also indicated in the table. As

expected, males and females are sexually dimorphic for all four dimensions as well as the ischio-pubic index. In general, males tended to have longer pelvic lengths and wider pelvic breadths. Pubis lengths in males were shorter than those of females, ischium lengths were longer in males than those of females, and the subsequent ischio-pubic index calculated was much smaller in males than in females. The F-value in Table 4.12 indicates the large distance between metric distributions of males and females, which designated a clear and significant difference between the groups for the measurements and the calculated index. All p-values, therefore, were at the level of <0.05, thus the distinct differences in size between males and females can once again be confirmed through this study.

These results were expected based on the considerable amount of past data dedicated to documenting the shape of the pelvic girdle in males and females, morphology that must exist in the act of child-bearing with females, and general sexual dimorphism of the os coxae and the pelvic region.

4.5.1

Comparison of pelvic metric data between sexes and populations

As expected, measurements of the pelvis corresponded to the known probability that black males would exhibit significantly larger coxal lengths, breadths, and ischium lengths; shorter pubis lengths (although not statistically significant); and a smaller ischio-pubic index than their female counterparts (Table 4.13).

White South Africans were observed to be metrically larger than their black counterparts for all values. In addition, the white population adhered to the same results as observed in the black South African sample; males were substantially (and significantly) different in their metric dimensions than the female sample. Table 4.14 illustrates the differences in males and females in the white South African population. Males were significantly larger in three metric values, and exhibited a smaller ischio-pubic index than their female counterparts. In addition, the pubis length of white

males was the only value smaller than that of the females, a characteristic that is distinctly sexually dimorphic. These differences show the quantitative disparity between males and females that make each sex overwhelmingly different in their morphology when observing metric characteristics of the pelvis. Metric differences were seen between females and males of both biological affiliations, and thus remained separated for the remainder of the analyses.

4.6

Comparison of female pelvic data between populations and age groups

Even though comparison of females from different population affinities was not the purpose of this study, it was necessary to first establish whether they were similar enough to pool all data. When pelvic measurements from the categories "black female" and "white female" were evaluated, it was clear that size differences existed between all measurements in the two groups on a statistically significant level (Table 4.15). White females tended to be larger on a general scale than their black female counterparts. All of these size discrepancies, as well as the ischio-pubic index, were great enough to quantify as statistically significant.

Metric data collected from the pelvis provided more than just variation in the size of the pelvic girdle dimensions; it provided a measurement of proportion differences, whether between males and females or divergent groups of the same sex. As seen above, females are most alike within the proportion of their ischio-pubic index, the holistic index value that makes these specimens uniquely "female". Because size differences were present when comparing black females and white females, it was essential to observe each population as discrete entities to distinguish differences with the onset of age. Since the two groups were observed to be different metrically, they remained separated for the remainder of the analyses.

4.6.1

Metric changes in pelvic measurements with the onset of age: black females

Much like in the other postcranial measurements of the black female sample, measurements of the pelvis remained static and largely unchanged with advanced age (Table 4.16).

Although not statistically significant, it was interesting to note that three measurements decreased slightly as well as the ischio-pubic index. Only coxal breadth increased in size. Since pubic lengths are usually longer in females than they are in males, the decrease in pubic length with black females indicated a decrease in sexual dimorphism with this isolated measurement. All males have a mean pubic length of 73.2 mm (refer to Table 4.12), while young black females have a mean pubic length of 73.0 mm and old black females have a mean pubic length of 71.6 mm (Table 4.16). This indicated that black females, with this particular skeletal site, might be nearer to males in skeletal size with regards to pubic length and thus misclassified as males more often if this measurement is utilized in isolation.

4.6.2

Metric changes in pelvic measurements with the onset of age: white females

None of the changes in white female pelvic measurements taken in this study were significant on a statistical level when comparing young white females to old white females over the age of 50 (Table 4.17).

However, an important observation was made when the metric data from the white female os coxae was examined. All pelvic measurements increased as age increased. Changes towards larger metric values in white females indicated a possibility for misclassification of females older than 50 years of age. For example, the general male pelvic length mean was 207.8 mm (Table 4.12) while the "old white

female" pelvic length mean was 208. 2 mm, larger in size than the general male mean with all male data pooled. In addition, the general male ischial length mean was 88.2 mm; the "old white female" ischial length mean was 87.1 mm, close to the general male mean. These two measurements were the only two that moved close to the general male means in pelvic measurements, but they were significant enough to note here. In fact, pelvic measurements from all white females (young and old) were larger than pelvic metric data from all black males (young and old) See Tables 4.13 and 4.14 for comparison.

In addition, the ischio-pubic index of white females decreased with age, although not significantly. Although the "male" and "old white female" means for this index were not close (83.0 mm and 93.8 mm, respectively) the decrease in the index suggested that this ratio was becoming less sexually dimorphic in white females. These results indicated a decrease in sexual dimorphism of the white female with the onset of age; that is, their metric values appear more male.

4.7

Comparison of male pelvic data between populations and age groups

The same approach was followed for males as for females. Analysis was performed to determine if the male pelvis is modified with the advancement of age, and if so, where those changes were taking place. The two biological affiliations of "black male", "white male" and their pelvic girdle measurements were left separate and subsequently compared. A statistically significant distinction was found between the two groups of male specimens; in general, white males tended to be larger in size than their black male counterparts (Table 4.18). When an analysis of variance of the means of each group was performed (ANOVA), the results were, as suspected, significant statistically except for the ischio-pubic index. Males categorized as "black"

and "white" were no different from each other when comparing this index, which assesses proportion or shape.

White male pelvic measurements (coxal length, coxal breadth, pubis length, and ischium length) were decidedly larger than their black male counterparts, confirming the past conclusion that these populations compared only differ in the principle component of size. The statistical insignificance of the ischio-pubic index between male populations indicated that male pelvic morphology is similar and non-population-specific. The important result here was the existence of marked sexual dimorphism between all males and all females in pelvic measurements.

4.7.1

Metric changes in pelvic measurements with the onset of age: black males

Black males increased slightly in their pelvic size dimensions with age on all metric measurements, although the increase in dimensions was not large enough to be deemed statistically significant (Table 4.19). The one metric value that was deemed statistically significant was the ischio-pubic index of the black male pelvis. This index increased significantly with the onset of age. All other metric dimensions of the black male pelvis increased, but not on a level deemed statistically significant.

4.7.2

Metric changes in pelvic measurements with the onset of age: white males

White males increased in size within the length and breadth of the pelvis, and measurements decreased with age in regard to pubis length and ischial length. Because it is comprised of the pubis and ischial lengths, the ischio-pubic index decreased significantly (Table 4.20).

The pubis length and ischio-pubic index in the white male pelvis changed the most with the onset of advanced age, with both being significantly different. Since

male ischio-pubic indices were smaller than female ischio-pubic indices in general (see Table 4.12) it appeared possible that white male pelves were becoming more "male" with age. Old white males had a smaller ischio-pubic index than the male population when pooled (82.55 mm for old white males and 83.01 mm for general males).

4.8

Implications of metric changes with age between males and females: the pelvis

When statistically significant changes with age were observed in the pelvic measurements for biological affiliation, that particular measurement site was compared to the opposite sex and their corresponding measurement to visualize whether the male and female values were diverging upon each other. Female and male groups were observed to increase in several pelvic measurement sites. They were subsequently compared to their male or female counterparts to observe the differences between the metric values. These differences were important to note, based on the possibility of metric misclassification between males and females if measurements were seen to increase, especially in the female population. In addition, metric decreases in pelvic measurements were observed and compared as well.

There were no statistically significant changes in the metric values of pelvic measurements between young females and those females over the age of 50 for either the black or white biological groups. The female pelvis appeared virtually unchanged with the advancement of age.

4.8.1

Statistically significant pelvic changes in black males with age

Black males did change in a statistically significant way in the ischio-pubic index, the numerical equivalent of proportion in the innominate. The ischio-pubic index of the black male increased with the onset of age, and was therefore compared to the black female ischio-pubic index to observe possible convergence of metric data (Figure 4.30).

Female ischio-pubic indices are significantly larger than any male group. Even though the ischio-pubic index of black males increased with the onset of age, it still does not metrically approach the general female ischio-pubic index mean (83.26 mm for old black males and 92.30 mm for old black females). Metric data between males and females was observed to near each other through age category five (51 years of age through 60 years of age); however the black male mean did not converge with the black female mean. In older ages, sexual dimorphism seemed to diverge from each other between males and females.

4.8.2

Statistically significant pelvic changes in white males with age

One measurement location and the ischio-pubic index in the white male pelvis changed significantly in metric size with the onset of age. The mean pubis length became smaller as white males increased with age (Figure 4.31). These changes were compared to white female pubis length measurement means to observe possible convergence.

The male mean closely paralleled the female mean within age category two (21 years of age through 30 years of age), and exceeded the white female mean within age category three (31 years of age through 40). In age category seven (71 - 80 years) the male mean again exceeded the female mean, demonstrating two occasions where the white male mean intersected with the white female mean in this

location of skeletal measurement. In addition, white male pubis length increased during the last age category. Pubic morphology is important because the pubis plays a major role in skeletal sex determination, influencing such element morphology as the subpubic concavity and the subpubic angle. The intersection of metric values from white male and female pubis length may indicate the possibility of misclassification.

The second location of significant metric change in the white male pelvis was the ischio-pubic index. Unlike the black male ischio-pubic index, this white male mean decreased metrically with the onset of advanced age since the pubis length decreased (Figure 4.32). The metric decrease in the ischio-pubic index demonstrated the continuance of established sexual dimorphism in the male and female pelvis; the white female mean began (as anticipated) well above the male mean and the two metric values did not come quantifiably close to each other at any age category.

4.9

Visual summary of metric results

Results obtained from metric data with regard to how the human skeleton changes with age were varied. The male skeleton showed different metric modifications with age than did the female skeleton. In addition, each ancestral group appeared different (although sometimes parallel) in their skeletal changes. Figures 4.33 – 4.36 were created to summarize these age-related changes in a skeleton in anatomical position, to better observe the location of such changes. These changes illustrate the most common location of skeletal size change within each biological group.

Table 4.1: Means, standard deviations, and univariate F-ratios for postcranial measurements of males and females.

	Males					Females					Univariate
Variables (mm)	N	Mean	Range	s.d.	S.E.	N	Mean	Range	s.d.	S.E.	F-ratio
Humerus:											
Vertical head diameter	403	45.2	32-55	3.55	0.2	189	41.0	34-52	3.26	0.2	**191.38***
Maximum midshaft diameter	404	22.4	17-29	1.94	0.1	189	20.0	16-29	1.76	0.1	**211.91***
Epicondylar breadth	404	63.2	49-73	3.90	0.2	189	56.1	49-68	3.36	0.2	**469.77***
Midshaft circumference	404	67.3	52-82	5.33	0.3	189	60.0	50-77	4.52	0.3	**264.48***
Ulna:											
Superior head diameter	402	27.1	21-34	2.16	0.1	189	26.0	18-34	2.59	0.1	**356.10***
Medial head diameter	402	20.8	15-30	2.02	0.1	189	18.5	14-23	1.54	0.1	**200.12***
Inferior head diameter	402	29.9	19-45	3.58	0.2	189	25.4	19-33	2.78	0.2	**241.22***
Maximum midshaft diameter	402	16.8	11-22	1.56	0.1	189	14.7	11-19	1.43	0.1	**242.25***
Distal diameter	401	20.2	15-25	1.54	0.1	189	18.1	14-26	1.59	0.1	**238.26***
Olecranon-coronoid	402	23.9	18-33	2.23	0.1	189	21.3	15-27	2.15	0.2	**186.57***
Radius:											
Head diameter	401	23.6	18-29	1.67	0.1	189	21.0	17-26	1.4	0.1	**358.77***
Maximum midshaft diameter	402	15.6	11-20	1.50	0.1	189	13.9	10-19	1.37	0.1	**198.67***
Distal diameter	402	34.8	26-45	2.37	0.1	189	30.7	25-38	2.09	0.2	**422.31***
Femur:											
Vertical head diameter	402	46.5	37-57	3.06	0.2	189	41.7	34-54	2.85	0.2	**341.00***
Maximum midshaft diameter	403	30.8	23-38	2.54	0.1	189	27.9	23-34	2.13	0.2	**194.71***
Distal bicondylar breadth	403	80.8	55-93	4.84	0.2	189	73.5	63-89	4.44	0.3	**314.63***
Midshaft circumference	403	91.6	75-110	6.22	0.3	189	83.9	69-100	5.81	0.4	**208.05***
Tibia:											
Proximal bicondylar breadth	403	77.2	66-90	4.12	0.2	189	69.3	60-81	3.77	0.3	**503.48***
Maximum midshaft diameter	403	30.9	23-42	2.51	0.1	189	27.7	22-35	2.11	0.2	**234.10***
Distal diameter	403	52.4	41-62	3.18	0.2	189	47.2	40-56	2.95	0.2	**360.40***
Fibula:											
Maximum proximal diameter	400	28.4	21-37	2.61	0.1	183	25.1	18-33	2.54	0.2	**194.12***
Maximum midshaft diameter	404	15.9	11-22	1.93	0.1	189	14.6	11-18	1.57	0.1	**58.44***
Distal diameter	404	27.8	21-38	2.44	0.1	189	25.2	20-35	2.19	0.2	**166.14***

**** p-values significant at <0.05***

Table 4.2: Means, standard deviations, and univariate F-ratios for postcranial measurements of black males and black females.

	Black males					Black females					Univariate
Variables (mm)	*n*	Mean	Range	s.d.	S.E.	*n*	Mean	Range	s.d.	S.E.	F-ratio
Humerus:											
Vertical head diameter	298	44.0	32-53	2.77	0.2	107	39.1	34-52	2.49	0.2	**264.68***
Maximum midshaft diameter	298	22.6	17-29	1.92	0.1	107	20.0	16-29	1.99	0.2	**109.13***
Epicondylar breadth	298	62.7	49-71	3.66	0.2	107	56.0	49-68	3.28	0.3	**288.43***
Midshaft circumference	298	66.7	53-82	5.17	0.3	107	59.5	50-77	4.57	0.4	**162.87***
Ulna:											
Superior head diameter	298	27.1	21-34	2.14	0.1	107	24.0	20-29	1.73	0.2	**187.74***
Medial head diameter	298	20.7	15-30	2.01	0.1	107	18.6	15-23	1.59	0.2	**101.48***
Inferior head diameter	298	29.7	20-46	3.56	0.2	107	25.6	20-32	2.74	0.3	**117.29***
Maximum midshaft diameter	298	16.6	11-22.0	1.55	0.1	107	14.4	11-18.0	1.34	0.1	**160.40***
Distal diameter	298	19.9	15-24	1.36	0.1	107	17.8	14-23	1.37	0.1	**179.16***
Olecranon-coronoid	298	23.9	18-33	2.22	0.1	107	21.8	15-27	2.3	0.2	**72.96***
Radius:											
Head diameter	298	23.3	18-29	1.55	0.1	107	20.9	17-26	1.48	0.1	**199.81***
Maximum midshaft diameter	298	15.4	11-20.0	1.49	0.1	107	13.7	10-19.0	1.39	0.1	**105.18***
Distal diameter	298	34.6	26-40	2.26	0.1	107	30.7	27-38	2.15	0.2	
Femur:											
Vertical head diameter	298	45.8	37-57	2.64	0.2	107	40.5	34-51	2.41	0.2	**332.11***
Maximum midshaft diameter	298	30.6	23-37	2.47	0.1	107	27.6	23-34	2.28	0.2	**123.11***
Distal bicondylar breadth	298	79.7	66-92	4.05	0.2	107	71.7	63-89	4.31	0.4	**299.52***
Midshaft circumference	298	90.6	75-107	5.85	0.3	107	82.1	69-100	5.49	0.5	**177.02***
Tibia:											
Proximal bicondylar breadth	298	76.6	66-89	3.85	0.2	107	68.6	60-81	3.99	0.4	**337.75***
Maximum midshaft diameter	298	30.8	23-42	2.47	0.1	107	27.8	22-35	2.08	0.2	**132.23***
Distal diameter	298	52.1	43-62	3.07	0.2	107	46.7	40-56	3.06	0.3	**243.64***
Fibula:											
Maximum proximal diameter	298	28.2	21-37	2.58	0.2	107	24.8	18-33	2.53	0.2	**137.13***
Maximum midshaft diameter	298	15.8	11-22.0	1.93	0.1	107	14.4	18-Nov	1.59	0.2	**43.37***
Distal diameter	298	27.6	21-38	2.46	0.1	107	25.1	20-35	2.49	0.2	**82.44***

**** p-values significant at <0.05***

Table 4.3: Means, standard deviations, and univariate F-ratios for postcranial measurements of white males and white females.

	White males					White females					Univariate
Variables (mm)	*n*	Mean	Range	s.d.	S.E.	*n*	Mean	Range	s.d.	S.E.	F-ratio
Humerus:											
Vertical head diameter	105	48.7	41-55	3.12	0.3	82	43.4	38-49	2.38	0.3	**169.32***
Maximum midshaft diameter	106	22.9	16-27	1.95	0.2	82	20.1	16-23	1.45	0.2	**124.68***
Epicondylar breadth	106	64.5	52-73	4.32	0.4	82	56.3	49-68	3.48	0.4	**198.66***
Midshaft circumference	106	68.8	52-80	5.56	0.5	82	60.7	52-71	4.41	0.5	**119.19***
Ulna:											
Superior head diameter	104	27.2	21-33	2.19	0.2	82	23.5	18-28	1.83	0.2	**156.44***
Medial head diameter	104	21.2	16-27	1.98	0.2	82	18.4	14-22	1.48	0.2	**112.99***
Inferior head diameter	104	30.4	21-42	3.66	0.4	82	25.1	19-33	2.83	0.3	**123.79***
Maximum midshaft diameter	104	17.3	12-21.0	1.48	0.1	82	15.0	12-9.0	1.49	0.2	**109.89***
Distal diameter	103	21.1	17-25	1.68	0.2	82	18.4	14-26	1.81	0.2	**111.11***
Olecranon-coronoid	104	24.0	19-30	2.18	0.2	82	20.7	15-25	1.77	0.2	**126.77***
Radius:											
Head diameter	103	24.4	20-29	1.78	0.2	82	21.1	17-25	1.32	0.1	**204.22***
Maximum midshaft diameter	104	16.4	13-20	1.38	0.1	82	14.1	11-18.0	1.31	0.1	**136.95***
Distal diameter	104	35.7	31-45	2.42	0.2	82	30.7	25-37	2.06	0.2	**227.45***
Femur:											
Vertical head diameter	104	48.7	40-57	3.14	0.3	79	43.2	38-54	2.68	0.3	**164.29***
Maximum midshaft diameter	105	31.4	24-38	2.56	0.3	81	28.2	23-32	1.91	0.2	**90.39***
Distal bicondylar breadth	105	84.1	55-93	5.39	0.5	81	75.7	67-84	3.51	0.4	**152.73***
Midshaft circumference	105	94.3	77-110	6.39	0.6	81	86.2	73-100	5.38	0.6	**85.14***
Tibia:											
Proximal bicondylar breadth	106	79.0	67-90	4.3	0.4	80	70.2	62-80	3.27	0.4	**237.97***
Maximum midshaft diameter	106	31.2	25-37	2.56	0.3	81	27.7	22-34	2.46	0.2	**105.35***
Distal diameter	106	53.2	41-60	3.31	0.3	80	47.8	42-54	2.69	0.3	**149.68***
Fibula:											
Maximum proximal diameter	102	29.0	22-35	2.6	0.3	76	25.6	19-31	2.49	0.3	**75.74***
Maximum midshaft diameter	106	16.1	11-21	1.87	0.2	82	14.9	11-18	1.49	0.2	**21.89***
Distal diameter	106	28.5	23-36	2.19	0.2	78	25.3	21-31	1.74	0.2	**123.01***

**** p-values significant at <0.05***

Table 4.4: Means, standard deviations, and univariate F-ratios for postcranial measurements of black females and white females.

	Black females					White females					Univariate
Variables (mm)		Mean	Range	s.d.	S.E.		Mean	Range	s.d.	S.E.	F-ratio
	n					*n*					
Humerus:											
Vertical head diameter	107	39.1	34-52	2.49	0.2	82	43.4	38-49	2.38	0.3	**147.50***
Maximum midshaft diameter	107	20.0	16-29	1.99	0.2	82	20.1	16-23	1.45	0.2	0.08
Epicondylar breadth	107	56.0	49-68	3.28	0.3	82	56.3	49-68	3.48	0.4	0.59
Midshaft circumference	107	59.5	50-77	4.57	0.4	82	60.7	52-71	4.41	0.5	3.48
Ulna:											
Superior head diameter	107	24.0	20-29	1.73	0.2	82	23.5	18-28	1.83	0.2	3.06
Medial head diameter	107	18.6	15-23	1.59	0.2	82	18.4	14-22	1.48	0.2	0.38
Inferior head diameter	107	25.6	20-32	2.74	0.3	82	25.1	19-33	2.83	0.3	1.87
Maximum midshaft diameter	107	14.4	11-18	1.34	0.1	82	15.0	9-21	1.49	0.2	**6.87***
Distal diameter	107	17.8	14-23	1.37	0.1	82	18.4	14-26	1.81	0.2	**6.36***
Olecranon-coronoid	107	21.8	15-27	2.3	0.2	82	20.7	15-25	1.77	0.2	**13.55***
Radius:											
Head diameter	107	20.9	17-26	1.48	0.1	82	21.1	17-25	1.32	0.1	0.41
Maximum midshaft diameter	107	13.7	10-19	1.39	0.1	82	14.1	11-18	1.31	0.1	**4.22***
Distal diameter	107	30.7	27-38	2.15	0.2	82	30.7	25-37	2.06	0.2	0.04
Femur:											
Head diameter	107	40.5	34-51	2.41	0.2	79	43.2	38-54	2.68	0.3	**52.25***
Maximum midshaft diameter	107	27.6	23-34	2.28	0.2	81	28.2	23-32	1.91	0.2	3.18
Distal bicondylar breadth	107	71.7	63-89	4.31	0.4	81	75.7	67-84	3.51	0.4	**47.95***
Midshaft circumference	107	82.1	69-100	5.49	0.5	81	86.2	73-100	5.38	0.6	**27.92***
Tibia:											
Proximal bicondylar breadth	107	68.6	60-81	3.99	0.4	80	70.2	62-80	3.27	0.4	8.65*
Maximum midshaft diameter	107	27.8	22-35	2.08	0.2	81	27.7	22-34	2.46	0.2	0.08
Distal diameter	107	46.7	40-56	3.06	0.3	80	47.8	42-54	2.69	0.3	**6.43***
Fibula:											
Maximum proximal diameter	107	24.8	18-33	2.53	0.2	76	25.6	19-31	2.49	0.3	**5.08***
Maximum midshaft diameter	107	14.4	11-18	1.59	0.2	82	14.9	11-18	1.49	0.2	**5.54***
Distal diameter	107	25.1	20-35	2.49	0.2	78	25.3	21-31	1.74	0.2	0.63

p-values significant at <0.05

Table 4.5: Statistical comparison of size differences between black and white females in the postcranial skeleton.

	Statistically Significant	Not statistically significant
Variables (mm)	p-value	p-value
Humerus:		
Vertical head diameter	0.00	
Maximum midshaft diameter		0.77
Epicondylar breadth		0.44
Midshaft circumference		0.06
Ulna:		
Superior head diameter		0.80
Medial head diameter		0.54
Inferior head diameter		0.17
Maximum midshaft diameter	0.00	
Distal diameter	0.03	
Olecranon-coronoid	0.00	
Radius:		
Head diameter		0.53
Maximum midshaft diameter	0.04	
Distal diameter		0.85
Femur:		
Head diameter	0.00	
Maximum midshaft diameter		0.07
Distal bicondylar breadth	0.00	
Midshaft circumference	0.00	
Tibia:		
Proximal bicondylar breadth	0.00	
Maximum midshaft diameter		0.78
Distal diameter	0.01	
Fibula:		
Maximum proximal diameter	0.03	
Maximum midshaft diameter	0.02	
Distal diameter		0.55

Table 4.6: Means, standard deviations, and univariate F-ratios for postcranial measurements of young black females (50 years and younger) and old black females (over 50 years).

	Young black females					Old black females					Univariate
Variables (mm)		Mean	Range	s.d.	S.E.		Mean	Range	s.d.	S.E.	F-ratio
	n					*n*					
Humerus:											
Vertical head diameter	66	38.9	34-43	2.09	0.3	40	39.4	35-52	3.03	0.5	1.15
Maximum midshaft diameter	66	20.1	16-29	2.09	0.3	40	19.8	17-26	1.82	0.3	0.73
Epicondylar breadth	66	55.9	49-63	3.07	0.4	40	56.1	50-68	3.62	0.6	0.04
Midshaft circumference	66	60.4	50-70	4.27	0.5	40	58.2	52-77	4.77	0.7	**6.15***
Ulna:											
Superior head diameter	66	23.9	20-29	1.62	0.2	40	24.1	21-28	1.91	0.3	0.50
Medial head diameter	66	18.7	15-23	1.58	0.2	40	18.3	15-23	1.61	0.3	1.60
Inferior head diameter	66	25.8	20-32	2.58	0.3	40	25.4	20-31	2.99	0.5	0.56
Maximum midshaft diameter	66	14.5	11-17	1.33	0.2	40	14.4	11-18	1.37	0.2	0.35
Distal diameter	66	17.9	15-20	1.12	0.1	40	17.8	14-23	1.69	0.3	0.13
Olecranon-coronoid	66	21.9	15-27	2.28	0.3	40	21.6	16-27	2.36	0.4	0.31
Radius:											
Head diameter	66	20.7	17-24	1.29	0.2	40	21.3	19-26	1.7	0.3	3.29
Maximum midshaft diameter	66	13.6	10-16	1.62	0.2	40	13.8	12-19	1.52	0.2	0.37
Distal diameter	66	30.8	27-35	1.94	0.2	40	30.7	27-38	2.48	0.4	0.05
Femur:											
Vertical head diameter	65	40.4	35-44	2.03	0.3	41	40.7	34-51	2.92	0.5	0.38
Maximum midshaft diameter	65	27.6	23-34	2.14	0.3	41	27.7	23-33	2.49	0.4	0.03
Distal bicondylar breadth	65	71.9	63-81	3.59	0.5	41	71.5	64-89	5.27	0.8	0.24
Midshaft circumference	65	82.5	72-100	4.93	0.6	41	81.4	69-99	6.26	0.9	0.95
Tibia:											
Proximal bicondylar breadth	65	68.6	60-77	3.43	0.4	41	68.6	60-81	4.77	0.7	0.00
Maximum midshaft diameter	65	27.9	22-32	1.88	0.2	41	27.5	23-35	2.35	0.4	0.91
Distal diameter	65	46.7	40-53	2.89	0.4	41	46.7	42-56	3.34	0.5	0.00
Fibula:											
Maximum proximal diameter	65	24.74	18-30	2.37	0.3	41	24.9	18-33	2.79	0.4	0.07
Maximum midshaft diameter	65	14.63	11-17	1.49	0.2	41	14.1	11-18	1.69	0.3	3.54
Distal diameter	65	25.13	20-35	2.68	0.3	41	25.0	30-31	2.68	0.4	0.11

**** p-values significant at <0.05***

Table 4.7: Means, standard deviations, and univariate F-ratios for postcranial measurements of young white females (50 years and younger) and old white females (over 50 years).

	Young white females					Old white females					Univariate
Variables (mm)	*n*	Mean	Range	s.d.	S.E.	*n*	Mean	Range	s.d.	S.E.	F-ratio
Humerus:											
Vertical head diameter	13	41.5	38-43	1.62	0.4	69	43.8	38-49	2.31	0.3	**15.95***
Maximum midshaft diameter	13	19.3	17-21	1.05	0.3	69	20.3	16-23	1.48	0.2	**5.61***
Epicondylar breadth	13	54.3	49-59	2.68	0.7	69	58.9	51-68	3.49	0.4	**7.93***
Midshaft circumference	13	59.7	52-68	4.15	1.01	69	61.0	52-71	4.47	0.5	1.12
Ulna:											
Superior head diameter	13	22.7	18-28	2.19	0.5	69	23.7	20-28	1.69	0.2	**3.97***
Medial head diameter	13	18.2	16-20	1.14	0.3	69	18.5	14-22	1.56	0.2	0.62
Inferior head diameter	13	22.8	19-27	2.27	0.6	69	25.6	20-33	2.69	0.3	**15.79***
Maximum midshaft diameter	13	14.2	12-16	1.34	0.3	69	15.2	12-19.0	1.47	0.2	**5.73***
Distal diameter	13	17.1	14-19	1.33	0.3	69	18.7	14-26	1.78	0.2	**11.57***
Olecranon-coronoid	13	19.6	15-22	1.75	0.4	69	20.9	17-25	1.68	0.2	**9.13***
Radius:											
Head diameter	13	20.3	17-22	1.35	0.3	69	21.2	18-25	1.25	0.2	**8.01***
Maximum midshaft diameter	13	13.5	11-15	1.02	0.2	69	14.2	11-18.0	1.34	0.2	**4.46***
Distal diameter	13	29.3	25-31	1.65	0.4	69	31.0	26-37	2.02	0.2	**10.25***
Femur:											
Vertical head diameter	13	41.3	38-45	1.56	0.4	67	43.6	38-54	2.69	0.3	**11.08***
Maximum midshaft diameter	13	27.1	24-29	1.62	0.4	68	28.4	23-32	1.89	0.2	**6.95***
Distal bicondylar breadth	13	73.4	68-77	2.46	0.6	68	76.6	67-84	3.5	0.4	**10.69***
Midshaft circumference	13	84.4	76-93	4.54	1.1	68	86.7	73-100	5.49	0.7	2.62
Tibia:											
Proximal bicondylar breadth	13	67.8	62-71	2.16	0.5	67	70.8	63-80	3.22	0.4	**13.74***
Maximum midshaft diameter	13	26.7	22-32	2.13	0.5	68	27.9	24-34	2.11	0.3	**4.06***
Distal diameter	13	46.8	42-49	1.78	0.4	67	48.0	42-54	2.84	0.3	3.04
Fibula:											
Maximum proximal diameter	13	24.3	19-28	2.32	0.6	59	26.0	20-31	2.42	0.3	**6.98***
Maximum midshaft diameter	13	14.3	11-16	1.32	0.3	69	15.1	11-18.0	1.51	0.2	3.59
Distal diameter	13	24.2	22-25	1.22	0.3	65	25.5	21-31	1.75	0.2	**8.92***

**** p-values significant at <0.05***

Table 4.8: Means, standard deviations, and univariate F-ratios for postcranial measurements of black males and white males.

	Black males					White males					Univariate
Variables (mm)	*n*	Mean	Range	s.d.	S.E.	*n*	Mean	Range	s.d.	S.E.	F-ratio
Humerus:											
Vertical head diameter	298	44.0	32-53	2.77	0.2	105	48.7	41-55	3.12	0.3	**212.40***
Maximum midshaft diameter	298	22.6	17-29	1.92	0.1	106	22.9	16-27	1.95	0.2	**8.52***
Epicondylar breadth	298	62.7	49-71	3.66	0.2	106	64.5	52-73	4.32	0.4	**15.92***
Midshaft circumference	298	66.7	53-82	5.17	0.3	106	68.8	52-80	5.56	0.5	**12.30***
Ulna:											
Superior head diameter	298	27.1	21-34	2.14	0.1	104	27.2	21-33	2.19	0.2	0.23
Medial head diameter	298	20.7	15-30	2.01	0.1	104	21.2	16-27	1.98	0.2	**4.03***
Inferior head diameter	298	29.7	20-46	3.56	0.2	104	30.4	21-42	3.66	0.4	3.25
Maximum midshaft diameter	298	16.6	11-22	1.55	0.1	104	17.3	12-21.0	1.48	0.1	**15.29***
Distal diameter	298	19.9	15-24	1.36	0.1	103	21.1	17-25	1.68	0.2	**54.91***
Olecranon-coronoid	298	23.9	18-33	2.22	0.1	104	24.0	19-30	2.18	0.2	0.03
Radius:											
Head diameter	298	23.3	18-29	1.55	0.1	103	24.4	20-29	1.78	0.2	**31.73***
Maximum midshaft diameter	298	15.4	11-20	1.49	0.1	104	16.4	13-20	1.38	0.1	**37.08***
Distal diameter	298	34.6	26-40	2.26	0.1	104	35.7	31-45	2.42	0.2	**18.13***
Femur:											
Vertical head diameter	298	45.8	37-57	2.64	0.2	104	48.7	40-57	3.14	0.3	**88.78***
Maximum midshaft diameter	298	30.6	23-37	2.47	0.1	105	31.4	24-38	2.56	0.3	**6.48***
Distal bicondylar breadth	298	79.7	66-92	4.05	0.2	105	84.1	55-93	5.39	0.5	**78.12***
Midshaft circumference	298	90.6	75-107	5.85	0.3	105	94.3	77-110	6.39	0.6	**28.76***
Tibia:											
Proximal bicondylar breadth	298	76.6	66-89	3.85	0.2	106	79.0	67-90	4.3	0.4	**27.17***
Maximum midshaft diameter	298	30.8	23-42	2.47	0.1	106	31.2	25-37	2.56	0.3	2.29
Distal diameter	298	52.1	43-62	3.07	0.2	106	53.2	41-60	3.31	0.3	**10.92***
Fibula:											
Maximum proximal diameter	298	28.2	21-37	2.58	0.2	102	29.0	22-35	2.6	0.3	**8.09***
Maximum midshaft diameter	298	15.8	11-22	1.93	0.1	106	16.1	11-21.0	1.87	0.2	2.22
Distal diameter	298	27.6	21-38	2.46	0.1	106	28.5	23-36	2.19	0.2	**12.38***

**** p-values significant at <0.05***

Table 4.9: Statistical comparison of size differences between black and white males in the postcranial skeleton.

	Statistically significant	Not statistically significant
Variables (mm)	p-value	p-value
Humerus:		
Vertical head diameter	0.00	
Maximum midshaft diameter	0.00	
Epicondylar breadth	0.00	
Midshaft circumference	0.00	
Ulna:		
Superior head diameter		0.64
Medial head diameter	0.04	
Inferior head diameter		0.07
Maximum midshaft diameter	0.00	
Distal diameter	0.03	
Olecranon-coronoid		0.87
Radius:		
Head diameter	0.00	
Maximum midshaft diameter	0.00	
Distal diameter	0.00	
Femur:		
Head diameter	0.01	
Maximum midshaft diameter	0.00	
Distal bicondylar breadth	0.00	
Midshaft circumference	0.00	
Tibia:		
Proximal bicondylar breadth	0.00	
Maximum midshaft diameter		0.13
Distal diameter	0.00	
Fibula:		
Maximum proximal diameter	0.01	
Maximum midshaft diameter		0.00
Distal diameter	0.00	

Table 4.10: Means, standard deviations, and univariate F-ratios for postcranial measurements of young black males (50 years and younger) and old black males (over 50 years).

	Young black males					Old black males					Univariate
Variables (mm)	*n*	Mean	Range	s.d.	S.E.	*n*	Mean	Range	s.d.	S.E.	F-ratio
Humerus:											
Vertical head diameter	125	43.7	32-50	2.81	0.3	173	44.1	37-53	2.77	0.2	1.86
Maximum midshaft diameter	125	21.9	17-26	2.01	0.2	173	22.5	18-29	1.79	0.1	**8.11***
Epicondylar breadth	125	62.3	49-71	3.8	0.3	173	63.1	51-70	3.49	0.3	**3.67***
Midshaft circumference	125	66.6	53-80	5.41	0.5	173	66.8	56-82	4.98	0.4	0.19
Ulna:											
Superior head diameter	125	26.8	21-32	2.11	0.2	173	27.4	22-34	2.16	0.2	**5.89***
Medial head diameter	125	20.6	16-26	1.74	0.2	173	20.8	15-30	2.21	0.2	0.56
Inferior head diameter	125	29.8	19-38	3.25	0.3	173	29.7	21-45	3.75	0.3	0.04
Maximum midshaft diameter	125	16.3	11-20	1.53	0.1	173	16.8	13-22	1.54	0.1	**7.94***
Distal diameter	125	19.7	15-24	1.49	0.1	173	20.0	16-23	1.23	0.1	2.65
Olecranon-coronoid	125	24.1	18-33	2.66	0.2	173	23.7	19-29	1.89	0.1	2.43
Radius:											
Head diameter	125	23.2	18-26	1.44	0.1	173	23.5	19-29	1.62	0.1	3.54
Maximum midshaft diameter	125	15.3	11-18	1.37	0.1	173	15.4	11-18	1.37	0.1	1.05
Distal diameter	125	34.5	26-39	2.31	0.2	173	34.6	28-40	2.27	0.2	0.08
Femur:											
Vertical head diameter	125	45.6	37-57	2.72	0.2	173	45.9	40-52	2.59	0.2	0.82
Maximum midshaft diameter	125	30.2	23-35	2.59	0.2	173	31.0	25-37	2.4	0.2	**6.71***
Distal bicondylar breadth	125	79.3	66-88	3.94	0.4	173	79.9	70-92	4.12	0.3	1.85
Midshaft circumference	125	90.3	75-107	6.26	0.6	173	90.9	76-106	5.61	0.4	0.67
Tibia:											
Proximal bicondylar breadth	125	76.1	66-86	3.69	0.3	172	77.0	67-89	3.97	0.3	**3.91***
Maximum midshaft diameter	125	30.7	23-37	2.51	0.2	172	30.9	26-42	2.47	0.2	0.16
Distal diameter	125	52.0	43-60	3.02	0.3	172	52.0	45-62	3.12	0.2	0.00
Fibula:											
Maximum proximal diameter	125	27.7	21-33	2.49	0.2	173	28.5	22-37	2.58	0.2	**6.94***
Maximum midshaft diameter	125	15.6	11-22	2.09	0.2	173	15.9	12-21	1.84	0.1	1.64
Distal diameter	125	27.4	22-38	2.59	0.2	173	27.8	21-36	2.39	0.2	2.02

**** p-values significant at <0.05***

Table 4.11: Means, standard deviations, and univariate F-ratios for postcranial measurements of young white males (50 and younger) and old white males (over 50 years).

Variables (mm)	Young white males					Old white males					Univariate
	n	Mean	Range	s.d.	S.E.	*n*	Mean	Range	s.d.	S.E.	F-ratio
Humerus:											
Vertical head diameter	26	48.5	41-53	2.51	0.6	79	48.7	41-55	3.24	0.4	0.14
Maximum midshaft diameter	26	22.7	16-26	1.99	0.4	80	23.0	17-27	1.93	0.2	0.55
Epicondylar breadth	26	63.1	52-69	3.76	0.7	80	64.9	52-73	4.42	0.5	3.44
Midshaft circumference	26	68.6	52-80	5.52	1.08	80	68.8	56-80	5.6	0.6	0.02
Ulna:											
Superior head diameter	25	26.7	24-29	1.45	0.3	79	27.4	21-33	2.36	0.3	2.13
Medial head diameter	25	20.9	16-23	1.63	0.3	79	21.2	16-27	2.08	0.2	0.55
Inferior head diameter	25	29.0	20-35	3.76	0.8	79	30.9	23-41	3.53	0.4	**5.47***
Maximum midshaft diameter	25	17.3	15-20	1.21	0.2	79	17.2	12-21	1.56	0.2	0.06
Distal diameter	25	21.0	17-25	1.67	0.3	78	21.1	17-25	1.69	0.2	0.19
Olecranon-coronoid	25	23.7	21-27	1.72	0.3	79	24.0	19-30	2.31	0.3	0.49
Radius:											
Head diameter	24	24.0	20-27	1.23	0.3	79	24.5	20-29	1.92	0.2	1.07
Maximum midshaft diameter	25	16.4	13-19	1.23	0.2	79	16.4	13-20	1.43	0.2	0.02
Distal diameter	25	34.7	31-37	1.79	0.4	79	36.0	31-45	2.52	0.3	**5.43***
Femur:											
Vertical head diameter	24	49.0	45-55	2.54	0.5	80	48.6	40-57	3.31	0.4	0.25
Maximum midshaft diameter	25	30.8	24-35	2.56	0.5	80	31.5	27-28	2.55	0.3	1.60
Distal bicondylar breadth	25	83.5	76-90	3.1	0.6	80	84.3	55-93	5.93	0.7	0.39
Midshaft circumference	25	93.4	77-110	6.8	1.4	80	94.5	80-109	6.28	0.7	0.58
Tibia:											
Proximal bicondylar breadth	26	77.5	70-83	3.16	0.6	80	79.4	67-90	4.53	0.5	**3.97***
Maximum midshaft diameter	26	31.0	25-37	2.83	0.6	80	31.3	26-37	2.48	0.3	0.18
Distal diameter	26	52.3	45-58	2.97	0.6	80	53.5	41-60	3.38	0.4	2.64
Fibula:											
Maximum proximal diameter	25	28.2	22-33	2.69	0.5	77	29.3	22-35	2.54	0.3	3.19
Maximum midshaft diameter	26	15.9	11-20.0	2.23	0.4	80	16.2	11-21.0	1.74	0.2	0.29
Distal diameter	26	28.2	23-31	1.68	0.3	80	28.6	24-36	2.33	0.3	0.82

**** p-values significant at <0.05***

Table 4.12: Means, standard deviations, and univariate F-ratios for pelvic measurements of males and females.

	Males					Females					Univariate
Variables (mm)		Mean	Range	s.d.	S.E.		Mean	Range	s.d.	S.E.	F-ratio
	N					*N*					
Pelvis length	401	207.8	177-248	13.52	0.7	182	197.8	170-245	13.95	4.03	**68.28***
Pelvis breadth	404	204.8	125-199	10.79	0.5	182	151.0	120-185	12.04	0.9	**3.92***
Pubis length	404	73.2	52-103	4.50	0.4	180	76.6	59-94	7.74	0.6	**25.42***
Ischium length	401	88.2	72-109	6.16	0.3	180	83.0	68-102	5.95	0.4	**93.08***
Ischio-Pubic index	404	83.0	60-105	6.61	0.3	180	92.3	73-126	7.37	0.5	**231.82***

p-value significant at <0.05

Table 4.13: Means, standard deviations, and univariate F-ratios for pelvic measurements of black males and black females.

	Black males					Black females					Univariate
Variables (mm)		Mean	Range	s.d.	S.E.		Mean	Range	s.d.	S.E.	F-ratio
	n					*n*					
Pelvis length	298	202.9	177-238	10.19	0.6	96	189.3	170-245	10.59	1.1	**127.63***
Pelvis breadth	296	149.4	125-199	8.79	0.5	96	143.0	120-175	8.6	0.9	**38.64***
Pubis length	298	71.4	52-92	6.54	0.4	96	72.4	59-94	6.09	0.6	1.84
Ischium length	298	86.2	72-98	4.66	0.6	96	79.8	68-102	5.15	0.5	**131.87***
Ischio-Pubic index	298	82.8	60-103	6.61	0.4	96	90.7	73-126	7.51	0.8	**98.06***

p-value significant at <0.05

Table 4.14: Means, standard deviations, and univariate F-ratios for pelvic measurements of white males and white females.

	White males					White females					Univariate
Variables (mm)		Mean	Range	s.d.	S.E.		Mean	Range	s.d.	S.E.	F-ratio
	n					*n*					
Pelvis length	106	222.3	192-248	11.52	1.1	82	207.3	178-240	10.76	1.2	**84.99***
Pelvis breadth	105	163.5	142-183	9.06	0.9	82	159.9	140-185	8.53	0.9	**7.79***
Pubis length	106	78.6	61-103	7.56	0.7	80	81.5	66-94	6.52	0.7	**7.66***
Ischium length	106	94.2	74-109	6.19	0.6	80	86.6	74-97	4.53	0.5	**86.93***
Ischio-Pubic index	106	83.5	68-105	6.6	0.6	80	94.1	78-113	6.81	0.7	**117.11***

p-value significant at <0.05

Table 4.15: Means, standard deviations, and univariate F-ratios for pelvic measurements of black females and white females.

	Black females					White females					Univariate
Variables (mm)		Mean	Range	s.d.	S.E.		Mean	Range	s.d.	S.E.	F-ratio
	n					*n*					
Pelvis length	96	189.3	170-245	10.59	1.1	82	207.3	178-240	10.76	1.2	**129.41***
Pelvis breadth	96	143.0	120-175	8.6	0.9	82	159.9	140-185	8.53	0.9	**177.02***
Pubis length	96	72.4	59-94	6.09	0.6	80	81.5	66-94	6.52	0.7	**93.06***
Ischium length	96	79.8	68-102	5.15	0.5	80	86.6	74-97	4.53	0.5	**88.83***
Ischio-Pubic index	96	90.7	73-126	7.51	0.8	80	94.1	78-113	6.81	0.7	**9.86***

p-value significant at <0.05

Table 4.16: Means, standard deviations, and univariate F-ratios for pelvic measurements of young black females (50 years and younger) and old black females (over 50 years).

	Young black females					Old black females					Univariate
Variables (mm)		Mean	Range	s.d.	S.E.		Mean	Range	s.d.	S.E.	F-ratio
	n					*n*					
Pelvis length	56	189.3	170-207	8.33	1.1	40	189.3	171-245	13.24	2.1	0.00
Pelvis breadth	56	142.7	120-154	7.04	0.9	40	143.4	128-175	10.49	1.7	0.15
Pubis length	56	73.0	59-94	6.56	0.9	40	71.6	61-81	5.32	0.8	1.17
Ischium length	56	79.8	68-90	4.46	0.6	40	79.8	69-102	6.05	0.9	0.00
Ischio-Pubic index	56	91.4	73-126	7.71	1.03	40	89.8	76-102	4.23	1.14	1.03

p-value significant at <0.05

Table 4.17: Means, standard deviations, and univariate F-ratios for pelvic measurements of young white females (50 years and younger) and old white females (over 50 years).

	Young white females					Old white females					Univariate
Variables (mm)		Mean	Range	s.d.	S.E.		Mean	Range	s.d.	S.E.	F-ratio
	n					*n*					
Pelvis length	13	204.8	184-217	9.47	2.2	69	208.2	178-240	10.79	1.3	1.52
Pelvis breadth	13	157.9	144-171	6.93	1.6	69	160.4	140-185	8.68	1	1.22
Pubis length	13	81.5	73-89	4.72	1.1	67	81.6	66-94	6.79	0.8	0.00
Ischium length	13	85.0	77-88	3.84	0.9	67	87.1	74-97	4.54	0.5	3.19
Ischio-Pubic index	13	96.0	87-103	4.54	1.1	67	93.8	78-113	7.14	0.9	1.50

p-value significant at <0.05

Table 4.18: Means, standard deviations, and univariate F-ratios for pelvic measurements of black males and white males.

	Black males					White males					Univariate
Variables (mm)		Mean	Range	s.d.	S.E.		Mean	Range	s.d.	S.E.	F-ratio
	n					*n*					
Pelvis length	298	202.9	177-238	10.19	0.6	106	222.3	192-248	11.52	1.1	**269.00***
Pelvis breadth	296	149.4	125-199	8.79	0.5	105	163.5	142-183	9.06	0.9	**201.25***
Pubis length	298	71.4	52-92	6.54	0.4	106	78.6	61-103	7.56	0.7	**89.21***
Ischium length	298	86.2	72-98	4.66	0.6	106	94.2	74-109	6.19	0.6	**194.07***
Ischio-Pubic index	298	82.8	60-103	6.61	0.4	106	83.5	68-105	6.6	0.6	0.93

p-value significant at <0.05

Table 4.19: Means, standard deviations, and univariate F-ratios for pelvic measurements of young black males (50 years and younger) and old black males (over 50 years).

	Young black males					Old black males					Univariate
Variables (mm)		Mean	Range	s.d.	S.E.		Mean	Range	s.d.	S.E.	F-ratio
	n					*n*					
Pelvis length	123	202.6	178-226	10.31	0.9	173	203.2	177-238	10.08	0.7	1.65
Pelvis breadth	123	149.1	128-199	8.93	0.8	171	149.6	125-180	8.72	0.6	0.71
Pubis length	123	70.4	55-84	5.5	0.5	173	72.0	52-92	7.09	0.5	2.29
Ischium length	123	85.9	73-97	4.67	0.4	173	86.5	72-98	4.62	0.3	2.47
Ischio-Pubic index	123	82.1	67-96	5.73	0.5	173	83.3	60-103	7.06	0.5	**3.08***

p-value significant at <0.05

Table 4.20: Means, standard deviations, and univariate F-ratios for pelvic measurements of young white males (50 years and younger) and old white males (over 50 years).

	Young white males					Old white males					Univariate
Variables (mm)		Mean	Range	s.d.	S.E.		Mean	Range	s.d.	S.E.	F-ratio
	n					*n*					
Pelvis length	26	221.4	192-239	11.07	2.1	80	222.6	194-248	11.73	1.3	0.18
Pelvis breadth	26	163.1	142-182	11.55	2.2	79	163.7	149-183	8.12	0.9	0.09
Pubis length	26	82.1	65-95	7.56	1.5	80	77.4	61-103	7.22	0.8	**8.38***
Ischium length	26	95.1	74-107	6.9	1.3	80	93.8	80-109	5.94	0.7	0.81
Ischio-Pubic index	26	86.5	76-105	6.82	1.3	80	82.6	68-98	6.26	0.7	**7.68***

p-value significant at <0.05

Table 4.21: Classification of age groups for comparison of means with the advancement of age.

Age Category	Age in Years
1	18-20
2	21-30
3	31-40
4	41-50
5	51-60
6	61-70
7	71-80
8	81-90
9	91-100

Figure 4.1: The relationship between the circumference of the humerus with age in black females and males.

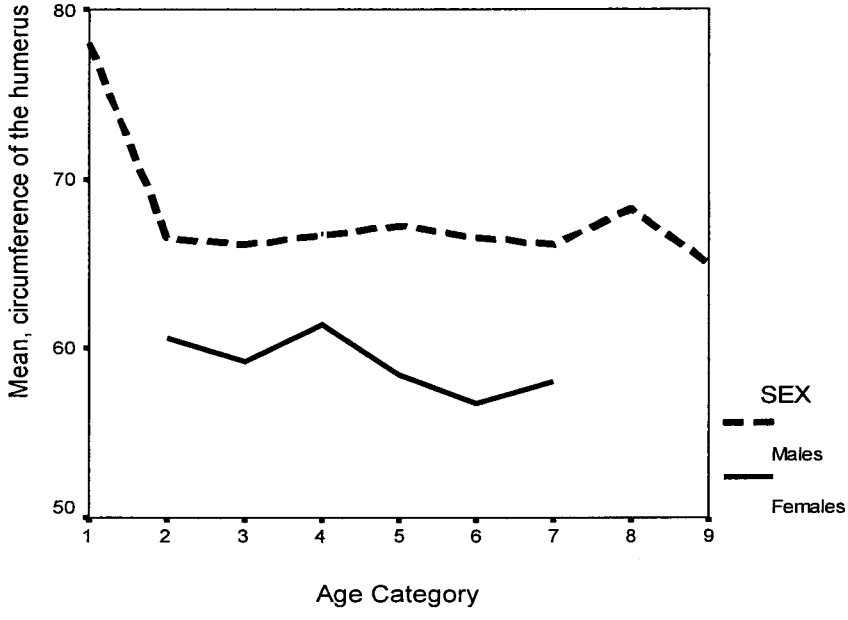

Figure 4.2: The relationship between the humeral head diameter with age in white females and white males.

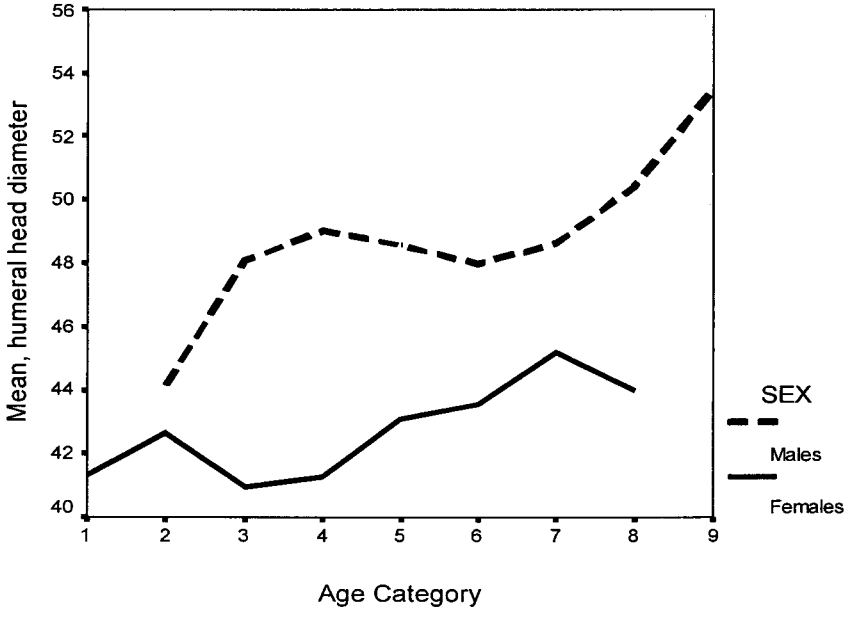

Figure 4.3: The relationship between the diameter of the humerus at midshaft with age in white females and males.

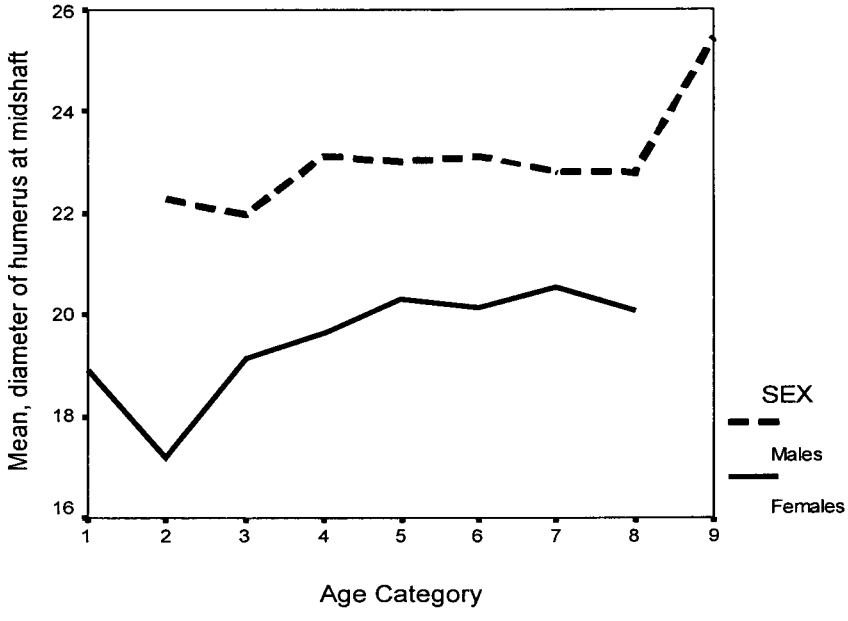

Figure 4.4: The relationship between the distal epicondylar breadth of the humerus with age in white females and white males.

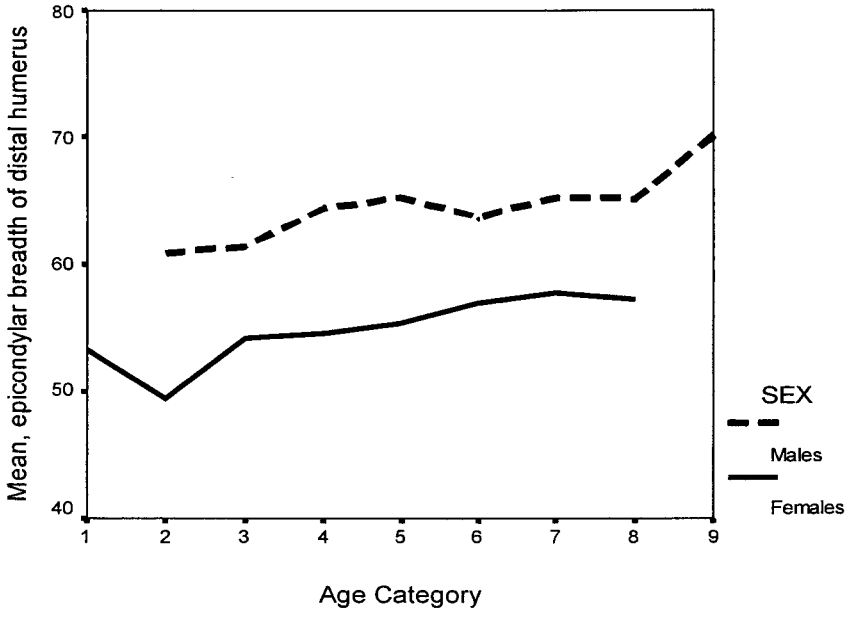

Figure 4.5: The relationship between the superior head diameter of the ulna with age in white females and white males.

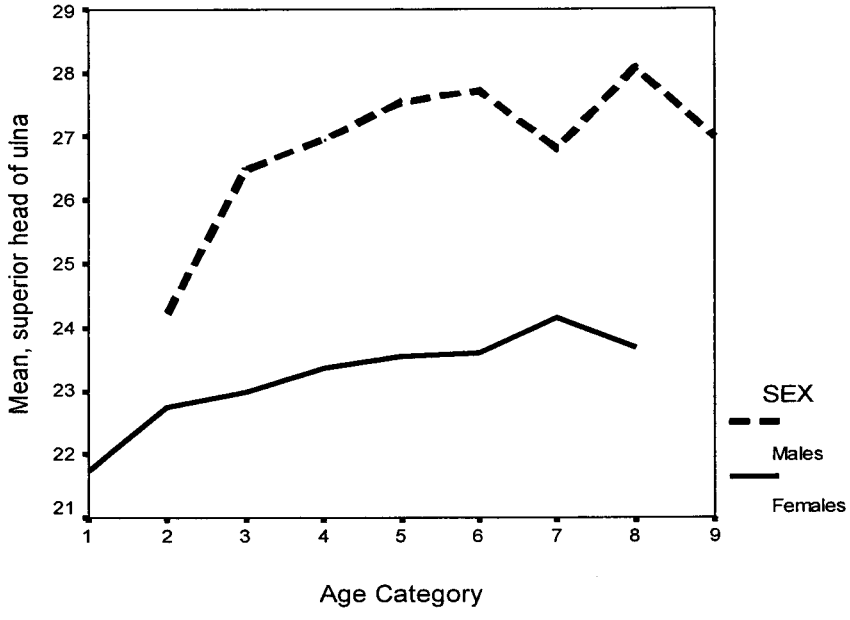

Figure 4.6: The relationship between the inferior head of the ulna with age in white females and white males.

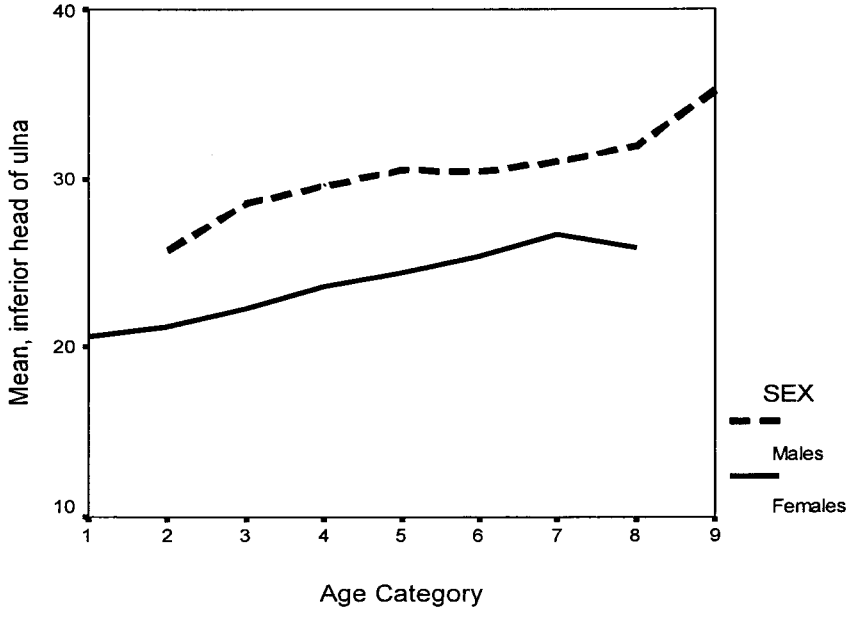

Figure 4.7: The relationship between the diameter of the ulna at midshaft with age in white females and white males.

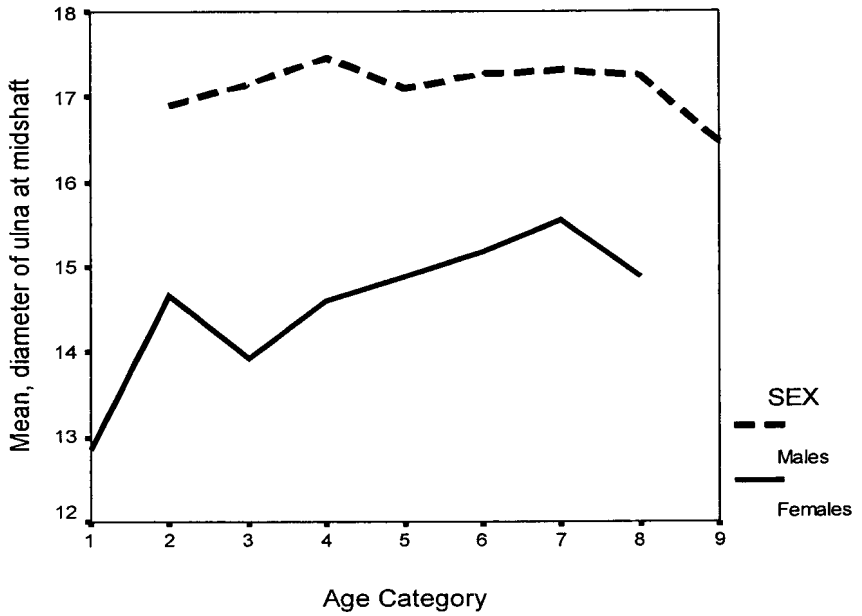

Figure 4.8: The relationship between the distal diameter of the ulna with age in white females and white males.

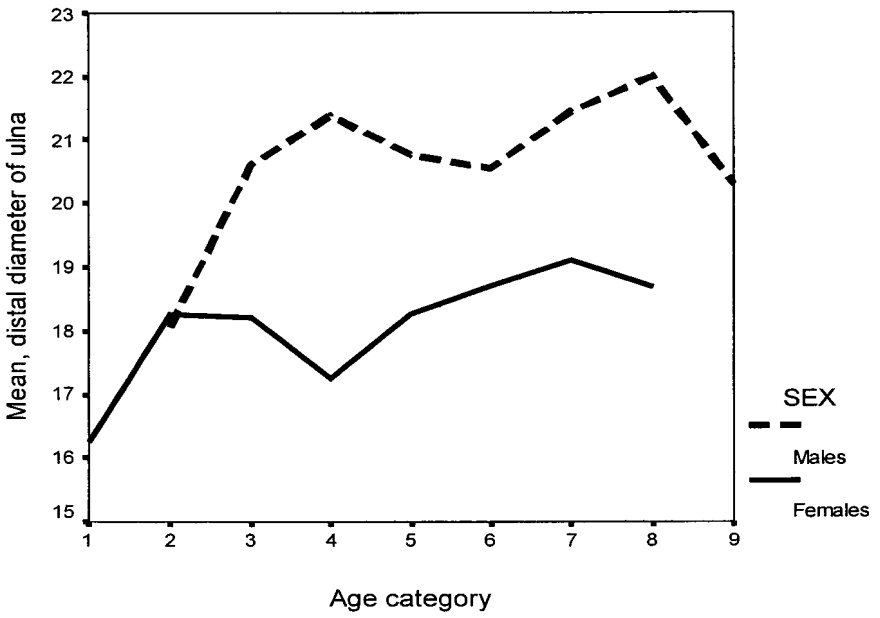

Figure 4.9: The relationship between the olecranon-coronoid diameter with age in white females and white males.

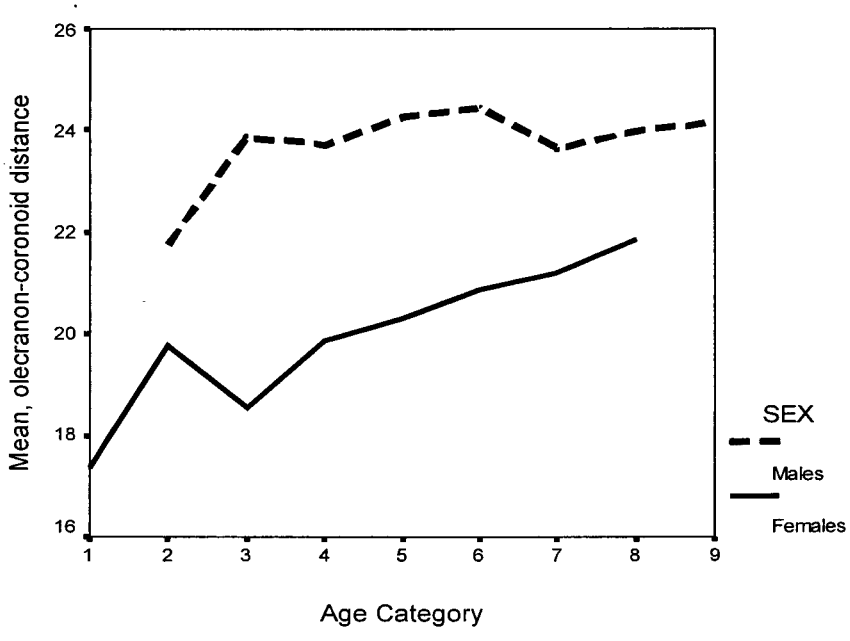

Figure 4.10: The relationship between the head of the radius with age in white females and white males.

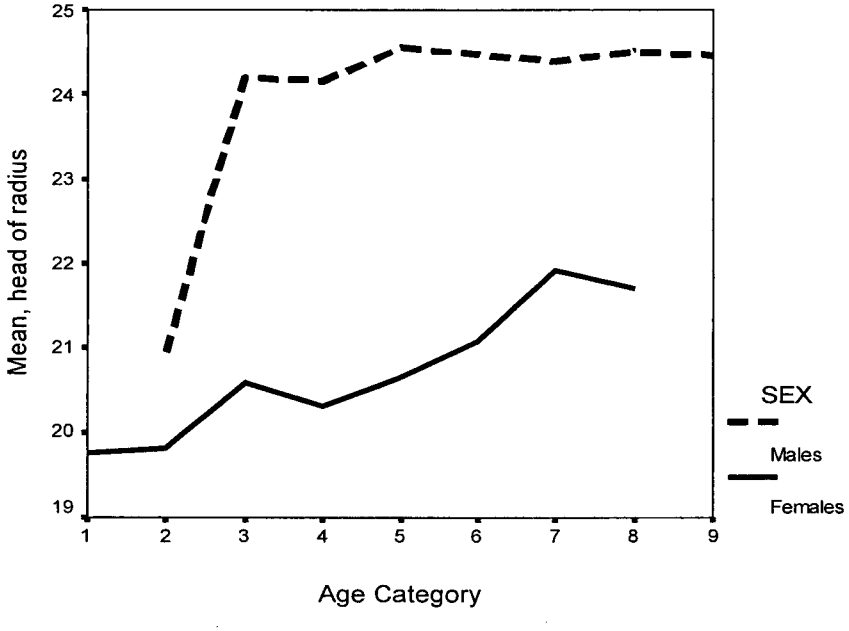

Figure 4.11: The relationship between the diameter of the radius at midshaft with age in white females and white males.

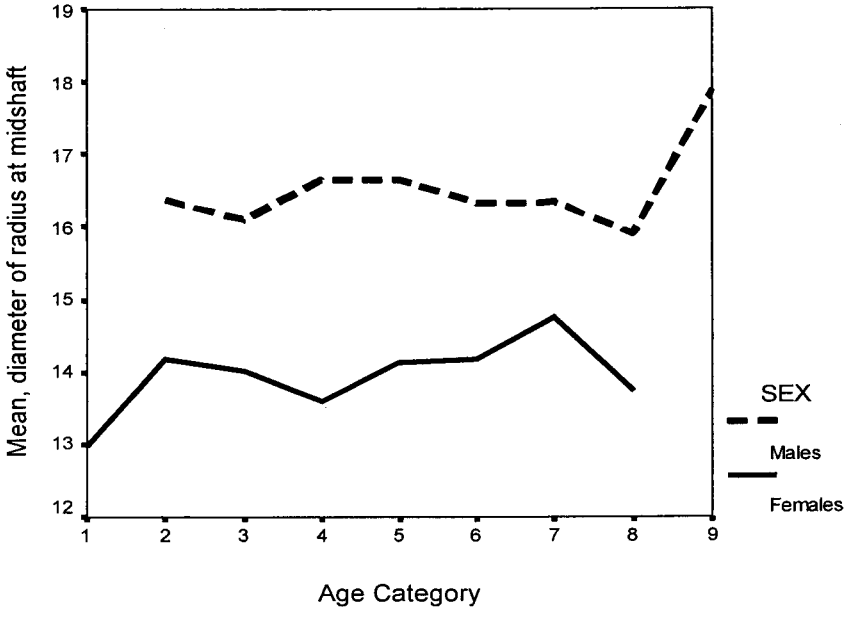

Figure 4.12: The relationship between the diameter of the distal radius with age in white females and white males.

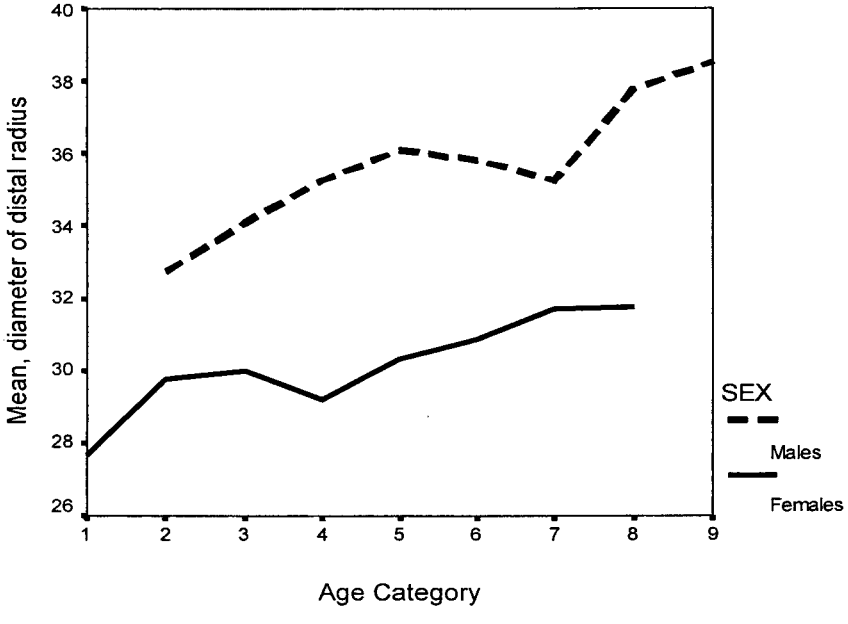

Figure 4.13: The relationship between the vertical diameter of the femoral head with age in white females and white males.

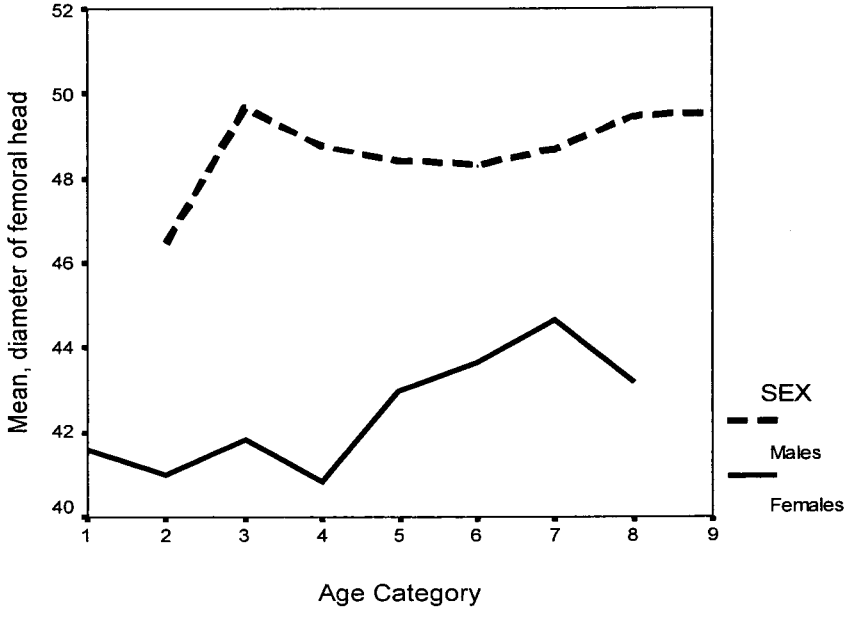

Figure 4.14: The relationship between the diameter of the femur at midshaft with age in white females and white males.

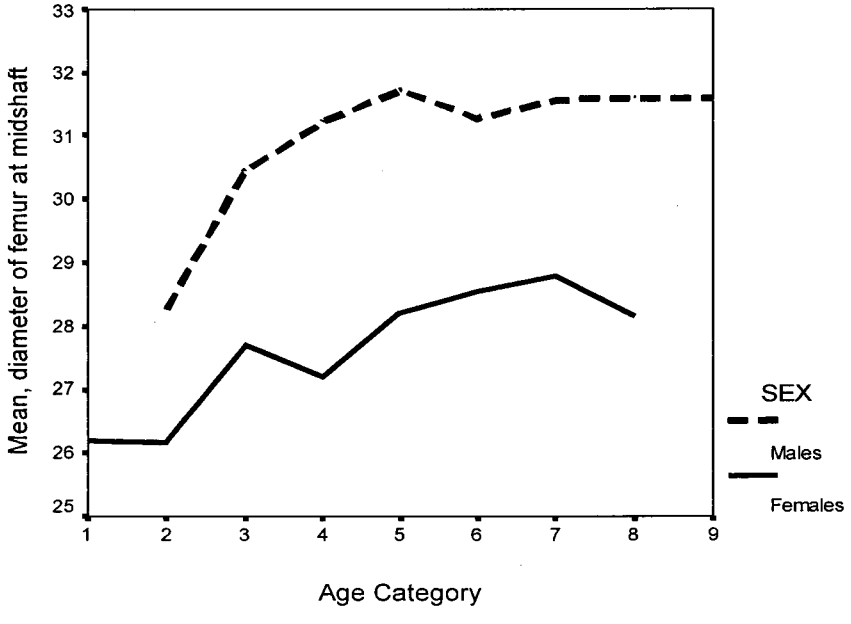

Figure 4.15: The relationship between the maximum bicondylar breadth of distal femur with age in white females and white males.

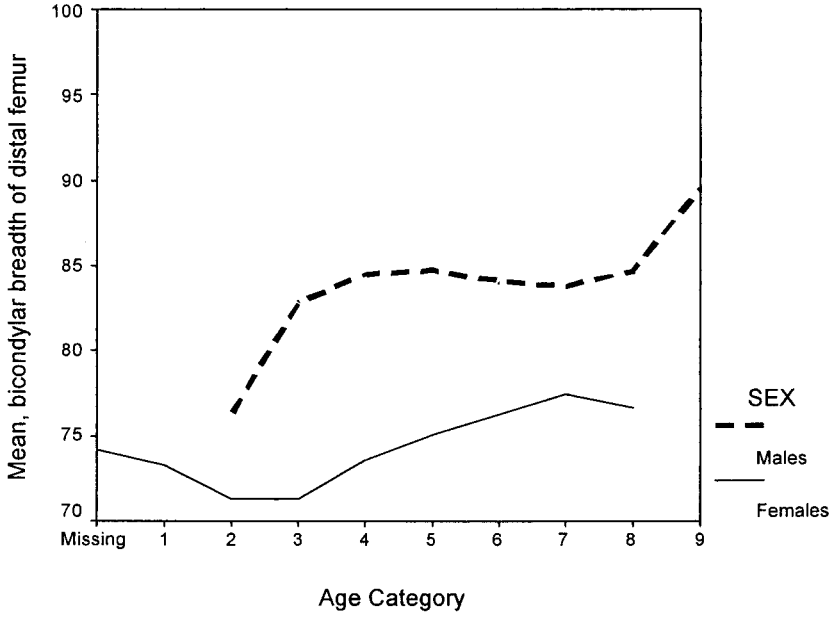

Figure 4.16: The relationship between the bicondylar breadth of the proximal tibia with age in white females and white males.

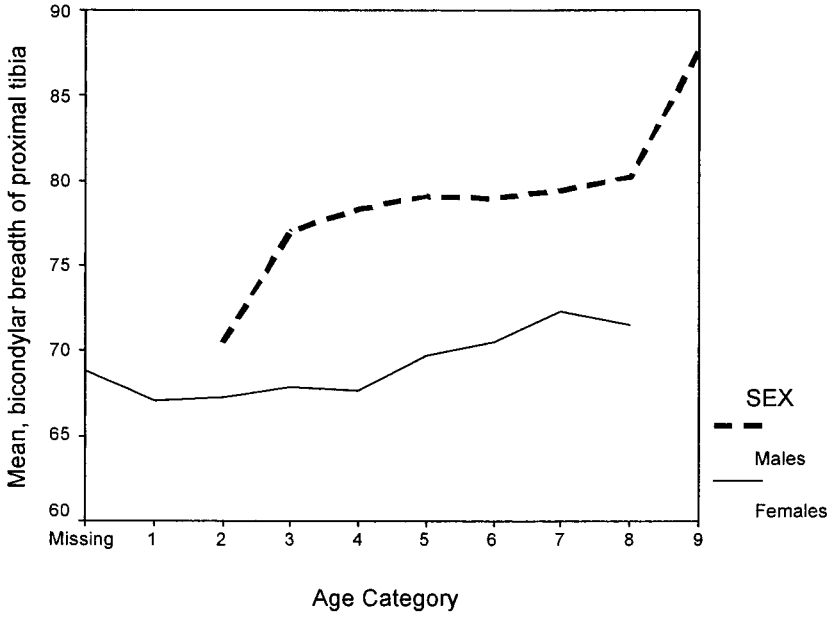

Figure 4.17: The relationship between the diameter of the tibia at midshaft with age in white females and white males.

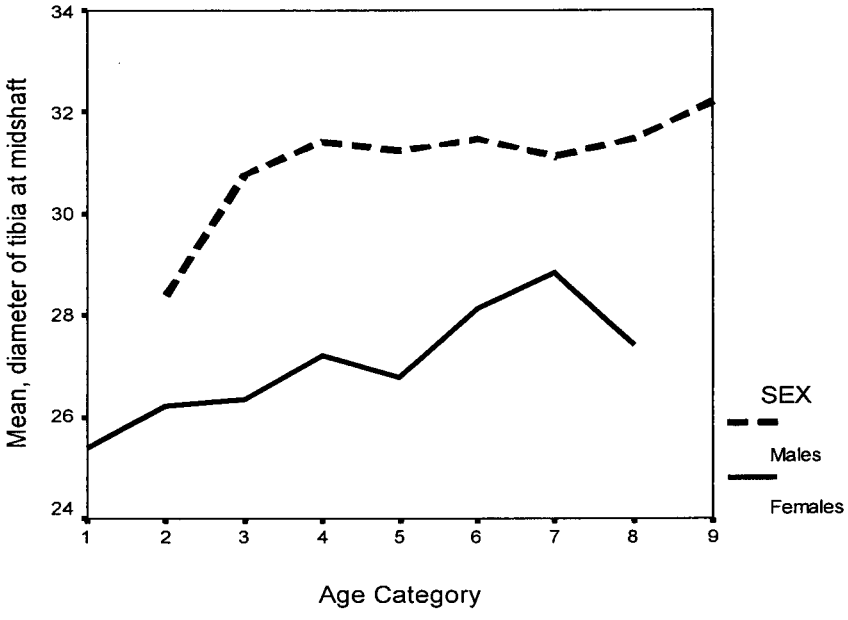

Figure 4.18: The relationship between the diameter of the head of the fibula with age in white females and white males.

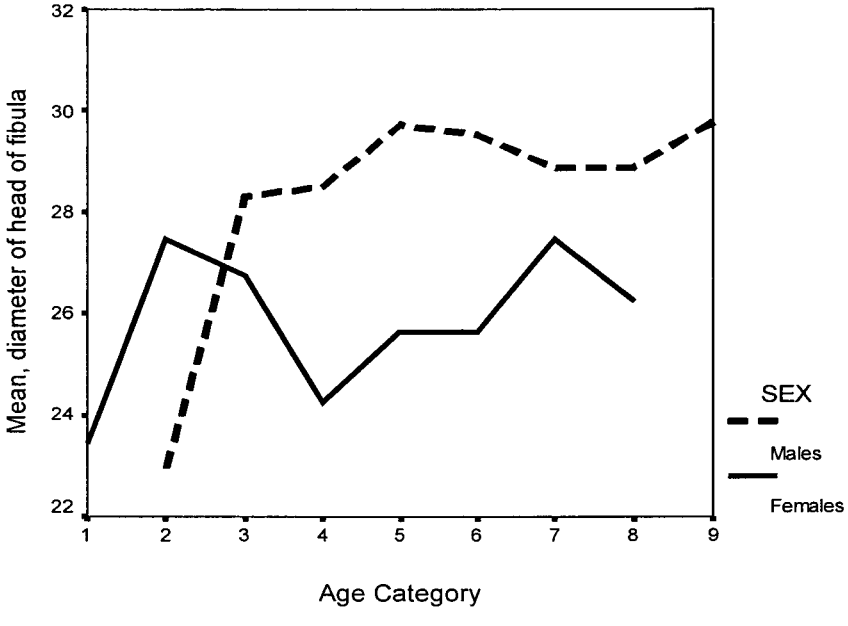

Figure 4.19: The relationship between the diameter of the distal fibula with age in white females and white males.

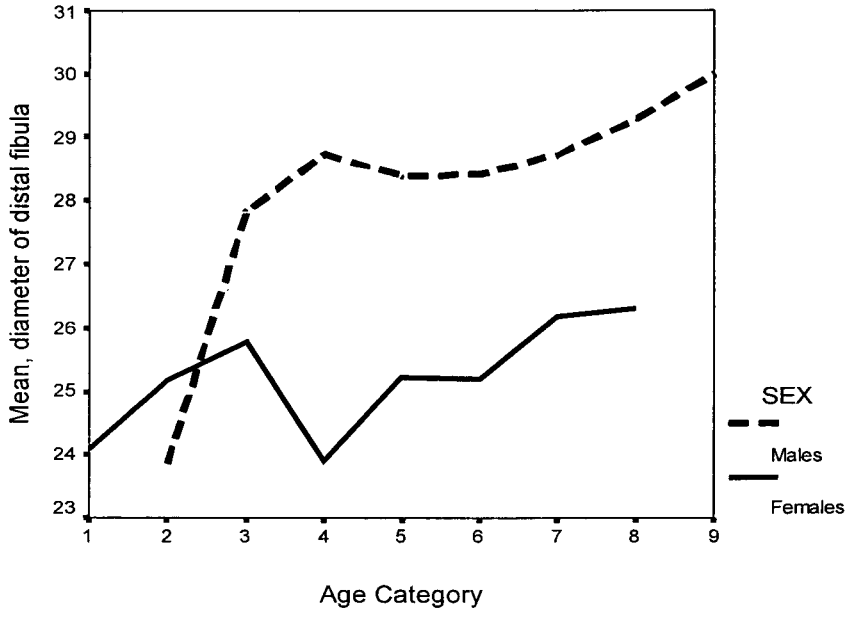

Figure 4.20: The relationship between the diameter of the humerus at midshaft with age in black males and black females.

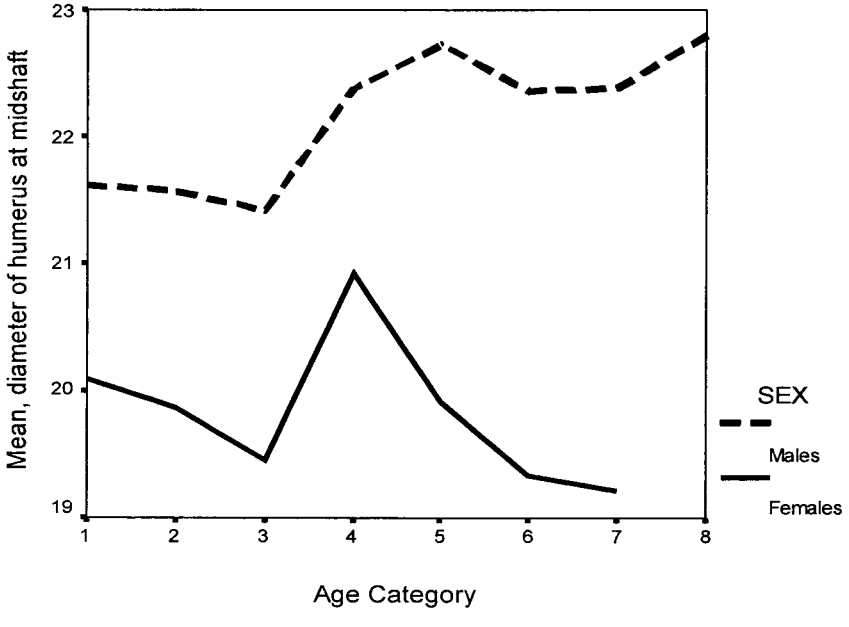

Figure 4.21: The relationship between the epicondylar breadth of the distal humerus with age in black males and black females.

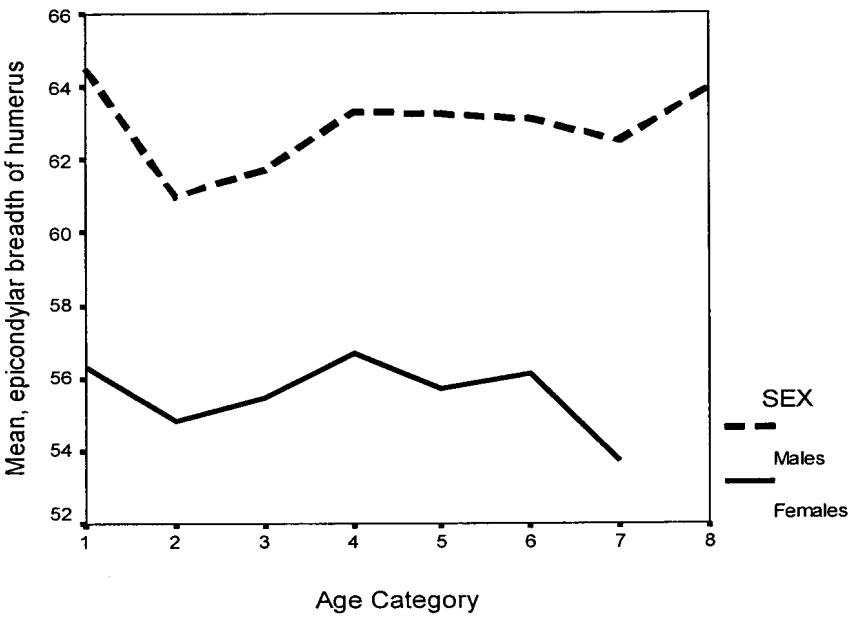

Figure 4.22: The relationship between the diameter of the superior head of the ulna with age in black males and black females.

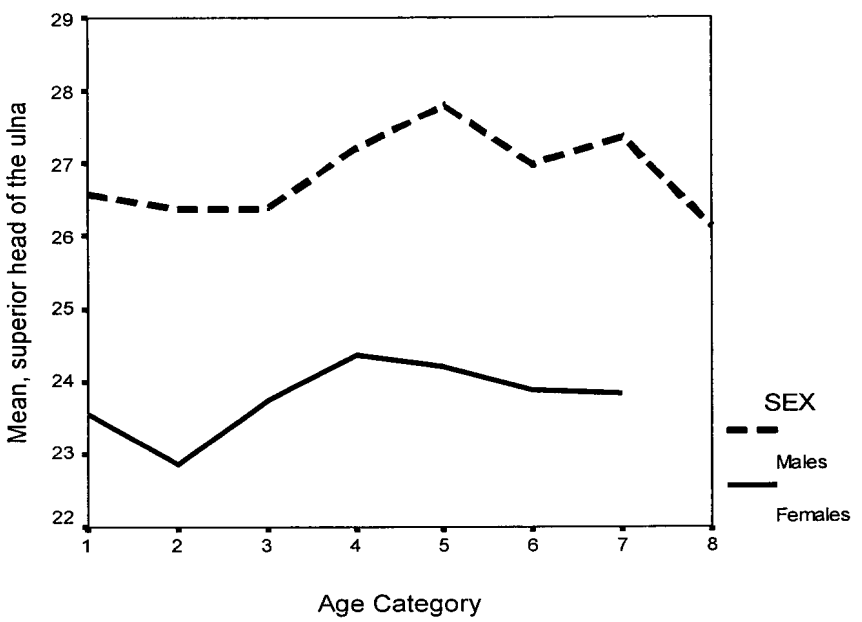

Figure 4.23: The relationship between the diameter of the ulna at midshaft with age in black males and black females.

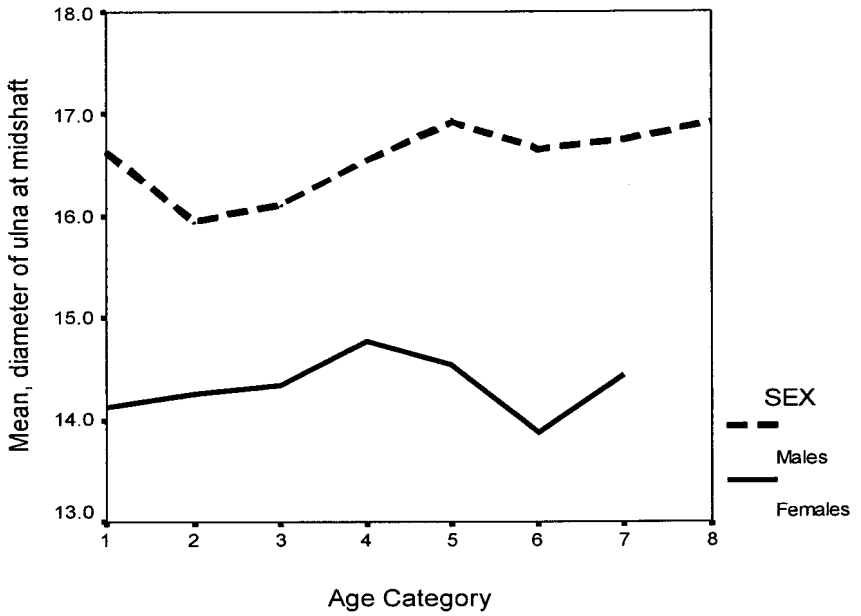

Figure 4.24: The relationship between the diameter of the femur at midshaft with age in black males and black females.

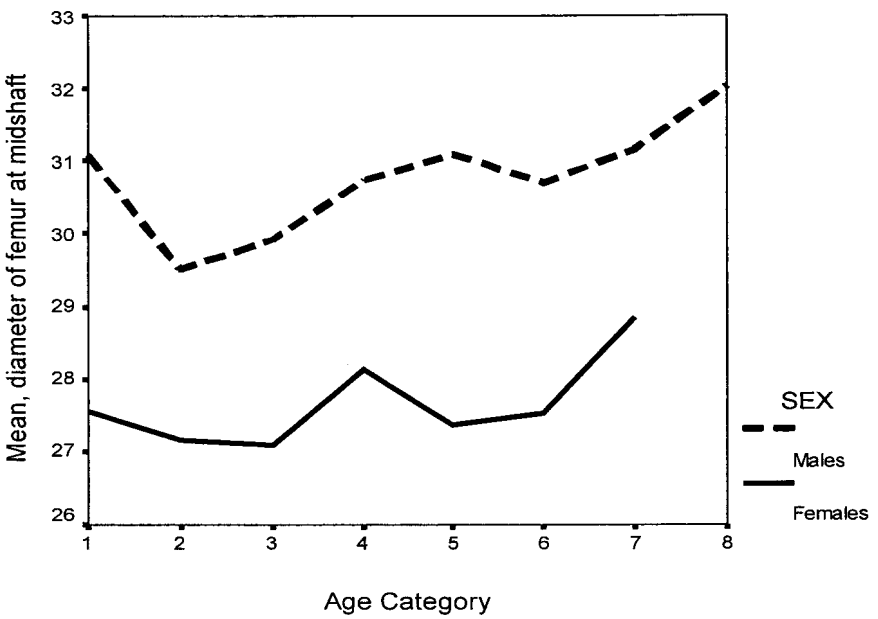

Figure 4.25: The relationship between the bicondylar breadth of the proximal tibia with age in black males and black females.

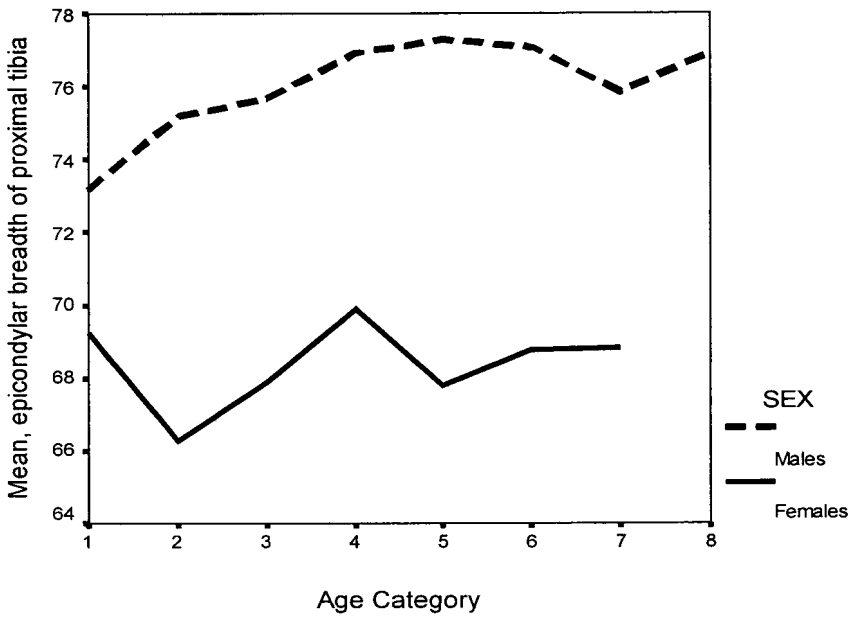

Figure 4.26: The relationship between the diameter of the head of the fibula with age in black males and black females.

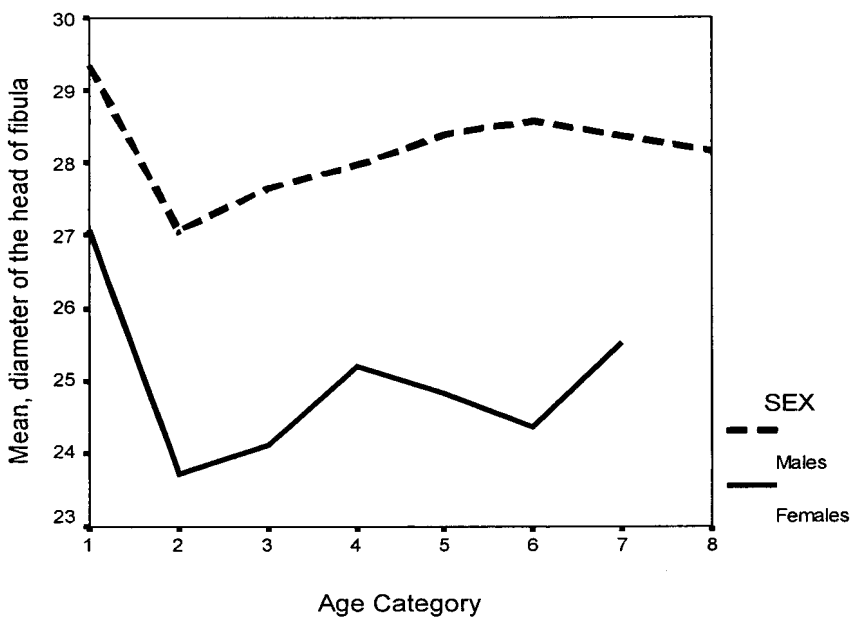

Figure 4.27: The relationship between the diameter of the inferior head of the ulna with age in white males and white females.

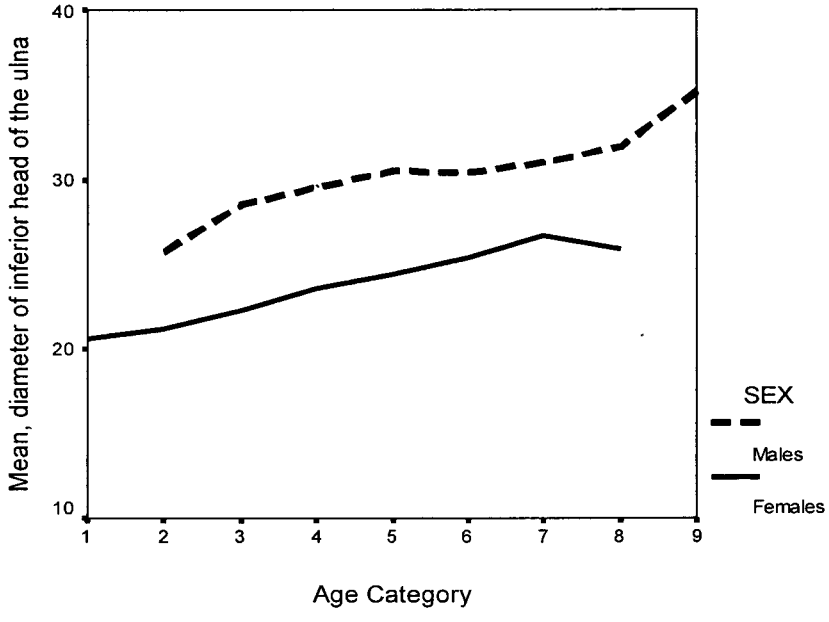

Figure 4.28: The relationship between the diameter of the distal radius with age in white males and white females.

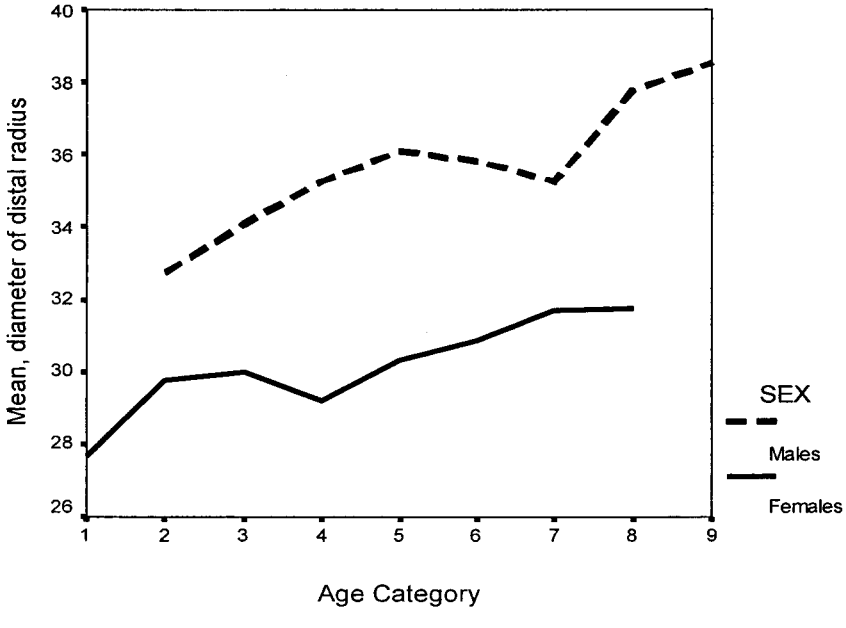

Figure 4.29: The relationship between the bicondylar breadth of the proximal tibia with age in white males and white females.

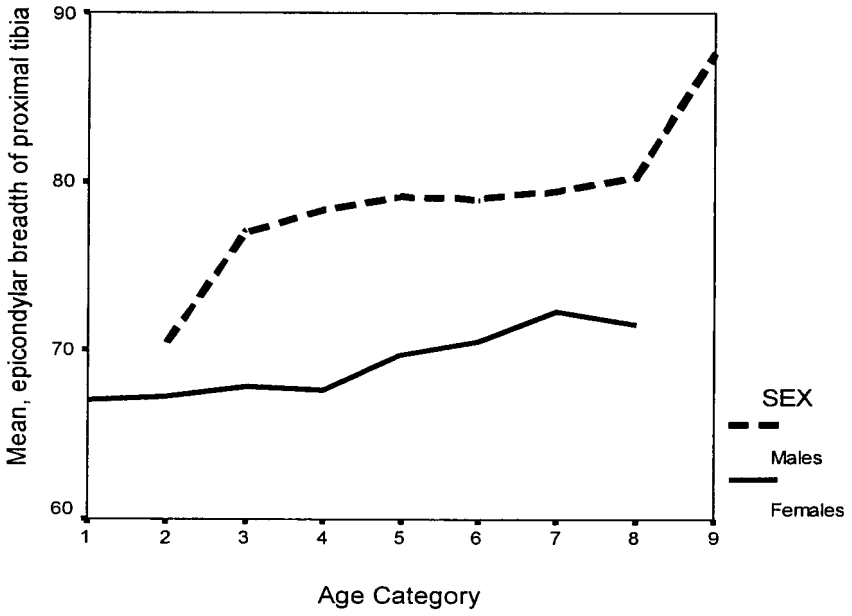

Figure 4.30: The relationship between the ischio-pubic index with age in black males and black females.

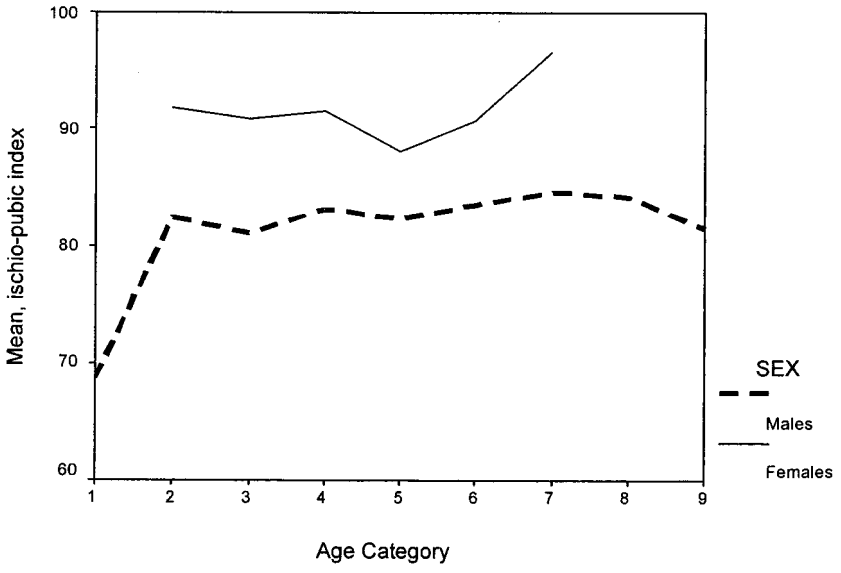

Figure 4.31: The relationship between the pubis length with age in white males and white females.

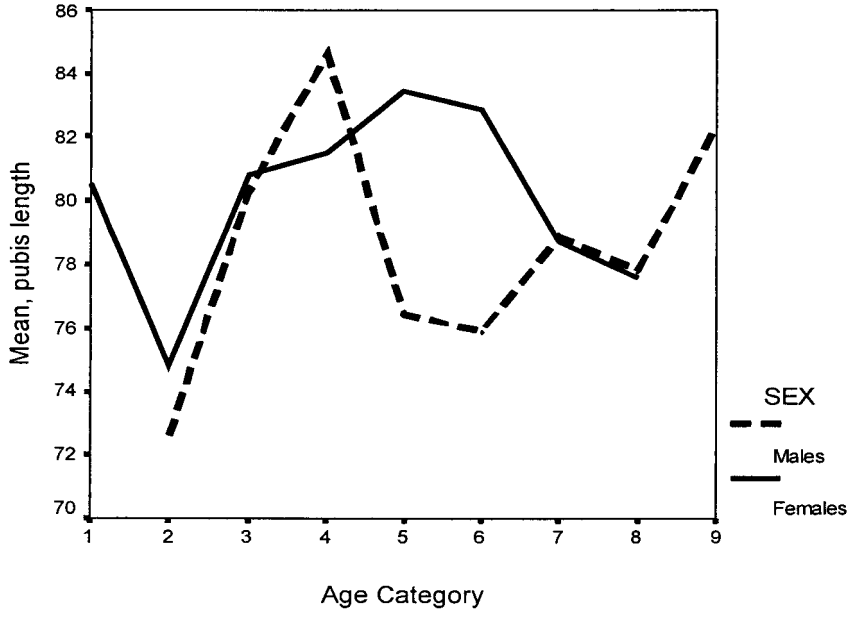

Figure 4.32: The relationship between the ischio-pubic index with age in white males and white females.

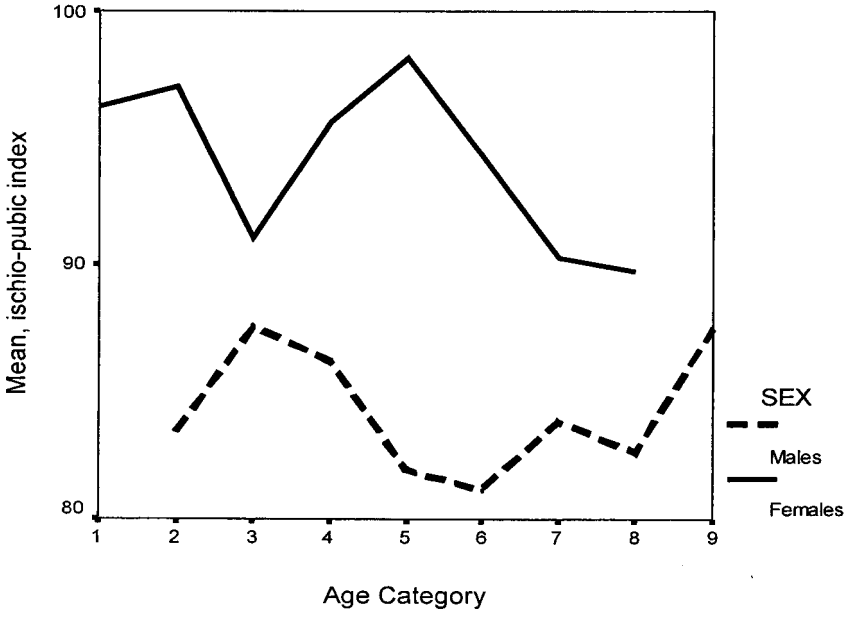

Figure 4.33: Statistically significant measurements that *decreased* (in blue) for the black female skeleton from the young age group (50 years and younger) to the old age group (over 50 years). None increased with age.

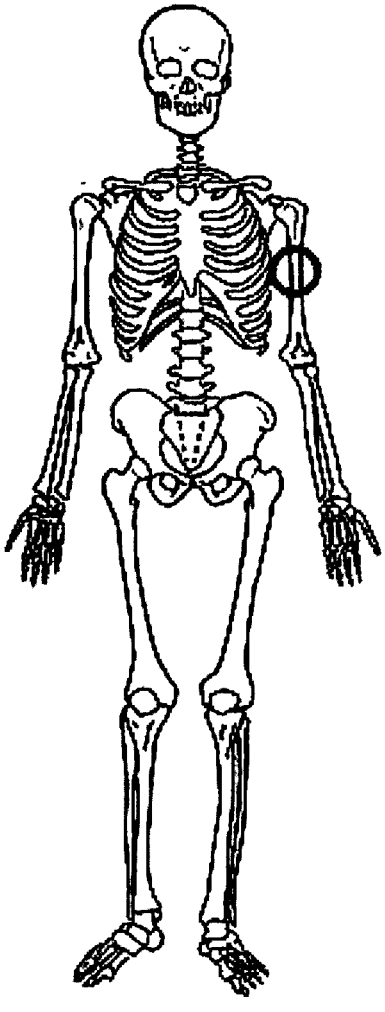

Figure 4.34: Statistically significant measurements that *increased* (in red) for the white female skeleton from the young age group (50 years and younger) to the old age group (over 50 years).

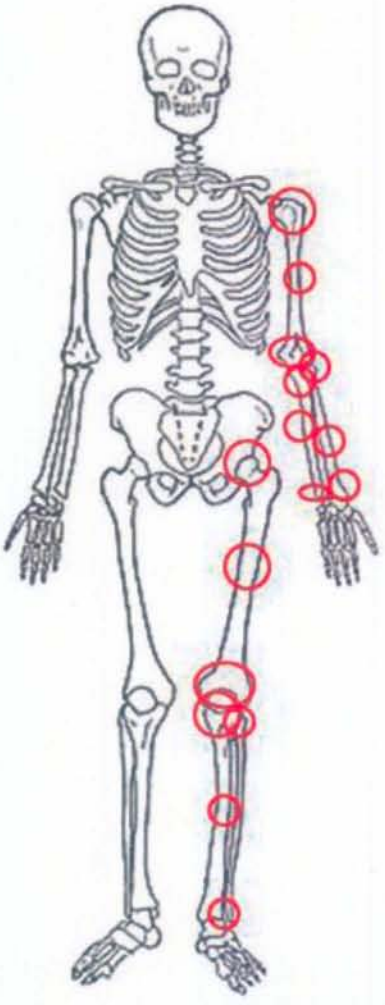

Figure 4.35: Statistically significant measurements that *increased* (in red) for the black male skeleton from the young age group (50 years and younger) to the old age group (over 50 years).

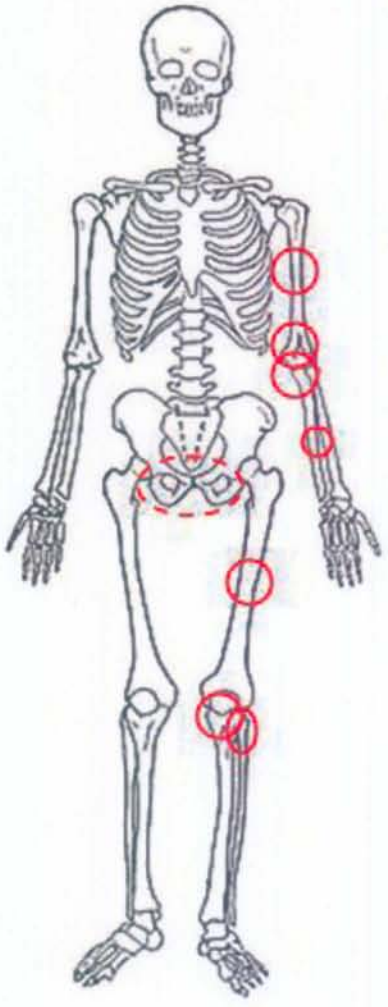

Figure 4.36: Statistically significant measurements that *increased* (in red) and *decreased* (in blue) for the white male skeleton from the young age group (50 years and younger) to the old age group (over 50 years).

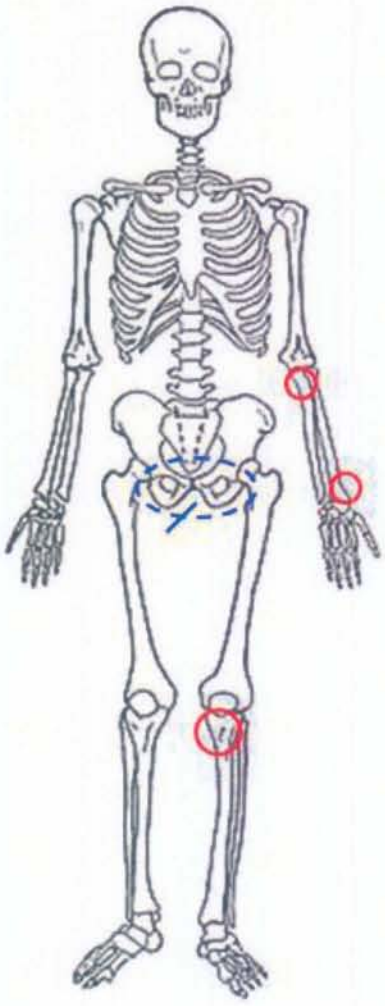

CHAPTER 5

RESULTS of NON-METRIC ANALYSIS

Based on published and known sexually dimorphic visual traits found on the postcranial skeleton (Bass 1995; Rogers 1999; Wanek 2002), two skeletal elements, the distal humerus and pelvis, were used in the attempt to successfully categorize skeletal sex. Subsequently, these visual assessments were subjected to statistical analysis to determine if the predictive value of each feature changed with the onset of age. If a change in accuracy was observed, the location and implications were addressed. The results of analyses of non-metric data from features present on the distal humerus are summarized in Section 5.1. The possibility of improving classification accuracy by removing one non-metric humeral trait is discussed in Section 5.2. Sections 5.3 and 5.4 summarize the analyses of non-metric data of the distal humerus in different male and female populations with the onset of age. Changes in non-metric data related to the pelvis in males and females with the onset of age is arranged in Sections 5.5, 5.6 and 5.7.

5.1

Results of non-metric data from the humerus

Four traits of the distal humerus, namely medial epicondylar symmetry, trochlear extension, olecranon fossa shape, and medial epicondylar angle were used as characteristics for sex determination of the humerus, and comprised an amalgamated score that resulted in the estimation of sex for each specimen. "Estimated sex" was then obtained based on a combination of all four visual traits.

Classic Pearson's chi square statistical analyses were performed on the total sample in order to determine the efficacy of humeral traits as a predictor of sex. Each humeral trait was individually analyzed to determine the relative efficacy of the

characteristic in its predictive value for accurately classifying sex. Scoring for each trait was completed with a [1] through [5] determination method to gauge the degree of sexual dimorphism in the individual characteristic. The allocation of a [1] represented the most typical male morphology, whereas [5] represented the most typical female morphology. Subsequently, [2] represented intermediate male morphology, [3] was considered ambiguous morphology, and [4] represented intermediate female morphology (see Chapter 3, section 3.2.1, "data collection for non-metric information" for a more detailed description of these features). Tables in this chapter display the number of specimens that exhibited each "grade" under each score of [1] through [5]. Based on chi square values observed for each trait, males and females appeared significantly different from each other on a statistical level.

5.1.1

Sex determination from epicondylar symmetry (all males and females)

Although the chi square test indicated significant differences between the male and female morphology, the placement of the medial epicondyle within the circular profile of the trochlea (epicondylar symmetry) was not considered an accurate predictor of sex in males; only 40% of males (168/420) were correctly identified from this trait (classified as [1] or [2], Table 5.1). This characteristic accurately placed more females in the correct category than males (classified as [4] or [5], 71%, 134/188). In addition, 14% of the total sample could not be classified as either male or female, meaning the individual element exhibited ambiguous morphology (classified as [3], Figure 5.1). In addition, a large number of male medial epicondyles and their symmetry patterns exhibited intermediate female/ [4] morphology.

5.1.2

Sex determination from trochlear extension (all males and females)

Trochlear extension was also a relatively inaccurate classification trait when observed in isolation. Only 45% of males were correctly classified, in contrast to 56% of females (Table 5.2). This trait was still considered sexually dimorphic based on the distribution of correctly assigned cases and the subsequent Pearson's chi square analysis, which showed statistically significant differences between the sexes (Figure 5.2).

5.1.3

Sex determination from olecranon fossa shape (all males and females)

Olecranon fossa shape was observed to be one of the better traits of the distal and posterior humerus to correctly classify skeletal sex. As seen in Table 5.3, 57% of males were correctly classified when combining the assignment of a [1] (male trait) and a [2] (intermediate male trait). The olecranon fossa shape as a female predictor was 60% accurate in isolation. Nineteen percent (113/ 608) of all specimens were ambiguous in their olecranon fossa morphology (Figure 5.3).

Pearson's chi square value determined that this characteristic was sexually dimorphic on a statistically significant level. The olecranon fossa shape was considered to be distinguishable between males and females.

5.1.4

Sex determination from the angle of the medial epicondyle (all males and females)

The angle of the medial epicondyle was also considered sexually dimorphic based on Pearson's chi square value and its significance level (Table 5.4). The angle of the medial epicondyle classified 71% of all males correctly, and 55% of females.

The angle of the medial epicondyle exhibited classification accuracies for males and females that indicated distinct sexual dimorphism in the feature, and produced a minimal number of ambiguous cases (6%, Figure 5.4). As seen in the bar graph for classification accuracy, the angle of the medial epicondyle appeared sexually dimorphic on a statistically significant level. This isolated trait of the distal humerus proved to be one of the better predictors of sex.

5.1.5

Final estimated sex from the distal humerus (all males and females)

Based on chi square values, a significant difference was observed between males and females for the ultimate determination of "estimated sex". Estimated sex was the final determination of sex classification when the four characteristics previously discussed were combined. To determine estimated sex, scores for each of the four humeral traits were combined, and a final value was placed on the specimen (4 through 11 for males, 12 for ambiguous, 13 through 20 for females). This value determined the final classification of the specimen as either a [1] male, [3] ambiguous, or [5] female (see Table 5.5). Final classification accuracies for sex estimation were 62% for male specimens and 72% for female specimens. Based on the chi square significance of estimated sex from the humerus, each characteristic was established as sexually dimorphic, as was the final determination of estimated sex from the distal humerus.

Distributions of final male and female classifications appear in Figure 5.5. Allocation based on the percentage of correct assignments showed the delineation between male and female morphology in the distal humerus. From these results it can be seen that each humeral characteristic, when used in isolation, was not necessarily an accurate predictor of sex. However, when taking a combined, total score based on a [1] through [5] determination from each trait, the deduction of estimated sex was moderately accurate for both males and females.

Based on chi square values, a statistically significant difference was observed between males and females and the characteristic morphology of medial epicondylar symmetry, trochlear symmetry, olecranon fossa shape, and medial epicondylar angle. In Table 5.6, under each column heading the number of specimens which were observed to exhibit each "grade" of morphology (and their resulting percentage of classification accuracy), is shown. Estimated sex in Table 5.6 (and all other subsequent tables) is *not* a column total for each value; it is a final amalgamation of the total scores of all humeral characteristics. Specimens exhibiting a majority of male characteristics were categorized as male under "estimated sex". Thus, humeral traits exhibiting a [1] and [2] were combined in the table under 1 (M), because both represented male morphology. Specimens exhibiting a majority of female characteristics were categorized as female under estimated sex, and placed in the table under 5 (F). Humeral traits exhibiting a [4] and [5] were combined because both represented female morphology. Some specimens exhibited an equal number of male and female characteristics, and were ultimately categorized under "estimated sex" as [3], or ambiguous. Estimated sex in each table should thus be viewed as the ultimate classification score (with the resulting percentage of accuracy noted in parentheses).

5.2

Removal of inaccurate trait (s) and the improvement in classification accuracy for the distal humerus

Because the non-metric analysis of traits from the distal humerus relied on features with fluctuating statistical significance, the trait that performed most poorly was discarded in an attempt to more accurately classify "estimated sex" and improve the classification accuracy of the sample. Medial epicondylar symmetry had a lower association with sex than the other three characteristics and did not associate

strongly with sex when analyzing data. Sex determination by medial epicondylar symmetry was removed from the data, and statistical analyses were then performed on the "estimated sex" determination based on a condensed suite of three morphological traits (trochlear symmetry, olecranon fossa shape, and medial epicondylar angle). The distribution of re-classification efforts is summarized in Table 5.7. A total of 97 cases were still misclassified after removing medial epicondylar symmetry. Twenty-four specimens in total were reclassified incorrectly with the removal of this trait, and a total of 60 specimens improved their classification accuracy from "misclassified" or "ambiguous" to being correctly classified. Seventeen cases were re-classified as ambiguous instead of being patently misclassified as the incorrect sex.

The removal of medial epicondylar symmetry from the data allowed for the correct assignment of a total of 60 otherwise ambiguous or misclassified cases. As seen in Table 5.8 and the corresponding bar graph in Figure 5.6, the classification accuracies for both males and females increased. Males were now classified with an increased accuracy rate of 74% (in contrast to 62% with four characteristics), and female estimated sex determination increased 5% in accuracy (from 72% to 77%). The removal of medial epicondylar symmetry allowed the remaining characteristics to classify skeletal sex equivalent to other anthropological methods used for non-metric sex determination (Albanese *et al.* 2005; Allen *et al.* 1987; Rogers 1999; Ubelaker and Volk 2002; Walrath *et al.* 2003; Wanek 2002).

5.3

Comparison of non-metric data from the humerus: females

After determining the degree of sexual dimorphism in the distal and posterior humerus, the variation between populations within the categories of "male" and "female" were examined. An assessment was done in order to establish whether

significant differences existed between the biological affiliations. If not, the results would be documented but groups would otherwise be combined in future analyses. Based on the separation of groups in Chapter 4: Results of Metric Analysis, the sample was separated into "black" and "white" categories, and the results tested to determine if sex classification was dependent on these biological groups for males and females. The categories of "black female", "white female", "black male", and "white male" were utilized. The non-metric classification accuracies of black females were therefore compared to that of white females by means of Pearson's chi square statistics, and differences noted where applicable. Similarly, black and white males were compared.

Non-metric traits of the humerus were categorized into populations to observe specific differences between "black females" and "white females". Populations were considered discrete in these initial analyses and each population data set was examined for classification accuracy fluctuations with the onset of age. A change in the predictive quality of each feature and a change in the classification accuracy for the ultimate determination of sex were noted when applicable.

5.3.1

Classification accuracy for black females vs. white females

A comparison of the categories "black female" and "white female" was performed to reveal the differences, if any, between the two groups (Table 5.9). When observing the specific traits in isolation, the shape of the olecranon fossa was observed to classify better in black than white females (73% and 45%, respectively). This difference in classification accuracy resulted in a statistically significant outcome between female groups. When sex was estimated from the amalgamation of the three humeral traits, this estimation was found to be different depending on the biological affiliation on a statistically significant level. Sex was estimated correctly in 84% of all black females, and 68% in all white females (Figure 5.7). Based on the

Pearson's chi square value (7.015, df=2, 0.030<0.05), estimated sex was dependent on the biological affiliation in females. Females from both populations were correctly classified on an accurate level. Characteristics of the distal humerus proved to be valid criteria for sex determination for both black and white females, although sex was predicted at a higher accuracy rate with black females. Based on Figure 5.7, it was interesting to note that 26% of the total white female sample was misclassified as male. A minimum number of females were deemed ambiguous between populations (5% for black females and 6% for white females).

5.3.2

Classification accuracy for young black females vs. old black females

Females were then separated and statistical analyses were performed to view changes with age in each biological group. Black females and their classification accuracy did not change significantly with age when observing any of the traits from the distal humerus (Table 5.10; 88% for young, 78% for old). Figure 5.8 illustrates the percentages of accuracy between young and old samples in this biological group when all variables were combined to observe "estimated sex".

5.3.3

Classification accuracy for young white females vs. old white females

In white females, the classification accuracy of two isolated humeral characteristics (olecranon fossa shape and medial epicondylar angle) changed on a significant level with the onset of age (Table 5.11). These significant changes increased the classification accuracy of the angle of the medial epicondyle from 36% accurate in young females to 56% accurate in old females, while decreasing the classification accuracy of the olecranon fossa shape from 79% accurate in young females to 38% accurate in old females.

Estimated sex is the final incorporation of isolated humeral trait scores used to predict skeletal sex. As seen in Figure 5.9, the percentage of white females

correctly classified by distal humeral traits decreased from 93% to 63% with the onset of age, which indicated a marked decrease in the classification accuracy of the feature. However, the 30% decrease in accuracy was statistically insignificant. The fact that this marked decrease in predictive value was statistically non-significant may be the result of the small sample size (n = 13) of the young white females.

The ultimate result of "estimated sex" is similar in both black females and white females. Changes in non-metric morphology were occurring that decreased the classification accuracy of the sex determination in all females. Thus, young female individuals were classified more accurately than older female individuals when utilizing characteristics from the distal humerus. In general, therefore, the results of the black and white females were congruent, as accuracies of both decreased (although not significantly on a statistical level) with age.

5.4

Comparison of non-metric data from the humerus: males

All data from males were observed in the same way as female non-metric data. Non-metric traits of the humerus were categorized into populations to observe specific differences between "black males" and "white males". Populations were considered discrete and each population data set was examined for classification accuracy fluctuations with the onset of age. A change in the predictive quality of each feature and a change in the classification accuracy for the ultimate determination of sex were noted where applicable.

5.4.1

Classification accuracy for black males vs. white males

A comparison of the categories "black male" and "white male" was performed to reveal the relative diversity between the two groups (Table 5.12).

The olecranon fossa shape exhibited statistically significant differences between male populations. This same trait also differed between the female populations. The remainder of the male traits, including the final estimated skeletal sex, were independent of the biological affiliation for their correct classification. Based on the Pearson's chi square value (0.606>0.05), estimated sex was not population-specific; the male sample was categorized with sufficient accuracy regardless of the biological affiliation of males (72% for black males, 78% for white males). The percentages of correct classification between the two male groups can be observed in Figure 5.10.

5.4.2

Classification accuracy for young black males vs. old black males

Young black males differed only slightly in morphology of the distal humerus from old black males (Table 5.13). The classification accuracy of the suite of 3 traits was accurate at 71% for young individuals of this group, and improved with the onset of age to a classification accuracy of 74%. This increase in accuracy was not statistically significant, however. The only trait that changed in a statistically significant manner was the shape of the olecranon fossa, in which accuracy decreased slightly with advanced age. These results indicated a slight general increase in accuracy with the onset of age in the black male humerus (Figure 5.11).

5.4.3

Classification accuracy for young white males vs. old white males

White males were predicted with more accuracy in general than their black male counterparts, but their classification accuracy decreased with age (black males 71% - 74%, white males 86% - 75%). This result was not statistically significant. Trochlear extension as an isolated element, however, was statistically different between young and old white males in its classification accuracy; correct categorization of white males decreased with age in this humeral characteristic from

64% accuracy to 46% accuracy (Table 5.14). The classification accuracy of sex determination with this suite of traits decreased with age, although not significantly (Figure 5.12). When age increased, more male samples were misclassified as female, which indicated a general change in morphology based on the lower classification accuracy of the features. In addition, more males were deemed ambiguous in their morphology as age increased. This is in direct contrast to the black male sample, where accuracy increased with the onset of advanced age. However, both differences in classification accuracy were considered statistically non-significant.

The pattern for a decrease in classification accuracy with the onset of age in white males was congruent with the female sample in both white and black populations.

5.4.4

Classification accuracy from the distal humerus: summary

In summary, physical traits from the distal and posterior humerus predicted sex at variable rates for different populations and sexes. Males and females across ancestral groups were quite similar comparatively in their morphology; black and white females exhibited similar morphology while black and white males also showed parallels in the anatomy of the distal humerus. When divided into population affinities and scrutinized between age groups (young=50 years old and younger, old=older than 50 years old), only black male classification accuracy increased with the onset of age. All others (black females, white females, and white males) were observed to decrease in their classification accuracy with age. In general, younger individuals were classified more accurately than older individuals in each of these population categories. Ultimately, although these changes were occurring, they could not be directly associated with age on a statistically significant level.

5.5

Results of non-metric data from the pelvis

Characteristics of the os coxae have been shown to be sexually dimorphic. Four non-metric visual traits (subpubic concavity, subpubic angle, ischio-pubic ramus width and greater sciatic notch width) were used to estimate sex. Based on an amalgamation of the first four visual traits, a final trait, "estimated sex" was determined for each specimen. Scoring of these traits was the same as with the distal humerus; [1] denoted the typical male morphology, [2] an intermediate male, [3] was ambiguous, [4] categorized an intermediate female and [5] denoted typical female morphology. Each pelvic trait was initially analyzed to determine the relative efficacy of the characteristic in its classification accuracy for correctly predicting sex.

5.5.1

Sex determination from the subpubic concavity (all males and females)

The subpubic concavity was an accurate predictor of sex as an isolated pelvic trait. If both categories [1] and [2] were deemed as an accurate diagnosis of a male, and both [4] and [5] deemed accurate as female, 76% of all male specimens and 88% of all female specimens were correctly classified when employing this trait (Table 5.15). Twenty-nine percent of all individuals could not be classified, and were assigned a score of [3] / ambiguous; only 3% of females and 6% of males were incorrectly classified. Males were predicted at a lower rate of accuracy than females, and more males exhibited "ambiguous" morphology with this trait than did females (18% and 10% respectively).

The subpubic concavity of individuals within this sample was sexually dimorphic on a statistically significant level. The results are graphically illustrated in Fig. 5.13, where it can also be seen that the overlap was quite small.

5.5.2

Sex determination from the subpubic angle (all males and females)

As expected, the subpubic angle of the os coxae predicted sex with a high rate of accuracy (Table 5.16). Males were correctly classified with this trait in isolation 67% of the time; in contrast, females were accurately predicted 95% of the time. Males appeared to exhibit more ambiguous morphology with the subpubic angle, while females virtually never exhibited ambiguous morphology (23% and 2%, Figure 5.14). Males exhibited both a wide and narrow subpubic angle based on the results. Females, however, exhibit subpubic angle morphology that is distinctly wide and unambiguous.

5.5.3

Sex determination from the ischio-pubic ramus width (all males and females)

The ischio-pubic ramus width in isolation was considered statistically significant in determining sex ($p = 0.000 < 0.05$). Males once again exhibited less defined morphology than females (Table 5.17).

The classification accuracy of this feature was much more robust with females than males, correctly predicting female skeletal sex 84% of the time, in contrast to only 48% of the time for male specimens. There were also numerous ambiguous cases in the male sample (Figure 5.15). This indicated that the width of the ischio-pubic index tends to be variable in males, yet quite consistently thin and gracile in its morphology in females. These results also imply that if a ramus is robust, it is almost definitively a male, while a thin and gracile morphology may indicate a male or female. The ischio-pubic index was observed to be the least-reliable trait in isolation of the four characteristics of the os coxae.

5.5.4

Sex determination from the width of the greater sciatic notch (all males and females)

Based on Pearson's chi square statistical analysis, this trait in isolation was considered sexually dimorphic on a statistically significant level (Table 5.18). Once again, females were correctly categorized with the use of this trait at a highly accurate rate (88%). Males were categorized at an accuracy rate of 70%. Figure 5.16 illustrates the classification accuracy of the greater sciatic notch in regards to sexual dimorphism. More males (13%) exhibited ambiguous morphology in this feature than did females (6%).

The number of ambiguous cases assigned to male specimens indicated again that male morphology was quite variable in this region with regard to greater sciatic notch width. Males exhibited a range of narrow and wide notch widths, while females appeared to remain constant in their characteristic wide morphology. This implies that an individual with a narrow greater sciatic notch is almost certainly a male, while an individual with a wide notch could possibly be male or female. More males exhibited female morphology than females exhibited male morphology.

5.5.5

Estimated sex (all males and females)

Sex was then estimated from incorporating all characteristics and establishing an ultimate determination of sex. As seen in Table 5.19, sex was predicted at a highly accurate rate, confirming that the non-metric pelvic morphology is sexually dimorphic. Table 5.20 indicates the delineation of trait accuracies with all males and females included within the sample, with 83% of the male sample and 94% of the female sample classified correctly (Figure 5.17).

5.6

Comparison of non-metric data from the pelvis: females

A comparison of the categories "black female" and "white female" was performed to reveal the relative diversity between the two groups. Populations were considered discrete and each population data set was examined for classification accuracy fluctuations with the onset of age. A change in the predictive quality of each feature and a change in the classification accuracy for the ultimate determination of sex were noted where applicable.

5.6.1

Classification accuracy for black females vs. white females

Females were first observed together to define similarities and differences in morphology based on classification accuracies of four characteristics of the pelvis. As seen in Table 5.21, all females regardless of their biological affiliation were classified with a high rate of accuracy with all pelvic traits utilized.

Accuracy rates between populations were congruent, and the ability to correctly categorize sex was independent of biological affiliation with every pelvic trait studied in the female sample. None of the p-values were significant. In other words, the characteristics of the female os coxae were non-population-specific; the population affinity was not needed in order to categorize female sex correctly. Both black and white females were categorized at a high rate of accuracy (Final estimated sex; Fig. 5.18, 93% and 96%, respectively). Black females were observed to be misclassified as males more often than white females; however, this was not statistically significant. The pelvis continued to be a highly accurate predictor of female sex in both populations studied.

5.6.2

Classification accuracy for young black females vs. old black females

The female sample was then divided into "black" and "white" and "young" and "old" groups to observe possible changes in accuracy rates within the groups. As seen in Table 5.22, the ability to determine sex from the pelves of black females is independent of age; sexual dimorphism remained high in black females with the onset of age.

Young females were classified more accurately than old females, although the difference between age groups was minimal (94% and 92%, respectively). This indicated that no considerable morphological changes were observed in visual traits of the os coxae with the onset of age, as seen with the high accuracy in which females were categorized regardless of age group (Figure 5.19).

5.6.3

Classification accuracy for young white females vs. old white females

White females performed much in the same manner as black females in their pelvic morphology, with accuracy in sex determination decreasing with the onset of age on a statistically non-significant level (Table 5.23). Although the accuracy rate decreased as age increased (final estimated sex; 100% for young white females, 94% for old white females), white female pelves were still categorized successfully regardless of the age; predictive values were independent of age (Figure 5.20).

As seen with the black female population, white females were also misclassified as males more often than being deemed ambiguous with the onset of advanced age. These numbers were not large, but indicated that when variation occurred, it occurred as an explicit departure in morphology for white females and not an "ambiguous" one. In general, sexual dimorphism remained constant with this biological group with the onset of age, and age was not considered a negative factor in determining skeletal sex from the os coxae.

5.7

Comparison of non-metric data from the pelvis: males

After confirmation of pelvic sexual dimorphism utilizing four non-metric visual traits and then a final estimate of sex based on these four traits, a comparison of the categories "black male" and "white male" was performed to reveal the relative range of variation between the two biological affiliations as was the case in the previous sections.

5.7.1

Classification accuracy for black males vs. white males

The two male groups were compared to observe any differences or contrasts in the morphology of the pelvis (Table 5.24). The subpubic concavity, the subpubic angle, and the greater sciatic notch width in black males differed significantly in morphology from their white male counterparts. Males from each group, however, were classified at a high rate of accuracy (85% for black males and 79% for white males). This indicated that although three morphological characteristics of the os coxae in males differed between populations in their predictive quality when observing each in isolation, the final determination of sex was not affected by these differences.

It was interesting to note that non-metric morphology in the greater sciatic notch exhibited a statistically significant divergence within biological groups. Greater sciatic notch width was dependent upon population in order to correctly classify skeletal sex in males divided between "black" and "white" groupings. Black males were categorized correctly with greater sciatic notch width morphology 73% of the time, while white males were assigned correctly with this pelvic trait 63% of the time. The greater sciatic notch width appeared to be far more variable in whites than in blacks. Not only are white males assigned to the correct sex less often than black

males, but that they are also misclassified as females more often than black males when observing the greater sciatic notch width in isolation.

When all of the traits were considered together and an estimated sex was obtained, however, this determination was independent of population on a statistically significant level. In other words, black males and white males were congruent with each other, and the population of a specimen was not needed in order to successfully assign it to the correct sex (Figure 5.21). The determination of sex was accurate in 85% of the black male sample when taking the suite of four pelvic traits into consideration, while the white male sample produced an accuracy of 79%.

This result indicated that although some non-metric visual techniques work better on some populations, the final determination of male sex from the pelvis is quite accurate across population affiliations.

5.7.2

Classification accuracy for young black males vs. old black males

As Table 5.25 illustrates, black males increased in their accuracy rates as their age increased. The subpubic angles as well as the greater sciatic notch width were significantly different in their classification accuracies with the onset of age; more characteristic male morphology was seen in older males. Both the greater sciatic notch and the final estimated sex differed significantly on a statistical level between the younger and older groups (Figure 5.22). This indicated that sexual dimorphism in the black male pelvis is significant for young individuals (79% accurate), but becomes even more pronounced with the onset of age (88% accurate).

5.7.3

Classification accuracy for young white males vs. old white males

The onset of age in the white male pelvis was significant when observing the subpubic concavity. When determining the final assessment of skeletal sex, age did not appear to play a role in the successful determination of sex (Table 5.26). In addition, male pelvic traits were independent of age in the majority of features; age did not play a role in the successful determination of sex from the subpubic angle, the ischio-pubic ramus width, or the greater sciatic notch width.

As seen in Figure 5.23, correct classification of white male sex decreased with the onset of age; younger white males were classified with more accuracy than older white males (93% and 74%, respectively). This was a statistically significant result. Older white males were found to have more ambiguous morphology than their younger counterparts and were misclassified as females more often than young males.

5.8

Repeatability for non-metric characteristics of the humerus and pelvis

An independent observer was utilized to determine if the non-metric characteristics of the distal humerus and the pelvis were apparent enough to reproduce accurate statistical results. This observer could not accurately predict sex with the first two humeral traits (trochlear extension and the olecranon fossa shape), but the angle of the medial epicondyle was categorized accurately as sexually dimorphic on a statistically significant level. When asked to ascertain a final determination of sex from the distal humerus, the independent observer was 91% accurate with male humeri and 75% accurate with female humeri (Appendix K). The distal humerus, therefore, appeared to show some ambiguity in the sexually

dimorphic features chosen for this study. As with any non-metric visual trait, experience in observing the characteristic may have played a role in determining sex from this element. Although the observer did not accurately categorize two of the three independent traits, ultimately the correct sex was determined accurately.

Non-metric pelvic features were assigned accurately by the independent observer for all four characteristics. Pelvic morphology as defined in this study was deemed to be reproducible, well-defined, and robust in its sexual dimorphism (Appendix L).

Table 5.1: Distribution of classification, all males and females, medial epicondylar symmetry. 1=M, 2=Intermediate M. 3=Ambiguous, 4=Intermediate F, 5=F

	1	2	3	4	5	Total
Male	41 (10%)	127 (30%)	63 (15%)	140 (33%)	49 (12%)	420
Female	10 (5%)	24 (12%)	20 (11%)	70 (37%)	64 (34%)	188
Total	51	151	83	210	113	*N* = 608

Pearson's chi square value=56.387, df=4, p=0.00<0.05

Table 5.2: Distribution of classification, all males and females, trochlear extension. 1=M, 2=Intermediate M. 3=Ambiguous, 4=Intermediate F, 5=F

	1	2	3	4	5	Total
Male	55 (13%)	135 (32%)	77 (18%)	137 (33%)	16 (4%)	420
Female	12 (6%)	40 (21%)	31 (17%)	79 (42%)	26 (14%)	188
Total	67	175	108	216	42	*N* = 608

Pearson's chi square value=31.951, df=4, p=0.00<0.05

Table 5.3: Distribution of classification, all males and females, olecranon fossa shape. 1=M, 2=Intermediate M. 3=Ambiguous, 4=Intermediate F, 5=F

	1	2	3	4	5	Total
Male	70 (17%)	170 (40%)	79 (19%)	86 (21%)	15 (4%)	420
Female	4 (2%)	36 (19%)	34 (18%)	67 (36%)	47 (24%)	188
Total	74	206	113	153	62	*N* = 608

Pearson's chi square value=110.370, df=4, p=0.00<0.05

Table 5.4: Distribution of classification, all males and females, medial epicondylar angle. 1=M, 2=Intermediate M. 3=Ambiguous, 4=Intermediate F, 5=F

	1	2	3	4	5	Total
Male	153 (37%)	144 (34%)	22 (5%)	76 (18%)	25 (6%)	420
Female	24 (13%)	49 (26%)	12 (6%)	64 (34%)	39 (21%)	188
Total	177	193	34	140	64	*N* = 608

Pearson's chi square value=73.6673, df=4, p=0.00<0.05

Table 5.5: Distribution of classification, all males and females, estimated sex. 1=Male, 3=Ambiguous, 5=Female

	1	3	5	Total
Male	**261 (62%)**	56 (13%)	103 (25%)	420
Female	30 (16%)	22 (12%)	**136 (72%)**	188
Total	291	78	239	*N*= 608

Pearson's chi square value=133.687, df=2, p=0.00<0.05

Table 5.6: Distribution of classification and chi square significance, all males and females (total *N* = 608). Estimated sex under "1 (M)" and "5 (F)" represents a total of the [1] and [2] "estimated sex" determinations for males, and [4] and [5] "estimated sex" determinations for females.

	Males (*n*=420)					**Females (*n*=188)**					Pearson's Chi Square	df	Sign. (2-tailed)
	1 (M)	2	3	4	5 (F)	1 (M)	2	3	4	5 (F)			
Epicondylar symmetry	41	127	63	140	49	10	24	20	70	64	56.387	4	**0.000***
	(10%)	(30%)	(15%)	(33%)	(12%)	(5%)	(13%)	(11%)	(37%)	(34%)			
Trochlear extension	55	135	77	137	16	12	40	31	79	26	32.994	4	**0.000***
	(13%)	(32%)	(18%)	(32%)	(4%)	(6%)	(21%)	(16%)	(42%)	(14%)			
Olecranon fossa shape	70	170	79	86	15	4	36	34	67	47	110.370	4	**0.000***
	(17%)	(40%)	(19%)	(20%)	(4%)	(2%)	(19%)	(18%)	(36%)	(25%)			
Epicondyle angle	153	144	22	76	25	24	49	12	64	39	69.388	4	**0.000***
	(36%)	(34%)	(5%)	(18%)	(6%)	(13%)	(26%)	(6%)	(34%)	(21%)			
Estimated sex	261		56		103	30		22		136	133.687	2	**0.000***
	(62%)		(13%)		(25%)	(16%)		(12%)		**(72%)**			

***Significant at <0 .05**

Table 5.7: Distribution and classification changes with "medial epicondylar symmetry" trait removed.

	YBF	YWF	OBF	OWF	YBM	YWM	OBM	OWM	**Total**
Misclassified originally to still misclassified	5	1	6	10	23	2	31	19	**97**
Ambiguous or correct to misclassified	1	0	0	10	7	0	6	0	**24**
Ambiguous or misclassified **to correct classification**	3	0	4	3	9	3	20	18	**60**
Misclassified to ambiguous	0	0	2	3	1	0	10	1	**17**

YBF = young black female, YWF = young white female, OBF = old black female, OWF = old white female, YBM = young black male, YWM = young white male, OBM = old black male, OWM = old white male.

Table 5.8: Distribution of classification, all males and females, estimated sex with the removal of epicondylar symmetry. 1=M, 2=Intermediate M. 3=Ambiguous, 4=Intermediate F, 5=F

	1	3	5	Total
Male	**310 (74%)**	56 (6%)	86 (20%)	420
Female	33 (17%)	10 (5%)	**145 (77%)**	188
Total	343	34	231	*N*= 608

Pearson's chi square value=182.593, df=2, p=0.00<0.05

Table 5.9: Distribution of classification and chi square significance, black females and white females (total *n* = 188). Estimated sex under "1 (M)" and "5 (F)" represents a total of the [1] and [2] "estimated sex" determinations and [4] and [5] "estimated sex" determinations.

	Black Females (*n*=106)					**White Females (*n*=82)**					Pearson's Chi Square	df	Sign. (2-tailed)
	1 (M)	2	3	4	5 (F)	1 (M)	2	3	4	5 (F)			
Trochlear extension	6	19	18	42	21	6	21	13	37	5	8.138	4	0.087
	(5%)	(18%)	(17%)	(40%)	(20%)	(7%)	(26%)	(16%)	(45%)	(6%)			
Olecranon fossa shape	1	13	15	39	38	3	23	19	28	9	21.230	4	**0.000***
	(1%)	(12%)	(14%)	(37%)	(36%)	(4%)	(28%)	(23%)	(34%)	(11%)			
Epicondyle angle	11	27	8	42	18	13	22	4	22	21	5.517	4	0.238
	(10%)	(25%)	(8%)	(40%)	(17%)	(16%)	(26%)	(5%)	(27%)	(26%)			
Estimated sex	12		5		89	21		5		56	7.015	2	**0.030***
	(11%)		(5%)		**(84%)**	(26%)		(6%)		**(68%)**			

Significant at <0 .05

Table 5.10: Distribution of classification and chi square significance for young black females vs. old black females (total *n* = 106). Estimated sex under "1 (M)" and "5 (F)" represents a total of the [1] and [2] "estimated sex" determinations and [4] and [5] "estimated sex" determinations.

	Young Black Females (*n*=65)					**Old Black Females (*n*=41)**					Pearson's Chi Square	df	Sign. (2-tailed)
	1 (M)	2	3	4	5 (F)	1 (M)	2	3	4	5 (F)			
Trochlear extension	4	9	9	30	13	2	10	9	12	8	4.417	4	0.353
	(6%)	(14%)	(14%)	(46%)	(20%)	(5%)	(24%)	(22%)	(29%)	(20%)			
Olecranon fossa shape	0	7	10	19	29	1	6	5	20	9	8.286	4	0.082
	(0%)	(11%)	(15%)	(29%)	(45%)	(2%)	(15%)	(12%)	(49%)	(22%)			
Epicondyle angle	5	15	6	30	9	6	12	2	12	9	4.959	4	0.292
	(8%)	(23%)	(9%)	(46%)	(14%)	(15%)	(29%)	(5%)	(29%)	(22%)			
Estimated sex	5		3		57	7		2		32	2.236	2	0.327
	(7%)		(5%)		**(88%)**	(17%)		(5%)		**(78%)**			

Significant at <0 .05

Table 5.11: Distribution of classification and chi square significance for young white females vs. old white females (total *n* = 82). Estimated sex under "1 (M)" and "5 (F)" represents a total of the [1] and [2] "estimated sex" determinations and [4] and [5] "estimated sex" determinations.

	Young White Females (*n*=14)					Old White Females (*n*=68)					Pearson's Chi Square	df	Sign. (2-tailed)
	1 (M)	2	3	4	5 (F)	1 (M)	2	3	4	5 (F)			
Trochlear extension	0	3	1	9	1	6	18	12	28	4	3.563	4	0.468
	(0%)	(21%)	(7%)	(65%)	(7%)	(9%)	(26%)	(18%)	(41%)	(6%)			
Olecranon fossa shape	0	0	3	7	4	3	23	16	21	5	11.380	4	**0.023***
	(0%)	(0%)	(21%)	(50%)	(29%)	(4%)	(34%)	(24%)	(31%)	(7%)			
Epicondyle angle	4	2	3	4	1	9	20	1	18	20	14.460	4	**0.006***
	(29%)	(14%)	(21%)	(29%)	(7%)	(13%)	(30%)	(1%)	(26%)	(30%)			
Estimated sex	1		0		13	20		5		43	4.769	2	0.092
	(7%)		(0%)		(**93%**)	(30%)		(7%)		(**63%**)			

Significant at <0.05

Table 5.12: Distribution of classification and chi square significance for black males vs. white males (total *N* = 420). Estimated sex under "1 (M)" and "5 (F)" represents a total of the [1] and [2] "estimated sex" determinations and [4] and [5] "estimated sex" determinations.

	Black Males (*n*=312)					White Males (*n*=108)					Pearson's Chi Square	df	Sign. (2-tailed)
	1 (M)	2	3	4	5 (F)	1 (M)	2	3	4	5 (F)			
Trochlear extension	35	101	60	104	12	20	34	17	33	4	4.012	4	0.404
	(11%)	(33%)	(19%)	(33%)	(4%)	(19%)	(32%)	(16%)	(30%)	(3%)			
Olecranon fossa shape	37	128	57	75	15	33	42	22	11	0	29.817	4	**0.000***
	(12%)	(41%)	(18%)	(24%)	(5%)	(30%)	(39%)	(21%)	(10%)	(0%)			
Epicondyle angle	117	109	19	50	17	36	35	3	26	8	5.601	4	0.231
	(38%)	(35%)	(6%)	(16%)	(5%)	(33%)	(33%)	(3%)	(24%)	(7%)			
Estimated sex	226		19		67	84		5		19	1.200	2	0.549
	(**72%**)		(6%)		(22%)	(**78%**)		(4%)		(18%)			

Significant at <0.05

Table 5.13: Distribution of classification and chi square significance for young black males vs. old black males (total *n* = 312). Estimated sex under "1 (M)" and "5 (F)" represents a total of the [1] and [2] "estimated sex" determinations and [4] and [5] "estimated sex" determinations.

	Young Black Males (*n*=127)					Old Black Males (*n*=185)					Pearson's Chi Square	df	Sign. (2-tailed)
	1 (M)	2	3	4	5 (F)	1 (M)	2	3	4	5 (F)			
Trochlear extension	18	46	19	38	6	17	55	41	66	6	5.856	4	0.210
	(14%)	(36%)	(15%)	(30%)	(5%)	(9%)	(30%)	(22%)	(36%)	(3%)			
Olecranon fossa shape	21	47	16	31	12	16	81	41	44	3	18.171	4	**0.001***
	(17%)	(37%)	(12%)	(24%)	(10%)	(9%)	(43%)	(22%)	(24%)	(2%)			
Epicondyle angle	45	43	11	20	8	72	66	8	30	9	2.936	4	0.569
	(35%)	(34%)	(9%)	(16%)	(6%)	(39%)	(36%)	(4%)	(16%)	(5%)			
Estimated sex	90		5		32	136		14		35	3.085	2	0.214
	(**71%**)		(4%)		(25%)	(**74%**)		(7%)		(19%)			

Significant at 0.05

Table 5.14: Distribution of classification and chi square significance for young white males vs. old white males (total *n* = 108). Estimated sex under "1 (M)" and "5 (F)" represents a total of the [1] and [2] "estimated sex" determinations and [4] and [5] "estimated sex" determinations.

	Young White Males (*n*=28)					Old White Males (*n*=80)					Pearson's Chi Square	df	Sign. (2-tailed)
	1 (M)	2	3	4	5 (F)	1 (M)	2	3	4	5 (F)			
Trochlear extension	6	12	7	3	0	14	22	10	30	4	10.056	4	**0.040***
	(21%)	(43%)	(25%)	(11%)	(5%)	(18%)	(28%)	(12%)	(37%)	(5%)			
Olecranon fossa shape	11	10	4	3	0	22	32	18	8	0	1.738	4	0.628
	(39%)	(36%)	(14%)	(11%)	(0%)	(28%)	(40%)	(22%)	(10%)	(0%)			
Epicondyle angle	11	10	1	5	1	25	25	2	21	7	1.973	4	0.741
	(39%)	(36%)	(4%)	(17%)	(4%)	(31%)	(31%)	(3%)	(26%)	(9%)			
Estimated sex	24		1		3	60		4		16	1.414	2	0.493
	(**86%**)		(3%)		(11%)	(**75%**)		(5%)		(20%)			

Significant at 0.05

Table 5.15: Distribution of classific subpubic concavity. 1=M, 2=Intermediate F, 5=F

	1	2	3	4	5	Total
Male	105 (25%)	214 (51%)	76 (18%)	15 (4%)	8 (2%)	418
Female	3 (2%)	2 (1%)	17 (9%)	56 (32%)	99 (56%)	177
Total	108	216	93	71	107	*N*= 595

Pearson's chi square value = 413.057, df = 4, p= 0.00<0.05

Table 5.16: Distribution of classification for all males and females, subpubic angle. 1=M, 2=Intermediate M. 3=Ambiguous, 4=Intermediate F, 5=F

	1	2	3	4	5	Total
Male	108 (26%)	173 (41%)	96 (23%)	26 (6%)	15 (4%)	418
Female	2 (1%)	4 (2%)	4 (2%)	43 (25%)	124 (70%)	177
Total	108	177	100	69	139	*N*= 595

Pearson's chi square value = 406.961, df = 4, p= 0.00<0.05

Table 5.17: Distribution of classification for all males and females, ischio-pubic ramus width. 1=M, 2=Intermediate M. 3=Ambiguous, 4=Intermediate F, 5=F

	1	2	3	4	5	Total
Male	91 (22%)	108 (26%)	110 (26%)	86 (20%)	23 (6%)	418
Female	3 (2%)	6 (3%)	20 (11%)	51 (29%)	97 (55%)	177
Total	94	114	130	137	120	*N*= 595

Pearson's Chi Square value = 230.774, df = 4, p = 0.00<0.05

Table 5.18: Distribution of classification for all males and females, greater sciatic notch width. 1=M, 2=Intermediate M. 3=Ambiguous, 4=Intermediate F, 5=F

	1	2	3	4	5	Total
Male	143 (34%)	152 (36%)	54 (13%)	48 (12%)	21 (5%)	418
Female	5 (3%)	5 (3%)	11 (6%)	41 (23%)	115 (65%)	177
Total	148	157	65	89	136	*N*= 595

Pearson's Chi Square Value = 314.215, df = 4, p= 0.00<0.05

Table 5.19: Distribution of classification for all males and females, estimated sex for the pelvis. 1=Male, 3=Ambiguous, 5=Female

	1	3	5	Total
Male	347 (83%)	24 (6%)	47 (11%)	418
Female	8 (4%)	3 (2%)	166 (94%)	177
Total	355	27	213	*N*= 595

Pearson's Chi Square Value = 369.551, df = 2, p = 0.00<0.05

Table 5.20: Distribution of classification and chi square significance, all males and females (total *N* = 595). Estimated sex under "1 (M)" and "5 (F)" represents a total of the [1] and [2] "estimated sex" determinations for males and [4] and [5] "estimated sex" determinations for females.

	Males (*n*=418)					**Females (*n*=177)**					Pearson's Chi Square	df	Sign. (2-tailed)
	1 (M)	2	3	4	5 (F)	1 (M)	2	3	4	5 (F)			
Subpubic concavity	105 (25%)	214 (51%)	76 (18%)	15 (4%)	8 (2%)	3 (2%)	2 (1%)	17 (8%)	56 (32%)	99 (56%)	413.057	4	**0.000***
Subpubic angle	108 (26%)	173 (41%)	96 (23%)	26 (6%)	15 (4%)	2 (1%)	4 (2%)	4 (2%)	43 (25%)	124 (70%)	406.961	4	**0.000***
Ischio-pubic ramus	91 (22%)	108 (26%)	110 (26%)	86 (20%)	23 (6%)	3 (2%)	6 (3%)	20 (11%)	51 (29%)	97 (55%)	230.774	4	**0.000***
Greater sciatic notch	143 (34%)	152 (36%)	54 (13%)	48 (12%)	21 (5%)	5 (3%)	5 (3%)	11 (6%)	41 (23%)	115 (65%)	314.215	4	**0.000***
Estimated sex	347 **(83%)**		24 (6%)		47 (11%)	8 (4%)		3 (2%)		166 **(94%)**	369.551	2	**0.000***

***Significant at 0.05**

Table 5.21: Distribution of classification and chi square significance, all black females and white females (total *n* = 177). Estimated sex under "1 (M)" and "5 (F)" represents a total of the [1] and [2] "estimated sex" determinations and [4] and [5] "estimated sex" determinations.

	Black Females (*n*=95)					White Females (*n*=82)					Pearson's Chi Square	df	Sign. (2-tailed)
	1 (M)	2	3	4	5 (F)	1 (M)	2	3	4	5 (F)			
Subpubic concavity	1	2	9	31	52	2	0	8	25	47	2.345	4	0.673
	(1%)	(2%)	(9%)	(33%)	(55%)	(2%)	(0%)	(10%)	(31%)	(57%)			
Subpubic angle	1	3	3	20	68	1	1	1	23	56	2.429	4	0.657
	(1%)	(3%)	(3%)	(21%)	(72%)	(1%)	(1%)	(1%)	(28%)	(69%)			
Ischio-pubic ramus	2	5	13	22	53	1	1	7	29	44	5.672	4	0.225
	(2%)	(5%)	(14%)	(23%)	(56%)	(1%)	(1%)	(9%)	(35%)	(54%)			
Greater sciatic notch	4	3	6	27	55	1	2	5	14	60	5.505	4	0.239
	(4%)	(3%)	(6%)	(29%)	(58%)	(1%)	(3%)	(6%)	(17%)	(73%)			
Estimated sex	5		2		88	3		1		78	0.484	2	0.785
	(5%)		(2%)		**(93%)**	(3%)		(1%)		**(96%)**			

Table 5.22: Distribution of classification and chi square significance, young black females (50 years and younger) and old black females (over 50 years) (total *n* = 95). Estimated sex under "1 (M)" and "5 (F)" represents a total of the [1] and [2] "estimated sex" determinations and [4] and [5] "estimated sex" determinations.

	Young Black Females (*n*=58)					Old Black Females (*n*=37)					Pearson's Chi Square	df	Sign. (2-tailed)
	1 (M)	2	3	4	5 (F)	1 (M)	2	3	4	5 (F)			
Subpubic concavity	1	1	6	23	27	0	1	3	8	25	4.934	4	0.294
	(1%)	(1%)	(11%)	(40%)	(47%)	(0%)	(3%)	(8%)	(21%)	(68%)			
Subpubic angle	1	2	2	10	43	0	1	1	10	25	1.881	4	0.758
	(1%)	(4%)	(4%)	(17%)	(74%)	(0%)	(3%)	(3%)	(27%)	(67%)			
Ischio-pubic ramus	1	3	9	13	32	1	2	4	9	21	0.517	4	0.972
	(1%)	(5%)	(16%)	(23%)	(55%)	(3%)	(5%)	(11%)	(24%)	(57%)			
Greater sciatic notch	3	2	4	17	32	1	1	2	10	23	0.679	4	0.954
	(5%)	(4%)	(6%)	(29%)	(55%)	(3%)	(3%)	(5%)	(27%)	(62%)			
Estimated sex	3		1		54	2		1		34	0.109	2	0.947
	(5%)		(1%)		**(94%)**	(5%)		(3%)		**(92%)**			

Table 5.23: Distribution of classification and chi square significance, young white females and old white females (total *n* = 82). Estimated sex under "1 (M)" and "5 (F)" represents a total of the [1] and [2] "estimated sex" determinations and [4] and [5] "estimated sex" determinations.

	Young White Females (*n*=14)					Old White Females (*n*=68)					Pearson's Chi Square	df	Sign. (2-tailed)
	1 (M)	2	3	4	5 (F)	1 (M)	2	3	4	5 (F)			
Subpubic concavity	0 (0%)	0 (0%)	3 (21%)	4 (29%)	7 (50%)	2 (3%)	0 (0%)	5 (7%)	21 (31%)	40 (59%)	2.947	4	0.400
Subpubic angle	0 (0%)	0 (0%)	0 (0%)	4 (29%)	10 (71%)	1 (1%)	1 (1%)	1 (1%)	19 (28%)	46 (68%)	0.644	4	0.958
Ischio-pubic ramus	0 (0%)	0 (0%)	1 (7%)	6 (43%)	7 (50%)	1 (1%)	1 (1%)	6 (9%)	23 (34%)	37 (55%)	0.760	4	0.944
Greater sciatic notch	0 (0%)	0 (0%)	2 (14%)	3 (22%)	9 (64%)	1 (1%)	2 (3%)	3 (5%)	11 (16%)	51 (75%)	2.844	4	0.584
Estimated sex	0 (0%)		0 (0%)		14 (**100%**)	3 (5%)		1 (1%)		64 (**94%**)	0.866	2	0.649

Table 5.24: Distribution of classification and chi square significance, black males and white males (total *N* = 418). Estimated sex under "1 (M)" and "5 (F)" represents a total of the [1] and [2] "estimated sex" determinations and [4] and [5] "estimated sex" determinations.

	Black Males (*n*=311)					White Males (*n*=107)					Pearson's Chi Square	df	Sign. (2-tailed)
	1 (M)	2	3	4	5 (F)	1 (M)	2	3	4	5 (F)			
Subpubic concavity	72 (23%)	161 (52%)	65 (21%)	7 (2%)	6 (2%)	33 (31%)	53 (50%)	11 (10%)	8 (7%)	2 (2%)	12.950	4	**0.012***
Subpubic angle	74 (24%)	124 (40%)	85 (27%)	17 (5%)	11 (4%)	34 (32%)	49 (46%)	11 (10%)	9 (8%)	4 (4%)	13.834	4	**0.008***
Ischio-pubic ramus	71 (23%)	81 (26%)	84 (27%)	57 (18%)	18 (6%)	20 (19%)	27 (25%)	26 (24%)	29 (27%)	5 (5%)	4.028	4	0.402
Greater sciatic notch	121 (39%)	107 (34%)	36 (12%)	39 (13%)	8 (2%)	22 (21%)	45 (42%)	18 (17%)	9 (8%)	13 (12%)	26.527	4	**0.000***
Estimated sex	263 (**85%**)		17 (5%)		31 (10%)	84 (**79%**)		7 (7%)		16 (14%)	2.273	2	0.321

Significant at 0.05

Table 5.25: Distribution of classification and chi square significance, young black males and old black males (total *n* = 311). Estimated sex under "1 (M)" and "5 (F)" represents a total of the [1] and [2] "estimated sex" determinations and [4] and [5] "estimated sex" determinations.

	Young Black Males (*n*=126)					Old Black Males (*n*=185)					Pearson's Chi Square	df	Sign. (2-tailed)
	1 (M)	2	3	4	5 (F)	1 (M)	2	3	4	5 (F)			
Subpubic concavity	29	59	30	5	3	43	102	35	2	3	4.859	4	0.302
	(23%)	(47%)	(24%)	(4%)	(2%)	(23%)	(55%)	(19%)	(1%)	(2%)			
Subpubic angle	22	55	33	8	8	52	69	52	9	3	9.469	4	**0.050***
	(18%)	(44%)	(26%)	(6%)	(6%)	(28%)	(37%)	(28%)	(5%)	(2%)			
Ischio-pubic ramus	25	33	31	31	6	46	48	53	26	12	6.220	4	0.183
	(20%)	(26%)	(24%)	(25%)	(5%)	(25%)	(26%)	(29%)	(14%)	(6%)			
Greater sciatic notch	53	39	9	19	6	68	68	27	20	2	9.909	4	**0.042***
	(42%)	(31%)	(7%)	(15%)	(5%)	(37%)	(37%)	(14%)	(11%)	(1%)			
Estimated sex	100		6		20	163		11		11	8.280	2	**0.016***
	(79%)		(5%)		(16%)	**(88%)**		(6%)		(6%)			

Significant at 0.05

Table 5.26: Distribution of classification and chi square significance, young white males and old white males (total *n* = 107). Estimated sex under "1 (M)" and "5 (F)" represents a total of the [1] and [2] "estimated sex" determinations and [4] and [5] "estimated sex" determinations.

	Young White Males (*n*=27)					Old White Males (*n*=80)					Pearson's Chi Square	df	Sign. (2-tailed)
	1 (M)	2	3	4	5 (F)	1 (M)	2	3	4	5 (F)			
Subpubic concavity	14	11	0	2	0	19	42	11	6	2	10.12(	4	**0.038***
	(52%)	(41%)	(0%)	(7%)	(0%)	(24%)	(53%)	(14%)	(7%)	(2%)			
Subpubic angle	12	13	1	0	1	22	36	10	9	3	6.425	4	0.170
	(44%)	(48%)	(4%)	(0%)	(4%)	(28%)	(45%)	(13%)	(11%)	(3%)			
Ischio-pubic ramus	3	10	5	8	1	17	17	21	21	4	3.758	4	0.440
	(11%)	(37%)	(19%)	(29%)	(4%)	(21%)	(21%)	(26%)	(26%)	(6%)			
Greater sciatic notch	6	10	8	2	1	16	35	10	7	12	5.949	4	0.203
	(22%)	(37%)	(30%)	(7%)	(4%)	(20%)	(44%)	(13%)	(8%)	(15%)			
Estimated sex	25		0		2	59		7		14	8.541	2	**0.049***
	(93%)		(%)		(7%)	**(74%)**		(9%)		(17%)			

Significant at 0.05

Figure 5.1: Classification accuracy for all males and females, epicondylar symmetry (total *N* = 595; males *n* = 420, females *n* = 188).

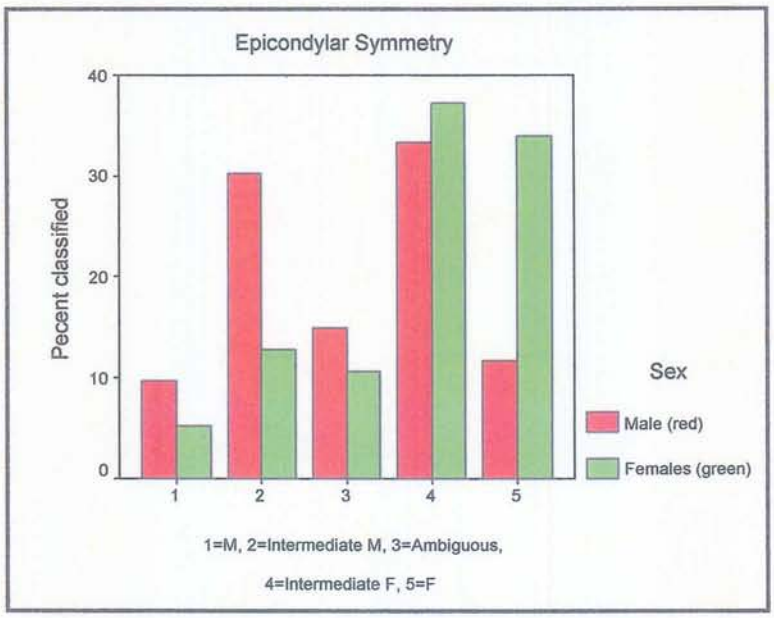

Figure 5.2: Classification accuracy for all males and females, trochlear extension (total *N* = 608; *n* = 420 males, *n* = 188 females).

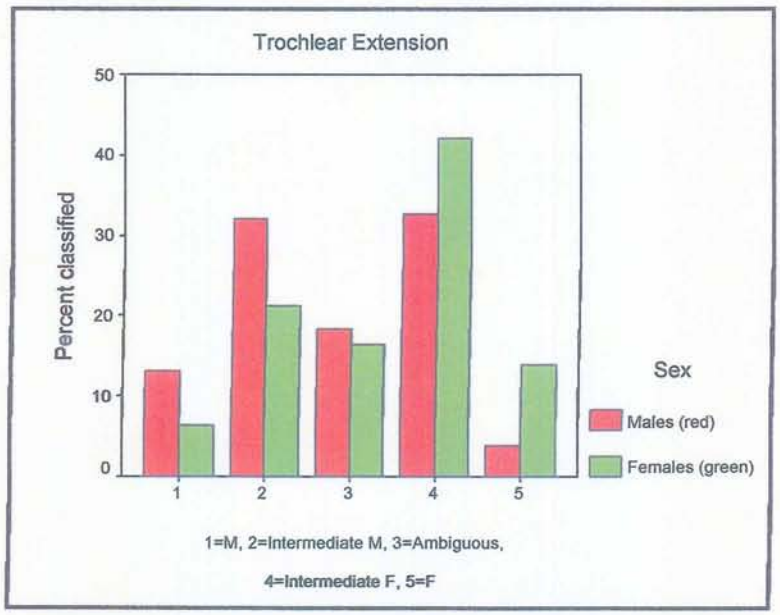

Figure 5.3: Classification accuracy for all males and females, olecranon fossa shape (total *N* = 608; *n* = 420 males, *n* = 188 females).

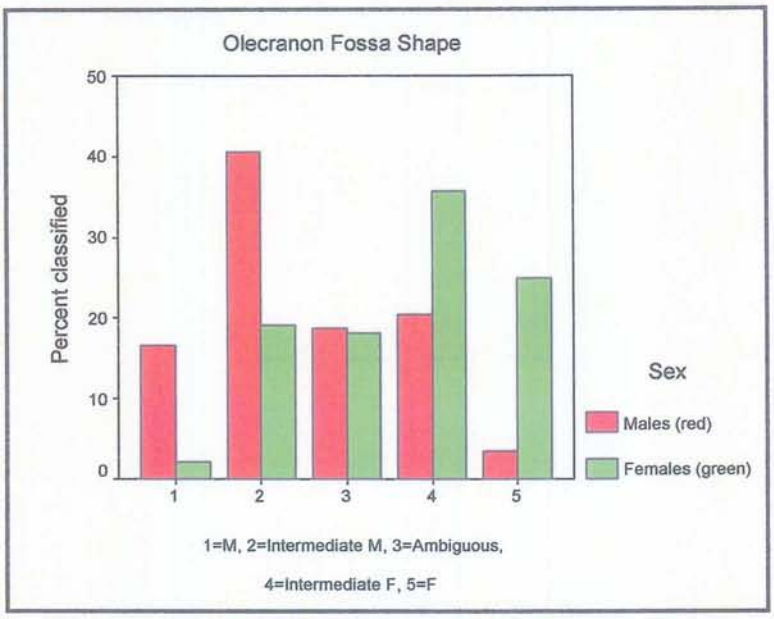

Figure 5.4: Classification accuracy for all males and females, angle of the medial epicondyle (total *N* = 595; *n* = 420 males, *n* = 188 females).

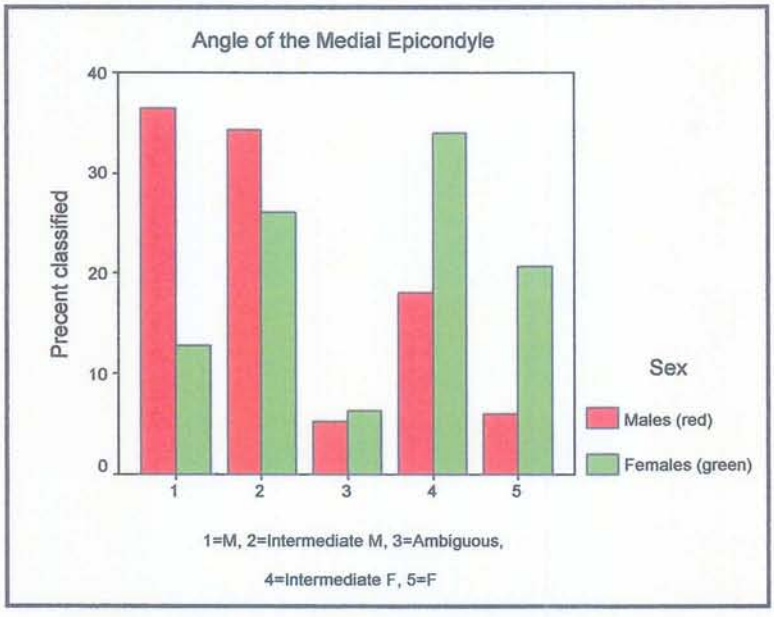

Figure 5.5: Classification accuracy for males and females, estimated sex (total *N* = 595; *n* = 420 males, *n* = 188 females).

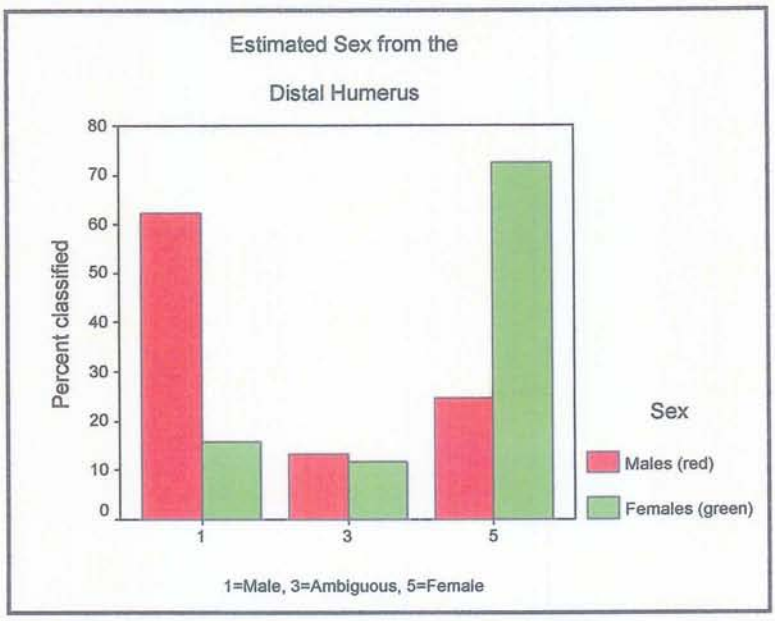

Figure 5.6: Classification accuracy for males and females with the three-trait combination of features, estimated sex (total *N* = 595; *n* = 420 males, *n* = 188 females).

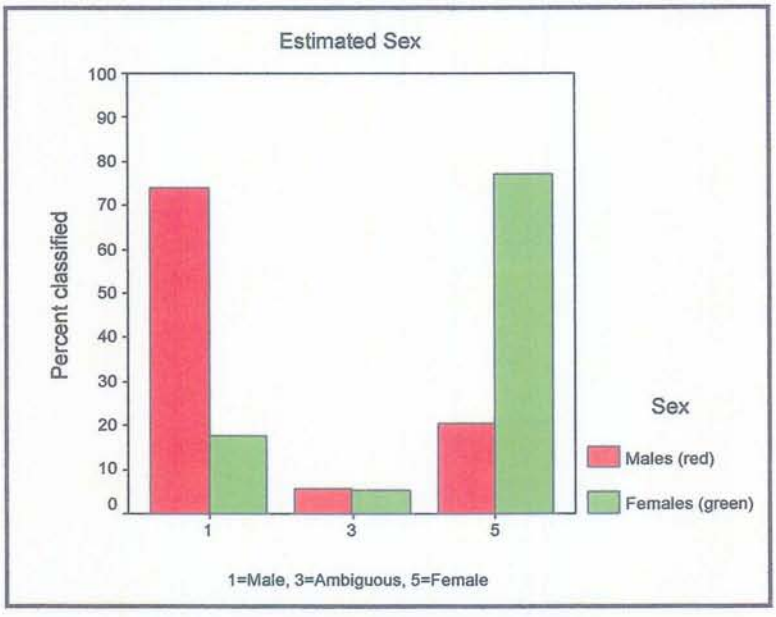

Figure 5.7: Classification accuracy for black females vs. white females, estimated sex (total *N*=188, black females *n*=106, white females *n*= 82).

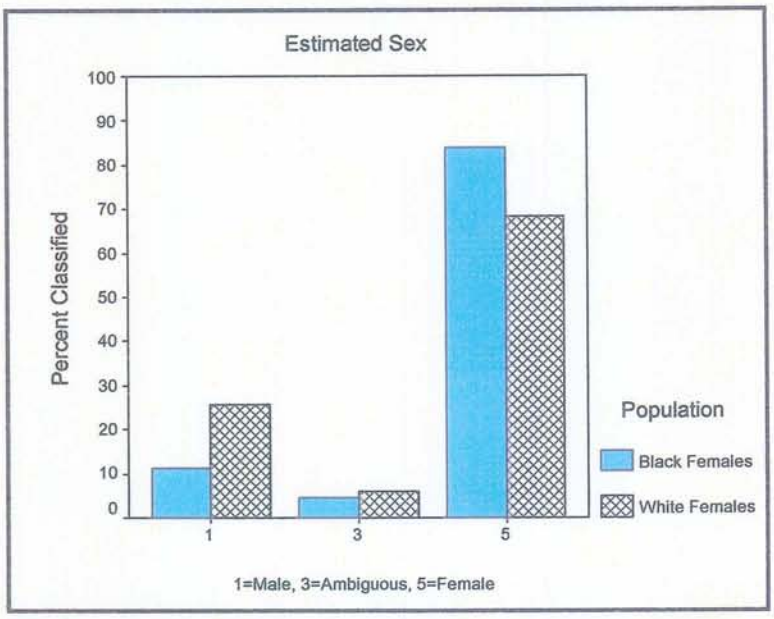

Figure 5.8: Classification accuracy for young black females vs. old black females, estimated sex (total *N*= 106, young black females *n*=65, old black females *n*=41).

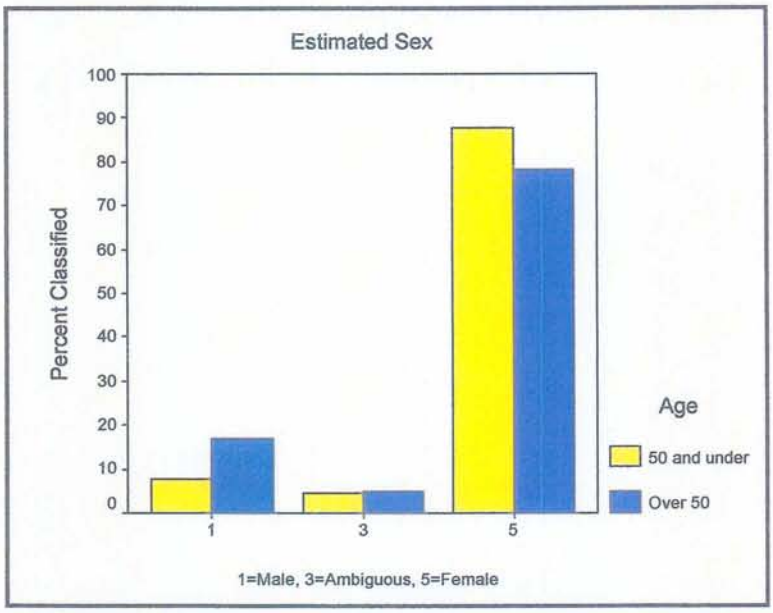

Figure 5.9: Classification accuracy for young white females vs. old white females, estimated sex (total *N*= 82, young white females *n*=14, old black females *n*=68).

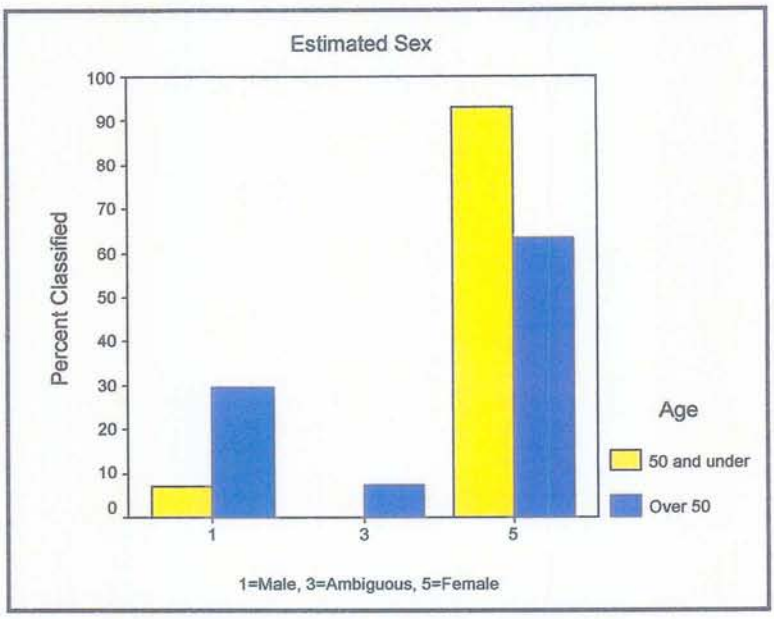

Figure 5.10: Classification accuracy for black males vs. white males, estimated sex (*N*=420, black males *n*=312, white males *n*=108).

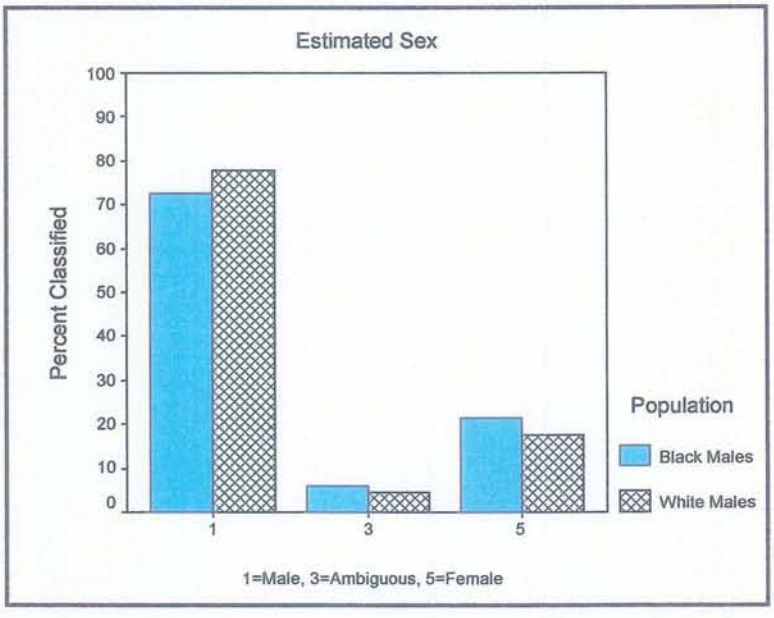

Figure 5.11: Classification accuracy for young black males vs. old black males, estimated sex (*N*=312, young black males *n*=125, old black males *n*=185).

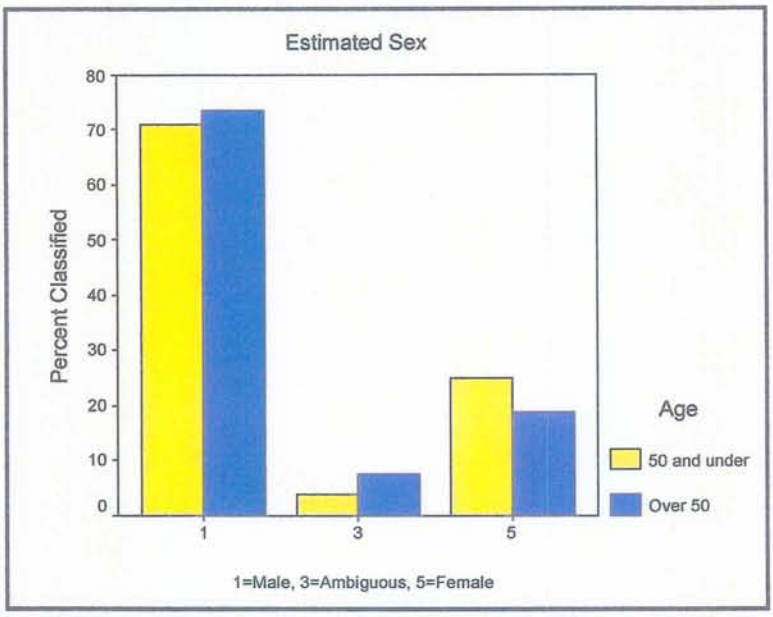

Figure 5.12: Classification accuracy for young white males vs. old white males, estimated sex (*N*=108, young white males *n*=28, old white males *n*=80).

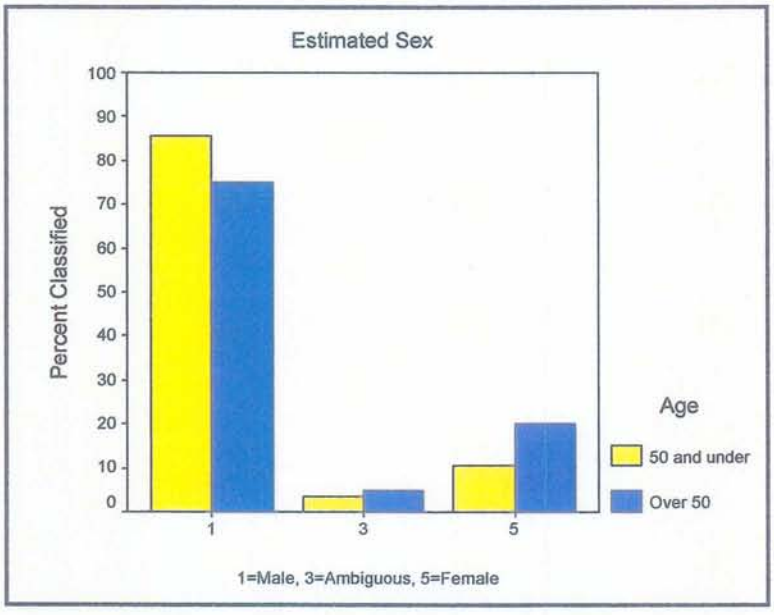

Figure 5.13: Classification accuracy for all males and females, subpubic concavity (total *N*=595, males *n*=418, females *n*=177).

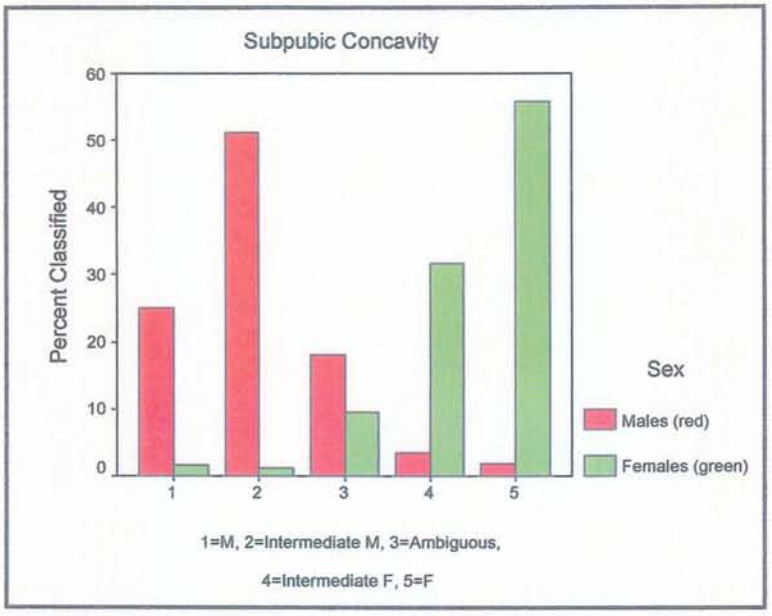

Figure 5.14: Classification accuracy for all males and females, subpubic angle (total *N*=595, males *n*=418, females *n*=177).

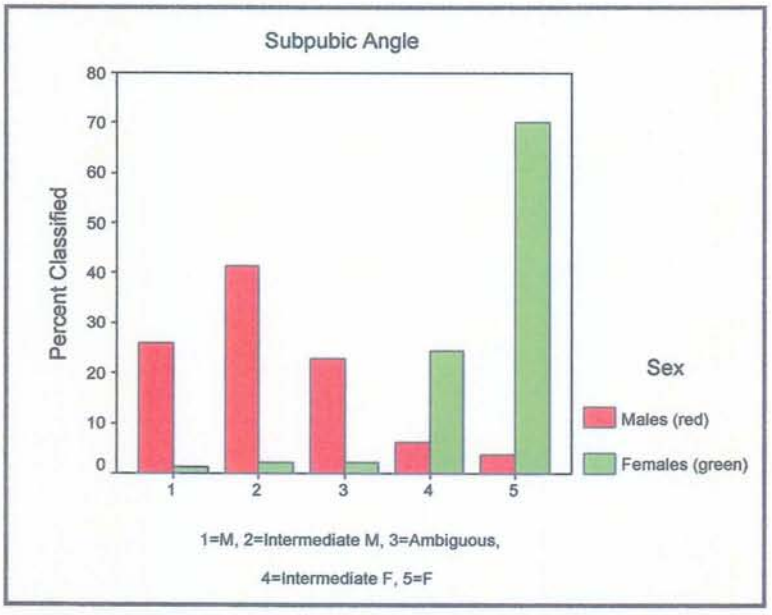

Figure 5.15: Classification accuracy for all males and females, ischio-pubic ramus width (total *N*=595, males *n*=418, females *n*=177).

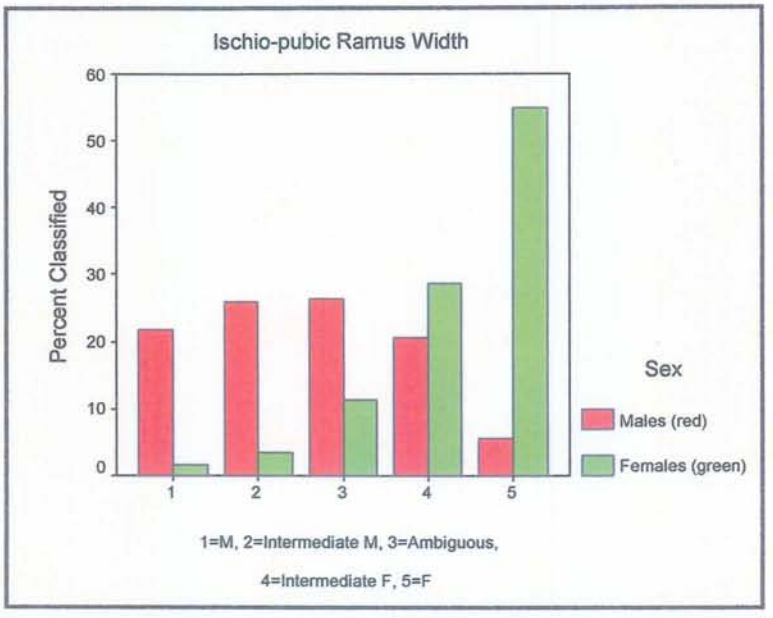

Figure 5.16: Classification accuracy for all males and females, greater sciatic notch width (total *N*=595, males *n*=418, females *n*=177).

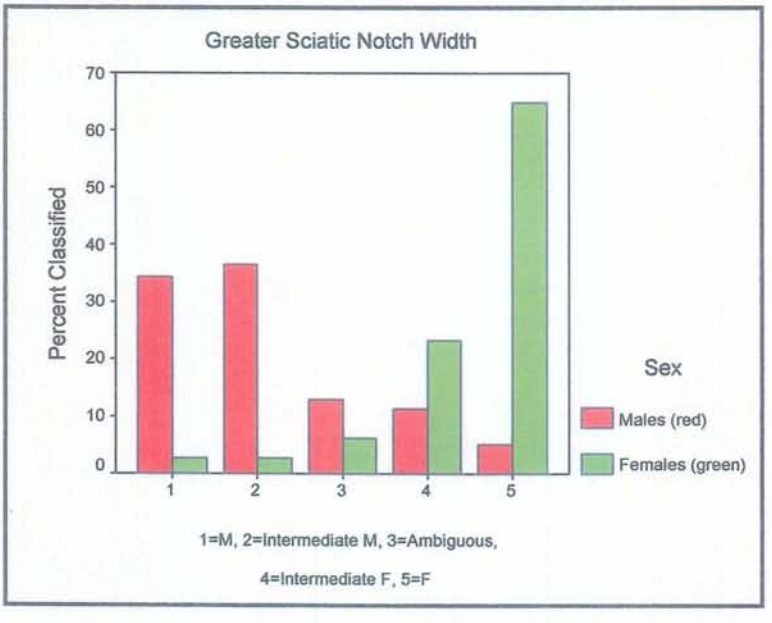

Figure 5.17: Classification accuracy for all males and females, estimated sex (total *N*=595, males *n*=418, females *n*=177).

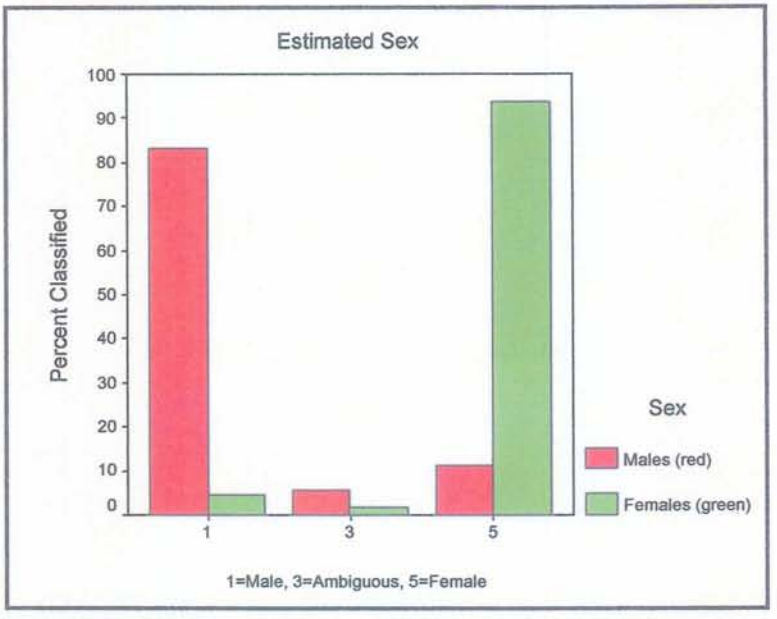

Figure 5.18: Classification accuracy for black females and white females, estimated sex (total *N*=177, black females *n*=95, white females *n*=82).

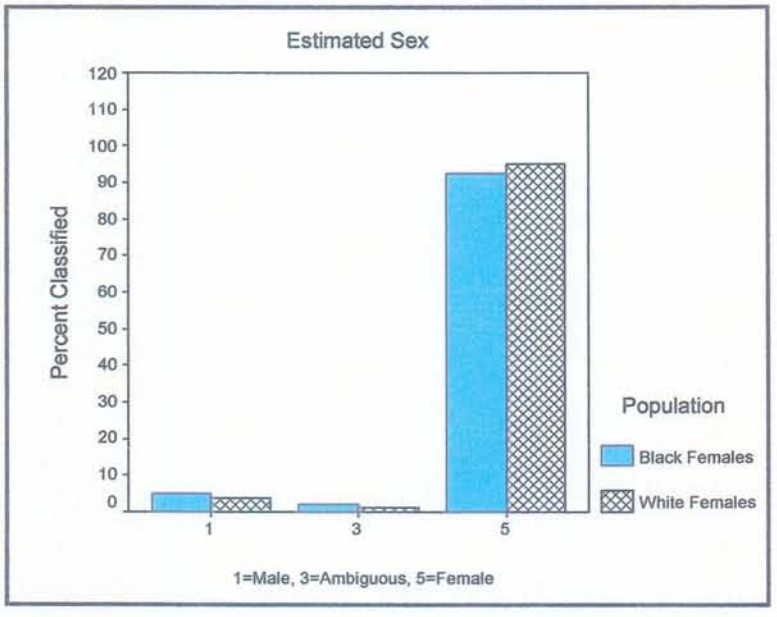

Figure 5.19: Classification accuracy for young black females and old black females, estimated sex (total *N*=95, young black females *n*=58, old black females *n*=37).

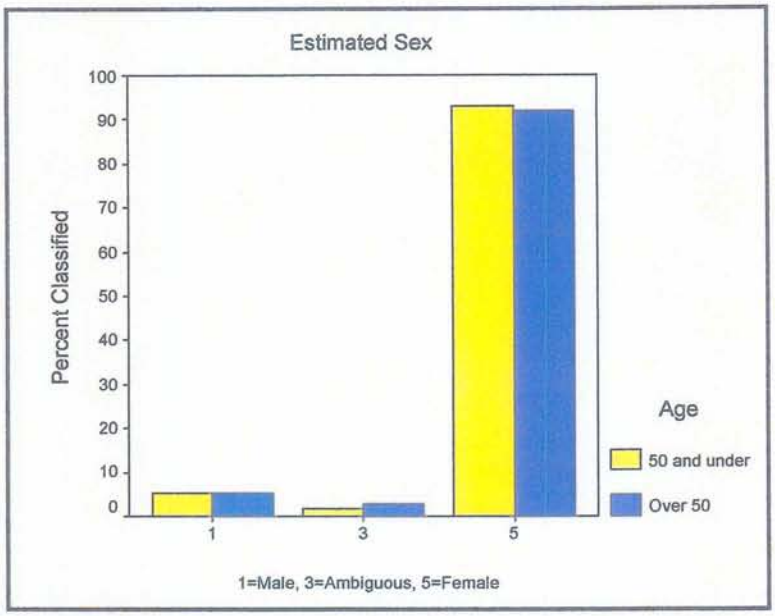

Figure 5.20: Classification accuracy for young white females and old white females, estimated sex (total *N*= 82, young white females *n*=14, old white females *n*=68).

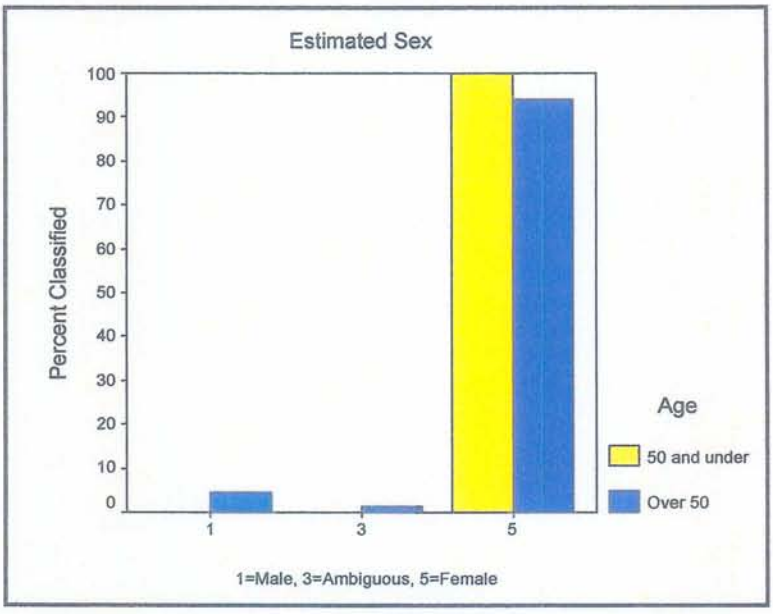

Figure 5.21: Classification accuracy for black males and white males, estimated sex (total *N*= 418, black males *n*=311, white males *n*=107).

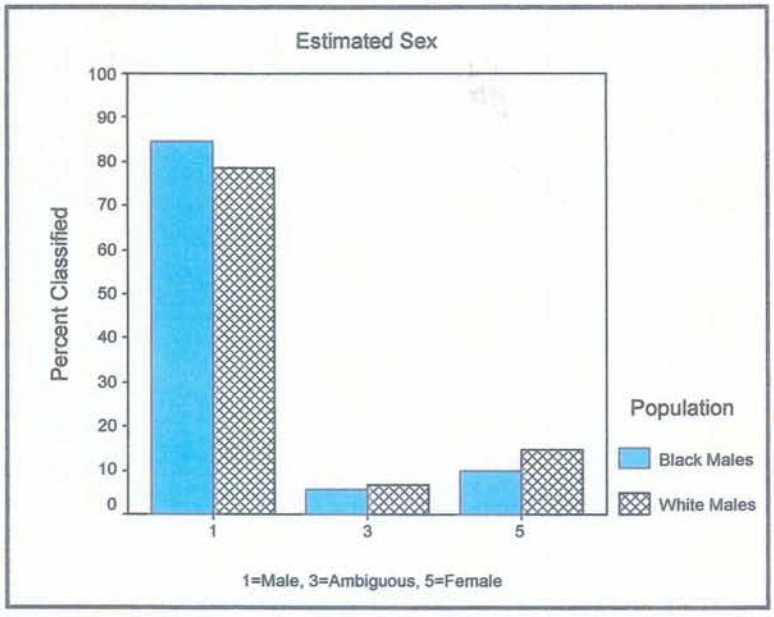

Figure 5.22: Classification accuracy for young black males and old black males, estimated sex (total *N*= 311, young black males *n*=126, old black males *n*=185).

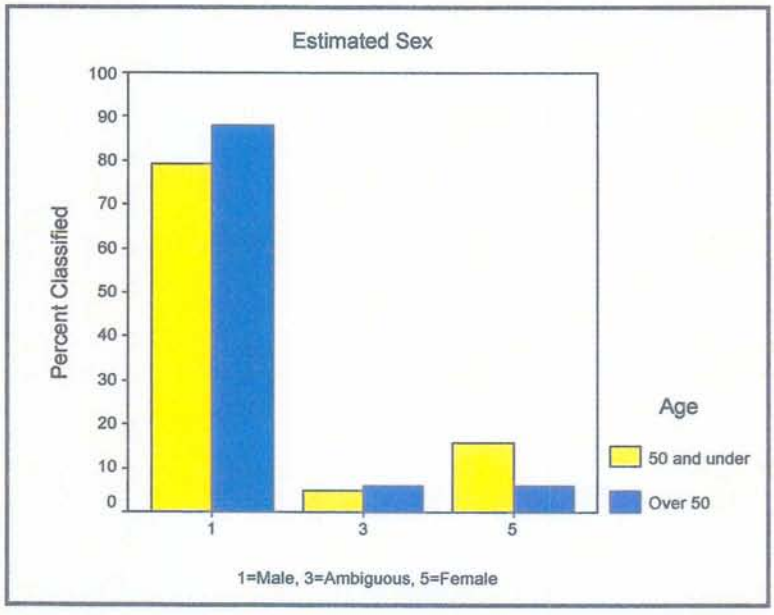

Figure 5.23: Classification accuracy for young white males and old white males, estimated sex (total *N*= 107, young white males *n*=27, old white males *n*=80).

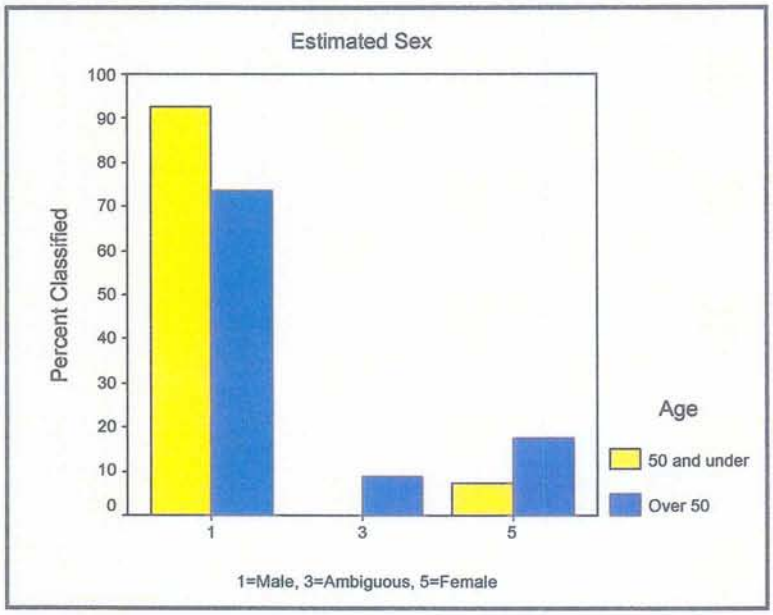

CHAPTER 6

RESULTS OF GEOMETRIC MORPHOMETRIC ANALYSIS

Results of geometric morphometric analyses were broken into sections. Sections 6.1 and 6.2 focus on the results obtained from two perspectives (and their corresponding homologous landmarks) of changes to the distal and posterior humerus with the onset of age. The "EPI" perspective indicates the location of the angle of the medial epicondyle, photographed from the distal aspect when the humerus was placed with the posterior side up. The "OL" perspective shows the olecranon fossa and the bony structures surrounding it. Both perspectives were assigned a series of standardized landmarks from which to base the statistical queries.

Sections 6.3 and 6.4 focused on results of two perspectives (and their corresponding homologous landmarks) between males and females with the onset of age in the os coxae. The "SUB" perspective focused specifically on the morphological features of the subpubic concavity and the subpubic angle, while the "SCI" perspective elucidated the anatomy of the greater sciatic notch. Each subsequent section was delineated further into comparisons between age groups and populations, as seen in previous chapters.

6.1

Sexual dimorphism in the distal humerus: EPI perspective

Nineteen homologous landmarks were assigned to the distal humerus, as shown in Figure 3.26. In order to confirm that the distal and posterior humerus was sexually dimorphic, the first analyses focused on establishing the degree of dimorphism and the classification accuracies between females and males.

Consensus relative warp analysis performed with the statistical package tpsRelw required the comparison of at least four groups within a sample. Therefore, the sample was divided into four initial assemblages based on biological affiliation to observe the presence of sexual dimorphism in this anatomical perspective of the posterior humerus. This separation of the sample into "black" and "white" male and female populations was to determine whether significant differences occurred between the groups, and if sexual dimorphism was of a sufficient magnitude to influence the accuracy with which sex can be determined. The presence of sexual dimorphism in this skeletal element is illustrated in Figure 6.1.

As can be seen, a distinct sexually dimorphic component exists with the EPI perspective, as well as a population component. All females were viewed to group below the x-axis, while all males were viewed to group above the x-axis. In addition, the consensuses for white females and white males appear to the left of the y-axis, while the consensus for black females and black males appear to the right of the y-axis. Black males and black females appear relatively close to one another in this relative warp analysis, while white males and females are more separated.

6.1.1

Results from the EPI perspective between females and males

Figure 6.1 illustrates the differences between females and males of each biological group. Statistical analyses in the form of Goodall's F test from the IMP TwoGroup statistical package were performed to quantify the magnitude of differences between these groups. Goodall's F-test assesses inter-group shape disparity between each group, taking sample variance into account. Analyses were performed to observe the magnitude of these differences. Table 6.1 illustrates the statistically significant differences between all groups compared in Figure 6.1. Females and males of both ancestries were observed to be sexually dimorphic on a statistically significant level in the EPI perspective.

Table 6.1 confirmed the results visualized in Figure 6.1. Males and females appear to be sexually dimorphic on a significant level, as observed by their separation in the consensus relative warp grid. White males and females appear more sexually dimorphic than their black counterparts, based on the distance separating them on the relative warp grid, and the comparative Goodall's F-statistic (white females and males Goodall's F-statistic = 12.78, black females and males Goodall's F-statistic = 6.65).

A reference consensus thin-plate spline was created to view the mean shape of all the individuals in the sample for the EPI perspective. Figure 6.2 is a representation of the average shape of the all males and females exemplified by an exactly perpendicular grid. Figure 6.3 demonstrates the thin-plate spline for the deformation from the EPI perspective. The deformation grid exemplifies the areas of form breakdown from the perpendicular reference, in this case the female shape. The female shape would have appeared as a perfect perpendicular grid, and this figure now gives the degree of deformation of the males on this female reference grid. Figure 6.4 demonstrates the differences exhibited between females and males in thin-plate spline vector mode. Vector mode thus represents not only the differences in morphology, but also the direction and magnitude of that change. In Figure 6.4 the points (or circles) represent the first shape (female) while the arrows represent the direction of the male shape.

As seen in Figures 6.3 and 6.4, most discrepancy between females (the point of origin of the arrow in vector mode) and males (the end length of the arrow in vector mode) existed in the portion of the medial epicondyle. The "root" of the medial epicondyle (landmark six) is lower and more defined from landmark five, making the medial epicondyle sit more centrally within the trochlea, instead of positioning itself in a more distal location. The surface of the medial epicondyle was lower and more compact in males, with the most distal point (landmark ten) closer to the table on which the bone rested. The female medial epicondyle appeared more elevated

through landmarks 6 to 12. Differences could also be seen in the lateral portion of the posterior humerus, where the most lateral point in males (landmark 19) was located higher, and the medial margin of the lateral epicondyle (landmark 1) was located in a more elevated position, in contrast to the female lateral epicondylar ridge existing lower on the posterior humeral surface. Landmarks 16 and 17, which document the morphology of the anterior border of the capitulum and trochlea, appeared slightly constricted upwards in males.

The accuracy by which these differences in the distal humerus can assign specimens was assessed by means of a canonical variates analysis (CVA). A CVA can test the accuracy with which this particular aspect of the distal humerus can be categorized as female or male. Table 6.2 represents the accuracies obtained from this analysis.

Female specimens were correctly categorized 79% of the time, (129/163) while male specimens were 78% accurate in their morphology (143/ 184). The significance value obtained by the canonical variates analysis (148.185) was greater than the critical value of chi square distribution at the significance value of 0.05 with 30 degrees of freedom (43.773). Both males and females were categorized correctly a large percent of the time, thus showing that the differences observed during standard non-metric morphological assessment could also be observed when using geometric morphometrics, and are quantifiable.

6.1.2

Results from the EPI perspective: black females vs. males

Sexual dimorphism between black females and black males is shown in Figure 6.1, and the statistical significance between the sexes is quantified by Goodall's F-statistic in Table 6.1. Sexual dimorphism in this perspective was lower in black South Africans than in white South Africans. Females and males were thus

compared independently so as to visualize sexually dimorphic changes in the EPI perspective, and to observe any differences in this specific sample.

Figure 6.5 demonstrates the thin-plate spline in deformation mode, which indicates the location on the EPI perspective where males deviate from the female reference grid. A warped or deformed portion of the grid designates morphological difference. Figure 6.6 is the thin-plate spline in vector mode, which illustrates the differences between black females and black males from the EPI perspective. Vector mode represents the direction and magnitude of change between the sexes in the sample. In Figure 6.6 the points (or circles) represent the first shape represented (black females) while the arrows represent the direction of the black male shape.

As seen in Figure 6.5, most discrepancy between black females and black males occurred along the lateral margin, which "tilted" the graph downwards on the left-hand (lateral) margin. Deformation was also observed along the points around the medial epicondyle. In vector mode as seen from Figure 6.6, females (the point of origin of the arrow in vector mode) and black males (the end length of the arrow in vector mode) differ in that the medial ridge of the lateral epicondyle (landmark 1) sits lower, or more towards the anterior, in males. This change of anteriorly migrating landmarks repeats with landmarks 18 and 19. In addition, landmark 15, the inferior edge of the trochlea, was seen to be higher in males, giving the inferior "spool" view of the humerus a less-constricted shape. Landmarks along the anterior surface of the medial epicondyle (landmarks 10 through 14) were observed to be higher in males than females. From this perspective, the medial epicondyle appears thinner in males than females. Because if this, the medial epicondyle in males may appear more angled away from the table with the position of landmarks 10 through 14; this angled aspect of the medial epicondyle is considered a "female" characteristic.

The accuracy by which these differences in the distal humerus can assign black South African specimens was assessed by means of a canonical variates analysis (CVA). A CVA can test the accuracy with which this particular aspect of the

distal humerus can be categorized as female or male. Table 6.3 represents the accuracies obtained from this analysis.

Black female specimens were correctly categorized 83% of the time, (83/ 100) while male specimens were 85% accurate (85/ 108). The significance value obtained by the canonical variates analysis (110.017) was greater than the critical value of chi square distribution at the significance value of 0.05 with 30 degrees of freedom (43.773). The classification accuracy was high for both black females and black males, thus showing that the sexual dimorphism in this population was quantifiable when using geometric morphometrics.

6.1.3

Results from the EPI perspective: white females vs. males

Sexual dimorphism between white females and white males was seen in Figure 6.1, as white females and white males appeared in different quadrants of a four-quadrant grid. The subsequent statistical significance between the sexes was quantified by Goodall's F-statistic in Table 6.1. Using this perspective, sexual dimorphism was evident for this group. Females and males were thus compared in this population independently so as to visualize these sexually dimorphic changes in the EPI perspective, and to observe any differences between the white and black samples.

Figure 6.7 demonstrates the thin-plate spline in deformation mode between females and males of the white group, which demonstrates the deviation males have from a perfect perpendicular grid (the female mean). Deformation in Figure 6.7 was seen primarily in the homologous landmarks placed around the medial epicondyle. Figure 6.8 subsequently shows the thin-plate spline in vector mode, which illustrates the magnitude and direction of differences between white females and white males from the EPI perspective. In Figure 6.7 the points (or circles) represent the first

shape represented (white female) while the arrows represent the direction of the white male shape.

As seen in Figure 6.8, females exhibited a markedly "raised" or angled medial epicondyle (considered classic "female" morphology), while male landmarks placed around this feature (landmarks 7 through 12) appeared lower and more towards the anterior surface of the bone. This would account for a more parallel angle to the medial epicondyle, which was considered a classic "male" profile. In addition, the landmarks placed on the lateral surface of the distal humerus (landmarks 18 and 19) were farther posteriorly on the male perspective than on the female perspective. These differences were similar to those seen in black South Africans in that the majority of the variation between males and females was observed through the surface of the medial epicondyle.

The accuracy by which these differences in the distal humerus can assign white specimens was assessed by means of a canonical variates (CVA) analysis. A CVA tests the accuracy with which this particular aspect of the distal humerus can be categorized as female or male. Table 6.4 represents the accuracies obtained from this analysis.

Female specimens were correctly categorized 91% of the time, (57/ 63) when compared to white males. White male specimens were classified at a 90% accuracy rate (68/ 76). The significance value obtained by the canonical variates analysis (107.188) was greater than the critical value of chi square distribution at the significance value of 0.05 with 30 degrees of freedom (43.773). The classification accuracy was high for both white females and white males, thus showing that the sexual dimorphism in this population was quantifiable when using geometric morphometrics.

Each biological affiliation, as well as the combined data of all females and all males, exhibited marked sexual dimorphism from the EPI perspective. Thus sexual dimorphism could be quantified, and correct classification of males and females was

sample used.

6.1.4

Sexual dimorphism and the onset of age: EPI perspective

Analyses were then performed in order to discern if characteristics from this perspective changed with the onset of age. Thus, each biological group and both sexes were further categorized as "young" (50 years of age or younger) and "old" (over 50 years of age). This provided an amalgamation of eight groups: young black females, young white females, old black females, old white females, young black males, young white males, old black males and old white males. The differences between males and females from each age group were subsequently examined.

A consensus relative warp analysis on all eight possible groups for the EPI perspective was performed to visualize the groupings between each combination of the sample (Figure 6.9). All eight permutations (1. young black female, 2. young white female, 3. old black female, 4. old white female, 5. young black male, 6. young white male, 7. old black male, 8. old white male) separate to a certain extent and cluster to a certain degree. Thus it is clear that there are differences between males and females, but population affinity and variations in age may also play roles in the separation of these groups.

Young and old groups appear commingled together, while those grouped in the black and white populations appear to cluster separately on the left and right side of the medial Y-axis, respectively. Females of each population clustered together (above the horizontal axis), and males of each population and age were observed to cluster together (mostly below the horizontal axis). Figure 6.9 also illustrates that young individuals of each biological affinity are quite separated from each other, while the old individuals of each biological affinity appear to "migrate" towards each other and become more similar.

6.1.5

Sexual dimorphism and the onset of age: black females and males

Evidence represented in Figure 6.9 shows that differences exist between black males and females, and that morphology of the posterior humerus from the EPI perspective appears to differ between young and old individuals. First, consensus thin-plate splines in vector mode were created for black females and black males independently to observe the differences between young and old consensus shapes. Figure 6.10 is the thin-plate spline in vector mode that exemplifies the changes females underwent with the onset of age.

As seen in Figure 6.10, changes from the young black female shape to the old black female shape took place primarily in the lateral and posterior surfaces of the perspective. Vector mode illustrates this expansion of the lateral and posterior surface. Landmarks 15 and 16 become lower along the border of the trochlea (which is medial) while landmarks 1, 2, 18 and 19 (all situated laterally) expand upwards, creating a thicker lateral portion. Changes in the medial epicondyle and its angle in the black female with age were minimal.

The changes that occur with age in black males can be seen in Figure 6.11. This graph shows the vector mode for black males as it transforms from "young" morphology to "old" morphology. Differences between young black males and old black males existed along the lateral and medial edges. These changes with the black male EPI perspective with age appeared more marked than in their female counterparts.

When observing the vector mode, several morphological differences are apparent. Landmark 1 appeared to rise higher, making the medial ridge of the lateral epicondyle more apparent. Landmark 14 was viewed lower or more anteriorly in old males, making the medial epicondyle take on a thicker appearance where it joins the trochlea. Landmark 15 also appeared lower (or more anteriorly) while landmark 17

rose upwards; the combination of this result may indicate more constriction within the area between the capitulum and the trochlea. Finally, landmarks 18 and 19 migrated towards the posterior, placing the tip of the lateral epicondyle and the lateral margin of the capitulum in a more posterior position.

Through viewing the direction and magnitude of change in thin-plate spline vector mode analyses, changes in black males and females with the onset of age were observable (Figures 6.10 and 6.11). In addition, Goodall's F-statistic comparing the young black sample (young black females vs. young black males) and the old black sample (old black females vs. old black males) was significant for both groups, but as seen in Table 6.5, the strength of the statistical significance decreased with the old sample (Goodall's F-statistic for the young sample = 5.50, df = 30, p = 0.000<0.05; Goodall's F-statistic for the old sample = 3.72, df = 30, 0.000<0.05). Because obvious changes were seen with age, the classification accuracies of both young and old individuals were calculated as a means to test whether sex could still be correctly assigned to the aged sample.

Table 6.6 illustrates the classification accuracy between males and females of both age groups. As can be seen in this table, young black individuals were classified at a high rate of accuracy when compared to each other (94% accurate for young black females, 89% accurate for young black males). The correct assignment of sex actually increased with the onset of age for old black females and old black males (96% and 94%, respectively). Both sets of changes were deemed statistically significant. This assessment of changes occurring with age may indicate that as the black population gets older, the classic "male" and "female" morphology of the inferior humerus and the angle of the medial epicondyle became more sexually dimorphic, and thus a higher percentage of individuals may be correctly classified. Changes with age to the distal humerus in the EPI perspective did not influence the classification accuracy for black South Africans. This trait is consistent in sorting between males and females regardless of age.

6.1.6

Sexual dimorphism and the onset of age: white females and males

In contrast to that observed in black South Africans, evidence represented in Figure 6.9 showed that differences existed between white males and females for the morphology of the posterior humerus from the EPI perspective. Consensus thin-plate splines in vector mode were created for white females and white males to observe the differences between young and old consensus shapes. Figure 6.12 is the thin-plate spline in vector mode that exemplified the changes white females underwent with the onset of age.

In vector mode, the landmarks in the region of the medial epicondyle (landmarks 7 through 14) appeared to increase in elevation and angle both posteriorly and medially from the young white female morphology (circles) to the old white female morphology (arrows). This result would create the appearance of a more slanting or "raised" medial epicondyle angle. Based on the fact that a posteriorly slanting medial epicondyle is considered a distinctly female characteristic, this may produce more explicit sexual dimorphism in old white females from the EPI perspective. Thus, old white females will take on a more classic "female" appearance.

In addition, the lateral surfaces of the medial epicondyle appeared to migrate towards the anterior surface. Landmarks 1, 2, 3, 16, 17, 18 and 19 shifted anteriorly from young white females to old white females, which may have created a less-constricted anterior capitulum spool and a thinner lateral epicondyle.

Young white males and old white males did exhibit small morphological differences, as seen in the relative warp analysis in Figure 6.9. To visualize these differences, thin-plate splines were created in vector mode to observe the location and direction of variation between the young white male EPI perspective, and the old white male EPI perspective. The changes that occur with age in white males can be

seen in Figure 6.13. This graph shows the vector mode for white males as it transforms from "young" morphology to "old" morphology.

As seen in Figure 6.13, differences between young white males and old white males existed along the lateral and medial edges. The vector arrows indicated directional change, where the posterior margin of the lateral epicondyle descended (landmark 1), as did landmarks three and four placed within the curvature of the distal posterior humeral surface. The posterior "root" of the medial epicondyle, represented by landmark six, migrated closer towards landmark five. This result would place the medial epicondyle more posteriorly within the profile of the trochlea, which is a more distinctly "female" characteristic.

Changes in white males and females with the onset of age were observable by viewing the direction and magnitude of change in thin-plate spline vector mode analyses (Figures 6.12 and 6.13). Visible changes in the white female EPI perspective were apparent; white female morphology appeared to diverge in numerous locations. In addition, Goodall's F-statistic comparing the young white sample (young white females vs. young white males) and the old sample (old white females vs. old white males) was significant for both groups, but as seen in Table 6.7, the significance in the statistic was not as considerable between young males and females (Goodall's F-statistic for the young sample = 4.44, df = 30, p = 0.014<0.05; Goodall's F-statistic for the old sample = 8.80, df = 30, 0.000<0.05). Because obvious changes were seen with age, the classification accuracies of both young and old individuals were calculated to determine if this accuracy rate decreased with the aging morphology of the white population.

Table 6.8 illustrates the classification accuracy between males and females of both age groups. As can be seen in this table, canonical variates analysis from the IMP statistical package could not correctly distinguish young white females from young white males with the EPI perspective; no statistics were generated when the analysis was performed. This indicated that the morphology of the EPI perspective

with these two groups compared was virtually the same. The sample size of the young population may also have played a role in the inability to perform statistical analysis. Old white females and males, however, were sorted successfully when compared to each other. Old white females were classified correctly 92% of the time when compared to their old male counterparts. The old male sample was classified at a rate of 85% accuracy. This assessment of changes occurring with age may indicate that as the white population gets older, the classic "male" and "female" morphology of the inferior humerus and the angle of the medial epicondyle become more sexually dimorphic, and thus a higher percentage of individuals may be correctly classified. Sexual dimorphism appeared to increase; with the females, in particular, becoming more "female" in their morphology, and the males acquiring a slightly more "male" morphology. Changes with age to the distal humerus in the EPI perspective did influence the classification accuracy for this biological group. The younger group appeared to exhibit more ambiguous or variable morphology from the EPI view than the older group.

6.2

Sexual dimorphism in the distal humerus: OL perspective

Fifteen homologous landmarks were assigned to the posterior humerus, as shown in Figure 3.27. The OL perspective quantified characteristics of the distal humerus that included the olecranon fossa shape and trochlear extension through landmark data analysis. In order to confirm that the posterior humerus was sexually dimorphic, the first analyses focused on establishing the degree of dimorphism and the classification accuracies between females and males. Consensus relative warp analysis performed with the statistical package tpsRelw required the comparison of a

minimum of four groups within a sample. Therefore, the sample was divided into four initial assemblages based on biological affiliation to observe the presence of sexual dimorphism in this anatomical perspective of the posterior humerus. This separation of the sample into "black" and "white" male and female populations was to determine whether significant differences occurred between the groups, and if sexual dimorphism was of a sufficient magnitude to influence the accuracy with which sex can be determined. The presence of sexual dimorphism in this skeletal element is illustrated in Figure 6.14.

As can be seen, a distinct sexually dimorphic component existed with the OL perspective, as well as a population component. All females were viewed to group below the x-axis, while all males were viewed to group above the x-axis. In addition, the consensuses for white females and white males appear to the left of the y-axis, while the consensus for black females and black males appear to the right of the y-axis. This initially indicated that the OL perspective and its quantified morphology might be distinct between males and females as well as between black and white South Africans.

6.2.1

Results from the OL perspective between females and males

Figure 6.14 illustrates the differences between females and males of each group, but does not indicate a statistical significance between those present in the assemblage. Statistical analyses in the form of Goodall's F test from the IMP TwoGroup statistical package was performed to quantify the magnitude of differences between the above four groups. Goodall's F-test assesses inter-group shape disparity between groups, taking sample variance into account. Analyses were performed to observe the magnitude of these differences. Table 6.9 illustrates the statistically significant differences between all groups compared in Figure 6.14.

Females and males of both ancestral groups were observed to be sexually dimorphic on a statistically significant level with the OL perspective.

Table 6.9 confirmed the results visualized in Figure 6.14. Males and females appear to be sexually dimorphic on a significant level, as observed by their separation in the consensus relative warp grid and by their significant Goodall's F-statistic. All permutations seen in Table 6.9 were significantly different enough to deem the OL perspective and the shape of the olecranon fossa sexually dimorphic.

A reference consensus thin-plate spline was created to view the mean shape of all the individuals in the sample for the OL perspective. Figure 6.15 is a representation of the average shape of the all males and females exemplified by an exactly perpendicular grid. Figure 6.16 demonstrates the thin-plate spline for the deformation from the OL perspective. The deformation grid exemplifies the areas of form breakdown from the perpendicular reference, in this case the female shape. The female shape would have appeared as a perfect perpendicular grid, and this figure now gives the degree and deformation of the males on this female/ reference grid. Figure 6.17 demonstrates the differences exhibited between females and males in thin-plate spline vector mode. Vector mode thus represents not only the differences in morphology, but also the direction and magnitude of that change. In Figure 6.17 the points (or circles) represent the first shape represented (females) while the arrows represent the direction of the male shape.

As seen in Figures 6.16 and 6.17, discrepancy between females (the point of origin of the arrow in vector mode) and males (the end length of the arrow in vector mode) existed in the olecranon fossa shape and the distal boundary of this view of the humerus. Females appeared to have a lower (more posteriorly placed) superior margin of the olecranon fossa. Landmark five, the point that makes the olecranon fossa decidedly oval (in females) or triangular (in males) is placed higher along the medial shaft of the bone with males. Subsequently, this would create a more triangular shape in the male olecranon fossa. This finding corresponds to the visual

characteristic in which males exhibited triangular olecranon fossa shapes (thus exhibiting a higher superior olecranon fossa margin, indicated by landmark five) and females have an oval olecranon fossa shape (exhibited by a lower superior olecranon fossa margin). Landmark 1 is in direct correlation with this observation, because it is based on the most-superior point on the olecranon fossa. As Figure 6.17 has shown, it also appears higher than the female adaptation of landmark 1. In addition, the medial margin of the olecranon fossa was located more posteriorly than females, indicated by landmark four. The most lateral point of the lateral epicondyle (landmark 11) is also higher in males than in females, while landmark 12 (denoting the most medial point of the medial epicondyle) appeared farther distally in males than females. Landmarks 13, 14 and 15 indicate the inferior border of the distal humerus. The edge of the posterior capitulum (landmark 13) was higher in males than females. This result, coupled with the extension and projection of the edge of the posterior trochlea (landmark fifteen) created a more "extended" trochlea past the margin of the capitulum, a feature that is considered to be distinctly "male". It appeared as if this feature (trochlear extension) might be successfully quantified as sexually dimorphic in addition to the shape of the olecranon fossa.

The accuracy by which these differences in the distal humerus can assign a specimen was assessed by means of a canonical variates analysis (CVA). Table 6.10 represents the accuracies obtained from this analysis.

Female specimens were correctly categorized 83% of the time (135/163) and male specimens 84% (156/ 185). As shown by the chi square value of 211.344 (significant at $p<0.05$) the OL perspective, which included a quantitative observation of the olecranon fossa shape as well as the extension of the trochlea, was sexually dimorphic on a statistically significant level. Males and females could be classified accurately 83% to 84% of the time.

6.2.2

Results from the OL perspective: black females vs. males

Sexual dimorphism between black females and black males was shown in Figure 6.14, and the statistical significance between the sexes was quantified by Goodall's F-statistic in Table 6.9. Sexual dimorphism in this perspective was higher in black South Africans than in white South Africans. Females and males were thus compared in this population independently so as to visualize these sexually dimorphic changes in the OL with sex and the onset of age.

Figure 6.18 demonstrates the thin-plate spline in deformation mode, which indicates the location on the OL perspective where females and males deviate from each other. A warped or deformed portion of the grid designates morphological difference. Figure 6.19 is the thin-plate spline in vector mode, which illustrates the differences between black females and black males from the OL perspective. In Figure 6.19 the points (or circles) represent the first shape represented (black female) while the arrows represent the direction of the black male shape.

As seen in Figure 6.18, most discrepancy between black females and black males occurred along the peripheral margins, which "tilted" the graph downwards on the right-hand (medial) margin. In vector mode as seen from Figure 6.19, black females (the point of origin of the arrow in vector mode) and black males (the end length of the arrow in vector mode) differ in that both lateral landmarks 1 and 11 appeared superiorly in males. The medial corresponding landmark that indicated the tip of the medial epicondyle (landmark 12) subsequently was viewed to be more inferior in males. Additional differences between black females and black males were exhibited along the inferior border of the humerus. The distal margin of the capitulum appeared higher in males (landmark 13). In addition, the distal margin of the trochlea appeared lower and more extended in males (landmark 15). This would create the visual characteristic of a more inferiorly projecting trochlea past the margin

of the capitulum from this perspective. This result is analogous to the total population thin-plate spline between females and males (Figure 6.17). Again, this extension of the trochlear margin was considered a distinctly male trait in non-metric morphology.

The accuracy by which these differences in the distal humerus can assign black specimens was assessed by means of a canonical variates (CVA) analysis (Table 6.11). Black female specimens were correctly categorized 82% of the time, (82/ 100) while male specimens were 81% accurate (89/ 110). The value obtained by the canonical variates analysis (123.551) was significant at $p < 0.05$. The classification accuracy was high enough such that sexual dimorphism fro the OL perspective is quantifiable in black females and males

6.2.3

Results from the OL perspective: white females vs. males

Sexual dimorphism between white females and white males was seen in Figure 6.14, as these groups appeared in different quadrants of a four-quadrant grid. The subsequent statistical significance between the sexes was quantified by Goodall's F-statistic in Table 6.9. Females and males were thus compared independently so as to visualize differences between the sexes and with the onset of age.

Figure 6.20 demonstrates the thin-plate spline in deformation mode between females and males, which demonstrates the deviation males have from a perfect perpendicular grid (the female mean). Deformation in Figure 6.20 was seen primarily in the homologous landmarks placed around the periphery of the distal humerus. Figure 6.21 subsequently shows the thin-plate spline in vector mode. In Figure 6.21 the points (or circles) represent the first shape represented (white females) while the arrows represent the direction of the white male shape.

As seen in Figure 6.21, those landmarks that denote the superior margin of the olecranon fossa (corresponding landmarks 1, 2, and 5) appear higher in the male

than the female humerus. This indicates the olecranon fossa projected farther up the medial shaft of the humerus in males, creating a more triangular shape in that region of the fossa. In addition, the projection of the inferior trochlea (landmark 15) appeared greater in males than in females. Landmark 15 appeared to project medially as well, causing the extension past the inferior margin of the capitulum (landmark 13) to be more pronounced in males. In all, the differences around the periphery of the trochlea and capitulum seemed to be more pronounced than differences seen in the olecranon fossa.

The accuracy by which these differences in the distal humerus can assign sex was assessed by means of a canonical variates (CVA) analysis. Table 6.12 represents the accuracies obtained from this analysis. Females were correctly categorized 87% of the time, (55/ 63) and males 88% (66/ 75). This was statistically significant at $p<0.05$. Therefore, this trait is sexually dimorphic and can be quantifiable when using geometric morphometrics in the OL perspective.

6.2.4

Sexual dimorphism and the onset of age: OL perspective

A quantifiable difference between males and females in both populations was observed when applying geometric morphometrics to the OL perspective, a view that exemplifies the olecranon fossa shape and trochlear extension in the posterior and distal humerus. This combination of these two characteristics was thus shown to be sexually dimorphic on a statistically significant level. Analyses were then performed in order to discern if characteristics from this perspective changed with the onset of age. Thus, each biological affiliation and both sexes were further categorized as "young" (50 years of age or younger) and "old" (over 50 years of age). This provided an amalgamation of eight groups: young black females, young white females, old black females, old white females, young black males, young white males, old black

males and old white males. The differences between males and females from each age group were subsequently examined.

A consensus relative warp analysis on all eight possible groups for the OL perspective was performed to visualize the groupings between each combination of the sample (Figure 6.22). All eight permutations (1. young black female, 2. young white female, 3. old black female, 4. old white female, 5. young black male, 6. young white male, 7. old black male, 8. old white male) separate into distinctive groupings or "clusters". Females of each biological affiliation clustered together, as did males of each affiliation. Females were observed below the margin of the x-axis, while males were above the x-axis. This indicated that the quantification of the OL perspective was sexually dimorphic. Young and old groups appeared to cluster together, which indicated that this characteristic changed little with age. Those grouped in the black and white groups appear to cluster separately on the right and left side of the medial Y-axis, respectively.

6.2.5

Sexual dimorphism and the onset of age: black females and males

Evidence represented in Figures 6.14 and 6.22 shows that differences exist between black males and females, and that morphology of the posterior humerus from the OL perspective varied little between the age groupings of "young" and "old". First, consensus thin-plate splines in vector mode were created for black females and males independently to observe the differences between young and old consensus shapes.

Figure 6.23 is the thin-plate spline in vector mode that exemplifies the changes black females underwent with the onset of age. The lateral and medial ridges of the humerus above both epicondyles migrated inferiorly and superiorly (landmark 1 and 2, respectively). The lateral and medial edges of each epicondyle migrated inferiorly and superiorly (landmark 11 and 12, respectively). Landmark 13,

the inferior margin of the capitulum, extended farther inferiorly while the inferior margin of the trochlea (landmark 15) contracted farther superiorly in old black females. These two changes between young black females and old black females would possibly cause a loss of trochlear extension in this portion of the humerus. A lack of trochlear extension (where the inferior edge of the capitulum and the inferior edge of the trochlea were more equal) was considered a distinctly "female" characteristic.

Each group of black females was different based on the separation from the relative warp analysis grid. This separation did not appear considerable, based on the fact that each clustered together in the lower right-hand portion of a four-quadrant grid. The subsequent canonical variates analysis, however, confirmed that the difference between young and old black females was great enough to quantify and categorize each with a high degree of accuracy.

The changes that occur with age in black males can be seen in Figure 6.24. This graph shows the vector mode for black males as it transforms from "young" morphology to "old" morphology. As seen in Figure 6.24, minimal changes were observed. The most lateral point of the olecranon fossa (landmark 3) travelled to a more superior position in old black males, while the lateral edge of the lateral epicondyle was seen to once again move superiorly as the medial edge of the medial epicondyle (landmark 12) positioned itself more inferiorly. Finally, the inferior edge of the trochlea (landmark 15) was observed to extend more inferiorly, and migrate slightly medially as well. These differences did appear subtle.

Changes in black males and females with the onset of age were observable by viewing the direction and magnitude of change in thin-plate spline vector mode analyses (Figures 6.23 and 6.24). In addition, Goodall's F-statistic comparing the young (young black females vs. young black males) and the old (old black females vs. old black males) was statistically significant. As seen in Table 6.13, the significance in the statistic decreased with the old sample (Goodall's F-statistic for

the young sample = 5.80, df = 22, p = 0.000<0.05; Goodall's F-statistic for the old sample = 2.45, df = 22, 0.000<0.05). Because obvious changes were seen with age, the classification accuracies were calculated and compared so as to observe a change, if any, to the assignment of sex with the onset of age.

Table 6.14 illustrates the classification accuracy between males and females of both age groups. As can be seen in this table, young black individuals were classified at a high rate of accuracy when compared to each other (84% accurate for young black females, 95% for young black males). The high classification rate indicates that males, when grouped in a young age category, exhibit marked male morphology that was easily quantifiable and discernable from the female shape.

Classification accuracy decreased for males with the onset of age (95% to 85%). This may indicate that as the black population gets older, the classic "male" and "female" morphology of distal humerus, including features such as the olecranon fossa shape, become less sexually dimorphic, and thus the ability to correctly assign a specimen to male or female declined.

6.2.6

Sexual dimorphism and the onset of age: white females and males

Evidence represented in Figures 6.14 and 6.22 showed that differences existed between white males and females, and that morphology of the distal humerus from the OL perspective appeared to not differ greatly between young and old individuals. Refer to Figure 6.22 for a summary of the clustering exhibited by all eight permutations in the OL perspective. Consensus thin-plate splines in vector mode were created for white females and males to observe the differences between young and old consensus shapes.

Figure 6.25 is the thin-plate spline in vector mode that exemplified the differences between young and old white females. The thin-plate spline in vector mode showed that little movement of homologous landmarks took place. The lateral

margin of the lateral epicondyle (landmark 11) migrated more superiorly between white females in the "young" and "old" groups. Landmark 13, the inferior margin of the capitulum, also migrated more superiorly in old white females, indicating an increase in trochlear extension on the medial side. This would provide a less "female" profile of the capitulum compared to the trochlea, which should be more equal in females. Landmark 2, the point placed upon the medial epicondylar ridge, moved inferiorly with age to a position lower than that of the young white female. In general, the morphological features of olecranon fossa shape and trochlear extension appeared to stay largely the same with the onset of age in the white female humerus.

Young white males and old white males did exhibit small morphological differences, as seen in the relative warp analysis in Figure 6.22. To visualize these differences, a thin-plate spline was created in vector mode to observe the location and direction of variation between the young and old in the OL perspective (Figure 6.26). Figure 6.26 indicated a lack of any variation with the absence of arrows indicating the direction of variation.

Small changes in white males and females with the onset of age were observable by viewing the direction and magnitude of change in thin-plate spline vector mode analyses (Figures 6.25 and 6.26). Goodall's F-statistic comparing the young white sample (young white females vs. young white males) and the old (old white females vs. old white males) were statistically significant for both groups, but as seen in Table 6.15, the significance in the statistic appeared to be greater with the old sample (Goodall's F-statistic for the young sample = 1.79, df = 22, p = 0.022<0.05; Goodall's F-statistic for the old sample = 3.32, df = 22, 0.000<0.05). Because the changes in the white population were very subtle with the OL perspective, the classification accuracies were calculated and compared so as to observe a change, if any, to the assignment of sex with the onset of age.

Table 6.16 illustrates the classification accuracy between males and females of both age groups. As can be seen in this table, young individuals were classified at a 92-100% rate of accuracy when compared to each other (92% accurate for young white females, 100% accurate for young white males). This shows females and males within this small sub-group of the white population exhibit enough divergent morphology to be categorized correctly the majority of the time. This classification accuracy was unusually high for any characteristic categorizing the differences between males and females. The small sample size for young white individuals (13 for females, 23 for males) may have played a role in the canonical variates analysis results being uncommonly accurate.

Classification accuracy decreased slightly with the onset of age in the white sample, however. Old white females and males were each classified correctly 90% of the time. This assessment of changes occurring with age may indicate that as the white population gets older, the classic "male" and "female" morphology of the inferior humerus and the angle of the medial epicondyle stayed relatively static in its sexual dimorphism. Females exhibited quantifiable "female" characteristics in the OL perspective, and these characteristics did not change with the onset of age, allowing for old females to be categorized correctly even when older individuals were assessed. Males exhibited the same absence of change with the onset of age. Morphological modification with age to the distal humerus in the OL perspective did not adversely influence the classification accuracy for this sample.

Although females and males from different samples exhibited variation in their classification accuracy, the OL perspective remained a good indicator of sex, when the shape of the olecranon fossa and the extension of the trochlea were quantified. Thus the OL perspective can bee seen as a sexually dimorphic feature that changes only subtly with the onset of age.

6.3

Sexual dimorphism in the pelvis: SUB perspective

Twenty-eight homologous landmarks were assigned to the subpubic portion of the pelvic bone as shown in Figure 3.28. The SUB perspective quantified characteristics of the subpubic concavity and subpubic angle through landmark data analysis. This view also included landmarks around the margin of the obturator foramen. The obturator foramen landmarks were included only to provide distinctive points of extrapolation for homologous landmarks placed around the periphery of the pubis and ischium, and its influence in the categorization of sex appeared minimal in this capacity. Even though the obturator foramen was not intended to provide results or influence the morphology of the subpubic region of the pelvis, changes in its morphology were noted when they were observed.

In order to confirm that the pubic region of the pelvis was sexually dimorphic, the first analyses focused on establishing the degree of dimorphism and the classification accuracies between females and males. Consensus relative warp analysis performed with the statistical package tpsRelw required the comparison of a minimum of four groups within a sample. Therefore, the sample was divided into four initial assemblages.

As can be seen in Figure 6.27, a distinct sexually dimorphic component existed with the SUB perspective, as well as a smaller population component. All females were viewed to group to the right of the y-axis, while all males were viewed to the left of the y-axis. Females, although in different quadrants of the four-quadrant graph, appeared relatively close together. Males, although on the same side of the y-axis, and approximately the same distance apart from the females, appeared to diverge dramatically from each other, indicating a difference in morphology between groups. The consensuses for white females and white males appeared above the x-axis, while the consensus for black females and black males appeared below the x-

axis. This initially indicated that the SUB perspective and its quantified morphology might be distinct between males and females. In addition, biological affiliations appeared to separate to a lesser degree into different morphological forms as well.

6.3.1 Results from the SUB perspective between females and males

Figure 6.27 illustrates the differences between females and males of each group, but does not indicate a statistical significance between those present in the assemblage. Statistical analyses in the form of Goodall's F test from the IMP TwoGroup statistical package were performed to observe the magnitude of these differences. Table 6.17 illustrates the statistically significant differences between all groups compared in Figure 6.27. Females and males, regardless of biological affiliation, were observed to be sexually dimorphic on a statistically significant level with the SUB perspective.

Males and females, regardless of their population, appeared distinctly apart from each other. Females of both population groups appeared closer together in consensus morphology than their male counterparts; it appeared as if black males and white males differed considerably in their anatomical features when the consensus relative warp grid was assessed. In addition, black females and males might be more sexually dimorphic than their white counterparts, based on the comparative Goodall's F-statistic (white females and males Goodall's F-statistic = 30.09, black females and males Goodall's F-statistic = 36.59). Both, however, were significantly different enough to deem the SUB perspective and the shape of the subpubic angle sexually dimorphic.

A reference consensus thin-plate spline was created to view the mean shape of all the individuals in the sample for the SUB perspective. Figure 6.28 is a representation of the average shape of males and females exemplified by an exactly perpendicular grid. Figure 6.29 demonstrates the thin-plate spline for deformation

from the SUB perspective. The deformation grid exemplifies the areas of form breakdown from the perpendicular reference, in this case the female shape. The female shape would have appeared as a perfect perpendicular grid, and this figure now gives the degree and deformation of the males on this female/ reference grid. The deformation grid exhibited a large amount of warping and collapse along all borders where homologous landmarks were placed. Figure 6.30 demonstrates the differences between females and males in thin-plate spline vector mode. Vector mode thus represents not only the differences in morphology, but also the direction and magnitude of that change. In Figure 6.30 the points (or circles) represent the first shape represented (female) while the arrows represent the direction of the male shape.

As seen in Figures 6.29 and 6.30, discrepancy between females (the point of origin of the arrow in vector mode) and males (the end length of the arrow in vector mode) existed in the length of the pubis (landmarks 14-18), the width of the ischium (landmarks 21, 22, 24, 27 and 28), the shape of the subpubic concavity (landmarks 19, 23, 25 and 26) and the obturator foramen shape (landmarks 1-13). The vector mode thin-plate spline illustrated numerous differences between males and females in the pelvic morphology of the subpubic angle and subpubic concavity. Based on landmarks 2, 5, 10 and 11 within the obturator foramen, it appears that the male obturator foramen (the end of the arrow boundaries) was wider through the inferior and dorsal margins than females (points). Landmarks 14 through 20 (demarcating the pubis bone and the vertical pubic symphysis) illustrated that this portion of the pelvis was much shorter in males than females. Male points in this region were seen to exist farther towards the acetabulum. In addition, landmarks 21, 23, 25 and 26 along the subpubic concavity were shorter and more medially inclined in the male than the female pelvis. This would create a thicker ischium and a narrow subpubic concavity without much extension or angling as it extended towards the ischium.

Finally, landmarks 22, 24, 27 and 28 demonstrated that the male ischium throughout this region was wider and thicker than that of females.

The accuracy by which these differences in the pelvis can assign a specimen was assessed by means of a canonical variates (CVA) analysis. Table 6.18 represents the accuracies obtained from this analysis.

Both females and males were correctly categorized 94% of the time (135/143 females; 165/ 175 males). The chi square value obtained by the canonical variates analysis was significant at the 0.05 level, which indicated that the SUB perspective, which included a quantitative observation of the subpubic angle and the subpubic concavity, was sexually dimorphic on a statistically significant level.

6.3.2

Results from the SUB perspective: black females vs. males

Sexual dimorphism between black females and males was initially shown in Figure 6.27, and the statistical significance between the sexes was quantified by Goodall's F-statistic in Table 6.17. Sexual dimorphism in this perspective appeared more statistically significant in this sample than in the white sample. Sex was compared independently so as to visualize sexually dimorphic differences in the SUB perspective and to observe any changes.

Figure 6.31 demonstrates the thin-plate spline in deformation mode, which indicates the location on the SUB perspective where females and males deviate from each other. A warped or deformed portion of the grid designates morphological difference. Figure 6.32 is the thin-plate spline in vector mode, which illustrates the differences between black females and males from the SUB perspective. As in previous graphs, the points (or circles) represent the first shape represented (black female) while the arrows represent the direction of the black male shape.

As seen in Figure 6.31, the most deformation between females and males occurred along the peripheral margin of the pubic bone and directly below the inferior

margin of the pubic symphysis, the location where the subpubic concavity is visualized. These differences were similar to what was observed in the combined male and female graph, but occurring to a lesser degree. These deformations between females (as the reference) and males (as the deformation) "tilted" the graph downwards on the right-hand (medial) margin. In vector mode as seen from Figure 6.32, females (the point of origin of the arrow in vector mode) and males (the end length of the arrow in vector mode) differ in that the landmarks assigned to the superior border of the pubis (landmarks 14 through 18) are positioned more superiorly in the male than in the female sample. This would visually give the pubis a thicker profile in males than in females. The landmarks which designated the subpubic angle and subpubic concavity (landmarks 19, 21, 23, 25 and 26) appear elongated and extended in the black females. In contrast, these same points in the black male sample appear closer to the acetabulum, truncating this segment of bone into appearing thicker, less angled, and contributed to a narrower subpubic angle. The obturator foramen showed little difference between females and males. Landmarks 1, 7, and 13 were positioned more superiorly in black males, giving the foramen a wider appearance through this portion of the feature. Other homologous landmarks around the border of the obturator foramen did not exhibit differences between males and females of this sample.

The accuracy by which these differences in the SUB perspective of the pelvis can assign black specimens was assessed by means of a canonical variates (CVA) analysis (Table 6.19). Black females were correctly categorized 96% of the time, (82/ 85) while males were 98% accurate (101/ 103). This is significant at $p<0.05$. The classification accuracy was high enough for both females and males to show that the sexual dimorphism in this population was quantifiable when using geometric morphometrics from the SUB perspective.

6.3.3

Results from the SUB perspective: white females vs. males

Sexual dimorphism between white females and males was seen in Figure 6.27, as they appeared in different quadrants of a four-quadrant grid. The subsequent statistical significance between the sexes was quantified by Goodall's F-statistic in Table 6.17. Sexual dimorphism in this perspective was evident. Females and males were thus compared independently in order to visualize these sexually dimorphic changes in the SUB perspective to observe any differences between this particular sample population and the black population sample analyzed above. Figure 6.33 demonstrates the thin-plate spline in deformation mode between females and males, which demonstrates the deviation males have from a perfect perpendicular grid (the female mean). Deformation in Figure 6.33 was seen primarily in the homologous landmarks placed along the subpubic angle. Other homologous landmarks assigned to this feature appeared to be similar between sexes, as illustrated by portions of the grid that were unaffected by deformation. Figure 6.34 subsequently shows the thin-plate spline in vector mode, which illustrates the magnitude and direction of differences between white females and white males from the SUB perspective. In Figure 6.34 the points (or circles) represent the first shape represented (white female) while the arrows represent the direction of the white male shape.

As seen in Figure 6.34, those landmarks that denote the margin of the pubis (landmarks 14-18) appear to be placed more superiorly in the white male pelvis. This result was similar to that in the black sample. In addition, the homologous points that delineate the shape of the subpubic angle and subpubic concavity (landmarks 19, 21, 23, 25 and 26) migrate closer to the medial portion of the pelvis, causing the white male subpubic concavity to be short and stout, with no projection or angling. The white female subpubic concavity, in contrast, would appear more elongated and

lengthened throughout this region, a feature that is mirrored in the non-metric visual morphology in females.

White female specimens were correctly categorized 97% of the time, (56/ 58) when compared to white males (Table 6.20). White male specimens were also classified at a 97% accuracy rate (70/ 72). The significance value obtained by the canonical variates analysis (163.348) was greater than the critical value of chi square distribution at the significance value of 0.05 with 48 degrees of freedom (65.171). The classification accuracy was high for both white females and white males, thus showing that the sexual dimorphism in this population was quantifiable when using geometric morphometrics in the SUB perspective.

Each population, as well as the combined data for both sexes, exhibited marked sexual dimorphism from the SUB perspective. Thus sexual dimorphism could be quantified, and correct classification of males and females was performed at a high rate of accuracy, regardless of the biological affiliation. This confirmed ample evidence that the subpubic angle and the subpubic concavity were sexually dimorphic between females and males. Results from this study now show that these features can be quantified successfully by employing geometric morphometrics.

6.3.4

Sexual dimorphism and the onset of age: SUB perspective

A quantifiable difference between males and females in both populations was observed when applying geometric morphometrics to the SUB perspective. This feature was thus shown to be sexually dimorphic on a statistically significant level. Analyses were then performed in order to discern if characteristics from this perspective changed with the onset of age. Thus, each group and both sexes were further categorized as "young" (50 years of age or younger) and "old" (over 50 years of age). This provided an amalgamation of eight groups: young black females, young

white females, old black female lack males, young white males, old black males and old white males.

A consensus relative warp analysis on all eight possible groups for the SUB perspective was performed to visualize the groupings between each combination of the sample (Figure 6.35). All eight permutations (1. young black female, 2. young white female, 3. old black female, 4. old white female, 5. young black male, 6. young white male, 7. old black male, 8. old white male) separate into distinctive groupings. Females of each *age* group clustered together. Males grouped with population affinity. Males and females were distinctly separated on either side of the y-axis, and this indicated that the quantification of the SUB perspective was sexually dimorphic. Young females were observed in the lower right quadrant, while old females presented in the top right quadrant of the grid. This indicated that morphology changes between all females as they advance through age. Males grouped in separate quadrants based on population affinity, and not age. This indicated that morphology was similar according to biological affiliation, and the male pelvis within the subpubic concavity region changed very little with the onset of age.

6.3.5

Sexual dimorphism and the onset of age: black females and males

Evidence represented in Figures 6.27 and 6.35 show that differences exist between black males and females, and that morphology of the pelvis from the SUB perspective varied between the age groupings of "young" and "old" for females, but varied minimally for males. To quantify and compare these differences and similarities between sexes, consensus thin-plate splines in vector mode were created for black females and black males independently to observe the differences between young and old consensus shapes.

Figure 6.36 is the thin-plate spline in vector mode that exemplifies the changes black females underwent with the onset of age. The surface of the pubis

(landmarks 14 through 18) appeared to extend superiorly with age and in this instance, also appeared to "retract" dorsally, shortening the length of the pubis. Landmarks 22, 24, 27 and 28 were broader in the ischium of old females as compared to the position of the young female landmarks. Landmarks denoting the obturator foramen appeared to change minimally. The changes along the ischium were indicative of changes seen in male pelves, thus suggesting the possibility that black females exemplify more male morphology as age increases.

The changes that occur with age in black males can be seen in Figure 6.37. This graph shows the vector mode for males as it transforms from "young" to "old" morphology. As seen in Figure 6.37, differences between young and old males existed along the pubic bone and the ischium. With this graph, changes were seen as a shortening of the pubis by the points located there (landmarks 14-18) contracting dorsally, and a broadening of the ischium through the area of the ischial tuberosity, as the points located there (landmarks 22, 24, 27 and 28) expanded out past the young black male points. When comparing the two graphs between sexes (Figures 6.36 and 6.37) the landmarks located directly below the inferior pubic symphysis that defined the subpubic angle and subpubic concavity (landmarks 19, 21, 23, 25 and 26) were distributed wider along the length of the bone in females. The same landmarks in the male sample appeared closer together and more "crowded" along the length of the bone. The changes along the subpubic concavity and ischium were indicative of changes seen in other male pelves samples in this study, thus indicating the possibility that black males demonstrated more male morphology as age increases.

Changes in black males and females with the onset of age were observable by viewing the direction and magnitude of change in thin-plate spline vector mode analyses (Figures 6.36 and 6.37). In addition, Goodall's F-statistic comparing the young (young black females vs. young black males) and the old(old black females vs. old black males) was significant for both groups (Goodall's F-statistic for the young

sample = 24.64, df = 30, p = 0.000<0.05; Goodall's F-statistic for the old sample = 14.30, df = 30, 0.000<0.05). This is illustrated in Table 6.21. Because changes were seen with age, the classification accuracy of both young and old individuals was calculated to determine if this accuracy rate decreased with the aging morphology of the black South Africans.

Table 6.22 illustrates the classification accuracy between males and females of both age groups. As can be seen in this table, young black individuals were classified at a high rate of accuracy when compared to each other (98% accurate for young black females, 100% accurate for young black males). The high classification rate between young females and young males indicated that males, when grouped in a young age category, exhibit marked male morphology which is easily quantifiable and discernable from standard female morphology. Classification accuracy decreased with the onset of age when old black females were compared to old black males (93% and 100%, respectively). This assessment of changes occurring with age may indicate that as the black females gets older, the classic "male" and "female" morphology of the pelvis became less sexually dimorphic, and thus a lower percentage of females may be correctly classified. As seen in Figure 6.36, female morphology appeared to exhibit the same differences (or undergo the same changes) as male morphology with the onset of age. Figure 6.35 illustrated this result by showing old black females closer to the male groupings on the left of the y-axis than any other of the female age/ ancestry groups. Sexual dimorphism was observed in the SUB perspective, and canonical variates analysis was able to categorize each age group with accuracy. Classification accuracies for black females and males declined with age; however, the classification accuracies are so high, that accuracy was maintained between the young and the old samples.

6.3.6

Sexual dimorphism and the onset of age: white females and males

Evidence represented in Figures 6.27 and 6.35 showed that differences existed between white males and females. Morphology of the subpubic angle from the SUB perspective appeared to not differ greatly between young and old white males. However, females exhibited distinct clusters defined by age, and not population affinity. As was seen in the previous section, this influenced the classification accuracy of old black females. Refer to Figure 6.35 for a summary of the clustering exhibited by all eight permutations in the SUB perspective. Consensus thin-plate splines in vector mode were created for white females and males to observe the differences between young and old consensus shapes.

Figure 6.38 is the thin-plate spline in vector mode that exemplified the changes white females underwent with the onset of age. The thin-plate spline in vector mode showed that little movement of homologous landmarks took place between the comparison of young and old white females. The landmarks quantifying the length of the pubis (14-18) appeared to rise superiorly in older females, causing the pubis to exhibit a thicker shape through the superior pubic region. Landmarks placed on the ischium (specifically landmarks 22, 24, and 28) appeared to be located in a more inferior position in older females, which suggested the ischium would be thicker and stouter through this region in the old females. Landmarks placed around the morphology of the obturator foramen did not appear to diverge with age. In addition, the elongated "rectangular" feature of the subpubic concavity in females did not change with age. In general, the morphological features of the subpubic angle and the subpubic concavity appeared to stay largely the same with the onset of age in the white female pelvis.

Young white males and old white males did exhibit morphological differences, as seen in the relative warp analysis in Figure 6.35. To visualize these differences, a

thin-plate spline was created in vector mode to observe the location and direction of variation between the young and old white male SUB perspective. The changes that occur with age in males can be seen in Figure 6.39. This graph shows the vector mode for males as it transforms from "young" morphology to "old" morphology.

Figure 6.39 indicated change around the periphery of the SUB view, as exemplified by distinct changes occurring in the pubic bone and the subpubic angle. Landmarks assigned to the span of the pubis (14 through 18) appeared to lengthen and expand towards the pubic symphysis, which would create a longer but thicker pubic region. The superior ischial region (landmarks 19, 21, 23, 25, and 26) migrated inferiorly between young (the point) and old males (the boundary of the arrow). These differences would change the shape of the superior subpubic region by elongating this area to an extent in the old white male population. Finally, landmarks 22, 24, 27 and 28 contracted inward, towards the obturator foramen, which created a thinner ischial margin. This may indicate a movement towards a more "female" appearing ischial region.

Changes in white males and females with the onset of age were observable by viewing the direction and magnitude of change in thin-plate spline vector mode analyses (Figures 6.38 and 6.39). Goodall's F-statistic comparing the young (young white females vs. young white males) and the old (old white females vs. old white males) resulted in differing statistical outcomes. Table 6.23 illustrates that differences between young females and males are insignificant (Goodall's F-statistic = 8.13, df = 48, 0.083>0.05), while the differences between old females and males in the SUB perspective are, in fact, statistically significant. The significance in the statistic increased with the old sample (Goodall's F-statistic = 23.65, df = 48, 0.000<0.05). Because of these discrepancies and the apparent variability of male morphology in the young white male SUB perspective, the classification accuracies of both young and old individuals were calculated to determine if this accuracy rate increased with the aging morphology of white South Africans.

Table 6.24 illustrates the classification accuracy between males and females of both age groups. As can be seen in this table, canonical variates analysis from the IMP statistical package could not correctly distinguish young white females from young white males with the SUB perspective; no statistics were generated when the analysis was performed. This indicated that the morphology of the SUB perspective with these two groups compared was the same.

The small sample size for young white individuals (11 for females, 23 for males) may have played a role in the canonical variates analysis results being unable to perform the analysis. However, the variability in morphology of the young white male pelvis may have influenced the lack of differences seen when comparing young white females to young white males. Male os coxae in this group appeared to exhibit either inconsistent male pelvic morphology, or exhibited pelvic morphology that has been historically (and with other populations) attributed to females. In other words, young white males and females appeared to have largely the same pelvic morphology through the characteristics of the SUB perspective.

Classification accuracy in the old sample provided accurate results, however. Old white females were classified correctly 98% of the time when compared to their old male counterparts. The old males were also classified at a rate of 98% accuracy. This assessment of changes occurring with age may indicate that as white South Africans get older, the classic "male" and "female" morphology of the pelvis changes dramatically in its degree of sexual dimorphism. Old females and males exhibited quantifiable characteristics in the SUB perspective, allowing for old females to be categorized correctly when compared to old males. Sexual dimorphism was present in the older group.

Although females and males from different ancestries exhibited differing rates of classification accuracy, the SUB perspective was still observed to be a highly accurate indicator of sex when the shape of the subpubic angle and the subpubic concavity were quantified, and males and females were compared to each other.

Thus the SUB perspective was deemed sexually dimorphic. However, unusual results with the young white sample population and the inability of the CVA program to correctly categorize males from females in this sample illustrated a peculiar divergence in this sample that is neither expected nor a classic divergence based on sexual dimorphism. White South Africans did not conform to the classic tenets of sexual dimorphism as seen in other populations.

6.4

Sexual dimorphism in the pelvis: SCI perspective

Five homologous landmarks were assigned to the portion of the pelvic bone as shown in Figure 3.29. The SCI perspective quantified characteristics of the greater sciatic notch through landmark data analysis. Confirmation of the sexually dimorphic nature in the SCI perspective was achieved; the presence of sexual dimorphism in this skeletal element is illustrated in Figure 6.40.

As can be seen, a sexually dimorphic component existed with the SCI perspective, as well as a population component between sexes. All females were viewed to group to the left of the y-axis and within the upper left hand quadrant of the grid. All males were viewed to the right of the y-axis, while males from each population presented in different quadrants on the right-hand side of the grid. Males, although on the same side of the y-axis, appeared to diverge dramatically from each other, indicating a difference in morphology between groups. In addition, white males were observed to be quite close to the nearest female consensus, the black females. This initially indicated that the SCI perspective and its quantified morphology might be distinct between males and females. In addition, population groups in males appeared to separate into different morphological forms as well, with white males presenting fairly close to the black female SCI consensus shape. Females appeared more congruent with each other across ancestry types

6.4.1

Results from the SCI perspective between females and males

Figure 6.40 illustrates the differences between females and males. Statistical analyses in the form of Goodall's F test from the IMP TwoGroup statistical package was performed to quantify the magnitude of differences between the above four groups. Goodall's F-test assesses inter-group shape disparity between groups, taking sample variance into account. Analyses were performed to observe the magnitude of these differences. Table 6.25 illustrates the differences between all groups compared in Figure 6.40. All groups were observed to be sexually dimorphic on a statistically significant level with the SCI perspective.

Table 6.25 confirmed the results visualized in Figure 6.40. Males and females appear to be sexually dimorphic on a significant level, as observed by their separation in the consensus relative warp grid. Males and females, regardless of their population, appeared distinctly apart from each other. Females appeared closer together in consensus morphology than their male counterparts; it appeared as if black and white males differed considerably in their anatomical features when the consensus relative warp grid was assessed. In addition, black females and males may be more sexually dimorphic than their white counterparts, based on the comparative Goodall's F-statistic (white females and males Goodall's F-statistic = 46.04, black females and males Goodall's F-statistic = 60.28). Both, however, were significantly different enough to deem the SCI perspective and the shape of the greater sciatic notch sexually dimorphic.

A reference consensus thin-plate spline was created to view the mean shape of all the individuals in the sample for the SCI perspective. Figure 6.41 is a representation of the average shape of the males and females exemplified by an exactly perpendicular grid. Figure 6.42 demonstrates the thin-plate spline for the deformation from the SCI perspective. The deformation grid exemplifies the areas of

form breakdown from the perpendicular reference, in this case the female shape. The female shape would have appeared as a perfect perpendicular grid, and this figure now gives the degree and deformation of the males on this female/ reference grid. The deformation grid exhibited a large amount of warping and collapse along the locations where all five homologous landmarks were placed. Figure 6.43 demonstrates the differences exhibited between females and males in thin-plate spline vector mode. In Figure 6.43 the points (or circles) represent the first shape represented (female) while the arrows represent the direction of the male shape.

As seen in Figures 6.42 and 6.43, discrepancy between females (the point of origin of the arrow in vector mode) and males (the end length of the arrow in vector mode) existed in the location of the inferior ischial spine, the location of the outer point of the greater sciatic notch, before the pelvis curves back towards the auricular surface, and the depth of the greater sciatic notch itself. The vector mode thin-plate spline illustrated numerous differences between males and females in the pelvic morphology of the greater sciatic notch (Figure 6.43). Females (represented by the point) exhibited a more elongated and extended greater sciatic notch surface through the curvature towards the auricular surface than their male counterparts (represented by the boundary of the arrow). Males appeared short and truncated along this margin. These differences are illustrated through landmarks 2, 3 and 4. In contrast, male morphology appeared to extend longer than female morphology along the inferior border of the greater sciatic notch, which included the curvature towards the inferior ischial spine (landmark 5) and the landmark placed on the inferior ischial spine itself (landmark 1). Landmark 2 is the point of maximum curvature in the sciatic notch. This region is seen to extend or "depress" the greater sciatic notch further inward with males than with females. This may result in the deep, narrow greater sciatic notch width seen visually in male morphology. The shallow position of landmark 2 in females may account for the wider, shallower morphology of females. It was interesting to note that the major differences are not in the width of the greater

sciatic, notch, but rather in its a "legs" were seen to be significantly different in length.

The accuracy by which these differences in the pelvis can assign a specimen was assessed by means of a canonical variates (CVA) analysis. Table 6.26 represents the accuracies obtained from this analysis. Female specimens were correctly categorized 70% of the time, (105/ 151) while male specimens were categorized correctly 79% of the time (142/ 180). The p-value obtained by the canonical variates analysis (132.160) was greater than the critical value of chi square distribution at the significance value of 0.05 with two degrees of freedom (5.991). This indicated that the SCI perspective, which included a quantitative observation of the greater sciatic notch, was moderately sexually dimorphic.

Morphology of the greater sciatic notch between the members of each group (females and males) was different, and correct classification of females vs. males was performed on a statistically significant level. However, the classification accuracy based on quantified morphology of the greater sciatic notch in the South African population is lower than other features used to determine sex from the human skeleton.

6.4.2

Results from the SCI perspective: black females vs. males

Sexual dimorphism between black females and males was initially shown in Figure 6.40, and the statistical significance between the sexes was quantified by Goodall's F-statistic in Table 6.25. Sexual dimorphism in this perspective appeared more statistically significant in black South Africans than in white South Africans. Black females and males were thus compared independently to visualize sexually dimorphic changes in the SCI perspective.

Figure 6.44 demonstrates the thin-plate spline in deformation mode, and Figure 6.45 is the thin-plate spline in vector mode. As was the case before, in Figure

6.45 the points (or circles) represent the first shape represented (black females) while the arrows represent the direction of the black male shape.

The most deformation between black females and males occurred at the margins of the greater sciatic notch. These deformations between females (as the reference) and males (as the deformation) "tilted" the graph downwards on the right-hand (inferior) margin. The two sexes differ in that males exhibited a shortened, truncated greater sciatic notch margin along the superior border (landmarks 2, 3, and 4) and appear extended along the inferior border (landmarks 1 and 5). In addition, the position of landmark 2, the point of most curvature of the greater sciatic notch, appears deeper within the notch of the black male than within the notch of the female.

Table 6.27 represents the accuracies obtained from the canonical variates analysis. Black females were correctly categorized 78% of the time (71/ 91) while males 86% (90/ 105). The significance value obtained by the canonical variates analysis (94.637) was greater than the critical value of chi square distribution at the significance value of 0.05 with two degrees of freedom (5.991). The classification accuracy was high enough for both males and females to show moderate sexual dimorphism, which was quantifiable when using geometric morphometrics from the SCI perspective.

6.4.3

Results from the SCI perspective: white females vs. males

Sexual dimorphism between white females and males was seen first in Figure 6.40 as a relative warp analysis separated each sex and population. White females and males appeared in different quadrants of a four-quadrant grid. The subsequent statistical significance between the sexes was quantified by Goodall's F-statistic in Table 6.25. Sexual dimorphism existed in this perspective.

Figure 6.46 demonstrates the thin-plate spline in deformation mode between females and males, which demonstrates the deviation males have from a perfect perpendicular grid (the female mean). Deformation in Figure 6.46 was seen primarily in position of the inferior and superior landmarks of the greater sciatic notch, as well as the depth of the notch itself when comparing females to males. Other homologous landmarks assigned to this feature appeared to be similar between male and female morphology, as illustrated by portions of the grid that were unaffected by deformation. Figure 6.47 subsequently shows the thin-plate spline in vector mode, which illustrates the magnitude and direction of differences between white females and white males from the SCI perspective

As seen in Figure 6.47, those landmarks that denote the outer margins of the greater sciatic notch differ from females (the circles) to males (the arrow boundaries). Landmark 1 (which indicated the most projecting point of the inferior ischial spine) was positioned in a wider and shorter region in females than in males. Landmark 1 in males was placed in a more extended position, but also appeared to decrease the visual width of the greater sciatic notch by being positioned closer to landmark 3. Landmark 3, in contrast, appeared to be positioned in a wider, more extended, and more superiorly location in females than in males. Landmark 3 in males was positioned closer within the notch itself and in a location that would shorten the length between landmark 3 and 4. Landmark 2, the point of maximum curvature of the greater sciatic notch, appeared shallow in females and deeper within the notch in males. Landmarks 4 and 5 did not exhibit any remarkable differences in placement between white females and white males. These two landmarks would delineate the actual width of the greater sciatic notch margins. Because they appear congruent between males and females, this indicated that the morphology of the actual width of the notch was similar between the sexes.

The accuracy by which these differences in the greater sciatic notch region can assign white specimens was assessed by means of a canonical variates (CVA)

analysis (Table 6.28). White female specimens were correctly categorized 80% of the time(48/ 60) and males 87% (65/ 75). The significance value obtained by the canonical variates analysis (85.785) was greater than the critical value of chi square distribution at the significance value of 0.05 with two degrees of freedom (5.991). The classification accuracy was significant for both white females and white males, thus showing that the sexual dimorphism in this population was quantifiable when using geometric morphometrics in the SCI perspective.

Each population, as well as the combined data of all females and all males, exhibited marked sexual dimorphism from the SCI perspective. Thus sexual dimorphism could be quantified, and correct classification of males and females was performed for all males and females, and for each population group. This confirmed ample evidence that the morphology of the greater sciatic notch was sexually dimorphic between females and males. Results from this study show that these features can be quantified successfully by employing geometric morphometrics.

6.4.4

Sexual dimorphism and the onset of age: SCI perspective

A quantifiable difference between males and females in both populations was observed when applying geometric morphometrics to the SCI perspective, a view that exemplifies the greater sciatic notch of the pelvis. This feature was thus shown to be sexually dimorphic on a statistically significant level. Analyses were then performed in order to discern if characteristics from this perspective changed with the onset of age. Thus, each population group and both sexes were further categorized as "young" (50 years of age or younger) and "old" (over 50 years of age) as seen before. The differences between males and females from each age group were subsequently examined.

A consensus relative warp analysis on all eight possible groups for the SCI perspective was performed to visualize the groupings between each combination of the sample (Figure 6.48). This figure illustrates the complex morphology of this

pelvic region. All females were observed on the right side of the y-axis, indicating a distinctive sexually dimorphic component. Most males (young black males, old black males, and old white males) clustered to the left of the y-axis. This, again, indicated that the quantification of the SCI perspective was sexually dimorphic. Most females (young white females, old black females, and old white females) were observed in the upper right quadrant, while young black females presented in the bottom right quadrant of the grid, and grouped most closely with the morphology of young white males.

Old black and white females clustered together, and old black and white males clustered together. Further, it appeared as if old black male and old white male morphology was indistinguishable from each other. This indicated a morphological change between all males and females to some extent as they advanced through age. The biological affiliation of each group did not seem to be a discriminating factor. Black population groups and white population groups clustered together. This indicated that morphology was similar according to age.

6.4.5

Sexual dimorphism and the onset of age: black females and black males

Evidence represented in Figures 6.40 and 6.48 show that differences exist between black males and females, and that morphology of the pelvis from the SCI perspective varied between the age groupings of "young" and "old" for both males and females. To quantify and compare these differences and similarities between sexes, consensus thin-plate splines in vector mode were created for black females and black males independently to observe the differences between young and old consensus shapes.

Figure 6.49 is the thin-plate spline in vector mode that exemplifies the changes black females underwent with the onset of age. Landmarks 1, 2 and 3 show quantifiable changes from young black females to old black females. Landmark 1 appears to be in a wider and more anterior position in old black females than in

young black females; this change would create a shorter but wider sciatic notch. Landmark 3, in contrast, projects inward toward the middle of the notch with the onset of age, producing a narrower notch for old black females. In addition, landmark 2 (the location of maximum curvature of the greater sciatic notch) was seen to be in a more superior position in old black females than in young black females. Landmarks 4 and 5 did not appear to migrate or deviate from their original positions between young black females and old black females.

The changes that occur with age in black males can be seen in Figure 6.50. This graph shows the vector mode for black males as it transforms from "young" morphology to "old" morphology in the SCI perspective. As seen in Figure 6.50, differences between young black males and old black males existed along the entire margin of the greater sciatic notch. All landmarks in the old male SCI perspective migrated around the sciatic notch. Landmarks 1 and 5 showed a slight migration inward, toward the medial section of the greater sciatic notch space. Landmarks 3 and 4 positioned themselves more towards landmark 2, the location of maximum sciatic notch curvature in old black males. This would have created a shorter, more truncated greater sciatic notch morphology in old black males than in young black males.

Changes in black males and females with the onset of age were observable by viewing the direction and magnitude of change in thin-plate spline vector mode analyses (Figures 6.49 and 6.50). In addition, Goodall's F-statistic comparing the young black sample (young black females vs. young black males) and the old black sample (old black females vs. old black males) was significant for both groups (Goodall's F-statistic for the young sample = 30.22, df = 2, $p = 0.000<0.05$; Goodall's F-statistic for the old sample = 32.50, df = 2, $0.000<0.05$) as seen in Table 6.29. Because changes were seen with age, the classification accuracy of both young and old individuals was calculated to determine if this accuracy rate decreased with the aging morphology of the black population.

Table 6.30 illustrates the classification accuracy between males and females of both age groups. Young black individuals were classified with accuracy when compared to each other (80% accurate for young black females, 85% for young black males). Classification accuracy remained basically the same with the onset of age when old black females were compared to old black males (81% and 84%, respectively). Assessment of classification accuracies between young and old age groups with the black population indicated that the classic "male" and "female" morphology of the pelvis maintained its sexually dimorphic nature throughout the onset of advanced age. Figure 6.48 showed old black females closer to the male groupings on the left of the y-axis than any other of the female age/ population groups. This could indicate a slight variance to more "male" morphology with the black female pelvis, although classification accuracies did not decrease with this sample, they increased. Regardless, sexual dimorphism was observed in the SCI perspective, and canonical variates analysis was able to categorize each age group with accuracy. Changes with age to the SCI perspective did not adversely influence the classification accuracy for females or males in this population group; as the age increased with black females and males, the ability to correctly assign a female specimen to its correct group remained virtually the same.

6.4.6

Sexual dimorphism and the onset of age: white females and males

Evidence represented in Figures 6.40 and 6.48 showed that differences existed between white males and females in the SCI perspective. Morphology of the greater sciatic notch appeared to differ greatly between young white male individuals and old white male individuals based on the separation of the two consensuses in the relative warp graph shown in Figure 6.48. Changes appeared to be taking place in the white male pelvis with age. Females in this same graph exhibited distinct clusters defined only by sex, and not population affinity. Consensus thin-plate

splines in vector mode were created for white females and white males to observe the differences between young and old consensus shapes.

Figure 6.51 is the thin-plate spline in vector mode that exemplified the changes white females underwent with the onset of age. The thin-plate spline in vector mode showed that little movement of homologous landmarks took place between the comparison of young white females and old white females. Landmark 1 appeared to migrate superiorly, towards the surface of the pubis, and slightly inward toward the point of most curvature in the greater sciatic notch (landmark 2). This would create a shorter and wider greater sciatic notch morphology in old white females as compared to young white females. Landmark 3, the end of the sciatic notch before the bone curves backwards towards the auricular surface, was positioned in a more extended position in old white females than in young white females. This would have the opposite effect of landmark 1's movement, producing a more elongated greater sciatic notch in this location when viewing old white females.

Young white males and old white males did exhibit marked morphological differences, as seen in the relative warp analysis in Figure 6.48. To visualize these differences, a thin-plate spline was created in vector mode to observe the location and direction of variation between the young white male SCI perspective, and the old white male SCI perspective. The changes that occur with age in white males can be seen in Figure 6.52. This graph shows the vector mode for white males as it transforms from "young" morphology to "old" morphology.

Figure 6.52 indicated alteration around the periphery of the SCI view, as exemplified by distinct changes occurring in all homologous landmarks within the greater sciatic notch. Landmark 3 migrated inward towards the iliac surface and towards the greatest curvature of the notch (landmark 2), shortening this aspect of the greater sciatic notch in old white males (categorized by the boundary of the arrow), as opposed to its elongated appearance in young white males (categorized

by the point). Landmark 4 also migrated towards the interior of the pelvis, increasing this "shortening" effect. Landmarks 1 and 5, however, elongate towards the inferior margin of the ischium in old white males, which may lengthen the morphology of the greater sciatic notch in this region. Finally, landmark 2 migrated medially and toward the auricular surface, creating what may be visually construed as constriction in the point of maximum curvature.

Changes in white males and females with the onset of age were observable by viewing the direction and magnitude of change in thin-plate spline vector mode analyses (Figures 6.51 and 6.52). Goodall's F-statistic comparing the young white sample (young white females vs. young white males) and the old white sample (old white females vs. old white males) resulted in differing statistical outcomes. Table 6.31 illustrates that differences between young white females and young white males just reached statistical significance (Goodall's F-statistic = 3.29, df = 2, 0.043<0.05), while the differences between old white females and old white males in the SCI perspective are highly significant (Goodall's F-statistic = 46.41, df = 2, 0.000<0.05). Because of these discrepancies and the apparent variability of male morphology in the young white male SCI perspective (as seen in the previous section with the SUB perspective), the classification accuracies of both young and old individuals were calculated to determine if this accuracy rate increased with the aging morphology of the white population.

Table 6.32 illustrates the classification accuracy between males and females of both age groups. As can be seen in this table, young white females were categorized correctly 73% of the time, while young white males were categorized with 74% accuracy. The young white male pelvis was quite variable in morphology. This may have influenced the inability to categorize young white males from young white females with a higher degree of accuracy. A lack of morphological differences was seen when comparing young white females to young white males. Male os coxae in this group appeared to exhibit either inconsistent male pelvic morphology, or

exhibited pelvic morphology that has been historically (and with other populations) attributed to females.

Classification accuracy in the old white sample provided accurate results, however. Old white females and males were categorized at a higher rate of accuracy than their younger counterparts (84% and 89%, respectively).

The assessment of changes occurring with age may indicate that as the white population gets older, the classic "male" and "female" morphology of the pelvis changes dramatically in its degree of sexual dimorphism. Young white females, when compared to young white males, were not distinguishable enough to provide very accurate canonical variates results. Old females and males, in contrast, exhibited quantifiable characteristics in the SCI perspective, allowing for old females to be categorized correctly when compared to old white males. Sexual dimorphism was present and marked in the old white population.

Although females and males from different population groups exhibited differing rates of classification accuracy, the SCI perspective was still observed to be a highly accurate indicator of sex when the shape of the greater sciatic notch was quantified, and males and females were compared to each other. Thus the SCI perspective was deemed sexually dimorphic. However, unusual results with the young white sample population and the inability of the CVA program to correctly categorize males from females with accuracy in this sample illustrated a peculiar divergence in this sample that is neither expected nor a classic divergence based on sexual dimorphism. Male pelvic morphology in white South Africans did not concur with the classic tenets of sexual dimorphism as seen in other populations. In fact, both perspectives of the pelvis (SUB perspective and SCI perspective) exhibited problematic results. Accurate classification of young white male pelvic morphology was either difficult or impossible to achieve.

Table 6.1: Statistical significance between females and males, EPI perspective.

	Statistical significance between groups, EPI		
Group	Goodall's F-test	df	p- value
All females vs. all males	13.48	30	**0.000***
Black females vs. Black males	6.65	30	**0.000***
White females vs. White males	12.78	30	**0.000***

Significant, < 0.05

Table 6.2: Percentage of males and females correctly assigned using canonical variates analysis, EPI perspective. *N* = 347

	CVA assignment based on shape data, EPI			
Group	Correctly assigned	Incorrectly assigned	Percentage correctly assigned	Chi square value
Females (*n*=163)	129	34	79%	**148.185***
Males (*n*=184)	143	41	78%	

**** Significant, at 0.05 level***

Table 6.3: Percentage of black males and black females correctly assigned using canonical variates analysis, EPI perspective. *N* = 208

	CVA assignment based on shape data, EPI			
Group	Correctly assigned	Incorrectly assigned	Percentage correctly assigned	Chi square value
Black females (*n*=100)	83	17	83%	**110.017***
Black males (*n*=108)	92	16	85%	

Significant, at 0.05 level

Table 6.4: Percentage of white males and white females correctly assigned using canonical variates analysis, EPI perspective. *N* = 139

Group	CVA assignment based on shape data, EPI			
	Correctly assigned	Incorrectly assigned	Percentage correctly assigned	Chi square value
White females (*n*=63)	57	6	91%	
White males (*n*=76)	68	8	90%	**107.188***

Significant, at 0.05 level

Table 6.5: Statistical significance between black females and males, EPI perspective.

Group	Statistical significance between groups, EPI		
	Goodall's F-test	df	p- value
Young black females vs. Young black males	5.50	30	**0.000***
Old black females vs. Old black males	3.72	30	**0.000***

Significant at 0.05 level

Table 6.6: Percentage of young and old black males and females correctly assigned using canonical variates analysis, EPI perspective. (*n* = 106 young, *n* = 102 old)

Group	CVA assignment based on shape data, EPI			
	Correctly assigned	Incorrectly assigned	Percentage correctly assigned	Chi square value
Young black females (*n*=50)	47	3	94%	
Young black males (n=56)	50	6	89%	**85.5835***
Old black females (*n*=50)	48	2	96%	
Old black males (n=52)	49	3	94%	**100.776***

Significant, at 0.05 level

Table 6.7: Statistical significance between white females and males, EPI perspective.

	Statistical significance between groups, EPI		
Group	Goodall's F-test	df	p- value
Young white females vs. Young white males	4.44	30	**0.014***
Old white females vs. Old white males	8.80	30	**0.000***

Significant, < 0.05

Table 6.8: Percentage of young and old white males and females correctly assigned using canonical variates analysis, EPI perspective. (n = 37 young, n = 102 old)

	CVA assignment based on shape data, EPI			
Group	Correctly assigned	Incorrectly assigned	Percentage correctly assigned	Chi square value
Young white females (*n*=13)	-	-	-%	-
Young white males (n=24)	-	-	-%	
Old white females (*n*=50)	46	4	92%	**81.2308***
Old white males (n=52)	44	8	85%	

Significant, at 0.05 level

Table 6.9: Statistical significance between females and males, OL perspective.

Group	Statistical significance between groups, OL		
	Goodall's F-test	df	p- value
All females vs. all males	9.30	22	**0.000***
Black females vs. Black males	7.08	22	**0.000***
White females vs. White males	3.86	22	**0.000***

Significant, < 0.05

Table 6.10: Percentage of males and females correctly assigned using canonical variates analysis, OL perspective. *N* = 348

Group	CVA assignment based on shape data, OL			
	Correctly assigned	Incorrectly assigned	Percentage correctly assigned	Chi square value
Females (*n*=163)	135	28	83%	
Males (*n*=185)	156	29	84%	**211.344***

**** Significant, at 0.05 level***

Table 6.11: Percentage of black males and black females correctly assigned using canonical variates analysis, OL perspective. *N* = 210

Group	CVA assignment based on shape data, OL			
	Correctly assigned	Incorrectly assigned	Percentage correctly assigned	Chi square value
Black females (*n*=100)	82	18	82%	
Black males (*n*=110)	89	21	81%	**123.551***

****Significant, at 0.05 level***

Table 6.12: Percentage of white males and white females correctly assigned using canonical variates analysis, OL perspective. *N* = 138

Group	CVA assignment based on shape data, OL			
	Correctly assigned	Incorrectly assigned	Percentage correctly assigned	Chi square value
White females (*n*=63)	55	8	87%	
White males (*n*=75)	66	9	88%	**111.226***

Significant, at 0.05 level

Table 6.13: Statistical significance between black females and males, OL perspective.

Group	Statistical significance between groups, OL		
	Goodall's F-test	df	p- value
Young black females vs. Young black males	5.85	22	**0.000***
Old black females vs. Old black males	2.45	22	**0.000***

Significant, < 0.05

Table 6.14: Percentage of young and old black males and females correctly assigned using canonical variates analysis, OL perspective. (*n* = 100 young, *n* = 110 old)

Group	CVA assignment based on shape data, OL			
	Correctly assigned	Incorrectly assigned	Percentage correctly assigned	Chi square value
Young black females (*n*=50)	42	8	84%	
Young black males (n=57)	54	3	95%	**102.773***
Old black females (*n*=50)	40	10	80%	
Old black males (n=53)	45	8	85%	**56.400***

Significant, at 0.05 level

Table 6.15: Statistical significance between white females and males, OL perspective.

Group	Statistical significance between groups, OL		
	Goodall's F-test	df	p- value
Young white females vs. Young white males	1.79	22	**0.022***
Old white females vs. Old white males	3.32	22	**0.000***

Significant, < 0.05

Table 6.16: Percentage of young and old white males and females correctly assigned using canonical variates analysis, OL perspective. (*n* = 35 young, *n* = 102 old)

Group	CVA assignment based on shape data, OL			
	Correctly assigned	Incorrectly assigned	Percentage correctly assigned	Chi square value
Young white females (*n*=13)	12	1	92%	**35.477***
Young white males (n=23)	23	0	100%	
Old white females (*n*=50)	45	5	90%	**78.459***
Old white males (n=52)	47	5	90%	

Significant, at 0.05 level

Table 6.17: Statistical significance between females and males, SUB perspective.

Group	Statistical significance between groups, SUB		
	Goodall's F-test	df	p- value
All females vs. all males	61.72	48	**0.000***
Black females vs. Black males	36.59	48	**0.000***
White females vs. White males	30.09	48	**0.000***

Significant, < 0.05

Table 6.18: Percentage of males and females correctly assigned using canonical variates analysis, SUB perspective. *N* = 318

Group	CVA assignment based on shape data, SUB			
	Correctly assigned	Incorrectly assigned	Percentage correctly assigned	Chi square value
Females (*n*=143)	135	8	94%	
Males (*n*=175)	165	10	94%	**397.806***

Significant, at 0.05 level

Table 6.19: Percentage of black males and black females correctly assigned using canonical variates analysis, SUB perspective. *N* = 188

Group	CVA assignment based on shape data, SUB			
	Correctly assigned	Incorrectly assigned	Percentage correctly assigned	Chi square value
Black females (*n*=85)	82	3	96%	
Black males (*n*=103)	101	2	98%	**262.356***

Significant, at 0.05 level

Table 6.20: Percentage of white males and white females correctly assigned using canonical variates analysis, SUB perspective. *N* = 130

Group	CVA assignment based on shape data, SUB			
	Correctly assigned	Incorrectly assigned	Percentage correctly assigned	Chi square value
White females (*n*=58)	56	2	97%	
White males (*n*=72)	70	2	97%	**163.348***

Significant, at 0.05 level

Table 6.21: Statistical significance between black females and males, SUB perspective.

Group	Statistical significance between groups, SUB		
	Goodall's F-test	df	p- value
Young black females vs. Young black males	24.64	48	**0.000***
Old black females vs. Old black males	14.30	48	**0.000***

Significant, < 0.05

Table 6.22: Percentage of young and old black males and females correctly assigned using canonical variates analysis, SUB perspective. (*n* = 96 young, *n* = 92 old)

Group	CVA assignment based on shape data, SUB			
	Correctly assigned	Incorrectly assigned	Percentage correctly assigned	Chi square value
Young black females (*n*=41)	40	1	98%	
Young black males (n=55)	55	0	100%	**165.780***
Old black females (*n*=44)	41	3	93%	
Old black males (n=48)	48	48	100%	**112.469***

Significant, at 0.05 level

Table 6.23: Statistical significance between white females and males, SUB perspective.

	Statistical significance between groups, SUB		
Group	Goodall's F-test	df	p- value
Young white females vs. Young white males	8.13	48	0.083
Old white females vs. Old white males	23.65	48	**0.000***

Significant, < 0.05

Table 6.24: Percentage of young and old white males and females correctly assigned using canonical variates analysis, SUB perspective. (*n* = 34 young, *n* = 96 old)

	CVA assignment based on shape data, SUB			
Group	Correctly assigned	Incorrectly assigned	Percentage correctly assigned	Chi square value
Young white females (*n*=11)	-	-	-%	-
Young white males (n= 23)	-	-	-%	
Old white females (*n*=47)	46	1	98%	**122.405***
Old white males (n=49)	48	1	98%	

Significant, at 0.05 level

Table 6.25: Statistical significance between females and males, SCI perspective.

	Statistical significance between groups, SCI		
Group	Goodall's F-test	df	p- value
All females vs. all males	88.85	2	**0.000***
Black females vs. Black males	60.28	2	**0.000***
White females vs. White males	46.04	2	**0.000***

Significant, < 0.05

Table 6.26: Percentage of males and females correctly assigned using canonical variates analysis, SCI perspective. *N* = 331

	CVA assignment based on shape data, SCI			
Group	Correctly assigned	Incorrectly assigned	Percentage correctly assigned	Chi square value
Females (*n*=151)	105	46	70%	
Males (*n=180*)	142	38	79%	**132.160***

**** Significant, at 0.05 level***

Table 6.27: Percentage of black males and black females correctly assigned using canonical variates analysis, SCI perspective. *N* = 196

	CVA assignment based on shape data, SCI			
Group	Correctly assigned	Incorrectly assigned	Percentage correctly assigned	Chi square value
Black females (*n*=91)	71	20	78%	
Black males (*n*=105)	90	15	86%	**94.637***

Significant, at 0.05 level

Table 6.28: Percentage of white males and white females correctly assigned using canonical variates analysis, SCI perspective. *N* = 135

Group	CVA assignment based on shape data, SCI			
	Correctly assigned	Incorrectly assigned	Percentage correctly assigned	Chi square value
White females (*n*=60)	48	12	80%	
White males (*n*=75)	65	10	87%	**85.785***

Significant, at 0.05 level

Table 6.29: Statistical significance between black females and males, SCI perspective.

Group	Statistical significance between groups, SCI		
	Goodall's F-test	df	p- value
Young black females vs. Young black males	30.22	2	**0.000***
Old black females vs. Old black males	32.50	2	**0.000***

Significant, < 0.05

Table 6.30: Percentage of young and old black males and females correctly assigned using canonical variates analysis, SCI perspective. (*n* = 98 young, *n* = 98 old)

Group	CVA assignment based on shape data, SCI			
	Correctly assigned	Incorrectly assigned	Percentage correctly assigned	Chi square value
Young black females (*n*=44)	35	9	80%	
Young black males (n=54)	46	8	85%	**44.457***
Old black females (*n*=47)	38	9	81%	
Old black males (n=51)	43	8	84%	**50.449***

Significant, at 0.05 level

Table 6.31: Statistical significance between white females and males, SCI perspective.

Group	Statistical significance between groups, SCI		
	Goodall's F-test	df	p- value
Young white females vs. Young white males	3.29	2	**0.043***
Old white females vs. Old white males	46.41	2	**0.000***

**Significant, < 0.05*

Table 6.32: Percentage of young and old white males and females correctly assigned using canonical variates analysis, SCI perspective. (*n* = 34 young, *n* =101 old)

Group	CVA assignment based on shape data, SCI			
	Correctly assigned	Incorrectly assigned	Percentage correctly assigned	Chi square value
Young white females (*n*=11)	8	3	73%	
Young white males (n=23)	17	6	74%	11.677
Old white females (*n*=49)	41	8	84%	
Old white males (n=52)	46	6	89%	**73.503***

Significant, at 0.05 level

Figure 6.1: Consensus relative warp analysis of females and males, EPI perspective.

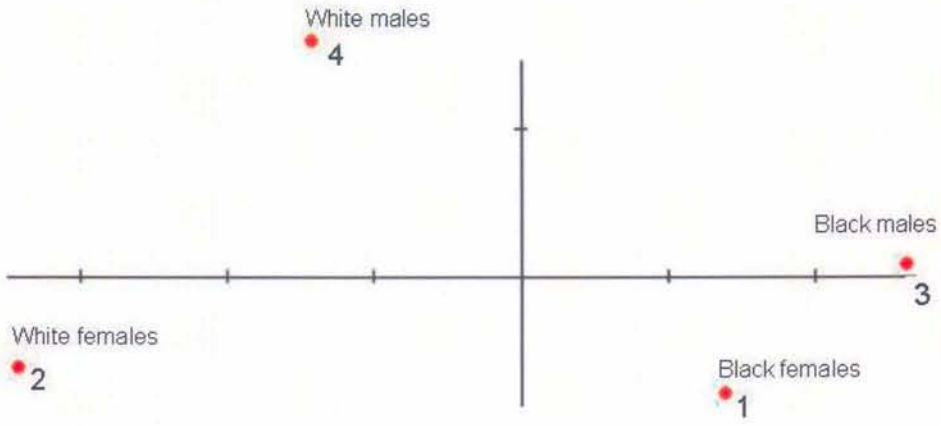

Figure 6.2: Consensus thin-plate spline reference shape of all females and all males from the EPI perspective.

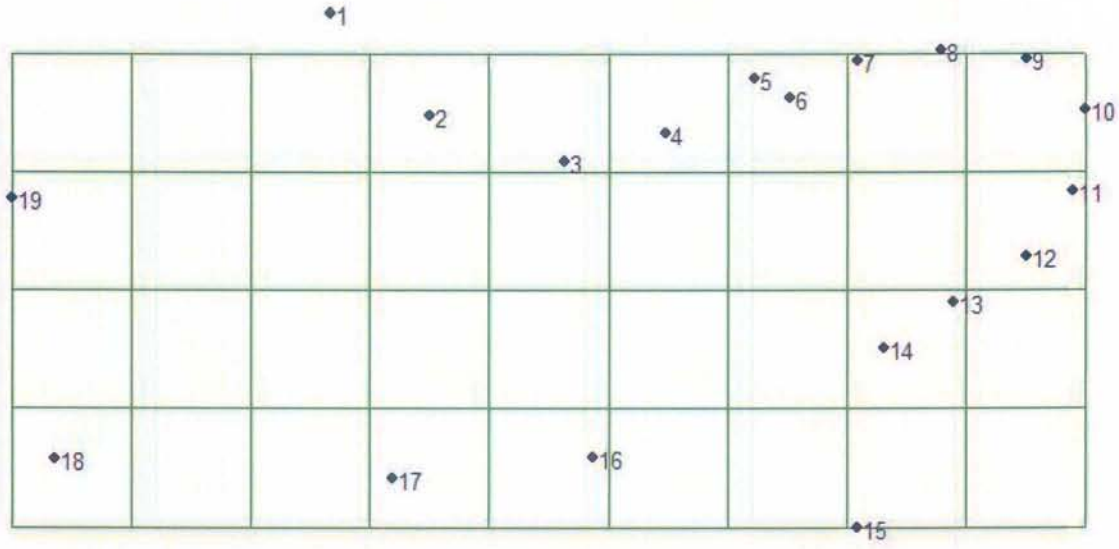

Figure 6.3: Consensus thin-plate spline in deformation mode demonstrating the differences between the reference shape (all females) and all males, EPI perspective.

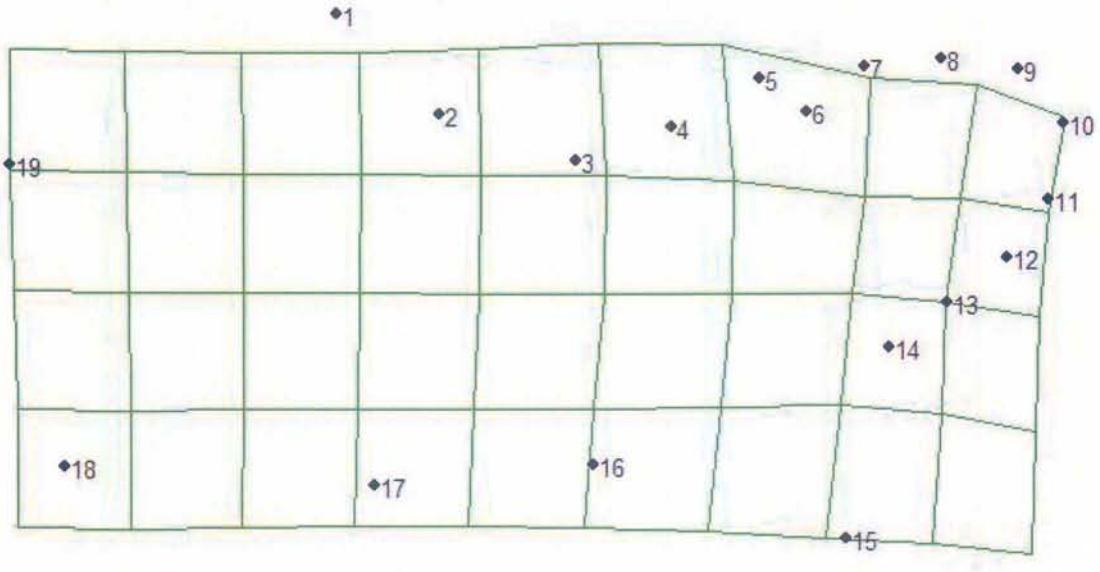

Figure 6.4: Consensus thin-plate spline (in vector mode) demonstrating the differences between all females and all males, EPI perspective.

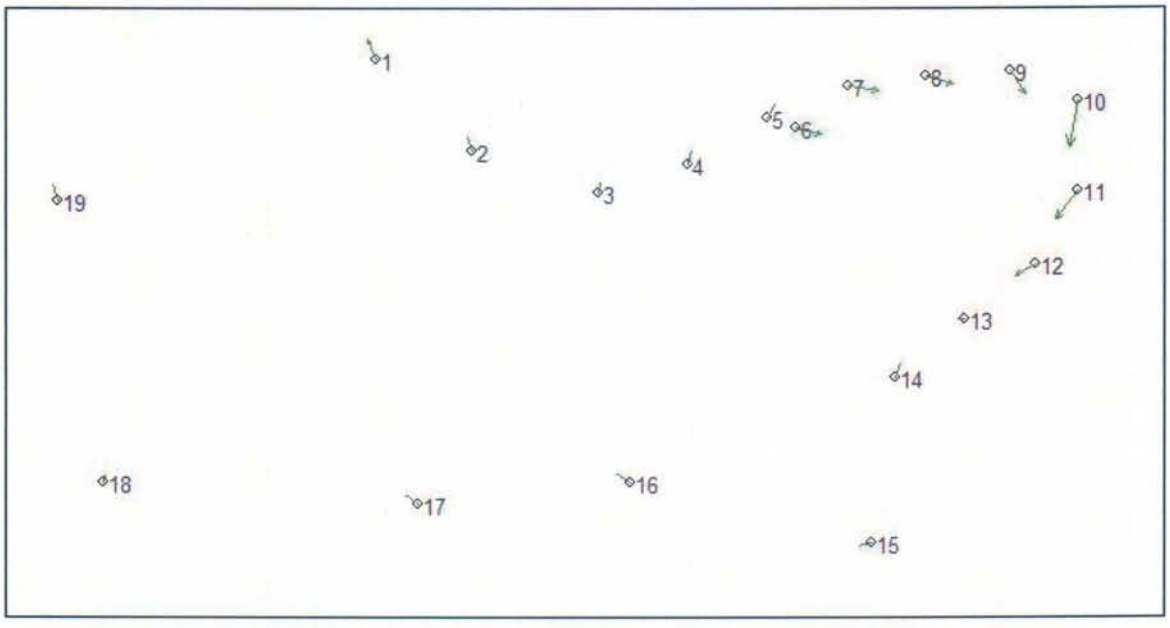

Figure 6.5: Consensus thin-plate spline in deformation mode demonstrating the differences between the reference shape (black females) and black males, EPI perspective.

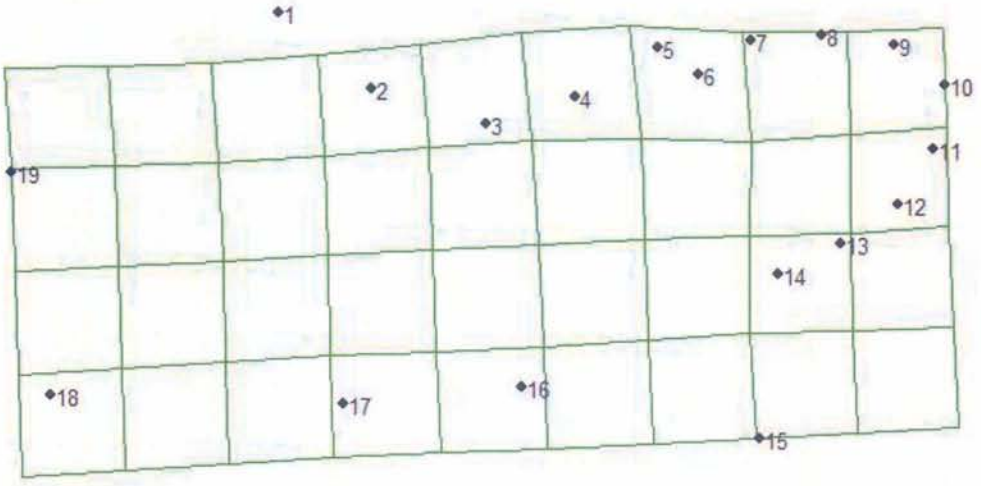

Figure 6.6: Consensus thin-plate spline (in vector mode) demonstrating the differences between black females and black males, EPI perspective.

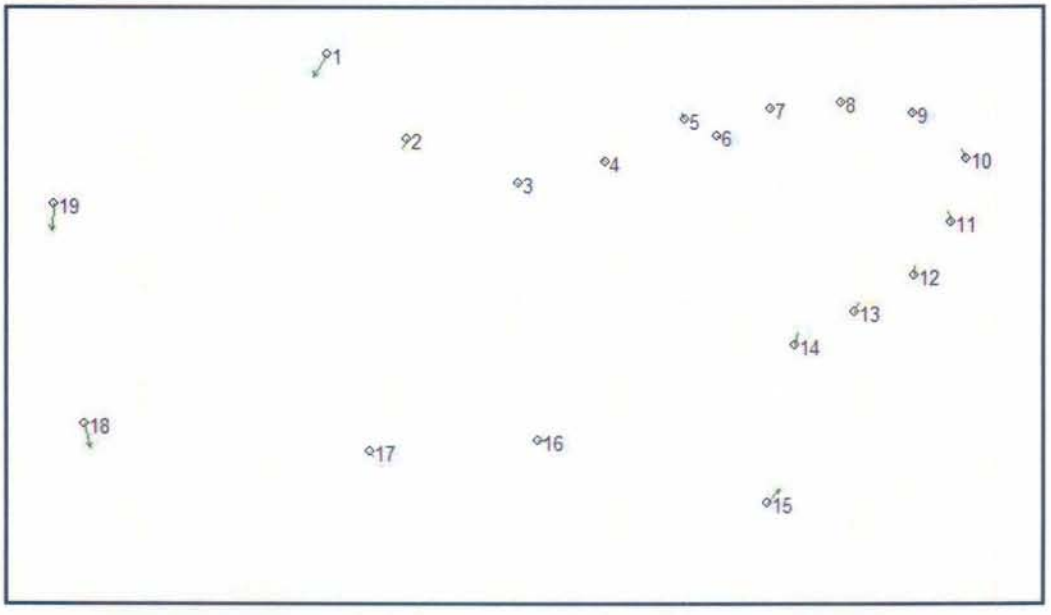

Figure 6.7: Consensus thin-plate spline in deformation mode demonstrating the differences between the reference shape (white females) and white males, EPI perspective.

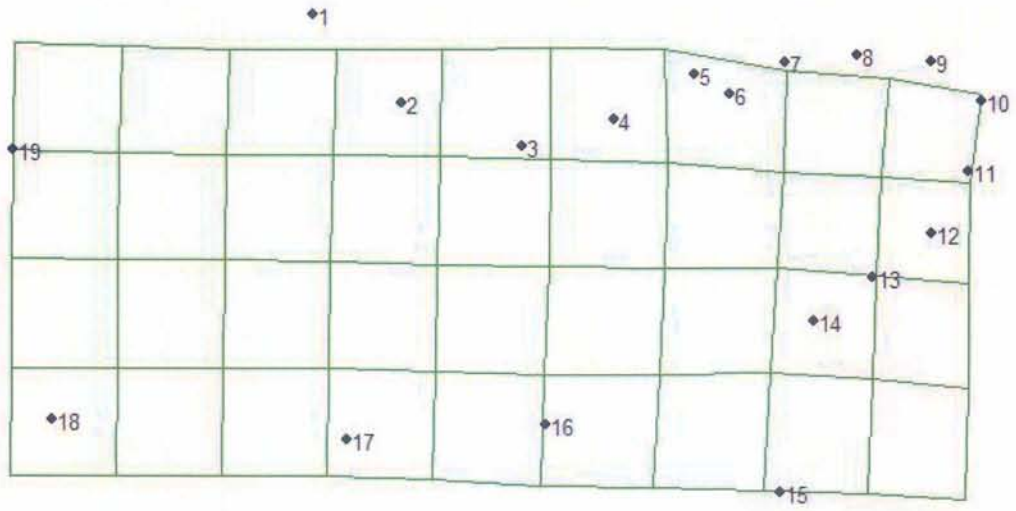

Figure 6.8: Consensus thin-plate spline (in vector mode) demonstrating the differences between white females and white males, EPI perspective.

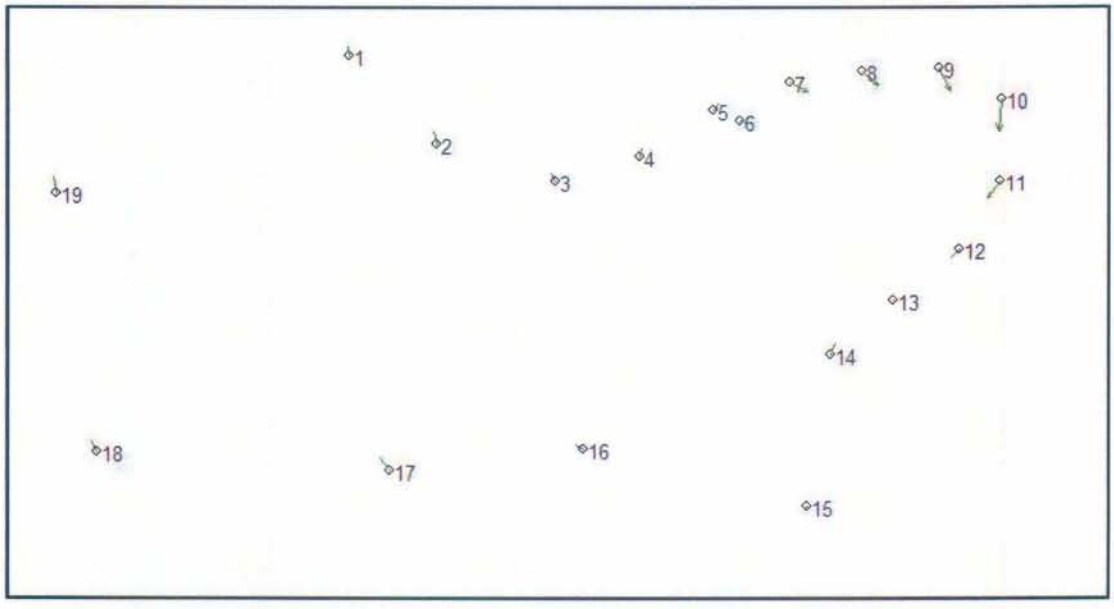

Figure 6.9: Relative warp consensus for eight groups of males and females, EPI perspective.

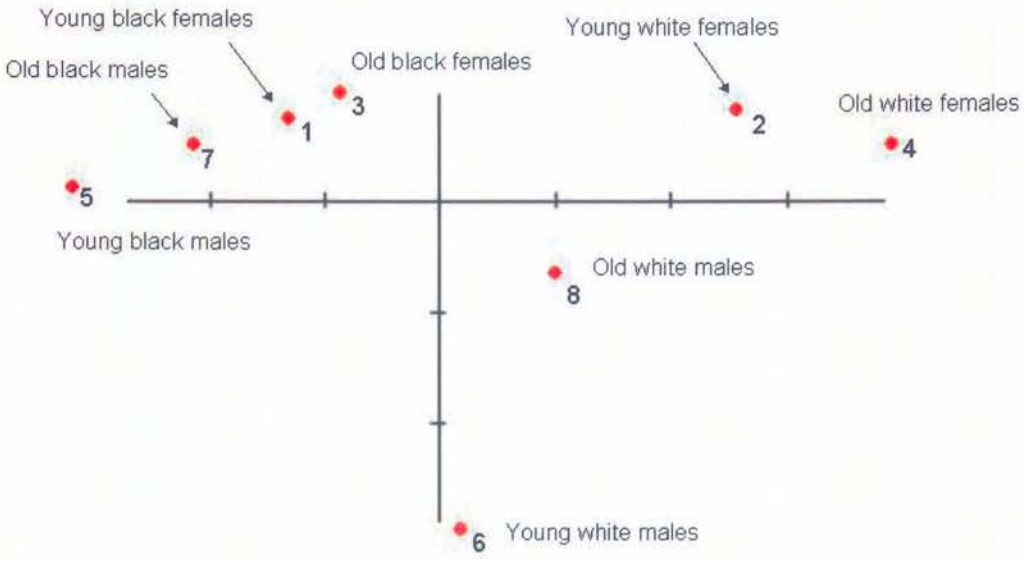

Figure 6.10: Consensus thin-plate spline (in vector mode) demonstrating the differences between young black females and old black females, EPI perspective.

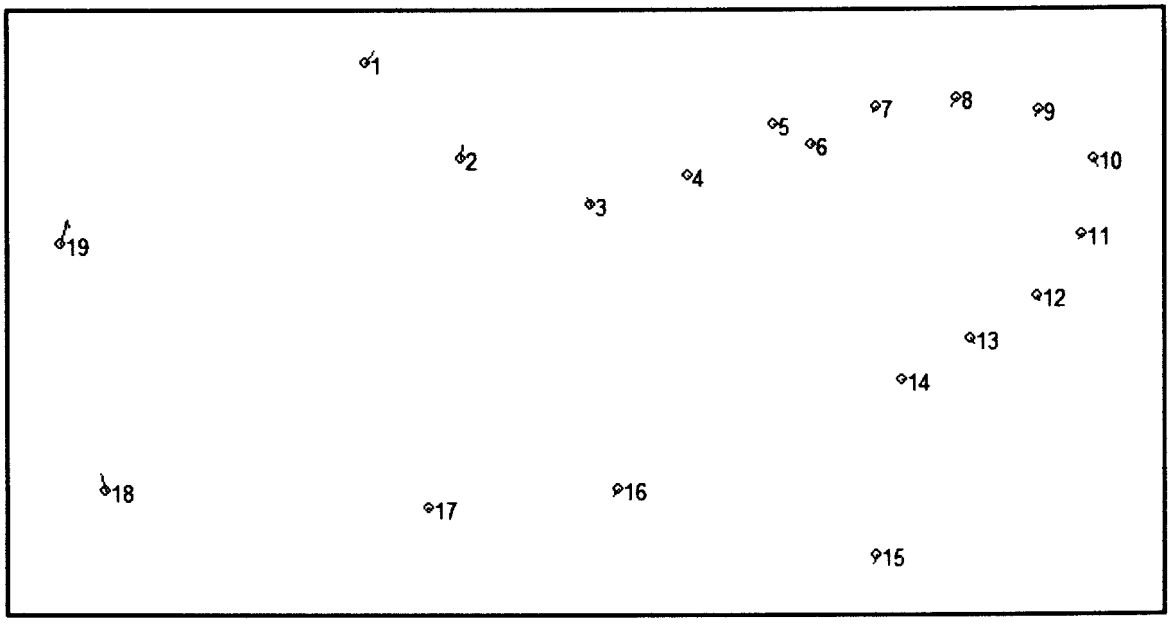

Figure 6.11: Consensus thin-plate spline (in vector mode) demonstrating the differences between young black males and old black males, EPI perspective.

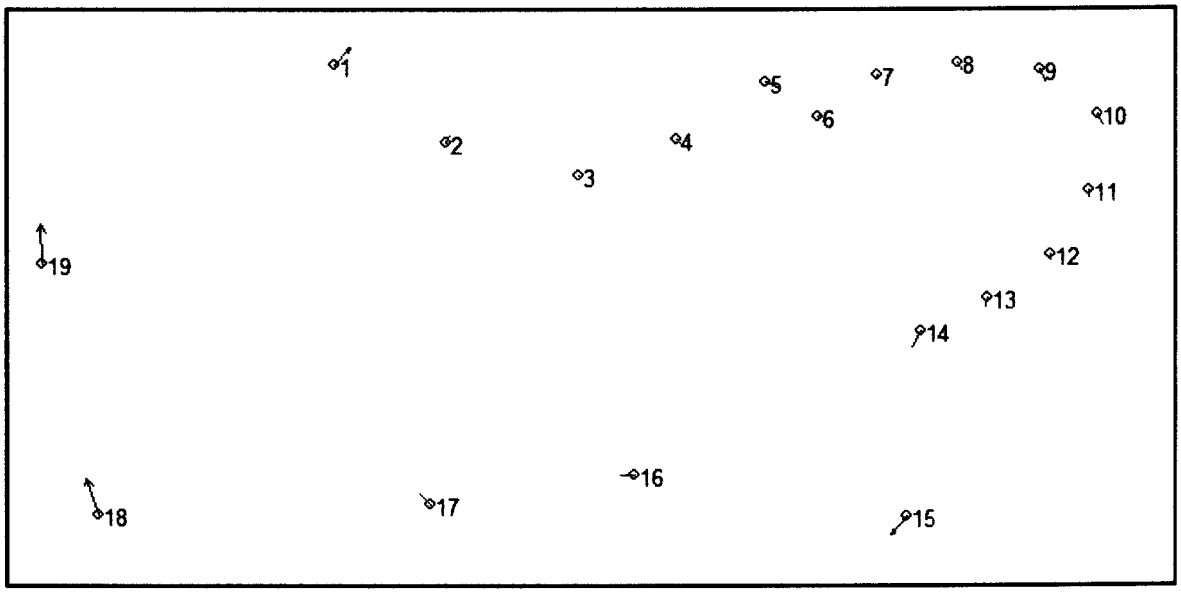

Figure 6.12: Consensus thin-plate spline (in vector mode) demonstrating the differences between young white females and old white females, EPI perspective.

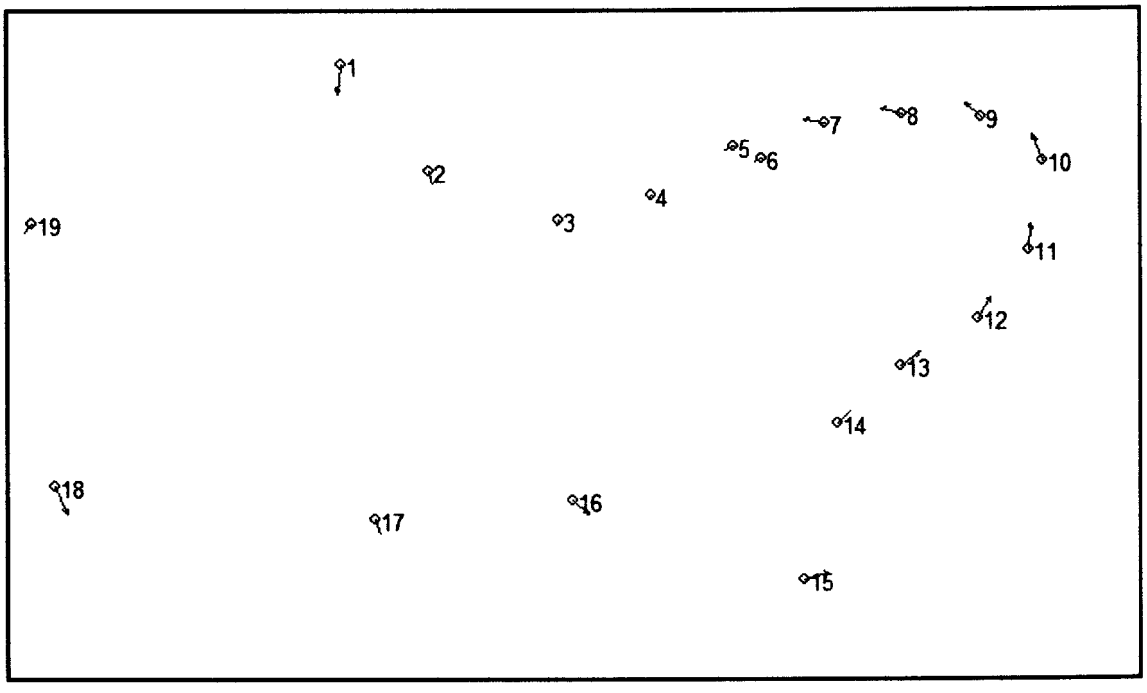

Figure 6.13: Consensus thin-plate spline (in vector mode) demonstrating the differences between young white males and old white males, EPI perspective.

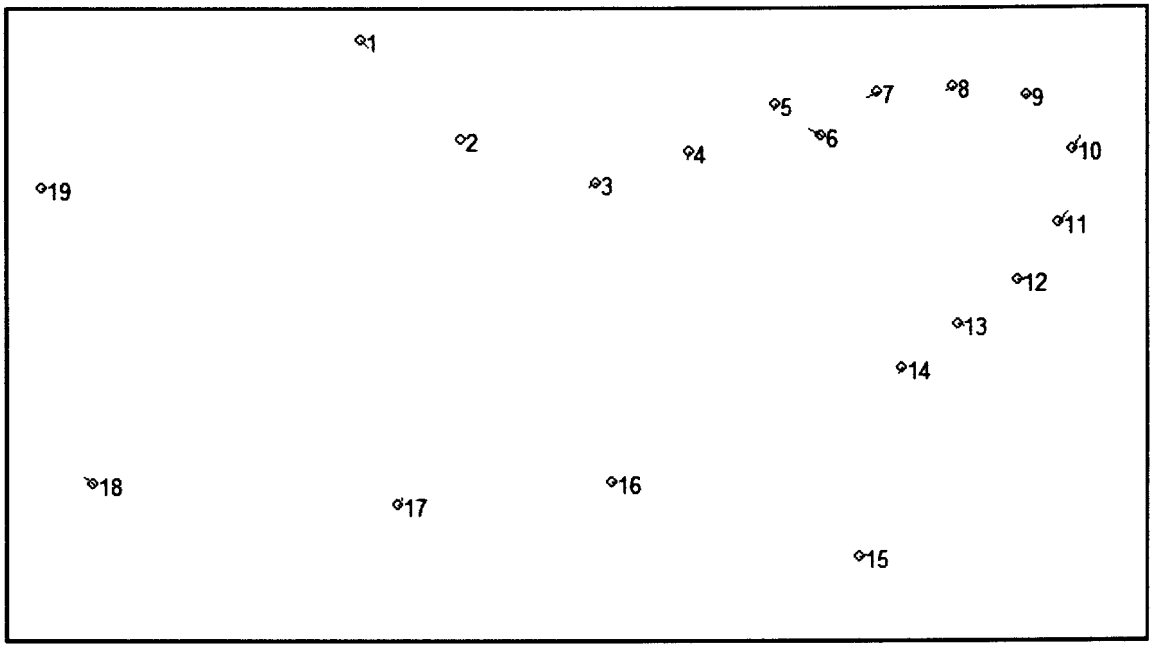

Figure 6.14: Consensus relative warp analysis of females and males, OL perspective.

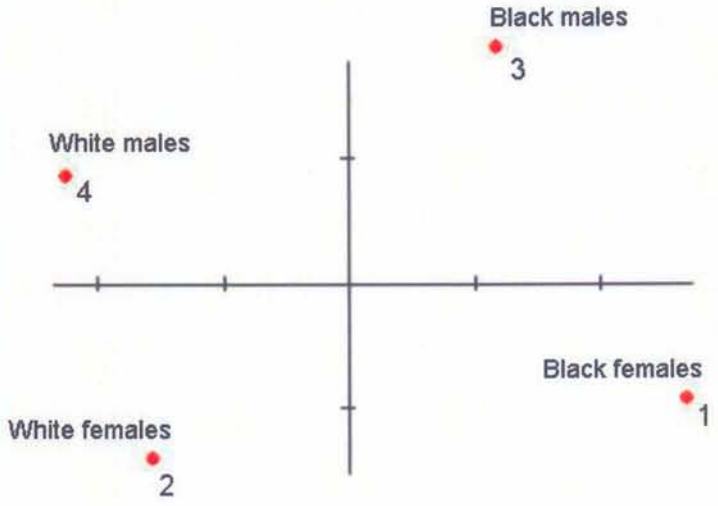

Figure 6.15: Consensus thin-plate spline reference shape of all females and all males from the OL perspective.

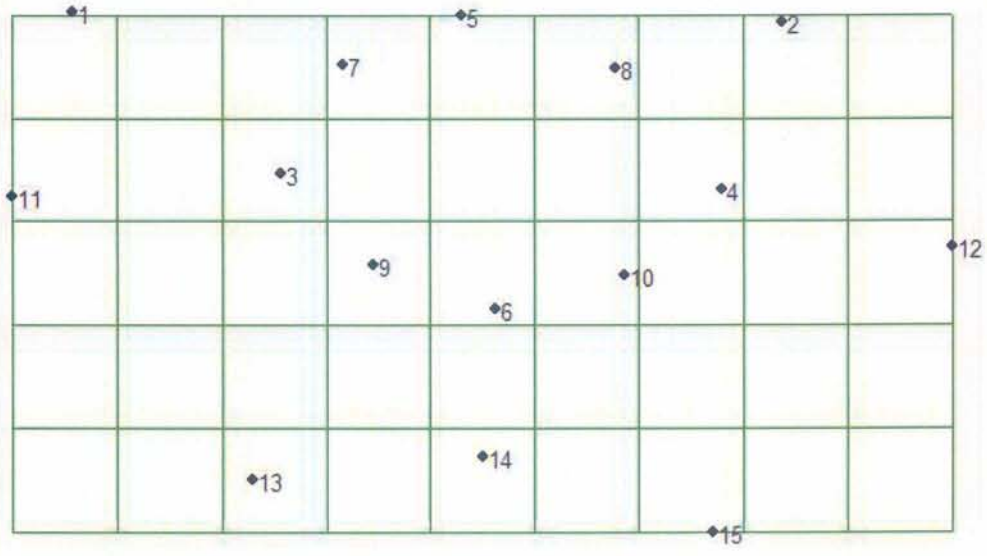

Figure 6.16: Consensus thin-plate spline in deformation mode demonstrating the differences between the reference shape (all females) and all males, OL perspective.

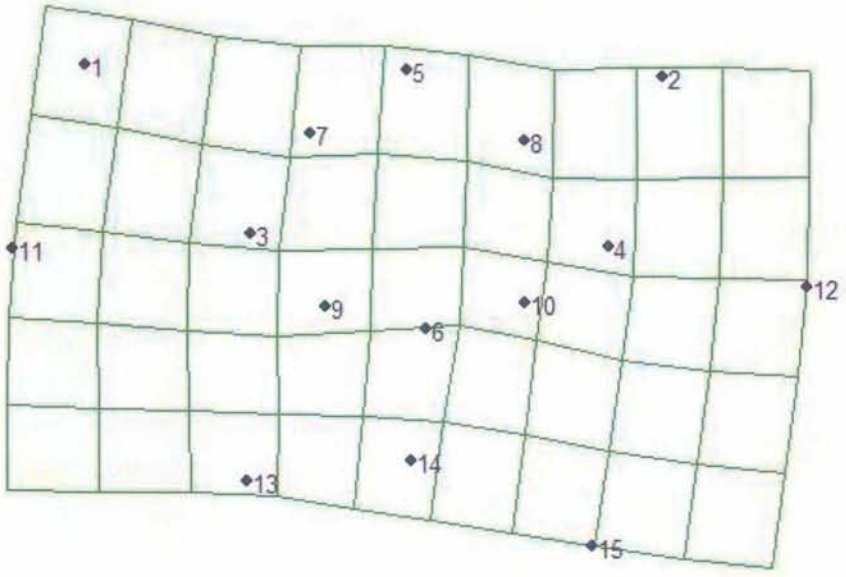

Figure 6.17: Consensus thin-plate spline (in vector mode) demonstrating the differences between all females and all males, OL perspective.

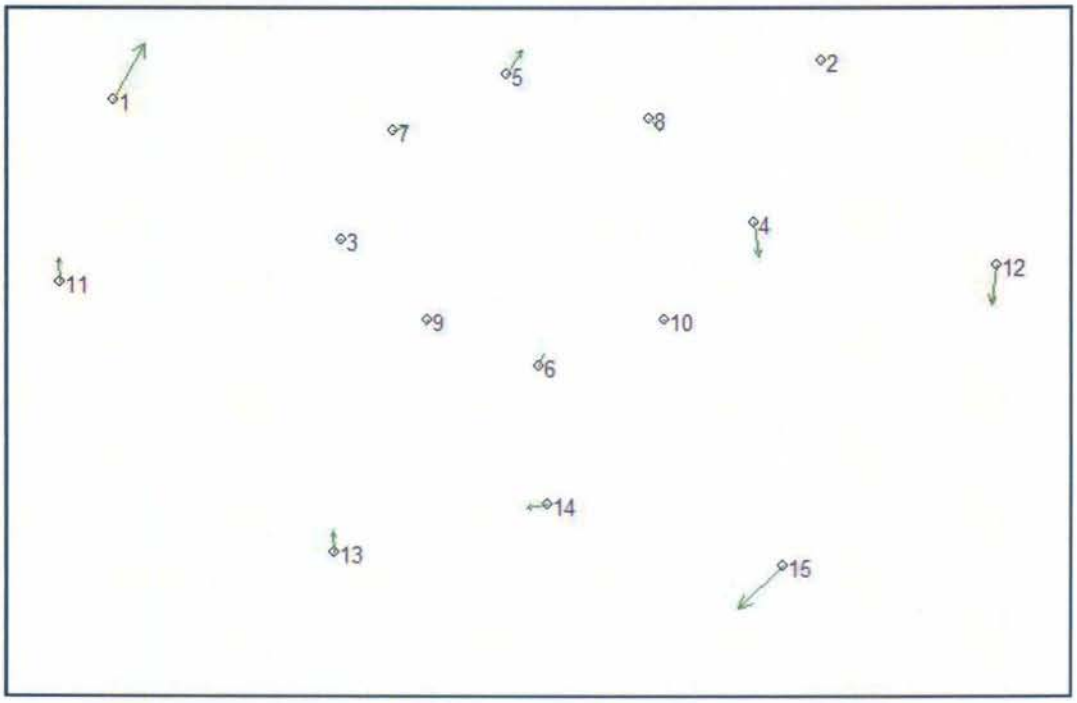

Figure 6.18: Consensus thin-plate spline in deformation mode demonstrating the differences between the reference shape (black females) and black males, OL perspective.

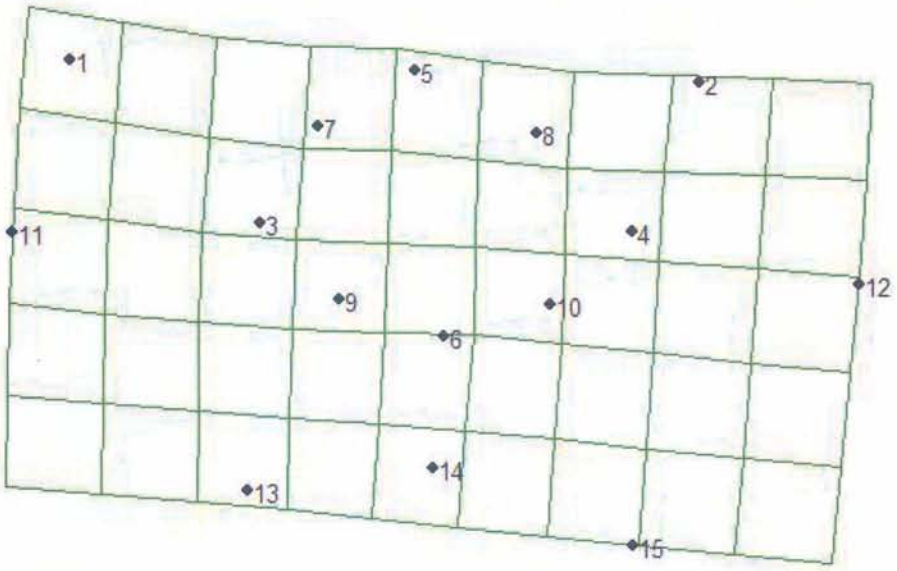

Figure 6.19: Consensus thin-plate spline (in vector mode) demonstrating the differences between black females and black males, OL perspective.

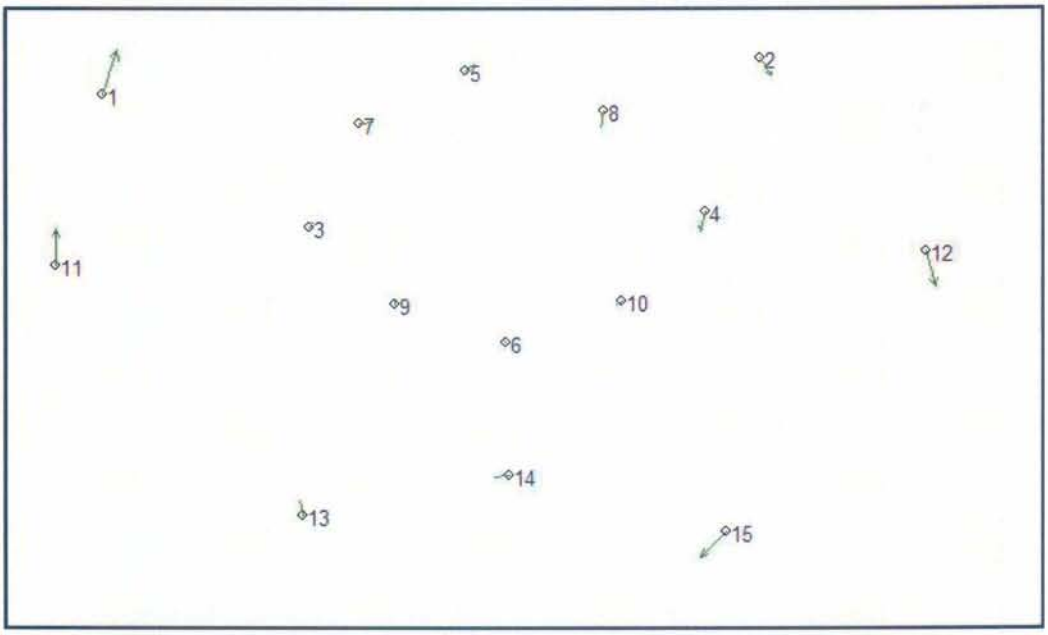

Figure 6.20: Consensus thin-plate spline in deformation mode demonstrating the differences between the reference shape (white females) and white males, OL perspective.

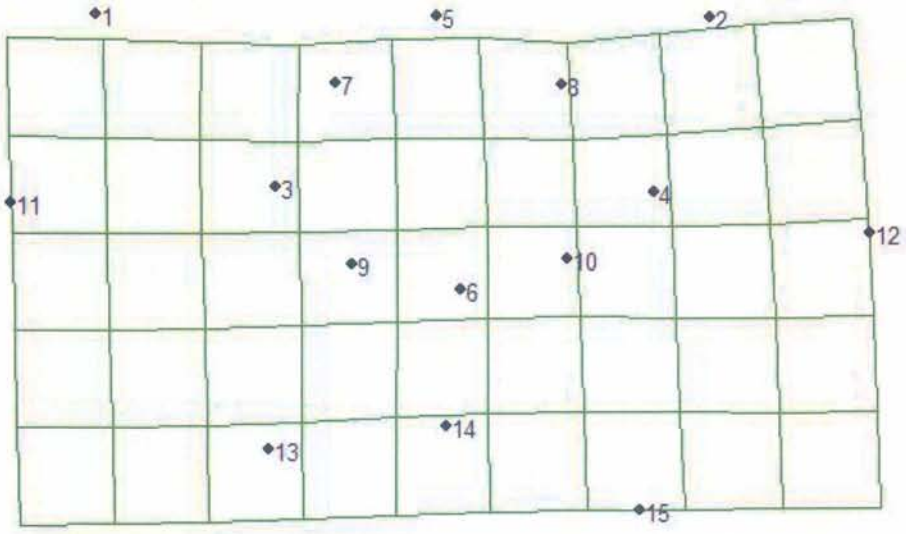

Figure 6.21: Consensus thin-plate spline (in vector mode) demonstrating the differences between white females and white males, OL perspective.

Figure 6.22: Relative warp consensus for eight groups of males and females, OL perspective.

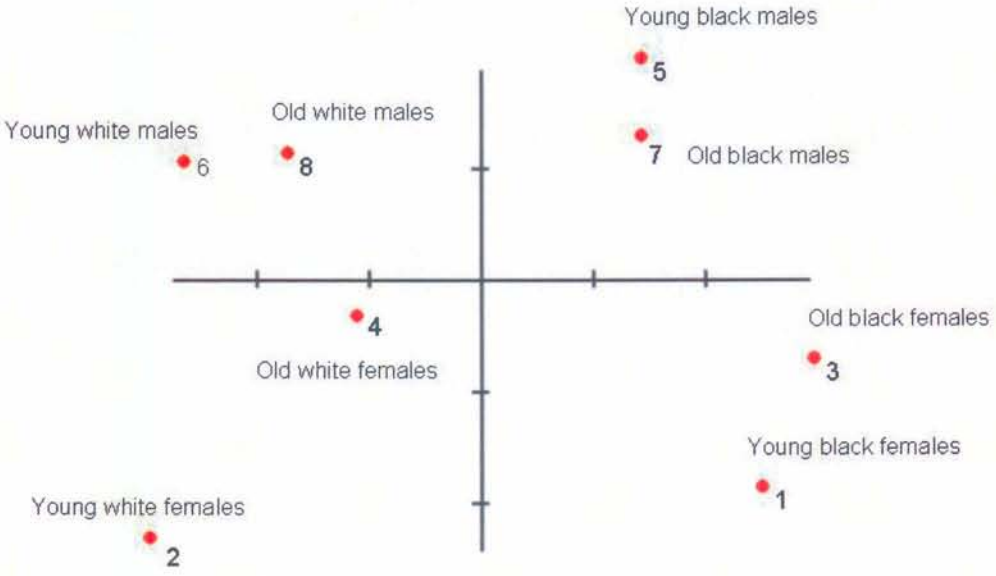

Figure 6.23: Consensus thin-plate spline (in vector mode) demonstrating the differences between young black females and old black females, OL perspective.

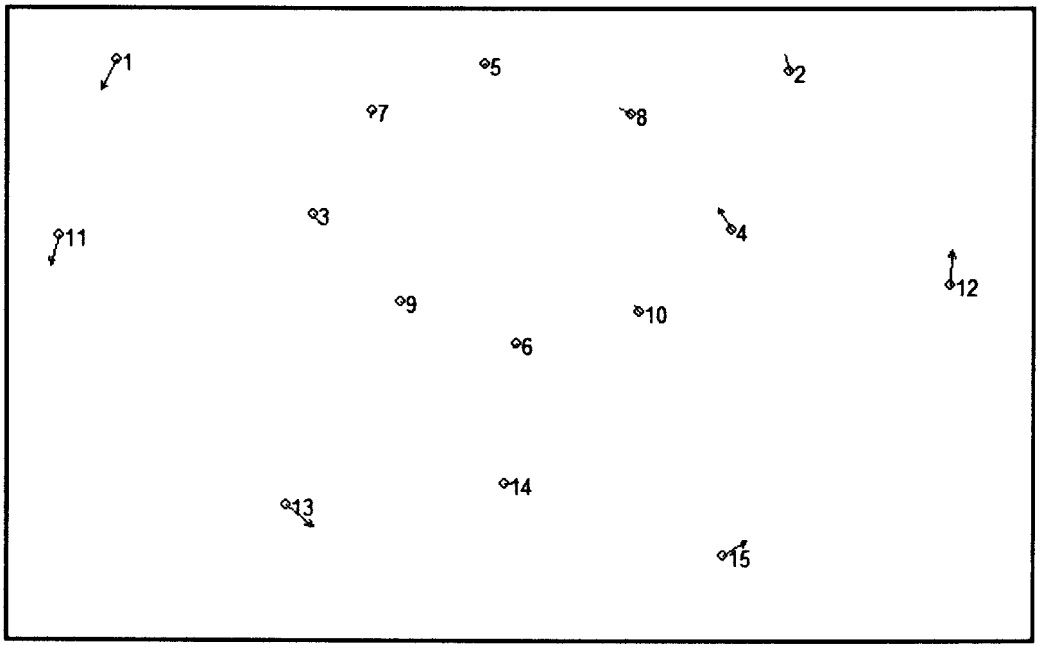

Figure 6.24: Consensus thin-plate spline (in vector mode) demonstrating the differences between young black males and old black males, OL perspective.

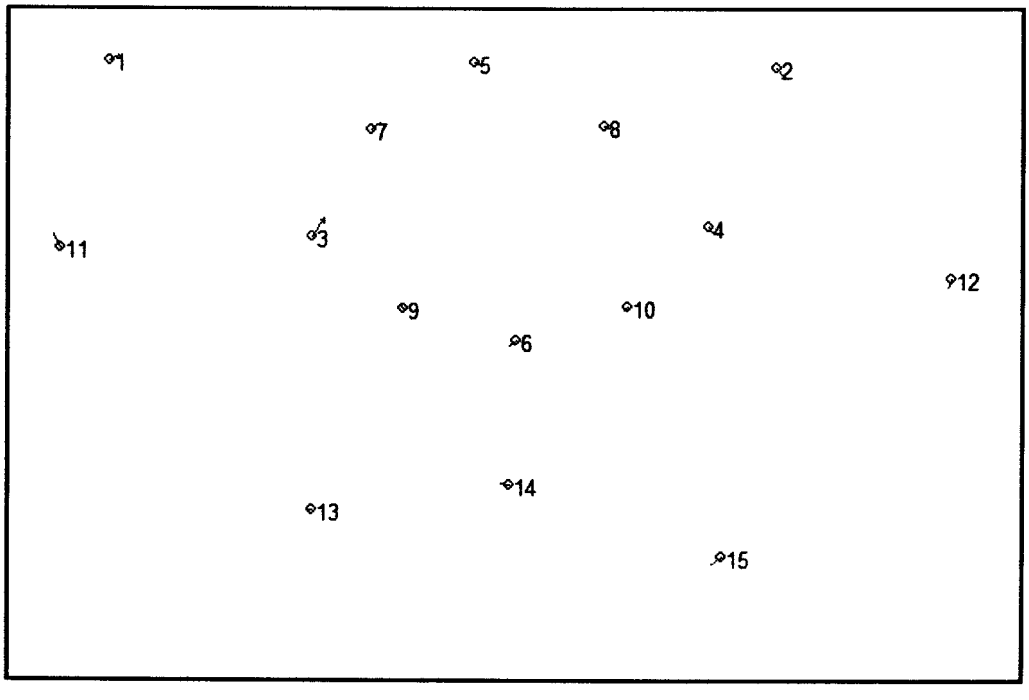

6.25: Consensus thin-plate spline (in vector mode) demonstrating the differences between young white females and old white females, OL perspective.

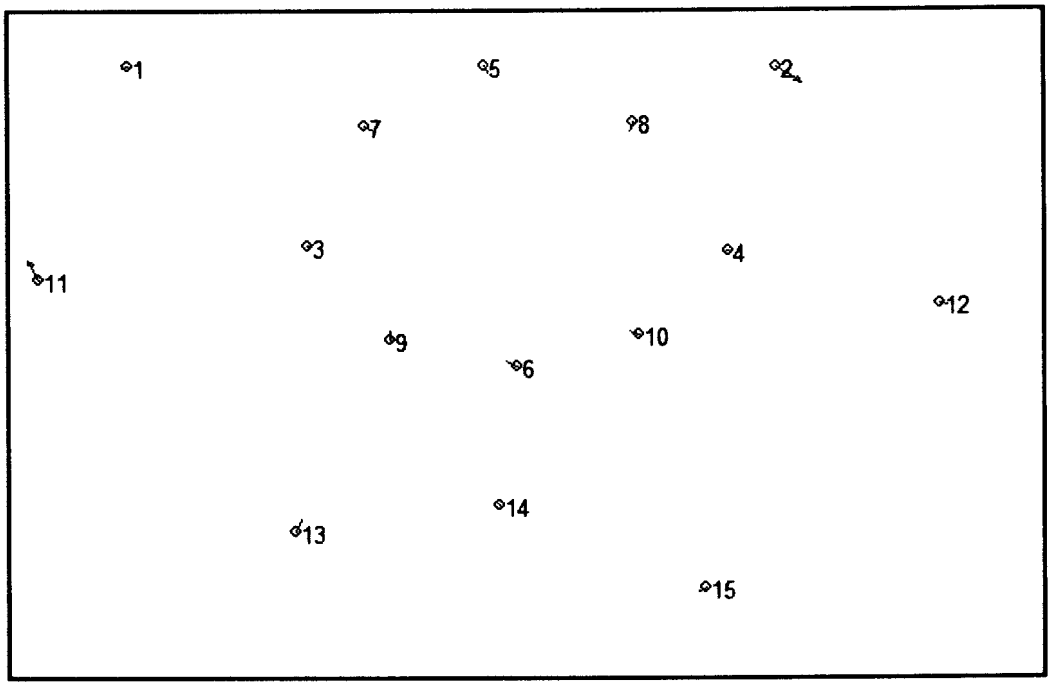

Figure 6.26: Consensus thin-plate spline (in vector mode) demonstrating the differences between young white males and old white males, OL perspective.

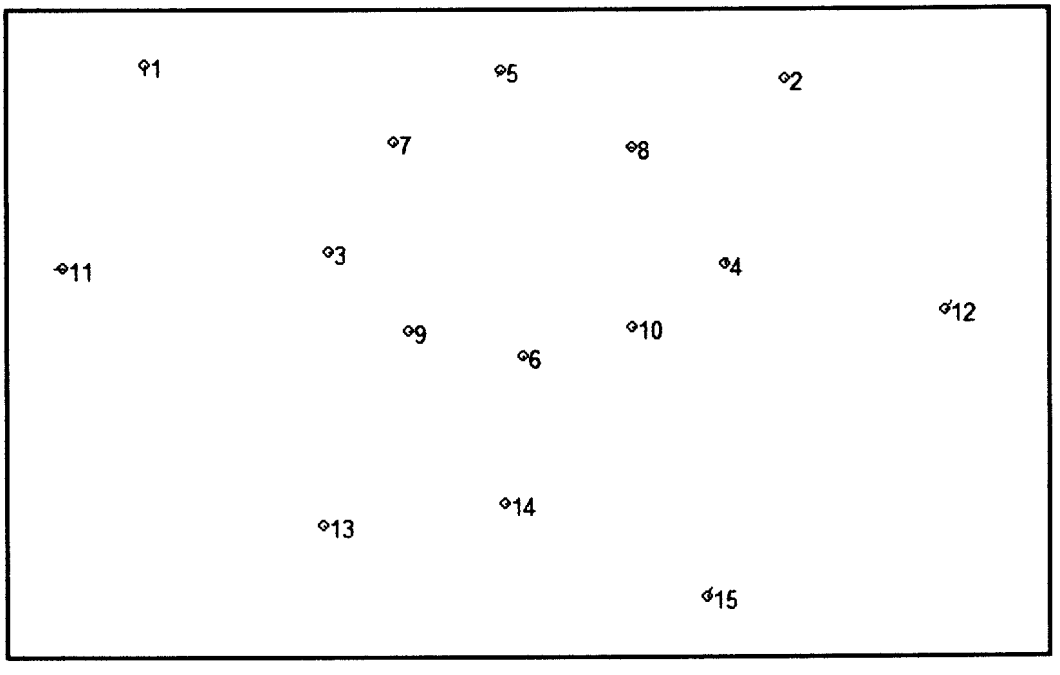

Figure 6.27: Consensus relative warp analysis of females and males, SUB perspective.

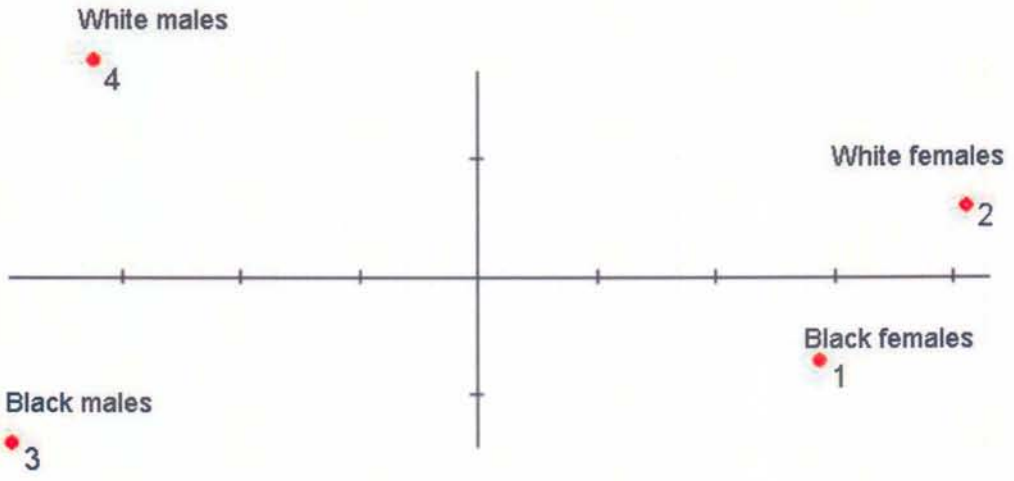

Figure 6.28: Consensus thin-plate spline reference shape of all females and all males from the SUB perspective.

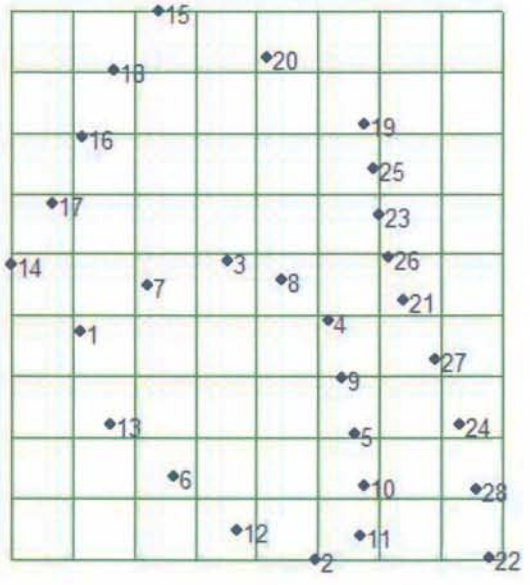

Figure 6.29: Consensus thin-plate spline in deformation mode demonstrating the differences between the reference shape (all females) and all males, SUB perspective.

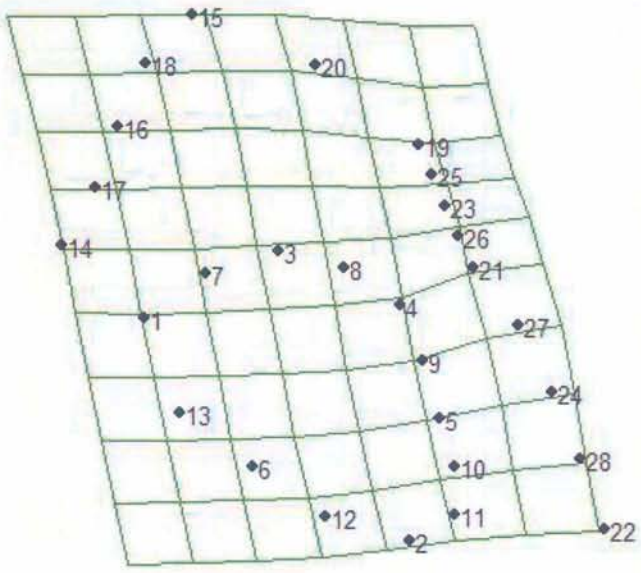

Figure 6.30: Consensus thin-plate spline (in vector mode) demonstrating the differences between all females and all males, SUB perspective.

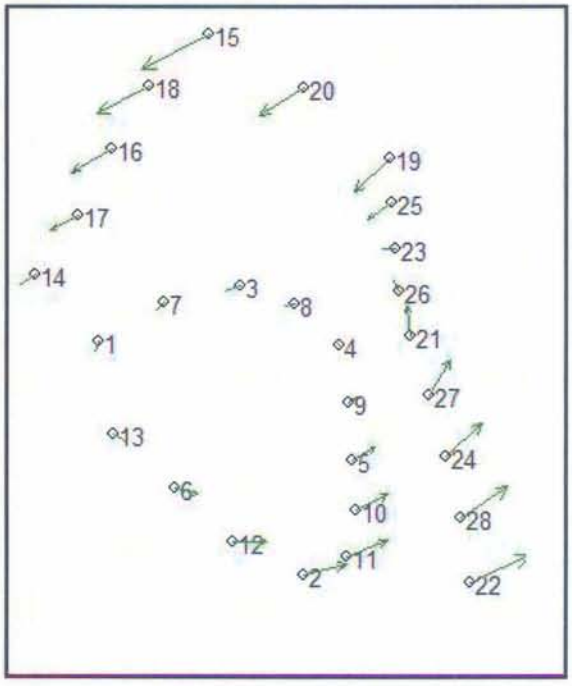

Figure 6.31: Consensus thin-plate spline in deformation mode demonstrating the differences between the reference shape (black females) and black males, SUB perspective.

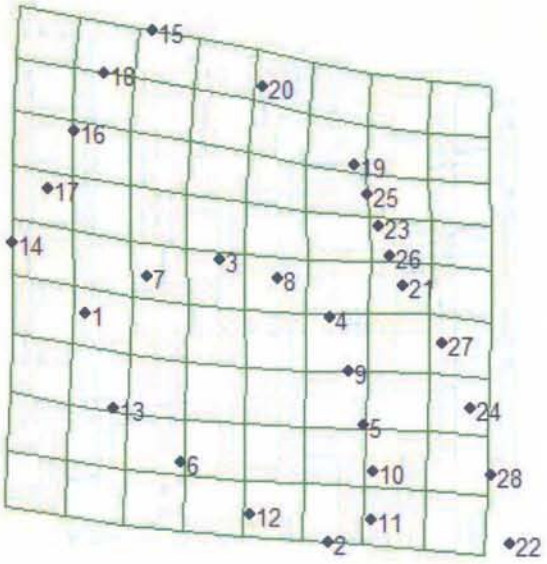

Figure 6.32: Consensus thin-plate spline (in vector mode) demonstrating the differences between black females and black males, SUB perspective.

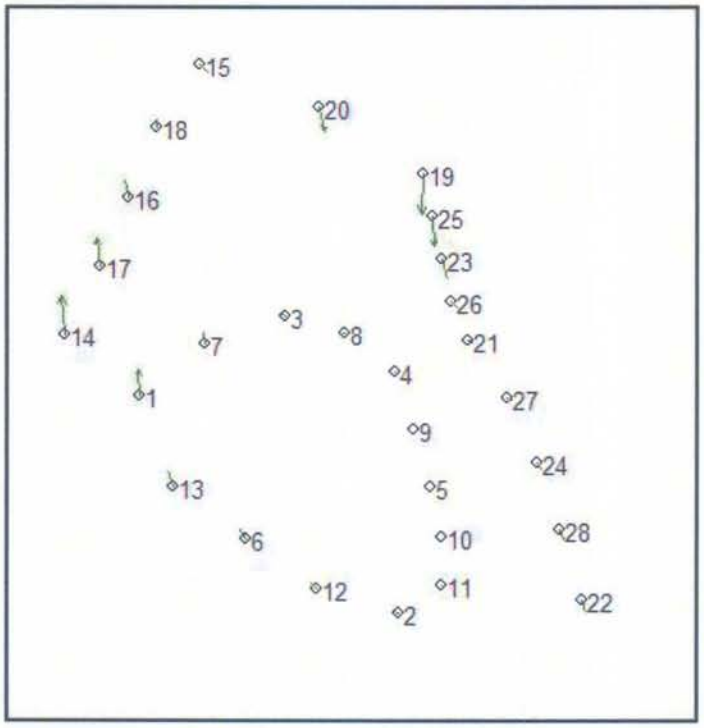

Figure 6.33: Consensus thin-plate spline in deformation mode demonstrating the differences between the reference shape (white females) and white males, SUB perspective.

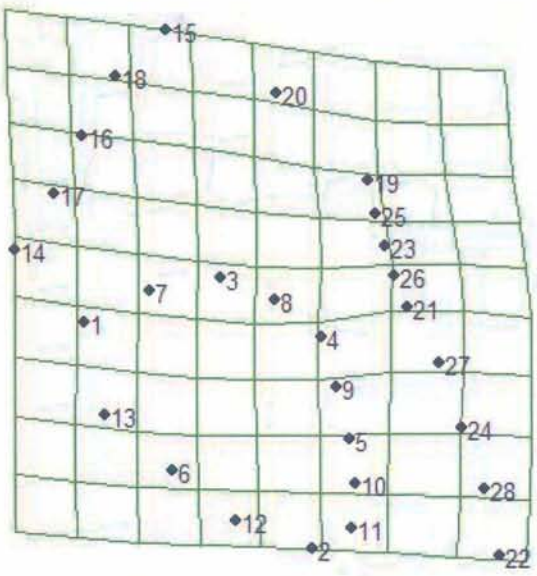

Figure 6.34: Consensus thin-plate spline (in vector mode) demonstrating the differences between white females and white males, SUB perspective.

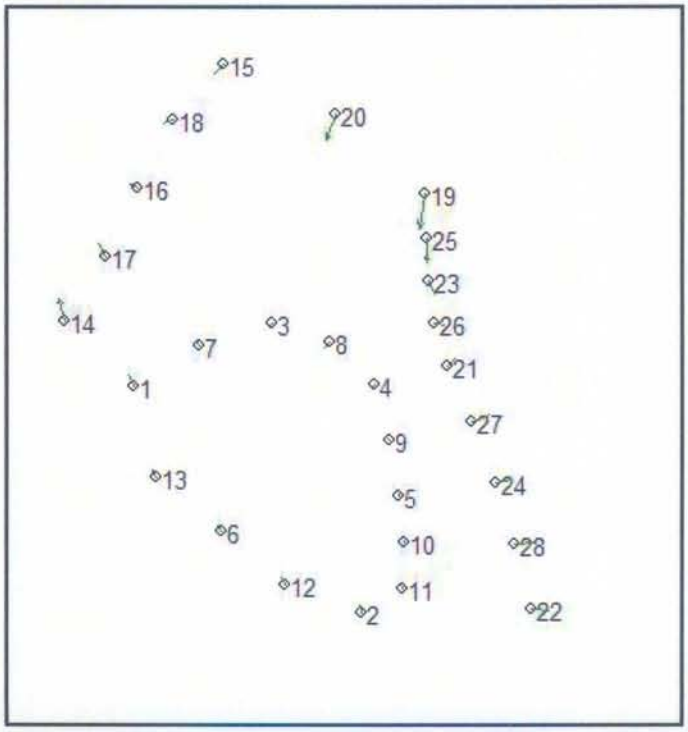

Figure 6.35: Relative warp consensus for eight groups of males and females, SUB perspective.

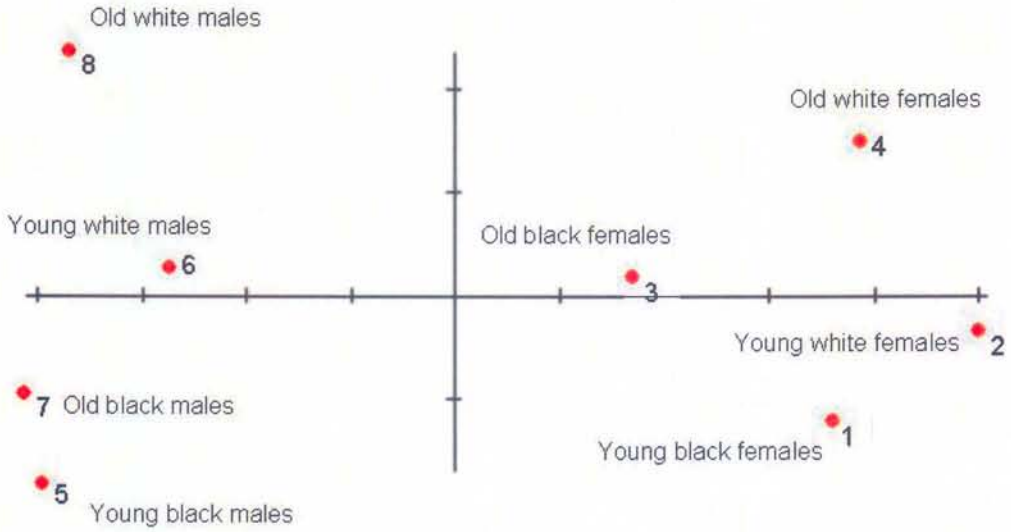

Figure 6.36: Consensus thin-plate spline (in vector mode) demonstrating the differences between young black females and old black females, SUB perspective.

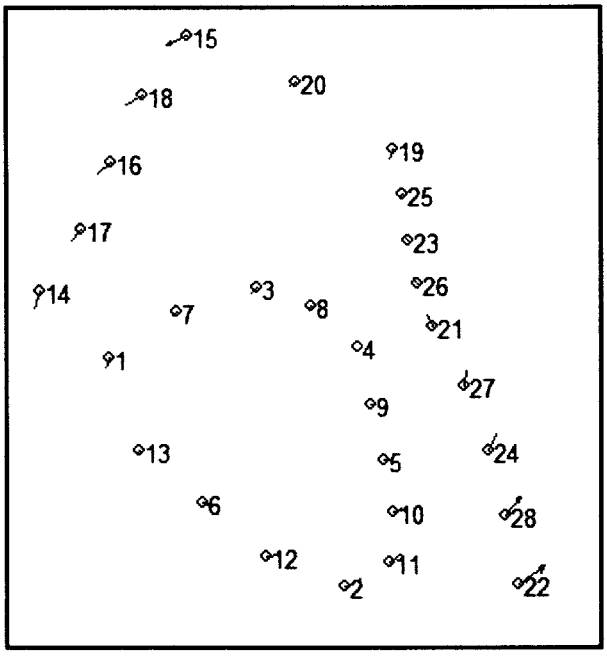

Figure 6.37: Consensus thin-plate spline (in vector mode) demonstrating the differences between young black males and old black males, SUB perspective.

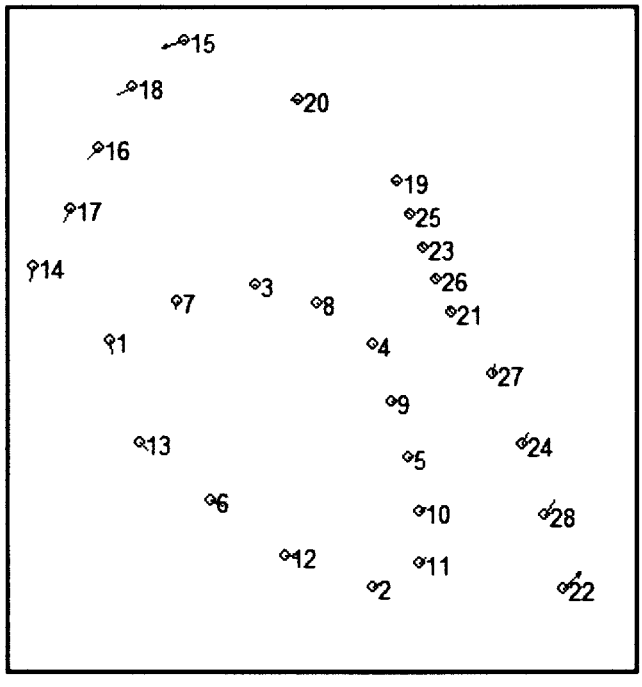

Figure 6.38: Consensus thin-plate spline (in vector mode) demonstrating the differences between young white females and old white females, SUB perspective.

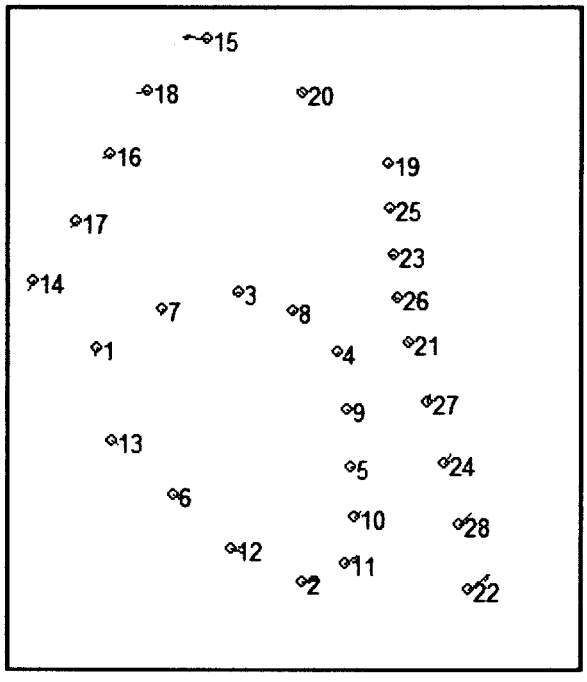

Figure 6.39: Consensus thin-plate spline (in vector mode) demonstrating the differences between young white males and old white males, SUB perspective.

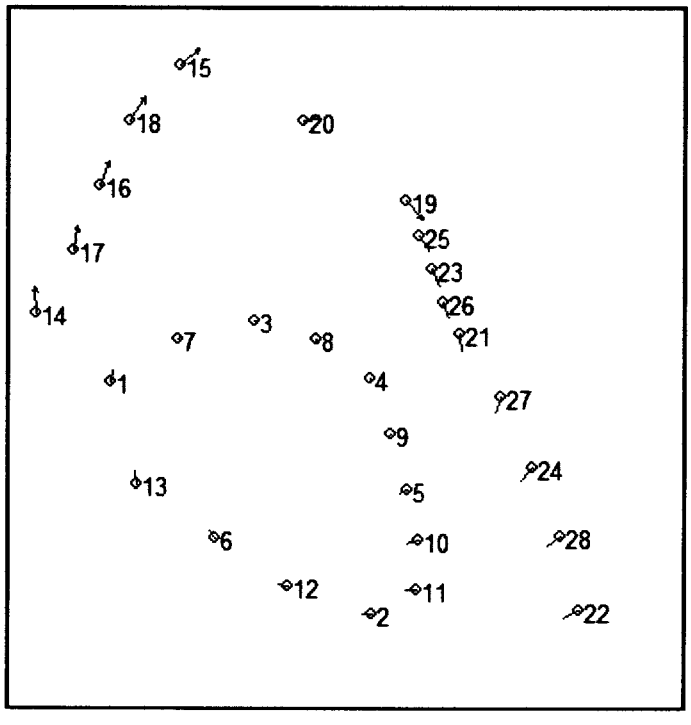

Figure 6.40: Consensus relative warp analysis of females and males, SCI perspective.

Figure 6.41: Consensus thin-plate spline reference shape of all females and all males from the SCI perspective.

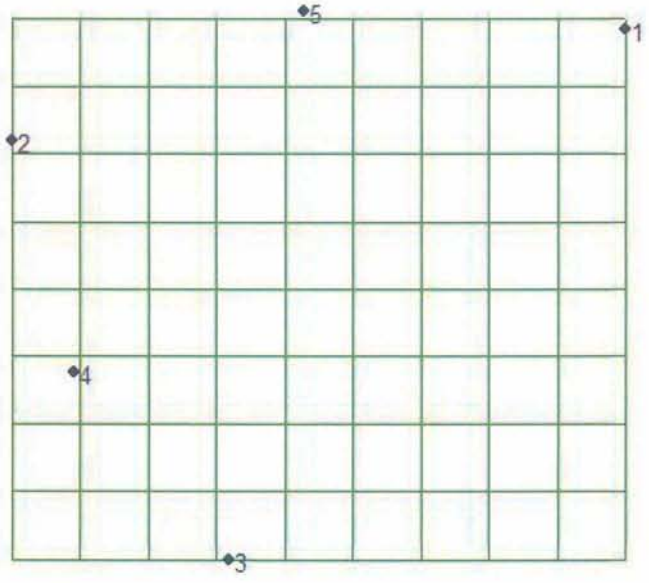

Figure 6.42: Consensus thin-plate spline in deformation mode demonstrating the differences between the reference shape (all females) and all males, SCI perspective.

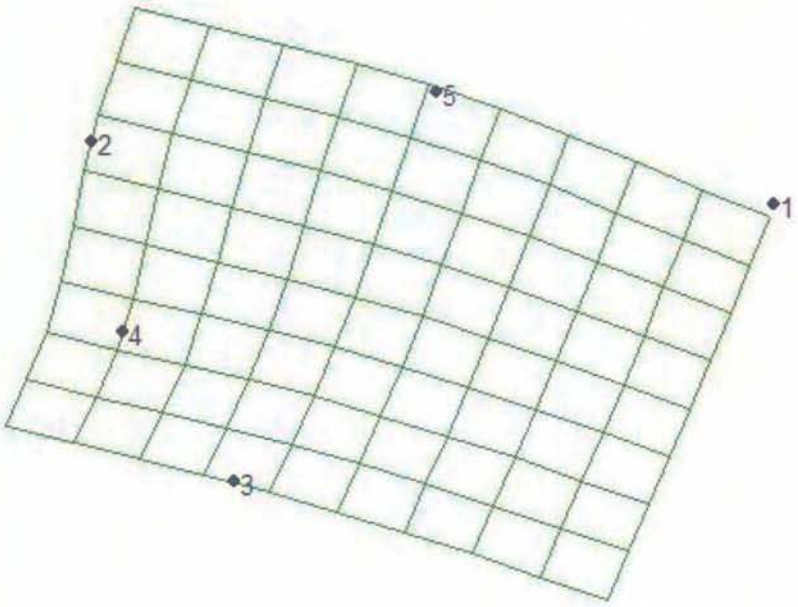

Figure 6.43: Consensus thin-plate spline (in vector mode) demonstrating the differences between all females and all males, SCI perspective.

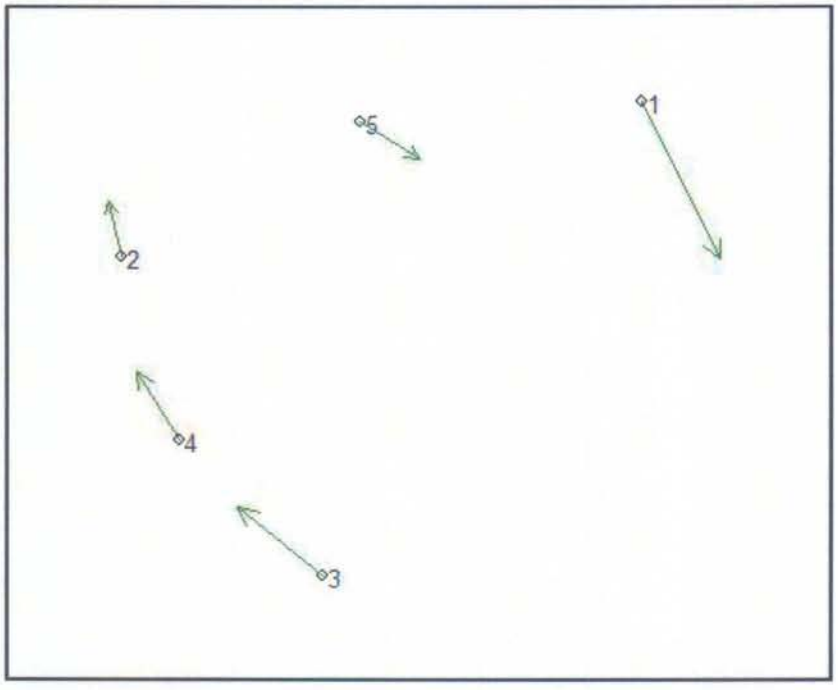

Figure 6.44: Consensus thin-plate spline in deformation mode demonstrating the differences between the reference shape (black females) and black males, SCI perspective.

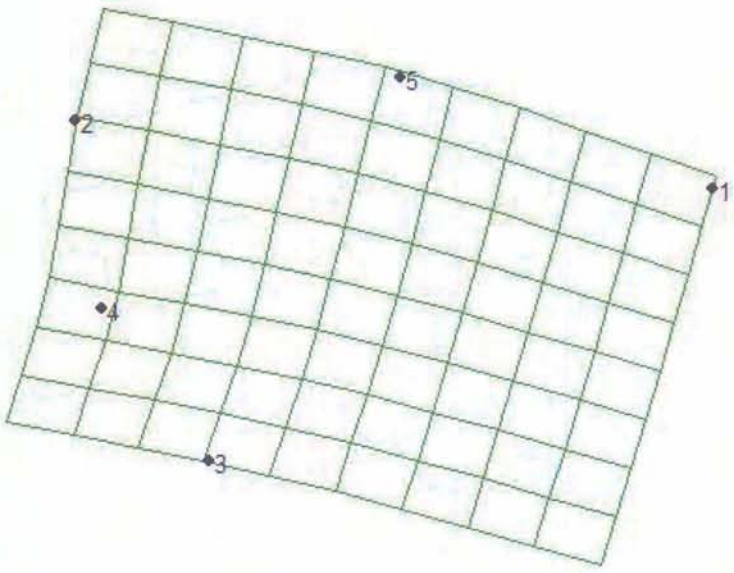

Figure 6.45: Consensus thin-plate spline (in vector mode) demonstrating the differences between black females and black males, SCI perspective.

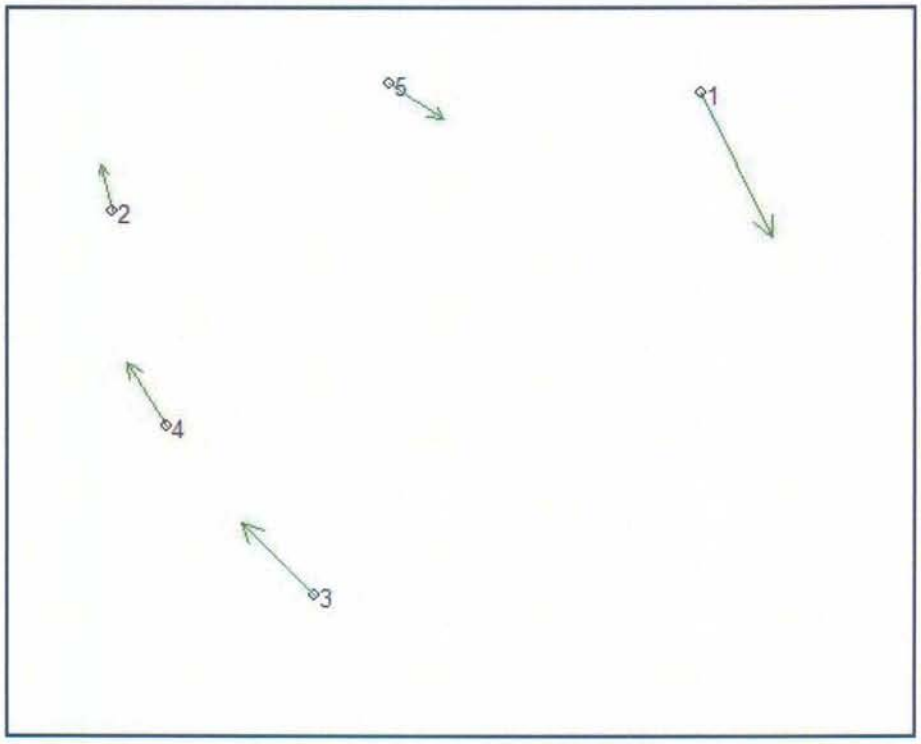

Figure 6.46: Consensus thin-plate spline in deformation mode demonstrating the differences between the reference shape (white females) and white males, SCI perspective.

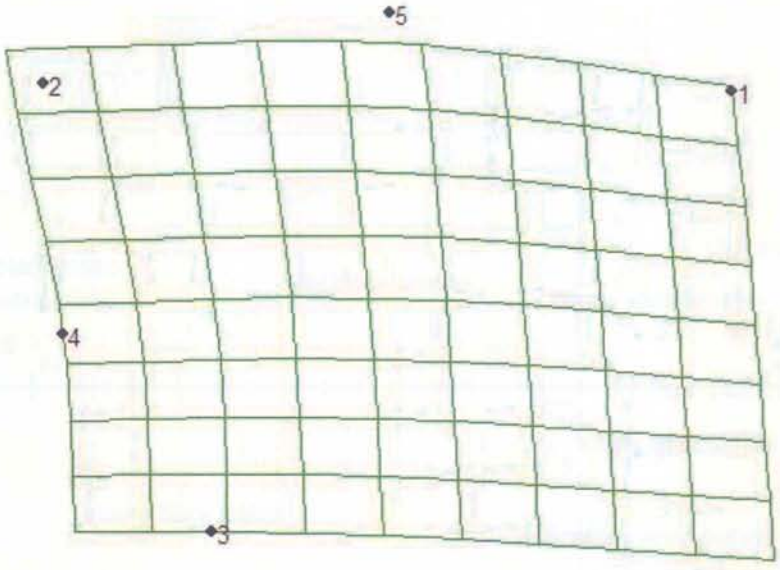

Figure 6.47: Consensus thin-plate spline (in vector mode) demonstrating the differences between white females and white males, SCI perspective.

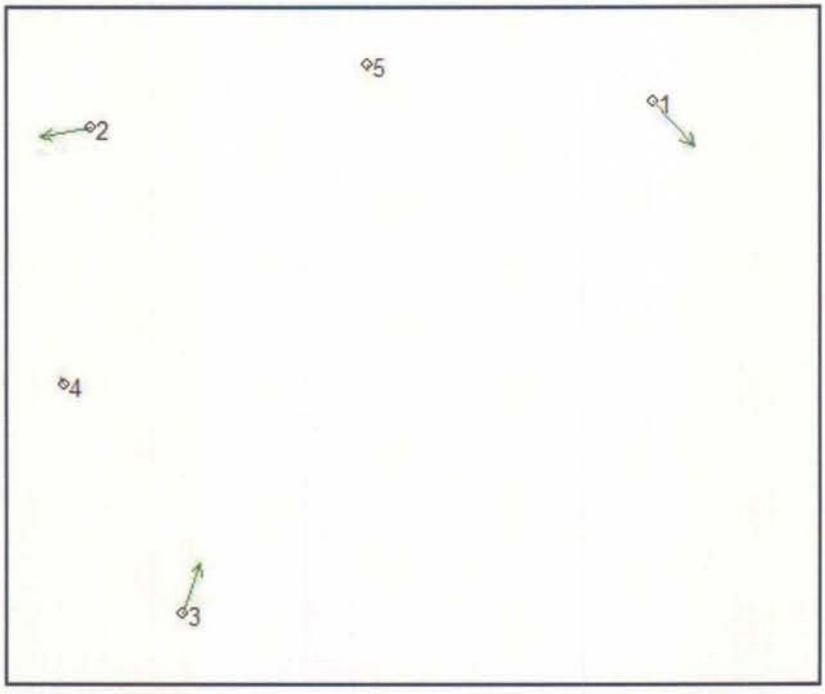

Figure 6.48: Relative warp consensus for eight groups of males and females, SCI perspective.

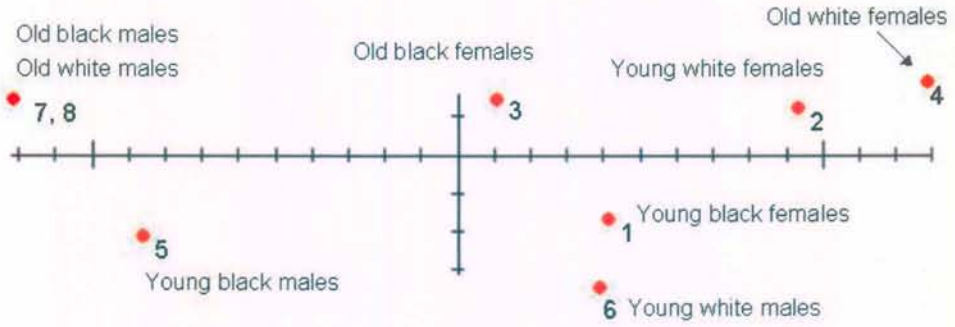

Figure 6.49: Consensus thin-plate spline (in vector mode) demonstrating the differences between young black females and old black females, SCI perspective.

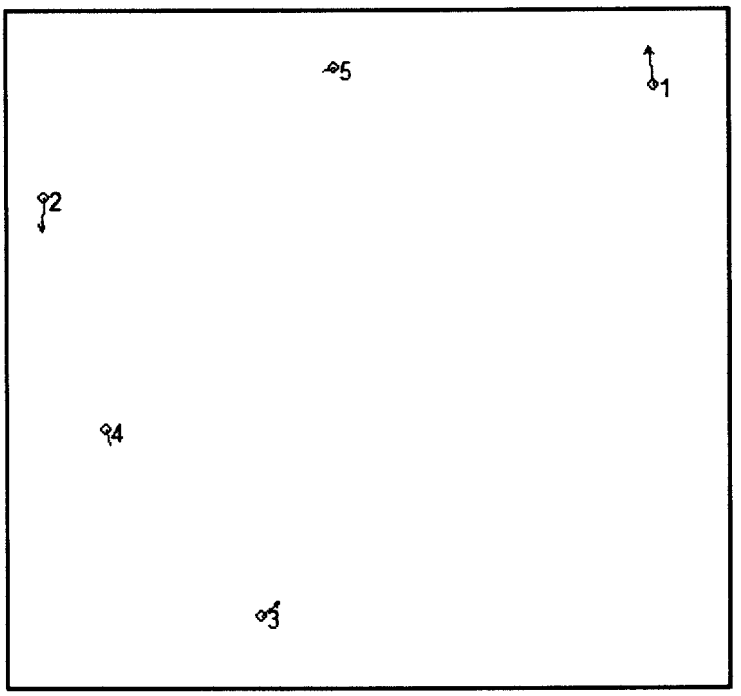

Figure 6.50: Consensus thin-plate spline (in vector mode) demonstrating the differences between young black males and old black males, SCI perspective.

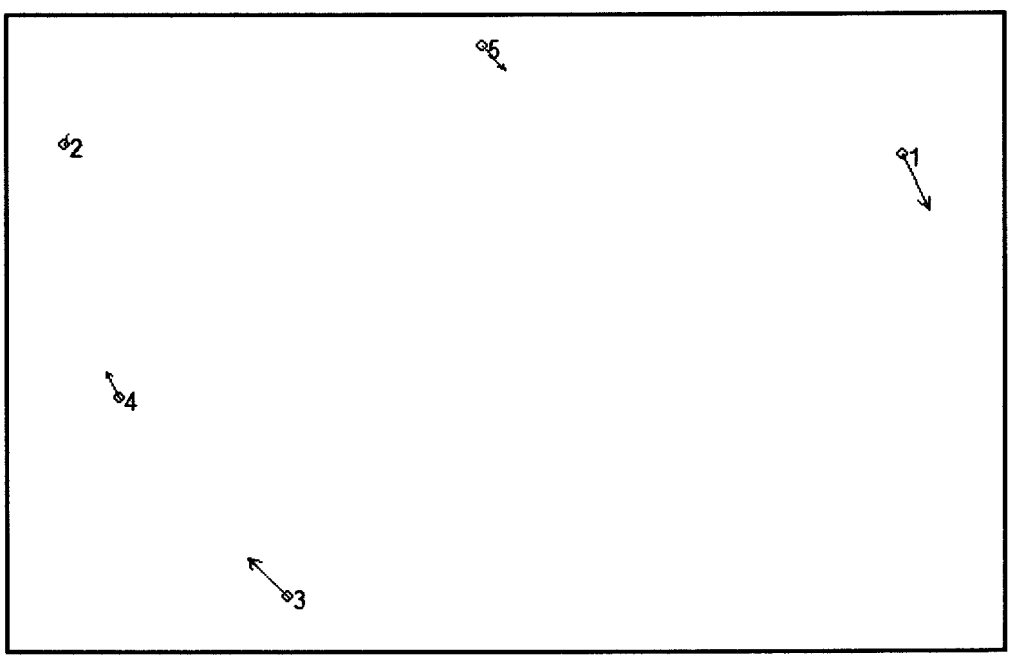

6.51: Consensus thin-plate spline (in vector mode) demonstrating the differences between young white females and old white females, SCI perspective.

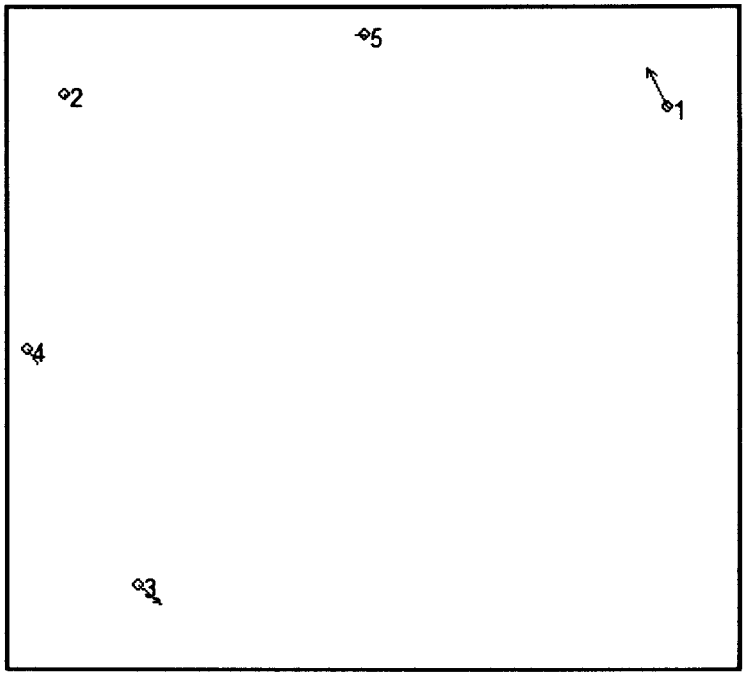

Figure 6.52: Consensus thin-plate spline (in vector mode) demonstrating the differences between young white males and old white males, SCI perspective.

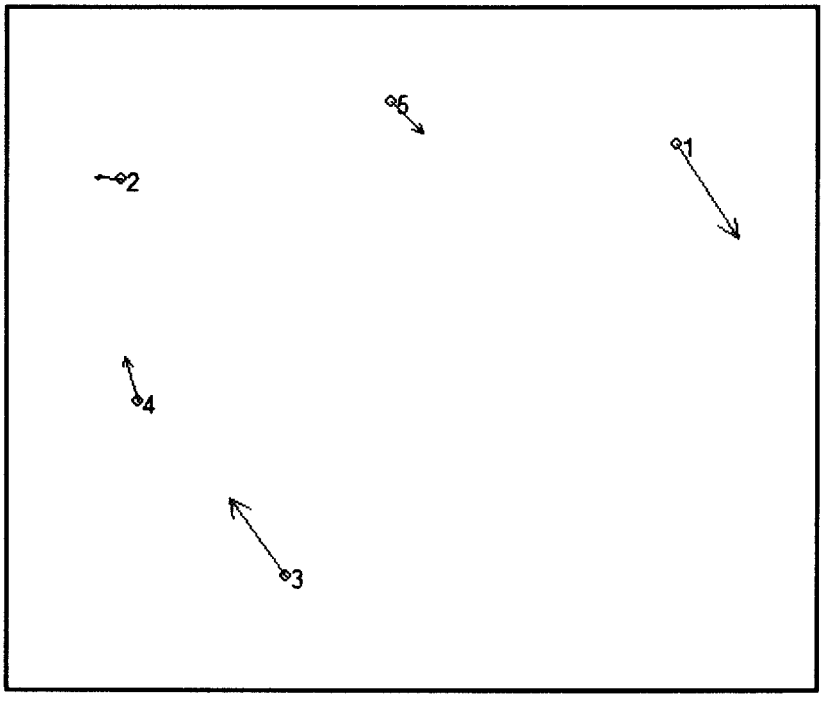

CHAPTER 7

DISCUSSION

Forensic anthropology uses comprehensive methods to recognize certain skeletal traits in the determination of sex. Quantitative analyses are the examination of measurements to illuminate information on sex or stature (Holman and Bennet 1991; Richman *et al.* 1979; Rother *et al.* 1977; Stewart 1954; Tagaya 1989; Wescott and Moore-Jansen 2001), and visual traits give information on the observed morphology and anatomy of the human skeleton (Donlon 2000; Hill 2000; van Dongen 1963; Ubelaker and Volk 2002; Walrath *et al.* 2003). Combined, these methods have proven quite effective in their accuracy rates for the determination of sex, in particular. In addition, geometric morphometrics provides a new way for anthropologists to quantify the shapes they visualize (Adams 1999; Bookstein 1982, 1986; Holliday and Falsetti 1999; Pretorius *et al.* 1994; Richtsmeier *et al.* 2002; Siegal and Benson 1982). All three methods are valuable tools by which analysts conduct research and identify skeletal remains in a medico-legal aspect.

However, modification in bone through degenerative processes may cause ambiguity in the expression of a trait or traits used for sex determination. The effect of age advancement on the human skeleton has been researched extensively with regard to living people and how these changes affect fracture patterns, healing, bone mineral density and general wellbeing (e.g., Bilezikian 1999; Dickenson *et al.* 1981; Heaney *et al.* 1989; Nordin 1966; Scientific Advisory Board 1988, 1996). As of yet, the effect of age on the human skeleton has not been studied to such a degree that we can understand its consequences on the successful establishment of skeletal sex in an unknown individual. Degenerative processes occur in a dynamic environment, with bone gain and loss occurring simultaneously to provide a complex picture of hard tissue morphology as humans age (Ebeling *et al.* 1998; Herd *et al.* 1992; Kolbe-Alexander *et al.* 2004; Leiel *et al.* 1988; Micklesfield *et al.* 2003; Riggs *et al.* 1982;

Steiger *et al.* 1992). These processes required further study in order to determine how they influence the way forensic anthropologists draw conclusions about sex with regard to aged human remains.

The aim of this study was to determine if sexual dimorphism changed with age in the human skeleton. If changes in the human skeleton with age are great enough to visualize, quantify, and ultimately are deemed significant through statistical analysis, then forensic anthropologists would have reason to be more cautious and prudent in their determination of sex based on these facts.

The goal to determine if sexual dimorphism changed with age was accomplished on three distinct levels. Using measurements and subsequent statistical analyses on 23 postcranial measurement sites, information was gained on patterns of metric increase or decrease at each skeletal site. These sites included articular joint ends of all six major long bones (both proximal and distal), shaft diameters and circumferences of these bones, and measurements of the pelvis. Biological populations were separated in order to take into account size discrepancies. When analyzing the size differences between young and old individuals, evidence was gained on where these changes were occurring and to what degree these changes were taking place. The magnitude of metric changes was important because of the potential misclassification of females if these bones metrically increased to such a degree that females may be misclassified as males, or if these bones decreased in size such that males were incorrectly classified as females. Changes in all dimensions were assessed between young and old individuals, and if the difference between the two were significant, they were compared to their male or female counterpart to reveal the possibility of metric overlap.

Secondly, non-metric traits of the pelvis and the distal humerus were employed to gain knowledge as to whether or not these visual indicators of sex changed with the onset of age. Four traits of the pelvis and four traits of the humerus

were used to determine sex. The classification accuracies for both young and old individuals of each biological affiliation were compared to determine if misclassification increased or decreased with advancing age.

Finally, geometric morphometric analysis was used on four 2-dimensional perspectives from the pelvis and the humerus to "quantify" the shape and form of each feature. These 2-dimensional views of the pelvis and humerus were directly correlated to those features used in the non-metric visual assessment of sex. In each perspective (especially the distal humerus) it was first attempted to prove that each view was sexually dimorphic. Subsequently, the geometric shape equivalent of young and old individuals from each group were calculated and compared to determine if any quantifiable changes in form took place with the onset of age. Geometric morphometric analysis achieved results that illuminated several issues with regard to the quantification of shape and form in anthropology. This visual and statistical tool is a powerful resource and produced interesting, highly accurate results on most occasions. However, drawbacks to the method will be discussed, as well as the future applicability of geometric morphometrics in forensic casework.

7.1

Research sample

The sample should ideally have included an equal number of females and males from all age groups and both population affiliations. Because the Pretoria Bone collection does not include a large number of young white individuals (both male and female), every effort was made to create a comprehensive sample that would include as many males and females in each population and age group as possible, and therefore specimens from the Raymond Dart collection (University of Witwatersrand) were added where possible.

Although this study does not focus on biological affinity, it was difficult not to note the abundance of young black male specimens in the collection, and the conspicuous absence of young black females and young whites (L'Abbe *et al.* 2005). The sample of young white specimens was not ideal, but every effort was made to acquire as much information as possible.

The Pretoria Bone and the Raymond Dart Skeletal Collections cannot be studied without addressing the issue of possible secular trends in the size of individuals throughout time. A secular trend is the tendency for each succeeding generation to mature earlier and become, on the average, larger (Kieser *et. al.* 1987). Slow but persistent alteration over a period of time in the mean shape or size of individuals in a population is referred to as a secular trend in human biological terms. A positive secular trend is one that demonstrates an increase in the dimensions under consideration, while a negative trend relates to a diminution of the structure (Cameron *et al.* 1989; Tobias 1975, 1985; Tobias and Netscher 1977).

This pattern of development towards an increase in size has numerous variables attributed to it. Factors include better nutrition and health care options which may allow for an increase in the stature of individuals in a healthier environment. The amount and quality of nutrition have increased, which allowed for more energy to be exerted in growth and development (Henneberg and George 1993; Jantz 2001). These factors may very well hold true with South African people. Sexual selection of taller individuals, decreased mortality rates and phenotypic adaptation to particular environmental conditions may also be mechanisms that drive secular trends towards an increase in size. However, studies focused on secular trends in humans concentrate largely on stature and cranial measurements (Henneberg and Louw 1997; Jantz 2001; Kelpinger 2001; Malina and Zavaleta 1980; Malena 1979; Susann 1985; Tanner 1994), which were not the focus of this study. However, these types of quantitative comparisons of past era samples to contemporary samples have provided data that support a general increase in stature

in recent generations. Research in South Africa has also shown certain positive secular trends, especially in cranial dimensions and the dentition of black South Africans, although the mid-20th century has shown an absence of a positive secular trend, which seemed to denote that environmental factors believed to produce a positive trend were absent in this time frame (Cameron *et al.* 1989; Kieser *et al.* 1987). Studies on the magnitude of secular trend in stature among South Africans found a weak positive trend (Henneberg and van den Berg 1990; Steyn and Smith 2007) but Tobias and Netscher (1977) and Ulijaszek (1996) found evidence of a reversal of this positive trend in the cranium and femur. Later, Tobias (1985) documented the reversal of a secular trend change in South Africans. Thus, it is difficult to determine what the effect of secular trend would be in this study, if any. Long bone length measurements were purposefully not included in this study because stature was not a priority for this particular research. Articular joint ends (such as those studied) were analyzed because they had unique properties in a degenerative sense that may illuminate differences with the onset of age. The possible addition of bone in old age (and subsequent degeneration) may be present regardless of whether a population was well or poorly nourished, as evidenced in Katzmarzyk and Leonard (1998) and Susann (1985). Long bone lengths, and thus secular trend in stature, would most likely not have influenced this study. The birth and death dates of each individual in the study were not recorded, eliminating the possibility of studying the mean birth dates for each group to see if a difference occurred between size and the era in which the individual was born. It should be mentioned that the Pretoria bone collection is the most contemporary sample in South Africa, with dates of birth ranging from 1863 to 1996.

This study was conducted with ideal parameters in mind. Every effort was made to collect data that was comprehensive, comparable, and that reflected the contemporary questions that were posed. Thus although the sample for each group was not ideal, it was considered sufficient for research purposes.

7.2

Metric analysis

The statistically significant size difference between males and females was initially apparent when comparing metric results, and continued to be the principle component of sexual dimorphism based on metric analysis as seen in other works (Bass 1995; White 2000; Steele and Bramblett 1988). The size (and size differences) in South Africans specifically have been well-documented by Asala (2001), Asala *et al.* (1998), Bidmos (2006), and Patriquin *et al.* (2005). All males were observed to be larger than their female counterparts in proximal and distal articular surfaces, midshaft diameters and circumferences, as well as most pelvic measurements; the only exception was the pubis length (males=73.2mm, females=76.6mm). The calculated ischio-pubic index of females presented a larger value than that of the male sample, based on the ratio of longer pubic lengths to shorter ischium lengths in females. These results correspond to all past research that detail South African osteometry.

7.2.1

Metric changes in females with the onset of age

In regard to the female specimens studied, metric differences between black and white female long bone dimensions were observed in several midshaft measurements and the head diameters of both the humerus and femur, among others. White female specimens have been shown to have larger skeletal measurements than their black counterparts (Steyn and Iscan 1999). Through analysis of the measurements, the degree of difference between the two populations was statistically significant in a majority of all variables. Thus, although there were some similarities in size between the two female groups, the groupings by population were made so as not to obscure small metric changes with age.

Clear size differences existed in pelvic dimensions between black and white females as well. All measurements of the pelvis and the ischio-pubic index calculation were greater in white females on a statistically significant level. This simply revalidates the results of the postcranial long bone measurement means indicating that white females are larger in size than their black counterparts.

Black females did not change much in their long bone dimensions with the onset of age. The absence of any size change showed that black females continued to exhibit the same level of sexual dimorphism (based on size) throughout life. Only one measurement changed on a statistically significant level with the onset of age in the black female, namely the circumference of the humerus at midshaft, which decreased with age. This decrease in the diaphyseal value of the upper arm bone is in general congruence with previous studies that showed both the addition and involution of bone within the cortical/ endosteal surface (Ericksen 1976; Evers *et al.* 1985; Garn *et al.* 1969; Garn 1970; Heaney *et al.* 1982; Nilas *et al.* 1988; Thompson 1980; Woddard 1962). Specifically, Heaney *et al.* (1989) found an increase in medullary cavity size does not always lead to the increase in midshaft circumference, especially if bone density is greater in cortical bone to begin with. Because bone density was found to be predominantly greater in black populations (Orwoll *et al.* 1996; Garn *et al.* 1969, 1972), a general loss of bone within the cortical/ endosteal surface of long bones in South African females seemed logical when viewing the results from both Heaney *et al.*'s and Orwoll *et al.*'s work. Thus, a net loss in the circumference of the humerus for black females with the onset of age appeared to be in conjunction within the framework of normal degenerative processes documented by Cummings *et al.* (1990), Herd *et al.* (1992) and Herrin (2001), and paralleled the findings of past research.

In addition, the high bone mineral content of black South African females may account for the lack of change with the onset of age in this sample. Numerous studies prove unequivocally that the population of black females in Africa inherently

have a greater bone density than white individuals. Adebajo *et al.* (1990) specifically saw less femoral fractures in black West African females than in European samples. Aspray *et al.* (1996) found even with a lower bone mineral content after menopause, Gambian females were less prone to osteoporotic fractures based on their elevated bone density. Schnitzler *et al.* (1990) attributed the lack of fragility in Black South African females as a combination of thicker and better connected trabeculae, even with the onset of age. Grynpas (1993) conclusion was the same; Black South African females were less likely to suffer from fragility fractures than others based on their bone mineral content. Black South African females commence with greater bone density, and thus theoretically have less bone density loss with the onset of age. In addition, pathological changes such as microfractures along muscle attachment sites and articular surfaces in black females during the 7^{th}, 8^{th}, and 9^{th} decades of life would be less prevalent than in white females of the same age category. All past studies concluded the lack of fragility in black South African female bone with the onset of age, and this current study corresponds to those conclusions. Black South African females change very little in their dimensions with the onset of age, because they do not lose as much bone tissue nor do they suffer as much from osteoporotic fractures and healing as white South African females.

Metric values from the pelvis for black South African females also remained static and largely unchanged with advanced age, much like they did in the other postcranial measurements. This indicated the absence of osteophytic changes that occur with decreased bone mineral density and the presence of robust bone tissue resilient to degenerative changes. Female pelvic morphology throughout life was maintained for this group, and the continuation of distinct sexual dimorphism with the onset of age was seen.

White females increased in all long bone metric dimensions with the onset of age. This result corresponded to the original notion that females may very well *decrease* in sexual dimorphism by *increasing* in size, thus making them more difficult

to categorize correctly. As found in Smith (1964), midshaft diameters of long bones did increase as age increased. Rother *et al.'s* research (1977) found 16% of female specimens overlapped metrically into the male mean when measuring older specimens. In addition, Walker (1995) found an increase in skeletal robusticity in white females 45 years old and older. Walker's results directly correspond to the metric increase in long bone articular ends and midshafts seen here.

White females in our study came metrically close to the white male mean with the humeral head diameter, the distal diameter of the ulna, the radial head, the femur diameter at midshaft, the bicondylar breadth of the distal femur, the bicondylar breadth of the proximal tibia, and the tibia diameter at midshaft. The mean of old white females through their 7th, 8th, and 9th decades of life came quite close to overlapping the mean of young white males. This raised a serious concern for the possible misidentification of an isolated bone shaft or fragment, if recovered in the field and only measurements were used to assess skeletal sex. Young white males in practice may rarely be misclassified as old white females for a number of reasons (visual techniques, bone density assessment, the presence of possible degenerative changes). However, misclassification may occur in instances of fragmentation and if other indicators of sex are absent.

One metric dimension of old white females crossed over into the metric dimension for black males; namely the humeral head diameter, which increased significantly in the white female population with the advance of age. The mean for black males and white females for this measurement not only converged as age progressed, but the female mean exceeded that of the males in the 6th decade of life. This result, again, was cause for concern based on the fact that many times measurements are often used exclusively to determine skeletal sex when remains are fragmented or incomplete, and ancestry of the individual cannot be determined from a fragmented bone.

The reasons for these changes are multi-faceted and may include normal degenerative factors as well as disease, e.g., osteoporosis (Aloia *et al.* 1985; Cummings *et al.* 2000; Dickenson *et al.* 1981; Frost 1963; Herd *et al.* 1992; Herrin 2001; Hurxthal *et al.* 1969; Jowsey 1960; Nilas *et al.* 1988; Orwoll *et al.* 1996; Riggs *et al.* 1982; Steiger 1992). White South African females commenced with less bone mineral density, and thus were more subject to degenerative processes as age progressed (Chavassieux *et al.* 2007; Cummings and Black 1995; Cummings *et al.* 1985; Evers *et al.* 1985). These degenerative processes include osteoporotic bone remodeling and the repair of possible microfractures at articular joint surfaces (Jowsey 1960; Kanis and McCloskey 1993; Martin and Atkinson 1977). Osteon count increases with age, which in turn allows for more potential microfracture points along the osteon margins. Also, bone mineral density has been directly correlated to the size of Haversian canals, and their increase in dimension with the onset of age (Thompson 1980). Thompson found that females tend to have significantly larger Haversian canal areas compared with males of the same advanced age, thus their bone mineral density values are smaller. Larger Haversian canals equate to larger expanses within osteons, thus less density in bone is seen in females than males. Because females of non-African origin have a lower bone mineral density with the onset of age (as seen in studies by Trotter *et al.* 1960, Ericksen 1976, and Martin *et al.* 1985), fractures are more likely to occur because the tensile strength of white female bone is not as substantial. As more bone is formed at these fracture sites due to hard tissue fracture response, metrically larger articular sites could occur.

The increase in long bone midshaft diameters with the onset of age in white females may also follow mechanisms found in past studies of cortical bone change with time. Endosteal bone loss and periosteal bone gain in long bones is characteristic of aging populations. As seen in the study by Nilas *et al.* (1988), an unexpected increase in bone width at two forearm sites was the result of research originally designed to observe bone loss over time. Smith and Walker (1964)

showed that in white females, the diameter of the midshaft periosteum increased as cortical thickness declined. Both processes worked together to increase the diameter of a long bone shaft. Since periosteal diameter increased and cortical thickness decreased, the endosteal diameter of long bones in white females were seen to expand when comparing the young and old groups. The same results were apparent in this current research as well, with an increase in dimensions of four skeletal sites (among others) of the arm in the white female sample when comparing young to old. The combined processes of an increase in the medullary cavity of long bones and the net bone gain at the periosteal surface with age, acts in tandem with osteophytic fracturing in less-dense bone to create a dual-process addition (thus net bone gain) in the white female skeleton.

Studies by Martin and Atkinson 1977, Leiel *et al.* 1988, and Heaney *et al.* 1989 showed the results of the complex process of addition and subtraction of bone on the periosteal surface and within the endosteal envelope. These changes can have an ultimate net bone gain or loss in regard to measurements such as midshaft diameters, cross-sectional periosteal widths, and circumferences. As seen in this current study, the female skeleton can show both bone loss (as in the black South African sample) and bone gain (white South African females), which directly correspond to the findings in past studies.

No measurements of the pelvis or the ischio-pubic index changed on a statistically significant level with the onset of age in either black or white females. This indicated the static nature of female pelvic morphology throughout life, and showed that cortical bone thinning and bone mineral density decline was not necessarily affecting white females in the os coxae as it was affecting them in their long bone measurements. Both white and black females appeared to maintain a relative stasis in their pelvic measurements, which indicated a lack of pelvic modification with the onset of age in both female groups. Although the size component between black South African females and white South African females

continued to be apparent (as seen in Patriquin *et al.* 2002), no dimension changes that may influence sexual dimorphism were observed with either group.

The possibility of misclassification from long bone measurements of white South African females was present. In addition, pelvic metric data from all white females, both young and old, were larger than pelvic metric data from all males, young and old. If size is truly the principle component for sex determination, then larger metric values in white females indicated the possible misclassification of females. However, sexual dimorphism in the pelvis can be seen as the amalgamation of many factors, only one of which is size. Visual characteristics may be the best predictor of sex from the pelvis (Bruzek and Soustal 1984; Krogman 1962; Moerman 1981; Stewart 1954), and measurements in this study do not indicate a change in sexual dimorphism in the female pelvis with the onset of advanced age.

Thus, the changes with age observed in white South African females and the lack of change in the black South African females can be attributed, in part, to original bone mineral density. Sexual dimorphism remained unchanged in black female long bones, while sexual dimorphism decreased in the form of increased metric dimensions of long bones in white South African females.

7.2.2

Metric changes in males with the onset of age

As in the white female sample, white males were observed to be markedly larger than black males. This discrepancy in the principle component of size was more discernible in males than in females, and the difference in size was significantly larger in 18 out of 23 postcranial measurements (Table 4.9).

Black males metrically increased significantly in seven long bone locations with the onset of age (Table 4.10). These statistically significant sites where metric increases took place were the midshaft diameters of the appendicular skeleton and the elbow and knee joint locations. Based on research indicating the increase in

medullary cavity dimensions with age (Garn et al. 1969; Garn 1970, 1972; Martin and Atkinson 1977; Rogers 1982; Thompson 1980), midshaft diameters may very well increase with the onset of age. The midshaft diameters of the black male humerus, ulna, and femur increased significantly with the onset of advanced age. These changes showed the where degenerative changes with age may occur; as stated and discussed earlier, black females showed a statistically significant *decrease* in the diameter of the humerus with the onset of age, a contrast to what was observed in their black male counterparts.

Elbow locations that increased in size included the distal epicondylar breadth of the humerus and the superior diameter of the head of the ulna. Additionally, the distal femur, being an integral component of the knee joint, increased in size when young were compared to their older counterparts. Black males became larger with age at these specific skeletal sites, and because sexual dimorphism in males may be categorized by size, the increase can be considered a trend towards more marked sexual dimorphism. These articular joint measurements increased to where they did not overlap any of the female measurements (of both populations) with the onset of age.

Based on the size increase of black males throughout the incremental age groups (and their distinct separation from black females with regard to size), sexual dimorphism can be said to "metrically" increase in this population with the onset of age. In addition to this, the metrics of black males tended to increase later in life, much later than the age category where epiphyseal closure occurs. This indicated that males continue to grow and show metric increases later in life, which subsequently separates them farther from black females with the onset of age.

White males increased in size significantly at three locations (Table 4.11). Interestingly, these three sites paralleled the results documented with the black male population; articular joint surfaces of the elbow and knee were exhibiting degenerative changes in which metric values were shown to increase. These

skeletal sites increased in size with the onset of age, and did not become more diminutive. This would indicate that white males (as with black males) are becoming "metrically" more sexually dimorphic based on their size attributes. White males are by far the biggest sample, size-wise, in the study population, and their increase in dimensions with the onset of advanced age only secures their position more definitively as the most robust sample in this study.

Also seen in the white male sample (and illustrated in part by Figures 4.2-4.19) most of the changes in size in young males could be seen shortly after epiphyseal closure, i.e. in the 2nd and 3rd decades of life. This meant that even though the epiphyses are closed, some form of "growth" or bone gain is taking place. This interesting result indicated that this population undergoes a type of increase in robusticity after the onset of puberty, which in some ways contrasts the notion that puberty provides the majority of bone growth and gain in the developing male skeleton, and after puberty metric gain appears nonexistent and size maintains a certain stasis (Bonjour *et al.* 1991; Sun *et al.* 2004; Tanner 1994). White males appear to not adhere to this pattern, and in fact show most of their size increase in robusticity after the fusion of most epiphyseal ends. Walker (1995) illustrated the residual feminine characteristics of male skeletons after maturation, and in part those results correspond to these measurement increases into the 3rd decade of life in white males.

Are the mechanisms for changes with age in male skeletons different than those for metric changes in females? Most often in past research including males and females, the net increase in size regarding midshaft diameters is correlated to thinning cortical bone and an increase in medullary cavity diameter in the aged, and not necessarily an increase in the thickness of cortical bone (Martin and Atkinson 1977; Leiel *et al.* 1988; Heaney *et al.* 1989). This increase in medullary cavity space might possibly be a mechanism for size increase in the both the black and white male population of this study. In addition, as stated above, net bone gain in males was

observed to increase fairly late in life, where they reached their final robusticity. This could not be due to degeneration. Males appear to become even more robust after the epiphyses have fused, thus implying some appositional "growth" in adult males. The cause of this is unknown, but the influence of testosterone in males may be a factor based hormonal influences already seen on hard tissue. Research from Jee *et al.* (1970) and Young and Heath (2000) emphasize the role hormones may have on the long term development and possible degenerative changes found in human bone. As seen in this current research, hormones may very well play a role in male skeletal modification.

Bones of the elbow joint in both black and white South Africans increased metrically with age. The epicondylar breadth of the humerus, being the main junction and stabilizing bone for the proximal ulna and radius, exhibits numerous muscle, ligament, and cartilage attachment sites along its borders (Amis *et al.* 1989; Fuss 1991; Grabiner 1989). These sites may become compromised due to the loss of cartilage normally covering the central areas of bone ends, and may compensate for this loss by net bone gain in the form of calcified cartilage or bone remodelling into additional bone or "osteophytes" as documented by Aufderheide and Rodriguez-Martin (1998).

Bones of the knee joint in the male skeleton exhibited increased metric dimensions in both black and white South African males. The knee joint is an extremely robust weight-bearing joint in humans, and past research has shown marked sexual dimorphism and changes with age in this location. Iscan and Steyn (1997) confirmed the sexually dimorphic nature of the knee joint (with research aimed at the femur and tibia of South African whites). Sakaue (2004), although studying a Japanese population, noted that elbow and knee joint measurements increased with age in females, "narrowing the gap" between male and female metric analysis. This result was in direct correlation to the metric increase in elbow and knee joint measurements with age found in three out of four populations studied here (black

males, white males, and white females). Finally, Ruff (1982) showed an increase in dimensions where bending and torsional rigidity are at their greatest in males and females, namely the knee joint. Ruff's findings are mirrored here, as metric dimensions also increased in the distal femur and proximal tibia. An increase in size with the onset of age may also signify signs of degenerative changes and progressive pathological conditions characterized by the loss of joint cartilage and the production of bony lesions for strength compensation. Both Compston *et al.* (2007) and Chavassieux *et al.* (2007) document remodeling patterns that increase size; this type of remodeling pattern may very well be present when observing the results from this current research as well.

Because white males, black males, and even white females show statistically significant metric increases in at least one of the three bones that comprise the knee joint, this area can be considered one of considerable modification with the onset of age in its bony components. Changes in these locations may be due not only to degenerative changes, but may also be attributed to reaching maximum levels of robusticity in middle age. As the size of males increased with age, it was observed that these increases did not occur late in life, but in mid-life constituting a sort of "late maturation" after puberty in adult males.

When black males were compared to white males with regard to pelvic measurements and the calculated ischio-pubic index, the common trend was extended in that white males were seen to present larger metric values in all measurements. However, the calculated difference with the ischio-pubic index was statistically insignificant between black and white males. This result should be considered a direct correlate to male morphology as it exists in both populations (and numerous others) as seen in research by Krogman (1962), Meindl *et al.* (1985), Patriquin *et al.* (2003), Phenice (1969), Richman *et al.* (1979), Rissech and Malgosa (1997), Ubelaker (2002), Walker (2005) and Washburn (1948). Males were considered the same statistically (regardless of their ancestry) in their ischio-pubic

index, even though white males were seen to be metrically larger on a statistically significant level.

Change in black male pelvic measurements when comparing young and old was only present in the ischio-pubic index. This indicated that a modification of the two measurements used to calculate the index, although not statistically significant in isolation, when combined altered the index to the point of increasing it with significance (82.1 in young black males to 83.3 in old black males). The length of the pubis was observed to increase with the onset of age. This increase in the ischio-pubic index brought the value closer to that of black females when viewing the incremental increase through the various age categories (Figure 4.30). However, old black males and their ischio-pubic index did not come close to converging with the female mean at any point. There appeared to be little possibility of metrically misclassifying black male pelves based on the ischio-pubic index.

Black male pelvic measurements, however, continued to be smaller than any of the white female pelvic measurements throughout the onset of age. This fact may still be considered a challenge where pelvic remains are incomplete and fragmented, because the determination of sex from metric analysis relies largely on the size of the bony element to correctly categorize the specimen as male or female. There is always the danger of misclassifying sex directly based on measurements of black males if these measurements were used in isolation and morphology was not considered. However, anthropologists tend to use a suite of techniques to come to an ultimate determination of sex, and the presence of additional remains and their subsequent morphology could provide insight into an ultimate establishment of sex.

Comparison of young and old white males in the metric values of the pelvis yielded two statistically significant differences. Pubis length and the ischio-pubic index both decreased significantly with the onset of age. The decrease in the pubis length could alter the visual characteristics of the pelvis. A shortening of the pubis would indicate a modification towards male morphology, based on the fact that

visually the male pubis is short, compact, stout and compressed. If the white male pubis became shorter with the onset of age, this would indicate that male pelves in this population exhibit more male morphology as they advance in age. To this end, the white male pelvis may very well become more sexually dimorphic in its metric values.

Length of the pubis increased in black males, and decreased in white males. Studies in pelvic morphology largely focus on sexual dimorphism in general, as with Bass (1995), Camacho *et al.* (1993), Steele and Bramblett (1988), and White (2000). Walker (2005) does illustrate the greater tendency for male pelves to shift in a masculine direction with increased age, resulting in greater sexual dimorphism with that particular study sample. However, the lengthening or shortening of the male pubis with age has not been extensively studied; Walker focused primarily on the greater sciatic notch. Reasons for the increased length of the black male pubis may include the ossification of pubic symphyseal cartilage with the onset of age. In addition, reasons for the decreased length of the white male pubis may include degenerative bone loss with age or the erosion of the pubic symphyseal borders that created length in a younger pubic bone.

7.3

Non-metric Analysis

In this study, traits from the distal and posterior humerus and the pelvis were used to determine sex; a comparison was then performed between young and old groups by population to determine if classification accuracies decreased with the onset of age. This analysis showed that different population groups had varying degrees of accuracy with each suite of traits. However, similarities in morphology between populations were noted as well.

Morphology of the elbow joint is known to be sexually dimorphic by observing the carrying angle of the articulated humerus and ulna (Amis 1989; Grabiner 1989; Fuss 1991; Wanek 2002). The lateral deviation of the human forearm from the axis of the humerus is distinctive between males and females, and each sex forms deviating angles that can be construed as sexually dimorphic (10 to 15 degrees in males, 20 to 25 degrees in females, Rogers 1999). The soft tissue anatomy of the ulnar collateral ligament (which originates on the medial epicondyle and inserts on the medial aspect of the coronoid process of the ulna) as well as the skeletal structure of the trochlear spool changes this carrying angle during elbow flexion. Grabiner (1989) also showed that the elbow and radioulnar joints are sexually dimorphic. Hard tissue morphology relating to the ulnar collateral ligament and the trochlear spool should therefore exhibit differences between males and females which have been shown in this research. The medial epicondyle is obviously the origin of ligaments that preserve the carrying angle; the olecranon fossa shape is the receptacle for the olecranon process superiorly, and is connected to the coronoid process inferiorly; and trochlear extension is an expansion of the trochlear spool and the articulation between the trochlea and the coronoid process. Anatomical soft tissue characteristics should influence the hard tissue sexual dimorphism of the bone at that location as well, and in fact have been documented as sexually dimorphic on a statistically significant level (Rogers 1999; Wanek 2002).

Examination of features from the distal and posterior humerus resulted in reasonably accurate classification rates with both males and females when utilizing a suite of three visual traits (trochlear extension, olecranon fossa shape, and the angle of the medial epicondyle). A fourth characteristic (medial epicondylar symmetry) was determined to be highly inaccurate, and was abandoned due to the increase in classification accuracy when it was excluded from the analysis. Each of these three characteristics in isolation were not particularly accurate in predicting sex on their own. However, when used in conjunction with each other as an amalgamated

recognition of sex, all males were classified with a 74% accuracy rate, while all females were classified accurately 77% of the time. This was accurate enough to deem these characteristics sexually dimorphic and moderately successful in predicting sex. These traits were also observed to be sexually dimorphic when utilizing geometric morphometrics, which confirmed the validity and efficacy of these traits by quantifying the form and shape of each characteristic.

Classic non-metric techniques based on the pelvic morphology of males and females has been used extensively to predict sex (Bass 1995; Krogman 1962; Steele and Bramblett 1988; White 200). Four characteristics of the pelvis were utilized to determine sex, then young and old determinations were compared to observe any changes in classification accuracy. Visual pelvic morphology remained unchanged in females with the onset of age, and exhibited differences with age in both the black and white South African males. These differences are discussed below.

7.3.1

Non-metric changes in females with the onset of age

Classification accuracy differed when comparing black to white females. When estimating sex from the distal humerus, black females performed better or exhibited more "female" morphological traits than did their white counterparts. Sex was estimated correctly in 84% of all black females, and 68% in all white females (Figure 5.7). This discrepancy in accuracy rates indicated that not only did black females exhibit "classic" female morphology of the distal and posterior humerus (as defined by Rogers 1999 and Wanek 2002) but exhibited a minimal amount of overlap into the male realm of morphological traits (black females were misclassified as males 11% of the time). In contrast, white females were misclassified as males 26% of the time. This is a significant amount of overlap into male morphology, and indicated that sexual dimorphism in this bony element is less apparent in white than black South Africans. If increased sexual dimorphism is based, in part, by

socioeconomic variables and nutritional factors, this suite of traits from the bony element of the elbow does not appear to be influenced by it. White females may simply exhibit less sexual dimorphism than their black female counterparts, or they may just appear more robust in their morphology than black females. Additionally, because of the abundance of old white females in the sample, the possibility that many were misclassified or ambiguous due to increased robusticity with age at the distal humerus site was apparent. White females would probably continue to look more female when compared to white males, but in isolation may cause confusion with their robusticity.

Black females and their classification accuracy in the determination of sex from the distal humerus decreased from 88% in young to 78% in old. This was not a significant drop in accuracy according to Pearson's chi square analysis, and simply indicated that there was a small amount of variation between young and old individuals of this population group. Black females continued to exhibit female morphology through the onset of advanced age, and results indicated that morphology was static with black females in this location.

This maintenance of sexual dimorphism in the humerus of black females may be due to several factors. As discussed previously, bone density indices are larger for black females as seen in past studies (Katzmarzyk and Leonard 1998; Kieser *et al.* 1987; Orwoll *et al.* 1996; Trotter *et al.* 1960). Degenerative processes that effect bone when it becomes structurally unsound may not necessarily affect black females, based on the higher bone density they exhibit.

It is important to note that virtually no metric changes occurred with the black female skeleton as well. Black females stayed approximately the same size throughout the onset of advanced age. These metric results correspond quite accurately with the non-metric results of the visual techniques employed in this study. Because no physiological changes appeared to be occurring (such as bone gain through osteoporosis or microfracture healing), no visual changes were observed.

Similar changes in classification accuracy were seen in the white female sample when comparing the young and old samples. The percentage of white females correctly classified by distal humeral traits decreased significantly from 93% to 63% with the onset of age, which indicated a marked decrease in the classification accuracy of the suite of characteristics. Thus, there is an apparent change of morphology between young and old white female specimens.

Specifically, two features exhibited marked, statistically significant changes in visual morphology which would either increase or decrease the predictive value of the trait. The olecranon fossa shape appeared to change visually with age, as young white females were classified with 79% accuracy and old white females with 38%. Results such as these indicated that a distinct change in the shape of this bony fossa was influencing the ability for to correctly determine sex using this trait. An oval shape is indicative of female morphology, with no upward projection of the fossa towards the shaft of the humerus to modify the shape into roughly triangular. The misclassification of 38% of old white females as males, in addition to the poor classification accuracy of 38% for this older group, gave two-fold evidence that old white females were exhibiting more triangular-shaped olecranon fossae than their young counterparts, and more than their black female counterparts as well.

The angle of the medial epicondyle increased in its predictive value as age increased in the white female sample. This change was in direct contrast to the modification of the olecranon fossa shape; classification accuracy in white females increased with age when viewing the medial epicondylar angle, from 36% (young white females) to 56% (old white females). An equal percentage of young and old white females were misclassified as males (43% in both groups). However, ambiguous cases in young white females were much greater (21%) than in old white females. This result indicated that old white females exhibited an array of distinct morphology that did not necessarily allow them to be correctly classified, but did allow for less ambiguous determinations. Although the sample size was small,

young white females did not appear to exhibit clear, definable female morphology *regarding the angle of the medial epicondyle* as their older counterparts, or as much as their black equivalents. A larger sample size of young white females may have allowed for different results.

The ultimate result of "estimated sex" was similar in both black and white females. Changes in non-metric morphology were occurring that decreased the classification accuracy of the sex determination in all females with the onset of age. Thus, young females were classified more accurately than older females when utilizing characteristics from the distal humerus. In general, therefore, the results of the black and white females were congruent, as accuracies of both decreased (although not significantly) with age.

Why morphology changes when viewing young and old white females may be, in part, a mechanism of the aging process. A decrease in elasticity of the joint's connective tissue structures may perhaps cause morphological modification to compensate for decreased range of motion, as documented in Aufderheide and Rodriguez-Martin (1998) as pathological conditions. In addition, bone density loss over time and with age (especially in white females) may cause the olecranon fossa to take on an alternate appearance, perhaps in an effort to combat simultaneous breakdown or osteophytosis of the olecranon process of the ulna, its main partner in the humero-ulnar junction (Grabiner 1989).

Metric increases of the elbow joint were seen on a statistically significant level in white females with the onset of age. These metric increases could very well be the result of early osteophytosis and its subsequent degenerative bone addition to the articular joint surface of the distal humerus. As osteoporotic bone gain increased, it was quite possible that non-metric visual characteristics within this bony element of the forearm changed as well. Even though the sample size of young white females was quite small, the fact remains that morphology with all traits combined was unambiguous in this sample group, estimating sex accurately 93% of the time. The

well-visualized female morphology in young white specimens declined dramatically with the onset of age within the population group. This can again be attributed directly to the degenerative processes with the onset of age, the decline of bone mineral density, and the propensity to incur microfractures at skeletal location most susceptible to stress, strain, and tensile strength reduction.

It may also be possible that the white population in this sample were considerably older than the black population, and that old age with degenerative changes masked the sexually dimorphic traits. Classification accuracy from the distal humerus decreased slightly in the black female sample with age, and the sample size was adequate. White females may perform better in these non-metric characteristics if the sample size of younger individuals was greater.

Classic non-metric morphology characteristics from the os coxae (the subpubic concavity, subpubic angle, ischio-pubic ramus width and the width of the greater sciatic notch) produced a 94% accuracy rate in the female sample, regardless of biological affiliation and the onset of age. Females provided a higher rate of classification accuracy than did males (83% accuracy) when combining the traits.

Both biological groups in the female sample appeared consistent in their pelvic morphology and had similar classification accuracies (93% black females, 96% white females). The biological affiliation of the specimen was not needed in order to successfully predict skeletal sex. This result was indicative of a highly sexually dimorphic skeletal trait that is may not be influenced as strongly by external factors such as socio-economic status, occupational stressors, dietary deficiencies, weight-bearing activities or childbirth statistics. Internal factors such as bone density measurements appeared not play a significant part in the sexually dimorphic nature of the female pelvis.

Although not statistically significant, a result of interest was the fact that more black females (young and old) were misclassified as male than were deemed having

ambiguous morphology. These numbers were not large, but indicated that when variation occurred, it occurred as an explicit departure in morphology for black females to male morphology, and not just to an "ambiguous" type.

The onset of advanced age did not appear to influence the distinct and unambiguous female pelvic morphology of either black females or white females. Pelvic non-metric traits in both black females and white females were highly predictive of sex with both age groups and neither group's classification accuracies decreased with statistical significance with the onset of age. Age was thus determined to not play a role in the successful determination of skeletal sex in the female skeleton, regardless of population group.

7.3.2

Non-metric changes in males with the onset of age

Examination of the two male population groups studied showed congruence in morphology between them. Only the classification accuracy of the olecranon fossa shape was significantly different between black males and white males when determining sex from that particular feature. Specifically, the black group had a varying morphology within the framework of the olecranon fossa shape, and a large percentage of black males would be considered "female" in their shape. Black males, however, were still classified at a relatively high rate of accuracy, along with their white male counterparts. These similarities between the two populations show that the technique is not population specific. Changes with age, however, were still viewed separately to determine possible trends.

Black males exhibited a slight increase in their classification accuracy when comparing the young (50 years of age or younger, 71% accurate) to the old sample (over 50 years of age, 74% accurate). Thus, the morphology of the black male distal humerus can be thought of as static with the onset of advanced age. As described above, this result is congruent with the black female sample in which no statistically

significant change in the classification accuracy was observed with the onset of age. The onset of advanced age in the black male skeleton appeared to not affect the bone of the distal and posterior humerus, thus indicating that degenerative changes were minimal in this location.

As a reference (and as exhibited by Figure 4.35), metric increases were seen in two locations of the elbow joint of black males with the onset of advanced age, one site being the distal epicondylar breadth of the humerus. These metric changes exhibited an increase in size; in conjunction, black males exhibited an increase in classification accuracy with the non-metric/ visual technique with the onset of age. Changes in *metric size*, then, appear to be linked to visual changes that increase the presence of *male morphology*.

White males exhibited little change with the onset of age from the distal humerus, as well. High classification accuracies for both age categories were seen and the difference between the young and old groups was statistically insignificant, although declining (86% vs.75% respectively). Both males in each population group appeared to remain static in their male morphology with the onset of advanced age, and in this fact can be considered quite similar.

Trochlear extension is the inferior projection of the trochlear edge past the inferior edge of the capitulum's border, and decreased in classification accuracy with statistical significance with the white male sample. There could be several reasons for this extension to become visually less pronounced with the onset of age. Most probable would be the induction of osteoporotic lesions along the lateral edge of the distal humerus, creating a more robust profile on that side and "evening out" the extension of the trochlea on the medial side. In addition, the loss of elasticity in the soft tissue anatomy of the elbow joint with age (Aufderheide and Rodriquez-Martin 1998) may cause a loss of movement in the joint. This, in turn, could cause degeneration of the junction of the coronoid process and the trochlear-capitulum surface, creating a certain amount of constriction within the space between the

posterior capitulum and the trochlea. Visually, this may cause the inferior edge of the trochlea to appear more congruent or equal to that of the capitulum. Regardless, this visual characteristic was seen as being the only statistically significant change with the onset of age in the white male distal humerus, and did not apparently affect the ultimate estimation of sex for the specimens over 50 years of age.

For comparison, no metric increase with age occurred at the distal humerus in white males. This result may indicate that *no metric increase* would equate to no definitive modification of visual characteristics, thus *no change in sexual dimorphism*. Size and shape, then, appear to go hand-in-hand with one another. If a metric increase occurred, visual male morphology would have appeared to change. Because a metric increase did not occur in the white male distal humerus, visual male morphology did not appear to increase.

Black and white males differed in their classification accuracy when assessing overall skeletal sex (85% accurate for black males, 79% accurate for white males). The discrepancy in these percentages were deemed non-significant, but black male pelvic morphology did appear different than white male pelvic morphology when observing the distribution of classification; black males exhibited a greater amount of "classic" male sexual traits.

Visually, results indicated that variation in the greater sciatic notch width for white males may lead the observer to misclassify the sex of the pelvis based largely on this feature. In this (and with results observed from geometric morphometrics), white male greater sciatic notch widths may very well be misleading in their visual morphology, and should be considered a tentatively reliable trait. Challenges in the visual determination of sex from the greater sciatic notch in this study paralleled past research in which male morphology in this region was surprisingly variable (Patriquin *et al.* 2003; Steyn *et al.* 2004; Walker 2005). White males in this study exhibited both wide and narrow sciatic notches, and were visually ambiguous with this isolated trait on many occasions.

With the onset of age, accuracies in black males increased as age increased. The older the individuals in the sample, the more accurate the prediction rates were for black male pelvic morphology. The subpubic angle specifically increased in its "classic" male visual morphology with age. The differences that make this characteristic statistically different from the young to old group was in how many are *misclassified* as females. More young black males were misclassified as females (12%) than their older black male counterparts (7%). These results show that it may not be the presence of male morphology that allows for the correct classification, but rather the presence of female morphology that allows for the incorrect classification. The misclassification of black males as females in the subpubic angle would indicate the presence of an elongated and more rectangular pubic region in young males, which subsequently changes into a more "male" appearing short and stout pubis. Black males, then, may follow the same trajectory observed by Walker (2005), in which male pelvic sexual dimorphism increased as age increased. This may be attributed to a type of maturation process (as seen in long bone measurements for black males as well), where full robusticity in the form of dimensions (or full sexually dimorphic characteristics) are not observed until middle or advanced age.

This same observation holds true with the other isolated trait that appeared significantly different in classification accuracy between young and old black males. There was little discrepancy between the predictive values of the width of the greater sciatic notch in young and old black males (73% accurate and 74% accurate, respectively). However, the number of young black males misclassified as females was more (20%) than those of old black males misclassified as females (12%). Black males, with the onset of age, appeared to exhibit more male morphology (and less female morphology) than their younger counterparts, making them essentially more sexually dimorphic. Again, this may very well be due to the presence of lingering female morphology from early adulthood, and the development of more observable male traits in middle age.

The results of white male pelvic morphology were contrary to the results of their black male counterparts. White males were correctly classified less often with old specimens than they were with young specimens (93% accuracy for young, 74% accuracy for old), and seemed to decrease in sexual dimorphism with age. The white male pelvis continued to be a challenge with morphological features providing a large amount of variation in this study sample. Specifically, the greater sciatic notch was markedly wider and more "female-looking" in young white males (30% were deemed ambiguous in their morphology as compared to 13% in the older sample), but characteristics such as the ischio-pubic ramus width appeared decidedly thin and gracile in the older male sample. These changes in the white male pelvis (that do not appear to occur in the black male pelvis) may be due to degenerative changes brought on by decreasing bone density. Specifically, Heaney *et al.* (1982) found that the average 30-40 year old white male has reached maximum bone density. The average elderly male is in negative calcium balance, and accordingly is losing bone mass. Decreased mechanical loading (which would increase structural integrity) was not seen in this population according to Heaney *et al.*'s study; visual characteristics of the white male pelvis, which include the thickness of the ischio-pubic ramus and the stout nature of the subpubic concavity, may very well be affected by cortical and endosteal bone loss in the os coxae. This, in turn, would create a more gracile visual description of the older male specimens.

7.4

Geometric Morphometric Analysis

Geometric morphometrics provided information that directly correlated to results found in the non-metric visual portion of this study in the fact that it "quantified" what the visual traits reportedly depicted. This union between a visual technique (which could be considered a qualitative technique) and a quantitative

technique has many promising aspects, several of which were apparent in this research. To be able to "test" a visual technique with a very robust secondary quantitative technique had several advantages and disadvantages.

Because aspects of the distal humerus have not been used extensively as sexually dimorphic features, geometric morphometrics provided definitive proof that there were, indeed, sexually dimorphic attributes of this skeletal feature that could be used with a fairly high degree of accuracy to determine sex. Visual techniques had already provided accurate determinations of sex from the features the distal humerus exhibited; geometric morphometrics provided additional verification that features researched in the past (Rogers 1999; Wanek 2002) were indeed accurate and reproducible. Two characteristics, namely the shape of the olecranon fossa and the angle of the medial epicondyle, were assessed with this method. An extensive discussion of the morphology related to both aspects follows, in order to illuminate the strong correlation between the distal humerus and its sexually dimorphic features.

Analysis of the pelvis and features relating to the sexual dimorphic nature of this pair of bones could be quantified in a way done only recently. This study employed four features of the pelvis, and quantified these existing highly accurate features and determined whether they changed with the onset of age. In addition, past geometric morphometrics research on the greater sciatic notch by Steyn *et al.* (2004) confirmed that this pelvic feature was sexually dimorphic, but also determined distinct differences in the white South African male population that appealed for more study. This current research confirmed the variable nature of the greater sciatic notch in the white South African male population.

7.4.1

Sexual dimorphism of the EPI perspective

In general, the EPI view (which depicted the angle of the medial epicondyle of the distal humerus) provided a unique and quantifiable way in which to accurately designate sex. The sexual dimorphism of the element was illuminated with the relative warp analysis first of the EPI perspective (Figure 6.1). This showed that males and females were divergent by grouping all females below the x-axis, while all males grouped above the x-axis. White males and females were seen at quite a distance from each other in this perspective, while black males and females were seen to be closer to each other within the grid than their white counterparts. This may indicate the fact that the black South African population is less sexually dimorphic in this feature. Statistical analysis confirmed this fact. However, males were always seen quite separate from their female equivalents and exhibited features of the medial epicondylar angle that were observed in visual assessment.

The medial epicondyle itself exhibited the most discrepancy between males and females, which was expected. First, when the medial epicondyle sits more centrally within the profile of the trochlea, there was more trochlear surface area surrounding the medial epicondyle. This, in turn, positioned the entire medial epicondyle further into an anterior position, thus closer to the tabletop on which the bone actually rested. This was the pattern most commonly seen in males. The amount of trochlear area between the posterior and anterior portion of the medial epicondyle allowed the male trochlea to project directly outward, parallel to the tabletop. With the lack of posterior surface area in the female trochlea surrounding the medial epicondyle, there was more possibility to angle away from the tabletop based on less physical bone for ligament and tendon insertion. The female medial epicondyle, in turn, appeared more elevated along the surface of the bone and provided for a large amount of deviation between the male and female form. These

skeletal features most probably correspond to soft tissue features that act upon the distal humerus, and these medial epicondylar angle differences were thought to be directly related to 1) the carrying angle of the arm, 2) where the ulnar collateral ligament actually originates on the female medial epicondyle as opposed to the male epicondyle, and 3) how this difference in tension, torsion, extension and flexion would affect the hard tissue anatomy of the elbow joint. This joint has been proven to be sexually dimorphic (Grabiner 1989) and thus the variation between males and females in this particular element can also be seen in hard tissue morphology.

Males and females were classified on a fairly accurate level with geometric morphometrics, and morphometrics could categorize males and females from each other more accurately than visual techniques. This skeletal feature was deemed sexually dimorphic, and geometric morphometrics increased the classification accuracy by observing differences in form that the human eye could not necessarily discern.

Male-female differences in black South Africans were different in the points assigned to the lateral margin of the distal humerus. These landmarks deviated downwards in the black male humerus, and surprisingly, the angle of the medial epicondyle appeared largely unchanged based on the vector mode arrows depicting shape variation between females and males (Figure 6.6). When viewing the relative warp analysis in Figure 6.1, black males and black females were quite close on the graph depicting the distance between shape configurations. This indicated a sexually dimorphic component between black females and males, although the distance between the two was not substantial.

White females and males were markedly sexually dimorphic in the EPI perspective, as seen in the relative warp analysis grid comparing all four population groups (Figure 6.1). The distance between the two groups proved that a distinct morphological difference existed between the two, and this was confirmed by viewing the vector mode thin plate spline that differentiated between female and male form

from the EPI perspective (Figure 6.8). The raised nature of the female medial epicondyle can be clearly delineated as the originating point in the vector mode thin plate spline, as shown in Figure 6.8. This positioned the female medial epicondyle in a more prominently angled perspective, much different than the male perspective which exhibited a flat and parallel profile. These characteristics were "classic" in the fact that they aligned clearly with the defined morphology attributes. The more posteriorly-placed landmarks assigned to features on the lateral surface of the distal humerus appeared in the same location as those seen in black males vs. black females, which indicated a common morphology throughout populations between both males and females, with the white South African population exhibiting a more marked degree of differentiation between the sexes.

The only discrepancy in this result was the apparent common morphology between young white females and males with the EPI perspective. Young white males and females did not produce statistical results when young females were compared to young males, indicating that they were virtually the same in form and shape. The CVA analysis was unable to divide specimens successfully into two distinct morphological groups, which implied that young white South Africans exhibited the same medial epicondylar angle and distal humeral attributes between males and females. These results may be due, in part, to the low sample number of young white female group. If the sample was larger, perhaps different results would have been observed. In addition, white male morphology may not exhibit marked sexual dimorphism in this location until later in life, as documented by research on gracile male specimens by Coleman (1969) and Walker (2005), who both noted lingering juvenile characteristics in the male pelvis, and Walker (1995), who documented gracile male crania in an adult sample from a historical collection.

Quantification of the sexually dimorphic features in the EPI perspective was, by in large, successful with geometric morphometrics, and correctly classified males and females at a high rate of accuracy. These morphometric results directly

correspond to those results found in Rogers (1999) and illuminate a different perspective when taking the hard tissue attributes of the radioulnar joint into account with sexual dimorphism, as outlined by Grabiner (1989). Steyn and Iscan (1999) concluded that the osteometrics of the humerus were sexually dimorphic; geometric morphometrics can now play a role in providing more information regarding the sexually dimorphic aspects of the distal end of this bone.

7.4.2

The EPI perspective: changes in females with the onset of age

The shape of the EPI perspective appeared almost the same with young black females as it did with old black females. This corresponds directly with both the metric analysis of black females as well as the non-metric visual analysis of black females with the onset of age.

Measurements of the distal humerus did not change on a statistically significant level (Table 4.6). This indicated the size component of black females remained static, even as this population group got older. In addition, the classification accuracy of the non-metric visual traits between young black females and old black females did not change on a statistically significant level (Tab le 5.10). Geometric morphometrics showed the lack of anatomical differences in the specific feature of the medial epicondyle and its angulation between young black females black females with advanced age. This feature was sexually dimorphic, was accurate in distinguishing black females from black males, and did not modify its shape in females with the onset of age.

These results indicated that the higher bone density in the South African black female skeleton found in studies by Micklesfield *et al.* (2003) Kolbe-Alexander *et al.* (2004) and Taitz (1998) very well "shielded" skeletal anatomy from degenerative changes, microfractures, and other possibly detrimental modification that may manifest themselves in the skeleton.

Determination of whether white females exhibited morphology change with the onset of age was depicted in the vector thin plate spline mode of Figure 6.12. Results showed a change in the location of virtually all landmarks assigned to the medial epicondyle (Landmarks 5-14), with the changes tilting the medial epicondyle into a more angled position. When evaluating the differences in change depicted in Figure 6.12, it was clear that morphological changes with age were occurring in the white female population. Landmarks in the white female EPI perspective were observed to migrate into different positions and forms, which apparently increased the degree of sexual dimorphism exhibited in this group. In addition, young white females could not be successfully separated from young white males in the EPI perspective, which indicated a lack of sexual dimorphism between males and females of the young white population. Old white females in the EPI perspective, however, were categorized successfully, which indicated a distinct change in morphology between the young population and the old population.

This morphometric result was in direct correlation to the non-metric visual results that were obtained when attempting to designate sex from the angle of the medial epicondyle and paralleled the visual classification accuracies. Young white females were highly variable in this feature, and the angle of the medial epicondyle only predicted sex in young white females a dismal 36% of the time. In contrast, old white females were correctly classified at a higher rate of accuracy, at 56% (Table 5.11). This indicated that as the white female population aged, the angle of the medial epicondyle began to exhibit the more "classic" form of female morphology as defined in this study.

White females were indeed changing in size at the distal humerus, as well as in shape and form as indicated from visual analysis and geometric morphometrics. The angle of the medial epicondyle moving from variable morphology in young white females to definitively angled in old white females may be caused by bone density loss (Aloia *et al.* 1985; Aspray *et al.* 1996; Cummings *et al.* 1990; Cummings and

Black 1995; Schnitzler and Mesquita 1998) or the effect of soft tissue degradation in the joint, with subsequent addition or loss of bone around the medial epicondyle for structural integrity (France 1998; Garn 1972; Seeman 2003). Regardless, a relationship between a *size change in the element* with the onset of age and the *morphology of the element* with the onset of age was seen.

7.4.3

The EPI perspective: changes in males with the onset of age

Black males were also compared in both age groups to observe discrepancies in shape with the onset of age. Young black males exhibited a distinctly different morphology mainly within the points assigned to the lateral surface of the humeral element, as well as aspects of anterior features of the bone (which are seen as landmarks 15, 16, 17 and 18, Figure 6.11). The way these landmarks migrate to a more posterior position in older black males may indicate a morphology change that may be correlated with increased torsion on the existing ligaments (Fuss 1991), degenerative changes at the lateral aspect of the distal humerus, or compensatory factors related with age as documented by Aufderheide and Rodriguez-Martin, 1998 (i.e., motion change with osteoarthritis).

However, the onset of age in the black male South African sample did not change the degree of accuracy obtained when assigning sex to specimens via canonical variates analysis. In fact, the older black individuals were placed correctly in their "male" or "female" category with more accuracy than their younger counterparts. The degree of classification accuracy increase in black males with the onset of age indicated that perhaps the sexually dimorphic traits that were visibly apparent were also becoming quantifiably more apparent.

In direct correlation with morphometric results are the results from the non-metric visual technique performed when observing sexually dimorphic features of the distal humerus. In general, classification accuracy increased with the onset of age in

the black male skeleton, very similarly to the geometric morphometric results. Even more comparable were the accuracy rates of the specific visual assessment of the angle of the medial epicondyle in comparison to the EPI view, which quantifies exactly that- the angle of the medial epicondyle. Just as the EPI perspective and its classification accuracy increased with the onset of age in black males, the classification accuracy for the visual trait in isolation increased with the onset of age. Geometric morphometrics quantified the visual characteristics of the angle of the medial epicondyle.

Finally, metric values for black males increased significantly with age at the site of the distal humerus (Figure 4.35). In black South African males, then, changes were occurring that not only increased the size of the element being studied, but morphology was modified to the point in which it became more sexually dimorphic, meaning more in congruence to "classic" male morphology as defined in this study. As stated before, an increase in *size* at a given element or feature appears to influence the *amount of sexual dimorphism* exhibited.

Shape change between young and old white males did not appear to be extensive as seen in the small amount of landmark movement depicted in Figure 6.13. Males appeared to stay the same in geometric morphometric analysis, as they did in both metric analysis and non-metric visual analysis. The distal epicondylar breadth measurement of white males did not increase nor decrease on a statistically significant level with the onset of age (Table 4.11). In addition, the difference in classification accuracy when observing the medial epicondylar angle in isolation as a visual trait was non-significant between young white males and old white. The absence of a size change in metric values equated to stasis in the classification accuracy and quantifiable morphology of the white male distal humerus.

The limitation to geometric morphometric analysis in this particular analysis was the perception of distance shown in the relative warp graph for the EPI perspective (Figure 6.9). Although statistical analysis proved that young white

females and males exhibited similar morphology (by being unsuccessful in dividing males from females in the young white population), the relative warp analysis, by viewing the graph, indicated a much larger distance in form between these two groups. In addition, old white males and females were successfully separated when subjected to CV analysis; however, these two groups and their consensus form appeared quite close on the relative warp analysis graph. This may very well be an unfortunate artefact of the sample size of the young white population.

7.4.4

Sexual dimorphism of the OL perspective

The olecranon fossa shape and trochlear extension was considered accurate predictors of sex when non-metric visual analysis was performed on each in isolation (Table 5.6). Analysis of the OL perspective, specifically the relative warp analysis of each population group divided by sex ("black female", "black male", "white female", "white male") indicated a distinct separation of males and females which signified that the male and female forms of these traits were in fact sexually dimorphic. This is important to note, based on the fact that features of the distal humerus have not been consistently utilized for sex determination. The olecranon fossa shape appears to be an accurate predictor of sex based on geometric morphometric analysis. Both features exhibited differences between males and females.

The most important feature to observe when viewing the olecranon fossa shape is the upward projection of the fossa towards the shaft, producing a superior "point" at the apex of the fossa. This made the fossa appear more triangular, which was considered a classic male trait. As seen in Figure 6.17 this point is located far more superiorly in males (the arrow of landmark 5) than in females (the point). In addition, trochlear extension clarifies male from female morphology by positioning the inferior margin of the trochlea farther downward (inferiorly) to that of females, which would form the visual equivalent of "extension" in this region.

Sexual dimorphism was evident in the OL perspective. Again, the morphology of the olecranon fossa and the trochlea most probably correspond to soft tissue features that act upon the distal humerus. These include the junction of the humerus to the ulna, which forms an articular surface between the two as described by Fuss (1991). Grabiner (1989) also documented the articulation between the distal humerus and the ulna within the olecranon fossa, and saw differences between males and females in the carrying angle of the arm at this location. Thus the variation between males and females in this particular element can also be seen in hard tissue morphology.

7.4.5

The OL perspective: changes in females with the onset of age

Young and old black South African females were observed to be close in morphology based on the relative warp consensus for the OL perspective (Figure 6.22). This indicated that morphology did not change drastically between the young and old samples of this population. In fact, black female South Africans were classified accurately in both young and old categories, confirming the clustering of both groups with the relative warp analysis. The majority of morphological changes with age occurred along the periphery of the feature, and not with the olecranon fossa shape itself or with the extension of the trochlea. The extension of the trochlea did appear to migrate superiorly in the older black female sample, which would indicate a less extended trochlea and a more equal margin with the edge of the capitulum. This change would theoretically make the OL feature more sexually dimorphic in this location than their younger counterparts. Although slight, the classification accuracy for young black females was better than that of their older counterparts.

Non-metric analysis of the distal humerus (specifically the olecranon fossa and trochlear extension) corresponded with the results found here in geometric

morphometrics in that the classification accuracy of both methods decreased non-significantly with the onset of age. However, both analyses appeared to show morphology change in the black female that, over time, made sex determination from this element slightly more difficult. The decrease in both the geometric morphometric accuracy and the non-metric accuracy may be attributed to a change in morphology due to compensatory actions or some sort of other physiological change. Regardless, geometric morphometrics confirmed that the black female olecranon fossa shape and trochlear extension stayed relatively static through time in its morphology.

Based again on the relative warp analysis (Figure 6.22), the fact that young and old consensus groups for white females clustered together in the same quadrant indicated that this feature changed little with age. This result was confirmed with the additional information from Figure 6.25, which indicated virtually no morphology change between young and old white females from the OL perspective. In fact, young whit females and old white females were categorized with an extremely high rate of accuracy, indicating that olecranon fossa morphology was easily quantified and again, quite sexually dimorphic regardless of the age of the white female specimen. Obviously, degenerative changes in the distal humerus of the white female did not affect the classification accuracy of geometric morphometrics.

When compared to the results from the non-metric visual analysis performed on the same features that comprise the OL perspective (olecranon fossa shape, trochlear extension), geometric morphometrics performed better than the non-metric visual analysis. Accuracy decreased from the young sample to the old in the visual technique, but geometric morphometrics correctly categorized both young and old white female specimens. Regardless, the sexually dimorphic features of an oval olecranon fossa shape and the lack of extension through the trochlea were seen to persist in the white female skeleton with the onset of age.

7.4.6

The OL perspective: changes in males with the onset of age

Black South African males (young and old) clustered closely together when viewing the consensus relative warp analysis for the OL perspective (Figure 6.22). The subsequent thin-plate spline graph (Figure 6.24) showed little difference between the morphological features of young black males and old black males, and in fact both were classified with a high rate of accuracy. The morphology of the male olecranon fossa and the extension of the trochlea in black South Africans was different than that of females, and continued to be different from females with the onset of age. Classic morphology defined in this study was maintained with the onset of age, and this feature provided a robust and discernable method of determining sex when utilizing geometric morphometrics.

Comparison of geometric morphometrics and the non-metric visual analysis of the same features in young and old black males (olecranon fossa shape, trochlear extension) showed similar results in that young and old black males were ultimately categorized correctly with a certain level of accuracy with the OL perspective. Non-metric techniques did show an increase in ambiguity of the olecranon fossa shape with the onset of age in black males (see Table 5.13). This would indicate a change of shape from distinctly triangular (a male characteristic) to a form that does not appear so triangular. Geometric morphometrics, however, does not show such a modification when viewing the comparison between the young and old black male forms in the OL perspective in vector mode (Figure 6.24). Geometric morphometrics confirmed the idea that many factors may play a role in the modification of bone throughout time, but a lack of morphology change found in geometric morphometrics may not correspond directly with the visual techniques employed for sex determination. Human error in the visual non-metric technique of observing olecranon fossa shape could have very well played a role in the significant

classification accuracy change with this trait, but geometric morphometric analysis continued to categorize both young and old black male specimens accurately with the OL perspective.

The same can be said for white male specimens with the OL perspective in that geometric morphometrics "quantified" what was seen visually with non-metric techniques, and performed better in the correct assignment of sex. Once again, the consensus shapes from the OL perspective for young and old white males were viewed near each other in the relative warp analysis graph, and again the corresponding thin-plate spline (Figure 6.26) showed no apparent morphological change between the young and the old white male samples. This lack of quantifiable physical changes in the olecranon fossa shape and trochlear extension allowed for the accurate classification of both young and old white males (92% and 90%, respectively), indicating that morphology in the OL perspective is static with the onset of age in white males.

Comparison of geometric morphometrics to non-metric visual techniques showed that the olecranon fossa shape was easily visualized as male in both young and old specimens and categorized with the same level of accuracy in young and old white males. Visualization of trochlear extension did not appear as distinctly with older white males as it did with younger ones, however. Trochlear extension with the non-metric technique misclassified old males as female (or deemed the trait ambiguous) more often than in young white males. This again illustrates the fact the geometric morphometrics may "visualize" the congruency of a trait more effectively than when employing the non-metric visual technique of sex determination. Morphometrics performed well in that it did not "observe" potential degenerative changes that may have influenced the correct categorization of old white male specimens.

All visual characteristics performed relatively well in the assignment of sex, while geometric morphometrics increased the classification accuracy on several

occasions of both young and old samples in the OL perspective. This indicated that what was observed in the anatomy of the distal humerus by physical characteristics was substantiated with the quantification method of landmark assignment and statistical testing in morphometrics. Again, this perspective did not appear to change with the onset of age, and thus can be considered a good representation of sexual dimorphism in the distal humerus for all young and old black and white South African males.

7.4.7

Sexual dimorphism of the SUB perspective

The SUB perspective quantified characteristics of the subpubic concavity and the subpubic angle (as well as the obturator foramen) through landmark data analysis. This perspective provided information that complemented the non-metric visual traits of the same characteristics used in this study which have been documented extensively in the past (Bass 1995; Bruzek and Soustal 1984; Humphrey 1998; Krogman 1962; Moerman 1982; Patriquin *et al.* 2003; Steele and Bramblett 1988). Geometric morphometrics confirmed that when utilized together, the subpubic concavity and subpubic angle were highly accurate in determining the sex of the human pelvic bone. Sexual dimorphism was marked and apparent, as shown in Figure 6.27 where males and females cluster separately from each other, and appear to span a large distance on the consensus relative warp graph. Dramatic differences in male and female pelvic morphology could also be seen in Figure 6.30, which demonstrates the magnitude and direction of change from male pelvic morphology to female morphology. Males were observed to have shorter and stouter pubic regions and thicker ischial surfaces than their female counterparts. Females had a more elongated pubis, thinner superior pubic profiles, and thinner inferior ischial profiles. This indicated that in general, this portion of the pelvis remained a

highly sexually dimorphic skeletal element in which sex determination was quantifiably apparent.

Black males and females specifically were also observed to be highly sexually dimorphic in their pelvic characteristics. Black females exhibited a thinner pubis and more elongated superior ischial region, which corresponds directly to the subpubic angle and subpubic cavity visual traits observed (Figure 6.32). White males and females exhibited a different and more subtle variation in traits when utilizing the SUB perspective for geometric morphometrics, with white females and males exhibiting much the same thickness in the pubic region, while the male ischial region appeared slightly more broad and robust. In addition, the male pubic symphyseal region was shorter and more truncated, possibly decreasing the visual aspect of the subpubic concavity (Figure 6.34).

However, when divided into age groups, geometric morphometrics had a difficult time discerning young white males from young white females. Statistically, the difference in morphology between young white males and females is not significant (Table 6.23) and in fact a CVA could not discern a difference between the two; statistics were not generated when this analysis was performed, indicating that morphology between the two were so close no meaningful statistics could be generated (Table 6.24). These results indicated variability in morphology of the young white male pelvis as seen in a previous study by Steyn *et al.* (2004). Male os coxae appeared to exhibit morphology that could be either considered distinctly male, variable, or female.

7.4.8

The SUB perspective: changes in females with the onset of age

In Figure 6.35, young females (of both populations) clustered together, while old females did the same above the x-axis of the graph. Thus, females separated out on the relative warp consensus graph into distinct age clusters, and not

necessarily by population. Old black females were the closest to the young contingency, which indicated that the morphology of this group of black females continued to maintain the skeletal structure of classic "young" morphology, while old white females deviated from this morphology by appearing farther apart on the graph. However, black females showed a progression with age that looked quite similar to the progression seen in the sexual dimorphism between females and males when viewing thin-plate spline data (Figure 6.36). The landmarks on the old black female pubis appeared to migrate laterally and superiorly, making this region appear thicker and broader (as in male morphology). In addition, landmarks placed on the ischium appeared to migrate inferiorly, allowing a thicker ischial region in the old black female pelvis to be present.

Despite this apparent trend towards possible robust "male" morphology, old black female classification accuracy was high at 93% (Table 6.22). In contrast, young black females were classified correctly by CVA 96% of the time, an even higher percentage. This result indicated the same point that was viewed in the non-metric visual portion of this study; if sexually dimorphic modification was to take place in the human skeleton, it apparently takes place in the form of *black females exhibiting more male morphology* with the onset of advanced age.

When compared to the visual techniques employed in this study to determine sex, virtually the same results were found in the black population sample as were found in geometric morphometrics. Young black females were categorized with more accuracy (94%) than old black females (92%), but both were highly sexually dimorphic. Specifically, the subpubic angle (directly correlated with the SUB perspective) in young black females provided an 87% accuracy rate, while old black females fared slightly better with an 89% accuracy rate. In addition, subpubic angle determination (a trait directly correlated with the SUB perspective) in young black females was 91% accurate, while old black females were 94% accurate. The change between young and old black female pelvic morphology was negligible. Even though

geometric morphometrics showed changes in morphology with the onset of age in the black female pelvis, this morphology change did not prevent the SUB perspective from being highly accurate as a sex predictor.

As stated above, young white females clustered with their young black female counterparts, exhibiting a morphology that was more related to age than to population affinity. In addition, young and old white females did not appear to change with the onset of age; Figure 6.38 illustrated migrating landmarks between young and old white females with this perspective. When viewing the small changes in morphology, it was observed that the changes that did occur were similar to the differences between females and males in general, just as observed with the black female population. When points did migrate with age, they migrated to create a thicker, broader pubis and a wider ischial region. Again, when female morphology changes, it was in the direction towards male morphology and not in the direction of becoming more sexually dimorphic, i.e., more "female". This is direct correlation with the metric and non-metric portions of this study. White females increased in metric dimensions with the onset of age, migrating towards male morphology in measurements, while classification accuracy in both the humeral and pelvic non-metric traits decreased with age, indicating that morphology of the white female is becoming, in the very least, more ambiguous and less sexually dimorphic.

7.4.9

The SUB perspective: changes in males with the onset of age

In the SUB perspective, males appeared to separate (to a point) into population groups, and appeared not to diverge too greatly with the onset of age (Figure 6.35). This result was different from that of females in the same perspective, where females were seen to cluster in age-specific groupings to the right of the y-axis. Male morphology in the SUB perspective also did not appear to change with age across both population groups.

When observing the respective results of geometric morphometrics and the non-metric techniques employed, young black males exhibited less sexually dimorphic features visually than they did with morphometrics; classification accuracy increased as black males got older when determining sex from the visual indicators of the subpubic angle and the subpubic concavity. Specifically, the subpubic concavity provided a 70% classification accuracy rate for young black males, and a 78% classification accuracy rate for old black males (Table 5.27). These statistics were less accurate than the morphometric results.

White males (young and old) clustered together as a population on the relative warp consensus graph. However, young white males were observed close to the x-axis, similar to old black females and young white females. Young white males were also closest in distance to all the female consensus shapes when comparing all male consensus shapes. Past research showed that white male pelves were different morphologically from other male populations (Patriquin *et al.* 2003). These results indicated that portions of the male pelvic structure may be similar to female morphology.

Old white males exhibited a thicker, stouter pubis and a more inferiorly blunted ischial region indicating a decrease in the subpubic angle from young specimens to old specimens (Figure 6.39). This suggested that as white males became older, their morphology began to modify to the point where it looked more classically "male". Young white males were quite variable in their morphology, but the SUB perspective indicated that with age, white males exhibited a more male structure and thus could be classified with more accuracy.

In comparison to the non-metric visual techniques that included the subpubic angle and the subpubic concavity, geometric morphometrics performed differently than the visual techniques normally used to determine sex. White males decreased in their classification accuracy with visual techniques when comparing the young populations to the old populations. This was the opposite result of geometric

morphometrics, which increased clearly in assignment accuracy from the young white population to the old white population. This inconsistency between the visual technique and the geometric morphometrics analysis was unusual to observe, based on the fact that the two, being complimentary to each other, should provide similar results. This may be attributed to the human factor in visual analysis; visual determination of sex from the pelvis is more of a holistic approach, where the observer cannot help but be influenced by not only the specific features observed, but other variables such as size, bone density, corresponding characteristics, robustness or gracility. Geometric morphometrics with the SUB perspective only focused on roughly a third of the entire pelvic bone, meaning it was a much more refined and concentrated endeavour to determine sex from a limited number of homologous landmarks placed on skeletal features.

7.4.10

Sexual dimorphism of the SCI perspective

The SCI perspective quantified one of the most well-known and accurate pelvic traits in which to discern sexual dimorphism, the greater sciatic notch. When viewing the relative warp analysis graph of the four-group consensus shapes (Figure 6.40), males and females were seen immediately to separate, indicating their marked sexual dimorphism in this feature. In addition, the sexual dimorphism of the greater sciatic notch was easily illustrated when observing Figure 6.43, the consensus thin-plate spline that demonstrated the differences in the placement of landmarks between all males and females. In general, female notches appeared wider and shallower than their male counterparts. Male notches tended to be more constricted with a shorter superior margin or "leg".

However, what was also clearly discernable from the consensus relative warp graph was the closeness of the black female consensus shape and the white male consensus shape, indicating a similarity in morphology that needed further

investigation. Because black females grouped in the same grid quadrant as their white female counterparts, the deviation in SCI morphology was thought to not be attributed to the black females; they clustered in a classic sense with other females. The white male consensus shape, however, did not group in the same grid quadrant as the black male consensus shape. This indicated that if one of the two groups were exhibiting a deviation from the "classic" morphology of the greater sciatic notch in males and females, it was the white male sample.

Through the analysis of the vector mode thin-plate spline, it was obvious that black females and males exhibited what was considered classic sexually dimorphic anatomy of the greater sciatic notch (Figure 6.45). Black females exhibited the same landmark locations, in general, as the larger population of all pooled females in the sample. Males, in turn, exhibited the same migration of points as the pooled male sample, in that black male notches appeared more constricted with a shorter superior margin.

When comparing white female greater sciatic notch morphology to the same characteristic in males, a contrasting set of differences in landmark distribution than that of the black population was observed (Figure 6.47). In other words, the differences between white male and female greater sciatic notch shape were unlike the differences between black male and female greater sciatic notch shape. Males in the white population did not exhibit the characteristic shorter superior margin. In white males compared to white females, each point migrates in a different direction creating a much different notch profile than that of black males compared to black females. The ischial spine is projected posteriorly in white males. Black male morphology also projects the ischial spine posteriorly, but also migrates more towards the inferior margin or "leg", constricting the two points towards each other, which may cause a narrower notch. This does not occur in white males. The white male inferior ischial spine "flares" more anteriorly as opposed to the female ischial spine position.

Differences continued when observing the relative warp consensus graph for all eight groups of males and females with the SCI perspective (Figure 6.48). Young white males clustered most closely with young black females and not another male group at all. In fact, the young white male consensus shape was the only male group that clusters closely to all the other female groups. Young white males clearly have different greater sciatic notch morphology than their other male counterparts. Statistical analysis showed that young white males were not markedly distinguishable from young white females, as seen by the barely significant p-value (0.043, Table 6.31).

This lack of sexual dimorphism in the white male greater sciatic notch has been recognized in past research (Patriquin 2003; Steyn *et al.* 2004) and illustrates the variability in the young white male pelvis. In particular, Walker (2005) found that younger individuals (males and females) exhibited more feminine morphology in the pelvis, and sexual dimorphism was strongly affected by age in males, especially in greater sciatic notch width. In Walker's study, greater sciatic notch width in an English sample shifted in a masculine direction with increasing longevity, which increased sexual dimorphism of the male sample. Walker also found that the sciatic notch width tended to decrease with increasing age at death, creating a more masculine notch in older individuals. The results of this current research in geometric morphometrics quantified this phenomenon by showing the wider, more feminine notch in young white males, which modified with age to become more sexually dimorphic in older males.

7.4.11

The SCI perspective: changes in females with the onset of age

Black females were seen to change morphologically with time through the greater sciatic notch when comparing the young population to the old population. However, the migration of landmarks between the young sample and the old sample

appeared to "cancel" each other, meaning movement from a wide position to a more narrow position was observed on the inferior margin, while movement from a narrow position to a wider position was observed on the superior margin. This signified change, but not necessarily change that would influence the classification accuracy of the sample when comparing young to old. In fact, young black females and old black females were classified with nearly the same accuracy rate when compared to their male counterparts (80% accurate and 81% accurate, respectively). Age did not greatly influence the shape of the greater sciatic notch in the black female, and the SCI perspective continued to provide acceptable levels of classification accuracy even with the onset of age.

When comparing geometric morphometric results from the quantification of the greater sciatic notch to the visual technique used to determine sex from the greater sciatic notch, similar results were observed. Young black females were extremely sexually dimorphic in this feature when used as a visual indicator of sex. In addition, old black females were sexually dimorphic in their greater sciatic notches as well and were actually classified correctly more often than their younger counterparts (89% and 84%, respectively). These visual results were very closely correlated to the morphometrics results in which the classification accuracy rate increased slightly with the onset of age in black females.

Young and old white females are seen clustered together in the relative warp analysis graph (Figure 6.48), which indicated that this feature, in addition to being sexually dimorphic in females, was also static and unchanging in the white female population with the onset of age. The consensus thin-plate spline that demonstrated differences between young white females and old white females confirmed that if changes occurred in morphology with the white female sample, they were minimal (Figure 6.51). The changes that did occur appear to create an even wider notch profile in old females as in their younger counterparts, which in turn indicated that sexual dimorphism was marked and quite apparent in both the young and old

sample. However, when compared to their male counterparts, females were distinguished from males at a much higher rate of accuracy in the old white population than in the young population. All data indicated that the greater sciatic notch was quite variable in the young sample, and then modified through age into a type of morphology that was better suited to the "classic" definition of sexual dimorphism with this population.

When comparing techniques, visual determination of sex and the classification accuracy for white females decreased with the onset of age; young white females were categorized more accurately (100%) with visual techniques than old females were (94%). Geometric morphometrics, on the other hand, saw an increase in statistical classification accuracy with the onset of age. One similar result between the two analyses was the fact that white females changed little with the onset of age, and the classification accuracies remained high for this female population, even over the age of 50.

7.4.12

The SCI perspective: changes in males with the onset of age

Black males exhibited a similar pattern as black females with the onset of age. Based on the vector mode thin-plate spline comparing the differences between young black males and old black males, morphology of the greater sciatic notch continued to be sexually dimorphic in advanced age (Figure 6.50). The migration of landmarks indicated that old black males exhibited an even shorter superior margin than the young sample, and changes appeared to create a notch that would be seen as more constricted. The combination of these modifications would indicate that the black male pelvis was getting even more sexually dimorphic with age, meaning the greater sciatic notch of old black males exhibited even more classic male morphology than the young sample. In fact, old black males were ultimately categorized with slightly less accuracy than the young black males based on the CVA (Table 6.30).

Ultimately, the classification accuracies of black males in the SCI perspective stayed relatively static through comparisons of the young and old samples. Sexual dimorphism was apparent even with advanced age from the SCI perspective.

The visual and geometric morphometric greater sciatic notch assessments gave the same results. The classification accuracy of the visual technique increased with the onset of age with black males (73% to 74%). These results, when combined with those from geometric morphometric analysis, indicated that the black South African male population was sexually dimorphic in this feature, and that these features of the pelvis did not change in a sexually dimorphic nature with the onset of age.

When viewing the relative warp consensus graph comparing age groups for the SCI perspective, it is easy to see the discrepancy between young and old white male morphology in the greater sciatic notch (Figure 6.48). The consensus thin plate spline in vector mode comparing young and old white males details the reason young white males appear morphologically similar to their female counterparts (and most closely to black females). The margins of the young white male greater sciatic notch were positioned wide and make the appearance of each margin to be roughly equal. The point of the most curvature in the notch was placed centrally and more forward, which produced a more "open" notch. The old white male greater sciatic notch, in contrast, has unequal margins with the inferior "leg" constricting inward and the superior "leg" extending outward, and the notch curvature is placed deeper within the pelvis. This constriction and inequality in margins seen with the old white male greater sciatic notch allowed this group to be categorized as male with more accuracy than their younger male counterparts (89% and 74%, respectively). Classification accuracy improved with the onset of age, and young white males may exhibit residual female pelvic characteristics through skeletal maturation and into the 3rd and 4th decades.

When comparing the visual technique of sex determination from the greater sciatic notch to the morphometric analysis of the greater sciatic notch, a divergent pattern emerged. Visual determination of sex and the classification accuracy for males decreased with the onset of age; geometric morphometrics saw an increase in statistical classification accuracy with the onset of age. With non-metric visual assessment, white males appeared to *visually* migrate towards a more "female" like morphology, with ambiguous cases increasing in the old age group, and more old white males being misclassified as females than their younger white male counterparts. Geometric morphometrics did not show this. In fact, geometric morphometrics did much better in correctly classifying old white males than it did classifying young white males. This indicated that sexual dimorphism in the SCI perspective increased with the onset of age in the white male pelvis, and features deemed classically "male" were more often viewed in the pelvic bones of older males. Young white males continued to be variable in their morphology, and geometric morphometrics quantified the young white male sciatic notch shape as more similar to female morphology than to male morphology.

7.4.13

Geometric morphometric analysis: summary

Geometric morphometrics complemented visual techniques in sex determination from the distal humerus and pelvis. This quantitative analysis provided generally accurate classification results in all four 2-dimensional perspectives studied. Males and females were markedly sexually dimorphic in both humerus views (EPI and OL) and both views of the pelvis (SUB and SCI). Each one of these perspectives can be considered a good indicator of sex in the human skeleton.

The EPI perspective showed age-related differences between white females and males. Young white females and males appeared so morphologically similar that neither could be successfully categorized with CVA analysis. Old white females

and males, on the other hand, were classified quite accurately when compared to each other. Both young and old black males and females were classified with significant accuracy in the EPI perspective. Therefore, age appeared to play a role in the white population with classification accuracy, but did not appear to affect the classification accuracy of blacks.

The OL perspective exhibited sexual dimorphism between all males and females in both population groups. These marked differences between males and females did not appear to statistically diminish with the onset of age.

The SUB perspective exhibited sexual dimorphism between all black South African males and females. When comparing young and old groups, age did not appear to affect the morphology of the subpubic angle and subpubic concavity of the black males and females; they remained sexually dimorphic from young age ranges to old age ranges. Differences in the morphology of white SUB perspective, however, were observed when comparing young and old samples. Young white females and males appeared so morphologically similar in this perspective that they could not be classified correctly with any amount of accuracy. Old white females and males were classified accurately, indicating a distinct age component to this view. Older white individuals were more sexually dimorphic than young individuals.

The SCI perspective exhibited sexual dimorphism between all black South African males and females, and age did not appear to diminish the classification accuracy for this group. The young white population was classified at a much lower accuracy than their old counterparts when comparing males and females. This indicated (again) that older white individuals were more sexually dimorphic than young individuals in the pelvis. In general, young white males exhibited more classically "female" morphology in the pelvis.

Based on classification accuracies between males and females, females presented male morphology on more occasions with all four perspectives, as seen by the female group's lower classification accuracies (in general). This was a good

indication that if age did play a role in morphology change, that role was to make females appear more "male". Males rarely appeared more "female" in their morphology, especially with the onset of age.

7.4.14

Geometric morphometric analysis: advantages and disadvantages

As seen in other published research, geometric morphometric analysis can be helpful in the determination of sexual dimorphism in the human skeleton (Pretorius *et al.* 2006; Pretorius and Steyn 2005). These studies successfully assess differences in the shape of several different skeletal elements, one of which is the greater sciatic notch also studied in this research. Pretorius *et al.* (2006) found a distinct separation between males and females in the greater sciatic notch width, but did not view changes with age as a parameter for the study. Results from this current research showed that homologous landmark analysis in geometric morphometrics successfully reflected the shape of each structure studied, and provided useful classification accuracies for each trait. In addition, geometric morphometric analysis, by and large, complemented the visual techniques utilized in this study to determine sex from postcranial skeletal remains. Results from the three perspectives used in this morphometric analysis (EPI, OL, SUB) showed results that appeared to be congruent with visual analysis. The SCI perspective did exhibit contradictory results in that its statistical analysis performed better on older individuals, while visual techniques were better at categorizing younger individuals.

Geometric morphometric results from the distal humerus (that confirmed visual results) implied that other features of the skeleton not normally explored could be considered sexually dimorphic as well. Specifically, other features of the elbow joint that contribute to the carrying angle of the arm may provide accurate results in sex determination if utilizing geometric morphometrics. The analysis provided

interesting results that were note-worthy and significant, especially in the fact that the distal humerus performed so well as a sexually dimorphic element.

In addition, geometric morphometrics quite often provided a higher accuracy rate in classification than the visual techniques alone did with regard to the distal humerus. This showed that as an observer, features were seen, but not to the extent or to the degree in which the computer-generated thin-plate spline could "see" them. This exposed advantages and disadvantages of a robust and complex shape-quantification package such as seen in geometric morphometrics.

Advantages to performing geometric morphometrics were clear. Visualization of a quantified shape allowed for explicit, defined analysis of the form (or aspects of the form) that were being modified with age. In many cases, subtle changes in form were observed with age, but ultimately did not alter the classification accuracy of designating one form "female" and the other form "male". Siegel and Benson (1982) viewed the complexities of interpreting small changes in form and determined that continuous research must be undertaken in order to correctly classify biological shapes. Geometric morphometrics also provided answers to questions posed regarding the efficacy of distal humeral traits as sex indicators. Because these features were not well-known and not yet well-established, morphometrics supplied the quantification of past visual techniques to solidify these physical features as sexually dimorphic. Just as Richtsmeier *et al.* (2002) used geometric morphometrics to quantify the description of characteristic traits in the identification of species, so can geometric morphometrics be used to characterize sexually dimorphic forms of a known species.

Geometric morphometrics provided answers to the specific question of sexual dimorphism changing with the onset of age. Visual sex determination techniques simply would not have been able to discern the subtle modifications in shape that were occurring in several locations. This analysis was compelling based on the fact that the human eye (and human bias) will always play a role in the visual

determination of sex from the skeleton. Geometric morphometrics attempts to eliminate all size bias so that only forms and shapes can be analyzed and compared. Finally, the fact that geometric morphometric statistical packages provided clear and concise accuracy rates and p-values (in most cases) made interpretation straightforward.

Disadvantages of geometric morphometric analysis became apparent during this study. Positioning of skeletal elements for correct image capture required an explicit research protocol that was comprehensive and clear. Little room for error was found in the digital image capture methods for morphometrics. These precise protocols made the analysis a robust one, but also hindered the analysis in the fact that image capture was extremely labour intensive. Digital image file storing, appropriate file names and the need to enhance photographs were consistent concerns that were addressed again and again. With such a large sample size for a geometric morphometric study, image files were in jeopardy of being renamed or stored incorrectly simply due to human error. Care was always taken to maintain digital image file integrity, but it must be noted that analysts not familiar with the effort in creating image files for morphometric analysis may find the procedure daunting. In addition, a small sample size in the young white female population was attributed to the lack of some statistical output. Better results may have been obtained if the sample size had been larger, but the lack of statistics made some interpretation difficult in these instances.

As shown, geometric morphometrics generally provided the same answers that visual techniques did. Where geometric morphometrics excelled was in the small morphological changes not discernable by the human eye; however, if those changes are, in fact, not easily discernable by visual techniques, would they ultimately play a role in the misclassification of sex of unidentified remains? This question could not be immediately answered.

CHAPTER 8

CONCLUSIONS

The results of this study answered several queries posed in an effort to determine if sexual dimorphism changed with age. These conclusions included the following:

♦ The human skeleton is not static in its modification through time. Changes in shape and size throughout a person's lifetime can be observed. However, changes in sexual dimorphism are limited.

♦ Size differences between the South African black and white populations were once again confirmed. Whites, in general, were larger, but the morphology of black and white South Africans was similar.

♦ Those more prone to osteoporotic modification (i.e., white females) increased metrically with the onset of age. This increase in size may indicate an increase in male morphology, and a subsequent decrease in sexual dimorphism. It also may indicate the possibility of misclassification of sex based on measurements.

♦ Those with higher bone densities in younger years (i.e., black females) had less osteoporotic modification in later years, and did not exhibit significant changes in size with the onset of age. Thus, sexual dimorphism stayed consistently marked.

♦ Males, in general, increased metrically at knee and elbow joint locations with the onset of age.

♦ Sexual dimorphism in non-metric traits of the humerus changed in females with the onset of age, but not with males. Females became more ambiguous in their morphology as age increased. Males exhibited distinct sexual dimorphism with classic "male" characteristics even with the onset of age.

♦ A relationship between a size change in the skeletal element and the morphology of that element with the onset of age was seen. If a feature was seen to increase metrically, it was more likely to exhibit male visual morphology in both females and males.

♦ The pelvic morphology of females stayed the same with the onset of age; sexual dimorphism was marked and apparent even in the aged individuals.

♦ The pelvic morphology of males became either more sexually dimorphic with age (as seen in black males) or less sexually dimorphic with age (as seen in white males). White South African male pelves showed the most variation with age, and continued to exhibit varying degrees of sexual dimorphism throughout age categories.

♦ Geometric morphometrics accurately quantified visually sexually dimorphic features of the distal humerus and the pelvis. Morphometrics rarely found a significant difference in sexual dimorphism between young and old males and females. The SCI perspective (which quantified the greater sciatic notch) increased in sexual dimorphism with the onset of age only in white males.

♦ A "late" maturation or increase in robusticity was observed in the male sample. This indicated that males apparently only reach their full adult, robust status (and thus their full set of sexually dimorphic characteristics) well after puberty (30's, 40's, and 50's). This held true in both long bone sexually dimorphic morphology and pelvic morphology.

The human skeleton does appear to change with age, but sexual dimorphism does not increase or decrease dramatically in the elements chosen for this research. An increase in size with age indicated an increase in male morphology, which again may pose some classification difficulty with older females. These changes, however,

would rarely influence an anthropologist's ability to determine sex from an unknown individual.

The methods used by anthropologists to determine sex should not be modified at this time, but the knowledge of possible changes in sexual dimorphism with the onset of age in the postcranial skeleton should be considered when observing individuals of differing ages. The presence of these changes should be taken into account by any anthropologist while attempting to sex specimens of unknown age, and great care should be used in the determination of sex with these changes in mind.

This research appeared to coincide with the findings of decreased sexual dimorphism/ increased robusticity in females with age as seen in past research on cranial morphology. More research is necessary to determine whether metric and visual changes in the long bones occur in conjunction with specific cranial robusticity as age increases, and if there is a correlation between populations and the differing levels of sexual dimorphism with age. Research on the increase in female cranial robusticity has only included populations of European origin. Interesting findings may be encountered when examining South African whites and blacks in this area of study.

Ultimately, the implications of this research rest with the anthropologist and their knowledge of the changes that occur with the onset of age. Sexual dimorphism does not change greatly in the long bones or the pelvis with the onset of age; however, changes do occur that make sex determination more challenging. Dynamic changes in bone with age were important to examine more closely and with a variety of sex determination methods. These modifications in bone must be understood and appreciated as anthropologists examine unknown specimens in forensic and paleodemographic fields.

Literature Cited

Adams D 1999. Methods for shape analysis of landmark data from articulated surfaces. Evolutionary Ecology Research 1:959-970.

Adebajo AO, Cooper C, and Grimley Evans J. 1990. Fractures of the hip and distal forearm in West Africa and the United Kingdom. Age and Ageing 20:435-438.

Albanese J, Cardoso HFV, and Saunders SR. 2005. Universal methodology for developing univariate sample-specific sex determination methods: an example using the epicondylar breadth of the humerus. J Archaeol Sci 32:143-152.

Aldridge S. 2005. Black women have lower fracture risk than whites with same bone density. J of Am Med Assoc 293:2102-2108.

Allen JC, Bruce MF, and MacLaughlin. 1987. Sex determination from the radius in humans. Hum Ev 2:373-378.

Aloia JF, Vaswani A, Ellis K, Yuen K, and Cohn SH. 1985. A model for involutional bone loss. J Lab Clin Med 106:630-636.

Amis AA, Miller JH, Dowson D, and Wright V. 1989. Axial forces in the forearm: their relationship to excision of the head of the radius. In: Stokes IAF, editor. Mechanical Factors and the Skeleton. London: John Libbey. p 29-37.

Anderson JY and Trinkaus E. 1998. Patterns of sexual, bilateral and interpopulational variation in human femoral neck-shaft angles. J Anat 192:279-285.

Angel JL, Kelley JO, Parrington M, and Pinter S. 1987. Life stresses of the free black community as represented by the First African Baptist Church, Philadelphia 1823-1841. Am J of Phys Anthro 74:213-229.

Asala SA, Mbajiorgu FE, and Papandro BA. 1998. A comparative study of femoral head diameters and sex differentiation in Nigerians. Acta Anatomica 162:232-237.

Asala SA. 2001. Sex determination from the head of the femur of South African whites and blacks. Forensic Sci Int 117:15-22.

Aspray TJ, Prentice A, Cole TJ, Sawo Y, Reeve J, and Francis RM. 1996. Low bone mineral content is common but osteoporotic fractures are rare in elderly rural Bambian women. J Bone Miner Res 11:1019-1025.

Aufderheide AC and Rodriguez-Martin C. 1998. The Cambridge Encyclopedia of Human Paleopathology. Cambridge UK: Cambridge University Press.

Bass W. 1995. Human Osteology: A Laboratory and Field Manual. Columbia, MO: Missouri Archaeological Society.

Beck TJ, Ruff CB, Warden KE, Scott WW Jr, and Rao GU. 1990. Predicting femoral neck strength from bone mineral data. A structural approach. Invest Radiol 25:6-18.

Beck TJ, Ruff CB, Scott WW Jr, Plato CC, Tobin JD, and Quan CA. 1992. Sex differences in geometry of the femoral neck with aging: a structural analysis of bone mineral data. Calcif Tissue Int 50:24-29.

Beck TJ, Looker AC, Ruff CB, Sievanen H, and Wahner HW. 2000. Structural trends in the aging femoral neck and proximal shaft: analysis of the Third National Health and Nutrition Examination Survey dual-energy x-ray absorptiometry data. J of Bone and Mineral Research 15:2304.

Bidmos M. 2006. Adult stature reconstruction from the calcaneus of South Africans of European descent. J Clin Forensic Med 13:247-252.

Bilezikian JP. 1999. Osteoporosis in Men. J of Clin Endocrin and Met 84:3431-3434.

Bonjour JP, Theintz G, Buchs B, Slosman D, and Rizzoli R. 1991. Critical years and stages of puberty for spinal and femoral bone mass accumulation during adolescence. J of Clin Endocrin and Metab 73:555-563.

Bookstein FL. 1982. Foundations of morphometrics. Annu Rev Ecol Syst 13:451-470.

Bookstein FL. 1986. Size and shape spaces for landmark data in two dimensions. Statistical Science 1:181-242.

Bookstein FL. 1990. Introduction to Methods for Landmark Data. In: Rohlf FJ and Bookstein FL, editors. Proceedings of the Michigan Morphometrics Workshop. Ann Arbor, Michigan: University of Michigan Museum of Zoology. p 215-225.

Bookstein FL. 1991. Morphometric tools for landmark data. New York: Cambridge University Press.

Bookstein FL. 1996. Landmark methods for forms without landmarks: morphometrics of group differences in outline shape. Medical Image Analysis 1:225-243.

Borgognini Tarli SM and Repetto E. 1986. Methodological Considerations on the Study of Sexual Dimorphism in Past Human Populations. Human Evolution 1:51-66.

Bruzek J and Soustal K. 1984. Contribution to ontogenesis of the human bony pelvis. Acta Univ Carol Biol 12:37-45.

Buckberry JL and Chamberlain A. 2002. Age estimation from the auricular surface of the ilium: a revised method. Am J of Phys Anthrop 119:231-239.

Burr DB and Martin RB. 1983. The effects of composition, structure and age on the torsional properties of the human radius. J Biomechanics 16:603-608.

Bushang PH, Baume RM, and Nass GG. 1983. A craniofacial growth maturity gradient for males and females between 4 and 16 years of age. Am J of Phys Anthrop 61:373-381.

Bushang PH, Tanguay R, Demirjian A, La Palme L, and Goldstein H. 1986. Sexual dimorphism in mandibular growth of French-Canadian children 6 to 10 years of age. Am J of Phys Anthrop 71:33-37.

Butler V. 2000. Lab Methods in Archaeology. Portland: Portland State University.

Camacho FJF, Pellico LG, and Rodriguez RF. 1993. Osteometry of the Human Iliac Crest: Patterns of Normality and Its Utility in Sexing Human Remains. J of Forensic Sci 38:779-787.

Cameron N, Tobias PV, Fraser WJ, and Nagdee M. 1989. Search for secular trends in calvarial diameters, cranial base height, indices, and capacity in South African Negro crania. Am J of Hum Biol 2:53-61.

Case DT and Ross AH. 2007. Sex determination from hand and foot bone lengths. J of Forensic Sci 52:264-270.

Chavassieux P, Seeman E, and Delmas PD. 2007. Insights into material and structural basis of bone fragility from diseases associated with fractures: how determinants of the biomechanical properties of bone are compromised by disease. Endocr Rev 28:151-164.

Chesnut III CH. 1993. Bone mass and exercise. The American Journal of Medicine 95:34s-36s.

Coats B and Margulies SS. 2006. Material properties of human infant skull and suture at high rates. J Neurotrauma 23:1222-1232.

Coleman WH. 1969. Sex differences in the growth of the human bony pelvis. Am J of Phys Anthrop 31:125-152.

Compston JE, Vedi S, Kaptoge S, and Seeman E. 2007. Bone remodeling rate and remodeling balance are not co-regulated in adulthood: implications for the use of activation frequency as an index of remodeling rate. J Bone Miner Res 22:1031-1036.

Cronk B. 1999. How to Use SPSS: A step-by-step Guide to Analysis and Interpretation. Los Angeles, CA: Pyrczak Publishing.

Cummings SR, Kelsey JL, Nevitt MC, and O'Dowd KJ. 1985. Epidemiology of osteoporosis and osteoporotic fractures. Epidemiologic Reviews 7:178-208.

Cummings SR, Black DM, Nevitt MC, Browner WS, Cauley JA, Genant HK, Mascioli SR, Scott JC, Seeley DG, Steiger P, and Vogt TM. 1990. Appendicular bone density and age predict hip fracture in women. JAMA 263:665-668.

Cummings SR and Black D. 1995. Bone mass measurements and risk of fracture in Caucasian women: a review of findings from prospective studies. Am J of Med 98:24s-28s.

Cummings SR, Palermo L, Browner W, Marcus R, Wallace R, Pearson J, Blackwell T, Eckert S, and Black D. 2000. Monitoring Osteoporosis Therapy With Bone Densitometry. JAMA 283:1318-1321.

Daniell HW. 1997. Osteoporosis after orchiectomy for prostate cancer. American Urological Association, Inc 157:439-444.

De Villiers H. 1968. The Skull of the South African Negro. Johannesburg: Witwaterstrand University Press.

Deakins M and Burt RL. 1944. The deposition of calcium, phosphorus, and carbon dioxide in calcifying dental enamel. Harvard School Laboratory of Dental Medicine77-83.

Devine A, Dhaliwal SS, Dick IM, Bollerslev J, and Prince RL. 2004. Physical activity and calcium consumption are important determinants of lower limb bone mass in older women. J Bone Miner Res 19:1634-1639.

Dibennardo R and Taylor JV. 1982. Classification and misclassification in sexing the black femur by discriminant function analysis. American J Phys Anthrop 58:145-151.

Dibennardo R and Taylor JV. 1983. Multiple Discriminant Function Analysis of sex and race in the postcranial skeleton. American Journal of Physical Anthropology 61:305-314.

Dickenson RP, Hutton WC, and Stott JRR. 1981. The mechanical properties of bone in osteoporosis. Journal of Bone and Joint Surgery 63-B:233-238.

Donlon DA. 2000. The value of infracranial nonmetric variation in studies of modern Homo sapiens: an Australian focus. Am J of Phys Anthrop 113:349-368.

Eastell R, Boyle IT, Ralston S, Compston J, Cooper C, Fogelman I, Francis RM, Hosking DJ, Purdie DW, Reeve J, Reid DM, Russell RGG, and Stevenson JC. 1998. Management of Male Osteoporosis: Report of the UK Consensus Group. Q J Med 91:71-92.

Ebeling PR, Erbas B, Hopper JL, Wark JD, and Rubinfeld AR. 1998. Bone mineral density and bone turnover in asthmatics treated with long-term inhaled or oral glucocorticoids. J of Bone and Mineral Research 13:1289.

Epker BN, Kelin M, and Frost HM. 1965. Magnitude and location of cortical bone loss in the human rib with aging. Clin Orthop Relat Res 41:198-203.

Ericksen MF. 1976. Cortical bone loss with age in three Native American Populations. American Journal of Physical Anthropology 45:443-452.

Evans F. 1976. Age changes in mechanical properties and histology of human compact bone. Yearbook of Physical Anthropology 20:57-72.

Evans F. 1976. Mechanical properties and histology of cortical bone from younger and older men. Anat Rec 185:1-11.

Evers SE, Orchard JW, and Haddad RG. 1985. Bone density in postmenopausal North American Indian and Caucasian females. Unknown journal 57:719-726.

Ferson S, Rohlf FJ, and Koehn RK. 1985. Measuring shape variation of two-dimensional outlines. Syst Zool 34:59-68.

Finkelstein JS, Klibanski A, Neer RM, Greenspan SL, Rosenthal DI, and Crowley Jr.WF. 1987. Osteoporosis in men with idiopathic hypogonadotropic hypogonadism. Annals of Internal Medicine 106:354-361.

France DL. 1998. Osteometry and muscle origin and insertion in sex determination. Am J Phys Anthrop 76:515-526.

Franklin D, Freedman L, Milne N and Oxnard CE. 2006. A geometric morphometric study of sexual dimorphism in indigenous southern African crania. South African Journal of Science 102, 5-6: 229-238.

Frost HM. 1963. Osteoporoses: Their Nature and Pathogeneses. JMSMS278-282.

Fuss FK. 1991. The ulnar collateral ligament of the human elbow joint. J Anat 175:203-212.

Garn SM, Rohmann CG, and Blumenthal T. 1966. Ossification sequence polymorphism and sexual dimorphism in skeletal development. Am J Phys Anthrop 24:101-115.

Garn SM, Rohmann CG, Wagner B, Davila GH, and Ascoli W. 1969. Population similarities in the onset and rate of adult endosteal bone loss. Clinical Orthopaedics and Related Research 65:51-60.

Garn SM. 1970. The earlier gain and the later loss of cortical bone in nutritional perspective. Springfield, IL: Charles C. Thomas.

Garn SM. 1972. The course of bone gain and the phases of bone loss. Orthopedic Clinics of North America 3:503-521.

Garnero P and Delmas PD. 1998. Biochemical markers of bone turnover. Osteoporosis 27:303-323.

Genant HK, Delmas PD, Chen P, Jiang Y, Eriksen EF, Dalsky GP, Marcus R, ann San MJ. 2007. Severity of vertebral fracture reflects deterioration of bone microarchitecture. Osteoporosis International 18:69-76.

Georgia R, Albu E, Sicoe M, and Georoceanu M. 1982. Comparative aspects of the density and diameter of haversian canals in the diaphyseal compact bone of man and dog. Morphology, Embryology, Physiology 28:11-14.

Georgopoulos NA, Markou KB, Theodoropoulou A, Vagenakis GA, Benardot D, Leglise M, Dimopoulos JCA, and Vagenakis AG. 2001. Height velocity and skeletal maturation in elite female rhythmic gymnasts. J of Clin Endocrin and Metab 86:5159-5164.

Giles E and Klepinger LL. 1998. Confidence intervals for estimates based on linear regression in forensic anthropology. JFS 33:1218-1222.

Goldberg CS, Antonyshyn O, Midha R, and Fialkov JA. 2005. Measuring pulsatile forces on the human cranium. J Craniofac Surg 16:134-139.

Gotfredsen A, Hadberg A, Nilas L, and Christiansen C. 1987. Total body bone mineral in healthy adults. J Lab Clin Med 110:362-368.

Grabiner MD. 1989. The elbow and radioulnar joints. London: Lea and Febiger.

Grasswick LJ and Bradford JMW. 2003. Osteoporosis associated with the treatment of paraphilias: a clinical review of seven case reports. J of Forensic Sci 48:1-7.

Grynpas M. 1993. Age and disease-related changes in the mineral of bone. Calcif Tissue Int 53:S57-S64.

Haglund WD and Sorg MH. 1997. Forensic Taphonomy: The Postmortem Fate of Human Remains. Boca Raton, Florida: CRC Press LLC.

Han Z-H, Palnitkar S, Sudhaker D, Nelson D, and Parfitt AM. 1997. Effects of ethnicity and age or menopause on the remodeling and turnover of iliac bone: implications for mechanisms of bone loss. J Bone Miner Res 12:498-508.

Harper AB, Laughlin WS, and Mazess RB. 1984. Bone mineral content in St. Lawrence Island Eskimos. Human Biology 56:63-77.

Heaney RP, Gallagher JC, Johnston CC, Near R, Parfitt AM, and Whedon GD. 1982. Calcium nutrition and bone health in the elderly. The Am J of Clinical Nutrition 36:986-1013.

Heaney RP, Avioli LV, Chesnut III CH, Lappe J, Recker RR, and Brandenburger GH. 1989. Osteoporotic bone fragility. JAMA 1989:20-2986.

Henneberg M and van den Berg ER. 1990. Test of socioeconomic causation of secular trend: stature changes among favored and oppressed South Africans are parallel. Am J of Phys Anthrop 83:459-465.

Henneberg M and George BJ. 1993. Possible secular trend in the incidence of an anatomical variant: Median artery of the forearm. Am J of Phys Anthrop 96:329-334.

Henneberg M and Louw GJ. 1997. Lack of secular trend in adult stature in white South African males born between 1954 and 1975. Homo 48:54-61.

Hennessy RJ and Stringer CB. 2002. Geometric morphometric study of the regional variation of modern human craniofacial form. Am J of Physical Anthropology 117:37-48.

Herd RJM, Ramalingham T, RP, Fogelman I, and Blake GM. 1992. Measurements of broadband ultrasonic attenuation in the calcaneus in premenopausal and post-menopausal women. Osteoporosis International 2:247-251.

Herrin Communications Group BP. 2001. American Association of clinical endocrinologists 2001 medical guidelines for clinical practice for the prevention and management of postmenopausal osteoporosis. Endocrine Practice 7:294-312.

Holliday TW and Falsetti AB. 1999. A new method for discriminating African-American from European-American skeletons using postcranial osteometrics reflective of body shape. JFS 44:926-930.

Holman DJ and Bennet KA. 1991. Determination of sex from arm bone measurements. American J Phys Anthrop 84:421-426.

Hoppa RD. 1992. Evaluating human skeletal growth: an Anglo-Saxon example. Int J Osteoarch 2:275-288.

Hui SL, Johnston CC, and MR. 1985. Bone mass in normal children and young adults. Growth 49:34-43.

Humphrey LT. 1998. Growth patterns in the modern human skeleton. Am J of Phys Anthrop 105:57-72.

Hurxthal LM, Vose GP, and Dotter WE. 1969. Densitometric and visual observations of spinal radiographs. Geriatrics93-106.

Imrie JA and Wyburn GM. 1958. Assessment of age, sex, and height from immature human bones. British Medical Journal January 18:128-131.

Inman VT, Saunders JB, DeC M, and Abbott LC. 1944. Observations on the function of the shoulder joint. The Journal of Bone and Joint Surgery 26:1-30.

Introna Jr F, Di Vella G, and Campobasso CP. 1998. Sex determination by discriminant analysis of patella measurements. Forensic Sci Int 95:39-45.

Iscan MY, Loth SR, and Wright R. 1985. Age estimation from the rib by phase analysis: white females. J of Forensic Sci 30:853-863.

Jantz RL, Hunt DR, and Meadows L. 1994. Maximum length of the tibia: how did Trotter measure it? American J Phys Anthrop 93:525-528.

Jantz RL. 2001. Cranial change in Americans: 1850-1975. J Forensic Sci 46:784-787.

Jee WSS, Park HZ, Roberts WE, and Kenner GH. 1970. Corticosteroid and bone. Am J Anat 129:477-480.

Jeffery N and Spoor F. 2001. Brain size and the human cranial base: A prenatal perspective. Am J Phys Anthrop 118:324-340.

Jowsey J. 1960. Age changes in human bone. Clin Orthop 17:217.

Kanis JA and McCloskey EV. 1993. Epidemiology of vertebral osteoporosis. Bone 13:S1-S10.

Katzmarzyk PT and Leonard WR. 1998. Climatic influences on human body size and proportions: ecological adaptations and secular trends. Am J of Phys Anthrop 106:483-503.

Kelly PJ, Eisman JA, and Sambrook PH. 1990. Interaction of genetic and environmental influences on peak bone density. Osteoporosis International 1:56-60.

Kendall DG. 1981. The statistics of shape. In: Barnet V, editor. Interpreting Multivariate Data. New York: Wiey-Liss. p 75-80.

Kendall M and Stuart A. 1979. The Advance Theory of Statistics. London: Griffin Publishers.

Kennedy KAR. 1995. But professor, why teach race identification if races don't exist? JFS 40:797-800.

Kieser JA, Cameron N, and Groeneveld HT. 1987. Evidence for a secular trend in the Negro dentition. Annals of Human Biology 14:517-532.

King CA, Iscan MY, and Loth SR. 1998. Metric and comparative analysis of sexual dimorphism in the Thai femur. J Forensic Sci 43:954-958.

Klepinger LL. 2001. Stature, maturation variation and secular trends in forensic anthropology. J Forensic Sci 46:788-790.

Kolbe-Alexander TL, Charlton KE, and Lambert E. 2004. Lifetime physical activity and determinants of estimated bone mineral density using calcaneal ultrasound in older South African adults. J Nutr Health Aging 8:521-530.

Kriewall TJ. 1982. Structural, mechanical, and material properties of fetal cranial bone. Am J Obstet Gynecol 143:707-714.

Krogman WM. 1962. The Human Skeleton in Forensic Medicine. Springfield, Illinois: Thomas Press.

L'Abbé EN, Loots M, and Mering JH. 2005. The Pretoria bone collection: A modern South African skeletal sample. Homo 56:197-205.

Lee S, Kim Y, Jo Y, Seo J, and Chi J. 1996. Prenatal development of cranial base in normal Korean fetuses. The Anatomical Record 246:524-534.

Leiel **Y, Edwards J, Shary J, Spicer KM, Gordon L, and Bell NH**. 1988. The effects of race and body habitus on bone mineral density of the radius, hip and spine in premenopausal women. J of Clin Endocrin and Met1247-1250.

Levine E. 1972. Carpal fusions in children of four South African populations. Am J of Phys Anthrop 37:75-83.

Linday R, MacLean A, Kraszewski A, Hart DM, Clark AC, and Garwood J. 1978. Bone response to termination of estrogen treatment. The Lancet June:1325-1327.

Looker AC, Bauer DC, Chesnut II CH, Gundberg CM, Hochberg MC, Klee G, Kleerekoper M, Watts NB, and Bell NH. 2000. Clinical use of biochemical markers of bone remodeling: current status and future directions. Osteoporosis International 11:480.

Loth SR and Henneberg M. 1996. Mandibular ramus flexure: a new morphologic indicator of sexual dimorphism in the human skeleton. Am J Phys Anthrop 99:473-485.

Loth SR and Henneberg M. 2001. Sexually dimorphic mandibular morphology in the first few years of life. Am J of Phys Anthrop 115:179-186.

Loy A, Boglion C, and Cataudella S. 1999. Geometric morphometrics and morpho-anatomy: a combined tool in the study of sea bream (*Sparus aurata*, sparidae) shape. J Appl Icthyol 15:110.

Maalouf G, Gannage-Yared MH, Alrawi Z, Ezzedine J, Larijani B, Badawi S, Rached A, Zakroui L, Masri B, Azar E, Saba E, Nammari R, Adib G, Abou Samra H, Salman S, El Muntasser K, Tarseen R, El Kharousi W, Al-Lamki M, Alothman AN, Almarzook N, El Dessouki M, Sulaimani R, Saleh J, Suhaili AR, Khan A, Delmas P, and Seeman E. 2007. Middle East and North Africa consensus on osteoporosis. J Musculoskelet Neuronal Interact 7:131-143.

Macho GA. 1990. Is sexual dimorphism in the femur a "population specific phenomenon"? Z Morph Anthrop 78:229-242.

Malina RM. 1979. Secular changes in size and maturity: causes and effects. Mon Soc Res Child Devl 179:59-120.

Malina RM and Zavalet AN. 1980. Secular trend in the stature and weight of Mexican-American children in Texas between 1930 and 1970. Am J of Phys Anthrop 52:453-461.

Mall G, Hubig M, Buttner A, Kuznik J, Penning R, and Graw M. 2001. Sex determination and estimation of stature from the long bones of the arm. Forensic Sci Int 117:23-30.

Manning PJ, Evans MC, and Reid IR. 1992. Normal bone mineral density following cure of Cushing's Syndrome. Clinical Endocrinology 36:229-234.

Marcus LF, Hingst-Zaher, and Zaher H. 2000. Application of landmark morphometrics to skulls representing the orders of living mammals. Hystrix 11:27-47.

Margulies SS and Thibault KL. 2000. Infant skull and suture properties: Measurements and implications ofr mechanisms of pediatric brain injury. J Biomech Eng 122:364-371.

Martin RB and Atkinson PJ. 1977. Age and sex-related changes in the structure and strength of the human femoral shaft. J Biometrics 10:223-231.

Martin RB, Burr DB, and Schaffler MB. 1985. Effects of age and sex on the amount and distribution of mineral in Eskimo tibiae. American J Phys Anthrop 67:371-380.

Matkovic V, Fontana D, Tominac C, Goel P, and Chesnut III CH. 1990. Factors that influence peak bone mass formation: a study of calcium balance and the inheritance of bone mass in adolescent females. Am J Clin Nutr 52:878-888.

McCormick WF and Stewart JH. 1983. Ossification patterns of costal cartilages as an indicator of sex. Arch Pathol Lab Med 107:206-210.

McVeigh JA, Norris SA, Cameron N, and Pettifor JM. 2004. Associations between physical activity and bone mass in black and white South African children at age 9 yr. J Appl Physiol 97:1006-1012.

Meindl RS, Lovejoy CO, Mensforth RP, and Don Carlos L. 1985. Accuracy and direction of error in the sexing of the skeleton: implications for paleodemography. American J Phys Anthrop 68:79-85.

Merchan VL and Ubelaker DH. 1977. Skeletal growth of the protohistoric Arikara. Am J of Phys Anthrop 46:61-72.

Meuller KH, Trias A, and Ray RD. 1966. Bone density and composition: age-related and pathological changes in water and mineral content. Journal of Bone and Joint Surgery 48:140-148.

Micklesfield L, Rosenberg L, Cooper D, Hoffman M, Kalla A, Stander I, and Lambert E. 2003. Bone mineral density and lifetime physical activity in South African women. Calcif Tissue Int 73:463-469.

Miles AE and Bulman JS. 1995. Growth curves of immature bones from a Scottish island population of sixteenth to mid-nineteenth century: shoulder, girdle, ilium, pubis and ischium. Int J Osteoarch 5:15-27.

Miller KWP, Walker PL, and O'Halloran RL. 1998. Age and sex-related variation in hyoid bone morphology. J of Forensic Sci 43:1138-1143.

Moerman ML. A longitudinal study of growth in relation to body size and sexual dimorphism in the pelvis. 1981. University of Michigan.
Ref Type: Thesis/Dissertation

Moerman ML. 1982. Sex differences in adolescent growth of the human pelvis. Am J of Phys Anthrop 57:211-217.

Moerman ML. 1982. Growth of the birth canal in adolescent girls. Am J Obstet Gynecol 143:58-532.

Moerman ML. 1992. Adolescent growth and maturation of the human acetabulum. Am J of Phys Anthropol Suppl 14:106-107.

Molleson T, Cruse K, and Mays S. 1998. Some sexually dimorphic features of the human juvenile skull and their value in sex determination in immature juvenile remains. J of Archaeological Science 25:719-728.

Moore-Jansen PM, Ousley SD, and Jantz RL. 1994. Data Collection Procedures for Forensic Skeletal Material. Knoxville: Department of Anthropology, Knoxville: University of Tennessee.

Navani S, Shah JR, and Levy PS. 1970. Determination of sex by costal cartilage calcification. Harvard J of Preventive Medicine 108:771-774.

Nelson DA, Pettifor JM, Barondess DA, Cody DD, Uusi-Rasi K, and Beck TJ. 2004. Comparison of cross-sectional geometry of the proximal femur in white and black women from Detroit and Johannesburg. J Bone Miner Res 19:560-565.

Newman KJ and Meredith HV. 1956. Individual growth in skeletal bigonial diameter during the childhood period from 5 to 11 years of age. Am J Anat 99:157-187.

Nilas L, Gotfredsen A, Hadberg A, and Christiansen C. 1988. Age-related bone loss in women evaluated by the single and dual photon technique. Bone and Mineral 4:95-103.

Nordin BEC. 1966. International patterns of Osteoporosis. Clinical Orthopaedics and Related Research 45:17-30.

Onat T and Iseri H. 1995. Rate of skeletal maturation in relation to secondary sexual development during female adolescence. Am J of Hum Biol 7:751-755.

Ortner DJ. 1975. Aging effects on osteons remodeling. Calif Tiss Res 18:27-36.

Orwoll ES, Bauer DC, Vogt TM, and Fox KM. 1996. Axial bone mass in older women. Annals of Internal Medicine 124:187-196.

Ozer I, Katayama K, Sahgir M, and Güleç E. 2006. Sex determination using the scapula in medieval skeletons from East Anatolia. Coll Anthropol 30:415-419.

Parfitt AM. 1997. Genetic effects on bone mass and turnover-relevance to black/ white differences. J Am Coll Nutr 16:333.

Patriquin M, Steyn M, and Loth SR. 2002. Metric assessment of race from the pelvis in South Africans. Forensic Sci Int 127:104-113.

Patriquin M, Loth SR, and Steyn M. 2003. Sexually dimorphic pelvic morphology in South African whites and blacks. Homo 53:255-262.

Patriquin M, Steyn M, and Loth SR. 2005. Metric analysis of sex differences in South African black and white pelves. Forensic Sci Int 147:119-127.

Peterson J and Dechow PC. 2002. Material properties of the inner and outer cortical tables of the human parietal bone. Anat Rec 268:7-15.

Peterson J and Dechow PC. 2003. Material properties of the human cranial vault and zygoma. Anat Rec A Discov Mol Cell Evol Biol 274:785-797.

Pfeiffer S and Zehr M. 1996. A morphological and histological study of the human humerus from Border Cave. J Hum Evol 31:49-59.

Phenice TW. 1969. A newly developed visual method of sexing the os pubis. Am J of Phys Anthro 30:297-302.

Pollitzer WS and Anderson JB. 1989. Ethnic and genetic differences in bone mass: a review with a hereditary vs. environmental perspective. Am J Clin Nutr 50:1244-1259.

Pons J. 1955. The sexual diagnosis of isolated bones of the skeleton. Human Biology 27:12-21.

Pretorius E and Scholtz CH. 2001. Geometric morphometrics and the analysis of higher taxa: a case study based on the metendosternite of the Scarabaeoidea (Coleoptera). Biol J Linn Soc 74:35-50.

Pretorius E and Steyn M. 2005. Geometric morphometric analysis of mandibular ramus flexure. Am J Phys Anthrop 128:623-629.

Pretorius E, Steyn M, and Scholtz Y. 2006. An investigation into the usability of geometric morphometric analysis in assessment of sexual dimorphism. American J Phys Anthrop.

Purkait R and Chandra H. 2004. A study of sexual variation in Indian femur. Forensic Sci Int 146:25-33.

Recker RR, Davies KM, Heaney RP, Hinders SM, Stegman MR, and Kinnel DB. 1992. Bone gain in young adult women. JAMA 268:2403-2408.

Reynolds EL. 1945. the bony pelvic girdle in early infancy. A roentgenometric study. Am J of Phys Anthrop 3:321-354.

Reynolds EL. 1947. The bony pelvis in prepuberal childhood. Am J of Phys Anthrop 5:165-200.

Richman EA, Michel ME, Schulter-Ellis FP, and Corrunccini RS. 1979. Determination of sex by discriminant function analysis of postcranial skeletal measurements. J Forensic Sci 24:159-163.

Richtsmeier JT, DeLeon VB, and Lele SR. 2002. The promise of geometric morphometrics. Yearbook of Physical Anthropology 45:63-91.

Riggs BL, Wahner HW, Seeman E, Offord KP, Dunn WL, Mazess RB, Johnson KA, and Melton III LJ. 1982. Changes in bone mineral density of the proximal femur and spine with aging. J Clin Invest 70:716-723.

Rissech C and Malgosa A. 1997. Sex prediction by discriminant functions with central portion measures of innominate bones. Homo 48:22-32.

Robling AG and Stout SD. 2000. Histomorphometry of human cortical bone: applications to age estimation. In: Katzenberg A and Saunders S, editors. Biological Anthropology of the Human Skeleton. New York: Wiley-Liss, Inc. p 187-213.

Roche AF and Davila GH. 1972. Late adolescent growth in stature. Pediatrics 50:874-880.

Rogers SL. 1982. The Aging Skeleton: Aspects of Human Bone Involution. Charles C. Thomas Publishers Ltd.

Rogers TL. 1999. A visual method of determining the sex of skeletal remains using the distal humerus. J Forensic Sci 44:57-60.

Rohlf FJ and Marcus LF. 1993. A revolution in morphometrics. Trends in Ecological Evolution 8:129-132.

Rohlf FJ. 2000. On the use of shape spaces to compare morphometric methods. Hystrix Ital J Mammol 11:9-25.

Rohlf FJ. 2000. Statistical power comparisons among alternative morphometric methods. Am J Phys Anthrop 111:463-478.

Rohlf FJ. 2003. Bias and error in estimates of mean shape in geometric morphometrics. J Hum Evol 44:665-683.

Rohlf FJ, Ferson S, and Koehn RK. 1985. Measuring shape variation of two-dimensional outlines. Systematic Zoology 34:59-68.

Ross AH, McKewon AH, and Konigsberg LW. 1999. Allocation of crania to groups via the "new morphometry". JFS 44:584-587.

Ross RW and Small EJ. 2002. Osteoporosis in Men Treated with Androgen Deprivation Therapy for Prostate Cancer. The Journal of Urology 167:1952-1956.

Rother VP, Hunger H, Leopold D, Kropf G, and Kruger G. 1977. The determination of age and sex from measures of the humerus. Anat Anz 142:243-254.

Ruff CB and Hayes WC. 1982. Subperiosteal expansion and cortical remodeling of the human femur and tibia with aging. Science 217:945-948.

Ruff CB. 1987. Sexual dimorphism in human lower limb bone structure: relationship to subsistence strategy and sexual division of labor. J Hum Evol 16:391-416.

Ruff CB, Holt B, and Trinkaus E. 2006. Who's afraid of the big bad Wolff?: "Wolff's law" and bone functional adaptation. Am J of Phys Anthrop 129:484-498.

Sakaue K. 2004. Sexual determination of long bones in recent Japanese. Anthrop Sci 112:75-81.

Scheuer L and Black S. 2004. The Juvenile Skeleton. New York: Elsevier Academic Press.

Schnitzler CM, Pettifor JM, Mesquita JM, Bird MDT, Schnaid E, and Smith AE. 1990. Histomorphometry of iliac breast bone in 346 normal black and white South African adults. Bone Miner 10:199.

Schnitzler CM. 1993. Bone quality: A determinant for certain risk factors for bone fragility. Calcif Tissue Int 53:S27-S31.

Schnitzler CM and Mequita JM. 1998. Bone marrow composition and bone microarchitecture and turnover in blacks and whites. J Bone Miner Res 13:1300-1307.

Scholtz Y. A geometric morphometric study into the ontogeny and sexual dimorphism of the human scapula. 22-24. 2006. University of Pretoria, Department of Anatomy.
Ref Type: Thesis/Dissertation

Schutkowski H. 1987. Sex determination of fetal and neonatal skeletons by means of discriminant analysis. International Journal of Anthropology 2:347-352.

Schutkowski H. 1993. Sex determination of infant and juvenile skeletons: 1. Morphognostic features. Am J of Phys Anthrop 90:205.

Scientific Advisory Board NOF. 1988. Clinical Indications for Bone Mass Measurements. National Osteoporosis Foundation Scientific Advisory Report, submitted to the Health Care Financing Administration November 4:1-28.

Scientific Advisory Board OSoC. 1996. Clinical practice guidelines for the diagnosis and management of osteoporosis. J of Canadian Medical Association 155:1113-1133.

Seeman E. 2003. Periosteal bone formation- a neglected determinant of bone strength. The New England J of Med 349:320-323.

Seeman E. 2003. The structural and biomechanical basis of the gain and loss of bone strength in women and men. Endocrin and Met Clin of North Am 32:25-38.

Sheets HD 2001. IMP software series. Buffalo, NY, Canisius College.

Siegel AF and Benson RH. 1982. A robust comparison of biological shapes. Biometrics 38:341-350.

Simmons DJ. 1985. Options for Bone Aging With the Microscope. Yearbook of Physical Anthropology 28:249-263.

Singer R and Kimura K. 1981. Body height, weight, and skeletal maturation in Hottentot (Khoikhoi) children. Am J of Phys Anthrop 54:401-413.

Skedros JG, Hunt KJ, and Bloebaum RD. 2004. Relationships of loading history and structural and material characteristics of bone: development of the mule deer calcaneus. J Morphol 259:281-307.

Slice DE, Bookstein FL, Marcus LF, and Rohlf FJ. A glossary for Geometric Morphometrics. http://life.bio.sunysb.edu/morph/ . 2005.
Ref Type: Electronic Citation

Slitor J. 1987. Statistics by Steps. Ginn Press.

Smith RW and Walker RR. 1964. Femoral expansion in aging women: implications for osteoporosis and fractures. Science 145:157.

Steele DG and Bramblett CA. 1988. The Anatomy and Biology of the Human Skeleton. Texas: Texas A & M University Press.

Steiger P, Cummings SR, Black DM, Spencer NE, and Genant HK. 1992. Age-related decrement in bone mineral density in women over 65. J of Bone and Mineral Research 7:625-632.

Stewart TD. 1954. Sex determination of the skeleton by guess and by measurement. American J Phys Anthrop 12:385-392.

Stewart TD. 1963. New developments in evaluating evidence from the skeleton. J Dent Res 42:264-273.

Steyn M and Iscan MY. 1997. Sex determination from the femur and tibia in South African whites. Forensic Sci Int 90:111-119.

Steyn M and Iscan MY. 1997. Sex determination from the femur and tibia in South African whites. Forensic Sci Int 90:111-119.

Steyn M and Iscan MY. 1998. Sexual dimorphism in the crania and mandibles of South African Whites. Forensic Sci Int 98:9-16.

Steyn M and Iscan MY. 1999. Osteometric variation in the humerus: sexual dimorphism in South Africans. Forensic Sci Int 106:77-85.

Steyn M, Pretorius E, and Hutten L. 2004. Geometric morphometric analysis of the greater sciatic notch in South Africans. Homo.

Steyn M and Smith J. 2007. Interpretation of ante-mortem stature estimates in South Africans. Forensic Sci Int 171:97-102.

Stini WA. 1969. Nutritional stress and growth: sex difference in adaptive response. Am J of Phys Anthro 31:417-426.

Sun Z, Lee E, and Herring SW. 2004. Cranial sutures and bones: growth and fusion in relation to masticatory strain. Anat Rec A Discov Mol Cell Evol Biol 276:150-161.

Susann C. 1985. Living conditions and secular trend. J Hum Evol 14:357-370.

Szulc P, Duboeuf F, Schott AM, Dargent-Molina P, Meunier PJ, and Delmas PD. 2006. Structural determinants of hip fracture in elderly women: re-analysis of the data from the EPIDOS study. Osteoporosis International 17:231-236.

Szulc P, Seeman E, Duboeuf F, Sornay-Rendu E, and Delmas PD. 2006. Bone fragility: failure of periosteal apposition to compensate for increased endocortical resorption in postmenopausal women. J Bone Miner Res 21:1856-1863.

Tagaya A. 1989. Development of a generalized discriminant function for cross-population determination of sex from long bones of the arm and leg. Can Soc Forens Sci J 22:159-175.

Taitz C. 1998. Osteophytosis of the cervical spine in South African blacks and whites. Clin Anat 12:103-109.

Takahasi H and Frost HM. 1965. Correlation between body habitus and cross-sectional area of ribs. Canadian J of Physiology and Pharmacology 43:773-781.

Tanner JM. 1962. Growth at Adolescence. Oxford: Blackwell Scientific Publications.

Tanner JM, Whitehouse RH, Marubini E, and Resele LF. 1976. The adolescent growth spurt of boys and girls of the Harpenden Growth Study. Ann Hum Biol 3:109-126.

Tanner JM. 1994. Introduction: growth in height as a mirror of the standard of living. In: Komlos J, editor. Stature, Living Standards and Economic Development. Chicago: University of Chicago Press. p 1-8.

Tarli SMB and Repetto E. 1986. Methodological considerations on the study of sexual dimorphism in past human populations. Human Evolution 1:51-66.

Thiebaud D, Krieg MA, Gillard-Berguer D, Facquet AF, Goy JJ, and Goy JJ. 1996. Cyclosporine induces high bone turnover and may contribute to bone loss after heart transplantation. European Journal of Clinical Investigation 26:549-555.

Thompson D. 1992. On Growth and Form: the complete revised edition. New York: Dover.

Thompson D. 1979. The core technique in the determination of age at death in skeletons. J of Forensic Sci902-914.

Thompson D. 1980. Age changes in bone mineralization, cortical thickness, and haversian canal area. Calcified Tissue International 31:5-11.

Tobias PV. 1975. Secular trend among southern African Negroes and San (Bushman). S Afr J Med Sci 40:145-164.

Tobias PV and Netscher D. 1977. Reversal of the secular trend, as evidenced by South African Negro crania and femora. Hum Biol 59:467-475.

Tobias PV. 1985. The negative secular trend. J Hum Evol 14:347-356.

Trotter M, Broman GE, and Peterson RR. 1960. Densities of bones of white and negro skeletons. The Journal of Bone and Joint Surgery 42-A:50-58.

Ubelaker DH and Volk CG. 2002. A test of the phenice method for the extimation of sex. J Forensic Sci 47:19-24.

Ulijaszek SJ. 1996. Seclar trends in growth: the narrowing of ethnic differences in stature. In: Making Health Work: Human Growth in Modern Japan. Berkeley, CA: University of California Press. p 16-56.

Van Dongen R. 1963. The shoulder girdle and humerus of the Australian Aborigine. Am J of Phys Anthro 21:469-487.

Vasireddy S and Swinson DR. 2001. Male osteoporosis associated with long term cyproterone treatment. The Journal of Rheumatology 28:1702-1703.

Vidulich L, Norris SA, Cameron N, and Pettifor JM. 2006. Differences in bone size and bone mass between black and white 10-year-old South African children. Osteoporosis International 17:433-440.

von Cramon-Taubadel N, Frazier BC, and Lahr MM. 2007. The problem of assessing landmark error in geometric morphometrics. Am J of Phys Anthrop 134:24-35.

Walker GF and Kowalski CJ. 1972. On the growth of the mandible. Am J of Phys Anthrop 36:111-118.

Walker JA. 2000. Ability of geometric morphometric methods to estimate a known covariance matrix. Syst Biol 49:686-696.

Walker PL. 1995. Problems of preservation and sexism in sexing: some lessons from historical collections for palaeodemographers. In: A Herring and SR Saunders, editors. Grave Reflections: Portraying the Past Through Cemetery Studies. Toronto, Canada: Canadian Scholars Press. p 31-47.

Walker PL. 2005. Greater sciatic notch morphology: sex, age, and population differences. American Journal of Physical Anthropology 127:385-391.

Wallin JA, Tkocz I, and Kristensen G. 1994. Microscopic age determination of human skeletons including an unknown but calculable variable. International Journal of Osteoarchacology 4:353-362.

Walrath DE, Turner P, and Bruzek J. 2003. Reliability test of the visual assessment of cranial traits for sex determination. Am J of Phys Anthrop 125:132-137.

Wanek VL. A qualitative analysis for sex determination in humans utilizing posterior and medial aspects of the distal humerus. 2002. Portland State University.
Ref Type: Thesis/Dissertation

Washburn SL. 1948. Sex differences in the pubic bone. Am J of Phys Anthro 6:199-208.

Weaver JK and Chalmers J. 1966. Cancellous bone: its strength and changes with aging and an evaluation of some methods for measuring its mineral content: I. Age changes in cancellous bone. J of Bone and Joint Surgery 48a:289-299.

Weaver JK and Chalmers J. 1966. Cancellous bone: its strength and changes with aging and an evaluation of some methods for measuring its mineral content: II. An evaluation of some methods for measuring osteoporosis. J of Bone and Joint Surgery 48a:299-308.

Weiss KM. 1972. On the systematic bias in skeletal sexing. American J Phys Anthrop 37:239-250.

Wescott DJ and Moore-Jansen PH. 2001. Metric variation in the human occipital bone: forensic anthropological applications. J o f Forensic Sciences 46:1159-1163.

White TD and Folkens PA. 2000. Human Osteology. San Diego: Academic Press.

Wiredu EK, Kumoji R, Seshadri R, and Biritwum RB. 1999. Osteometric analysis of sexual dimorphism in the sternal end of the rib in a West African population. J of Forensic Sci 44:921-925.

Woodard HQ. 1962. The elementary composition of human cortical bone. Health Physics 8:513-517.

Young B and Heath JW. 2000. Skeletal Tissues. In: Functional Histology. London: Churchill Livingstone. p 172-192.

APPENDIX A: Research Data Sheet used in data collection procedures.

RESEARCH DATA SHEET

Reference Number: **Sex:** **Age:**
Population:
Date/ Recorder:

METRICS:

Humerus	Ulna
Max. Vert. Diam of Head =	Max. Diam of Head =
Max. Diam At Midshaft =	Max. Diam at Midshaft =
Epicondylar breadth =	Max. Distal Diameter =

Radius	Femur
Max. Diam of Head =	Max. Vert. Diam of Head =
Max. Diam at Midshaft =	Max. Diam at Midshaft =
Max. Distal Diameter =	Epicondylar breadth =

Tibia	Fibula
Max. Prox Epi Breadth =	Max. Diam of Head =
Max. Diam at Midshaft =	Max. Diam at Midshaft =
Max. Distal Epi Breadth =	Max Distal Diameter =

NONMETRICS:

(1=M, 2=Int. M, 3=Ambiguous, 4=Int. F, 5=F)

Humerus	Os Coxae
Medial epicondylar symmetry:	Subpub concavity:
Trochlear extension:	Subpub angle width:
Olecranon fossa shape:	Ischiopub ramus W:
Angle of medial epicondyle:	Greater sciatic notch:

APPENDIX B: Specimens used for geometric morphometric analysis – young white females

Number	Specimen Number	View Present/ Absent	Reason
1	5079	Absent SUB, SCI view	No os coxae available
2	2819	Present	
3	3069	Absent SUB, SCI view	No os coxae available
4	3275	Present	
5	3617	Present	
6	6782	Present	
7	4247	Present	
8	4678	Present	
9	3486	Present	
10	15683	Present	
11	6068	Present	
12	6338	Present	
13	6512	Present	

APPENDIX C: Specimens used for geometric morphometric analysis – young black females.

Number	Specimen Number	View Present/ Absent	Reason
1	1543	Absent SUB, SCI view	No os coxae available
2	2866	Present	
3	3041	Present	
4	3120	Present	
5	3266	Present	
6	3385	Present	
7	3609	Present	
8	3843	Present	
9	3854	Absent SUB, SCI view	No os coxae available
10	4198	Absent SUB, SCI view	No os coxae available
11	4256	Present	
12	4436	Present	
13	4448	Absent SUB view	Degraded pubic area
14	4598	Absent SUB, SCI view	No so coxae available
15	4604	Present	
16	4786	Present	
17	4956	Present	
18	5086	Present	
19	5150	Present	
20	5201	Present	
21	5259	Present	
22	5286	Absent SUB view	Degraded pubic area
23	5306	Present	
24	5335	Absent SUB view	Degraded pubic area
25	5384	Present	
26	5628	Present	
27	5692	Present	
28	5797	Present	
29	5878	Present	
30	5932	Present	
31	5957	Present	
32	6000	Present	
33	6094	Present	
34	6139	Present	
35	6157	Present	
36	6177	Present	
37	6192	Present	
38	5256	Present	
39	6290	Present	
40	6358	Present	
41	6372	Present	
42	6390	Present	
43	5767	Present	
44	5714	Present	
45	4060	Absent SUB, SCI view	No os coxae available
46	3154	Present	
47	5783	Present	
48	5316	Present	
49	5079	Absent SUB, SCI view	Bilaterally fused sacro-iliac joint
50	5892	Present	

APPENDIX D: Specimens used for geometric morphometric analysis – old black females.

Number	Specimen Number	View Present/ Absent	Reason
1	4763	Present	
2	1855	Present	
3	5018	Present	
4	5073	Present	
5	5148	Present	
6	5197	Present	
7	5511	Present	
8	5602	Present	
9	5682	Present	
10	5705	Present	
11	5717	Present	
12	5319	Present	
13	5342	Absent SUB, SCI view	No os coxae available
14	3015	Absent SUB view	Degraded pubic area
15	4584	Absent EPI, OL view	No humerus available
16	5013	Present	
17	2632	Present	
18	2900	Absent SUB, SCI view	No os coxae available
19	4564	Present	
20	4240	Present	
21	3538	Present	
22	1803	Absent SUB, SCI view	No os coxae available
23	6315	Present	
24	6328	Present	
25	6369	Present	
26	5005	Present	
27	4417	Absent SUB, SCI view	No os coxae available
28	5785	Present	
29	5635	Present	
30	5654	Present	
31	1696	Present	
32	2885	Present	
33	4990	Present	
34	5292	Present	
35	5316	Present	
36	5390	Present	
37	5698	Present	
38	6024	Present	
39	6388	Present	
40	4492	Present	
41	4998	Present	
42	5708	Present	
43	2905	Present	
44	2939	Present	
45	5323	Present	
46	5203	Present	
47	5033	Present	
48	5629	Present	
49	5039	Present	
50	5734	Absent SUB view	Degraded pubic area
51	4543	Present	

APPENDIX E: Specimens used for geometric morphometric analysis – old white females.

Number	Specimen Number	View Present/ Absent	Reason
1	5098	Present	
2	5270	Present	
3	5406	Present	
4	5452	Present	
5	5489	Present	
6	5610	Absent SUB view	Degraded pubic area
7	5634	Present	
8	5660	Present	
9	5716	Present	
10	5790	Absent SUB view	Degraded pubic area
11	5818	Present	
12	5373	Present	
13	7402	Present	
14	7329	Present	
15	7743	Present	
16	7798	Present	
17	7622	Present	
18	7419	Present	
19	7549	Present	
20	7865	Present	
21	7683	Present	
22	7677	Absent SUB view	Degraded pubic area
23	7685	Present	
24	7781	Present	
25	7864	Present	
26	7857	Present	
27	7818	Present	
28	7356	Present	
29	7094	Present	
30	7009	Present	
31	6837	Present	
32	7083	Present	
33	6997	Present	
34	6686	Present	
35	6420	Present	
36	6170	Present	
37	6168	Present	
38	4837	Present	
39	6407	Present	
40	6166	Present	
41	4047	Present	
42	4787	Present	
43	6003	Present	
44	5962	Present	
45	5858	Absent SCI view	Degraded sciatic notch area
46	5677	Present	
47	5499	Present	
48	5898	Present	
49	5437	Present	
50	5827	Present	

APPENDIX F: Specimens used for geometric morphometric analysis – old black males.

Number	Specimen Number	View Present/ Absent	Reason
1	2865	Present	
2	2978	Present	
3	3441	Present	
4	3700	Present	
5	4244	Present	
6	4258	Present	
7	4265	Present	
8	4396	Absent SUB view	Os coxae/ sacral fusion
9	4405	Present	
10	4542	Present	
11	4608	Present	
12	4617	Present	
13	4731	Present	
14	4947	Present	
15	4961	Present	
16	5000	Present	
17	5020	Present	
18	5024	Present	
19	5053	Present	
20	5063	Present	
21	5144	Present	
22	5149	Present	
23	5170	Present	
24	5175	Present	
25	5177	Present	
26	5209	Absent SUB view	Degraded pubic area
27	5222	Present	
28	5260	Present	
29	5265	Absent SUB view	Degraded pubic area
30	5273	Present	
31	5287	Absent SUB, SCI view	No os coxae available
32	5365	Present	
33	5372	Present	
34	5392	Present	
35	5447	Present	
36	5461	Present	
37	5466	Present	
38	5513	Present	
39	5532	Present	
40	5535	Present	
41	5566	Present	
42	5646	Present	
43	5665	Absent SUB, SCI view	No os coxae available
44	5753	Present	
45	5772	Present	
46	5805	Present	
47	5837	Present	
48	5309	Present	
49	5142	Present	
50	4979	Present	
51	5050	Present	
52	5078	Present	
53	5167	Present	

APPENDIX G: Specimens used for geometric morphometric analysis – old white males.

Number	Specimen Number	View Present/ Absent	Reason
1	4372	Present	
2	4837	Present	
3	5127	Present	
4	5434	Present	
5	5476	Present	
6	5531	Present	
7	5673	Present	
8	5684	Present	
9	5777	Present	
10	5805	Present	
11	5864	Present	
12	5877	Present	
13	5908	Present	
14	5348	Present	
15	4601	Present	
16	5907	Present	
17	3299	Present	
18	3012	Present	
19	3292	Present	
20	3295	Present	
21	3201	Present	
22	3311	Present	
23	3567	Present	
24	3446	Present	
25	3243	Present	
26	3193	Present	
27	3188	Absent SUB view	Degraded pubic area
28	3432	Present	
29	3474	Present	
30	3453	Present	
31	3242	Present	
32	4006	Present	
33	5715	Present	
34	5225	Present	
35	4953	Present	
36	5949	Absent SUB view	Degraded pubic area
37	5929	Present	
38	5587	Present	
39	5731	Present	
40	5784	Present	
41	5407	Present	
42	5642	Present	
43	5325	Present	
44	5724	Present	
45	5873	Present	
46	4589	Present	
47	5759	Present	
48	5711	Present	
49	5872	Present	
50	5304	Absent SUB view	Degraded pubic area
51	5570	Present	
52	6223	Present	

APPENDIX H: Specimens used for geometric morphometric analysis – young black males.

Number	Specimen Number	View Present/ Absent	Reason
1	1694	Present	
2	2019	Present	
3	2858	Present	
4	2889	Present	
5	2991	Present	
6	3096	Present	
7	3153	Absent EPI view	No medial epicondyle
8	3298	Present	
9	3561	Absent SUB, SCI view	No os coxae available
10	4236	Present	
11	4522	Present	
12	4535	Present	
13	4599	Present	
14	4794	Present	
15	4948	Absent SCI view	Degraded sciatic notch area
16	5010	Present	
17	5022	Present	
18	5025	Absent SUB view	Degraded pubic area
19	5031	Present	
20	5037	Present	
21	5080	Present	
22	5082	Present	
23	5124	Present	
24	5130	Present	
25	5152	Present	
26	5192	Present	
27	5262	Present	
28	5293	Present	
29	5351	Present	
30	5354	Present	
31	5361	Present	
32	5369	Present	
33	5394	Present	
34	5415	Present	
35	5428	Present	
36	5429	Present	
37	5431	Present	
38	5493	Present	
39	5569	Present	
40	5572	Present	
41	5591	Present	
42	5627	Present	
43	5638	Present	
44	5656	Absent SCI view	Degraded sciatic notch area
45	5663	Present	
46	5670	Present	
47	5691	Present	
48	5751	Present	
49	5761	Present	
50	5816	Present	
51	5856	Present	
52	5870	Present	
53	5885	Present	
54	5904	Present	
55	6353	Present	
56	6391	Present	
57	5868	Present	

APPENDIX I: Specimens used for geometric morphometric analysis – young white males.

Number	Specimen Number	View Present/ Absent	Reason
1	4220	Present	
2	6109	Present	
3	115	Present	
4	4485	Present	
5	3632	Present	
6	3441	Present	
7	3142	Present	
8	2546	Present	
9	4296	Present	
10	2656	Present	
11	3106	Present	
12	6680	Present	
13	3291	Present	
14	2615	Present	
15	2467	Present	
16	1835	Present	
17	814	Present	
18	7327	Present	
19	7507	Absent OL view	Pathology
20	6675	Present	
21	7147	Present	
22	8317	Present	
23	6046	Absent SUB, SCI view	No os coxae available
24	6008	Present	

APPENDIX J: Means, standard deviations, and univariate F-ratios for postcranial measurements of males and females, intra-observer results.

	Males					Females				Univariate
Variables (mm)		Mean	Range	s.d.	S.E.		Mean	Range	s.d.	S.E.	F-ratio
	N					*N*					
Humerus:											
Vertical head diameter	11	46.1		3.87	0.2	20	40.4		3.26	0.2	**19.26***
Maximum midshaft diameter	11	23.7		1.78	0.1	20	20.7		2.12	0.1	**15.32***
Epicondylar breadth	11	64.4		3.90	0.2	20	56.5		3.36	0.2	**34.38***
Midshaft circumference	11	70.4		5.23	0.3	20	61.6		4.84	0.3	**22.12***
Pelvis:											
Pelvis length	11	210.9		15.23	0.1	19	193.9		13.97	0.1	**9.57***
Pelvis breadth	11	153.2		9.65	0.1	19	148.8		11.51	0.1	1.15
Pubis length	11	67.0		7.03	0.2	20	71.3		8.55	0.2	1.98
Ischium length	11	80.7		6.16	0.1	20	78.6		6.71	0.1	0.76

**** p-values significant at <0.05***

APPENDIX K: statistical analyses of non-metric humerus characteristics, intra-observer results.

Distribution of classification, all males and females, trochlear extension.

		1=M, 2=Intermediate M. 3=Ambiguous, 4=Intermediate F, 5=F					Total
		1	2	3	4	5	
SEX	Male	5 (46%)	3 (27%)	2 (18%)	1 (9%)	0 (0%)	11
	Female	8 (40%)	4 (20%)	3 (15%)	5 (25%)	0 (0%)	20
Total		13	7	5	6	0	*N* = 31

Pearson's chi square value=1.189, df=3, p=0.76>0.05

Distribution of classification, all males and females, olecranon fossa shape.

		1=M, 2=Intermediate M. 3=Ambiguous, 4=Intermediate F, 5=F					Total
		1	2	3	4	5	
SEX	Male	2 (18%)	6 (55%)	2 (18%)	1 (9%)	0(0%)	11
	Female	4 (20%)	7 (35%)	2 (10%)	7 (35%)	0 (0%)	20
Total		6	13	4	8	0	*N* = 31

Pearson's chi square value=2.873, df=3, p=0.412>0.05

Distribution of classification, all males and females, medial epicondylar angle.

		1=M, 2=Intermediate M. 3=Ambiguous, 4=Intermediate F, 5=F					Total
		1	2	3	4	5	
SEX	Male	4 (36%)	3 (28%)	1 (9%)	2 (18%)	1 (9%)	11
	Female	0 (0%)	2 (10%)	1 (5%)	15 (75%)	2 (10%)	20
Total		4	5	2	17	3	*N* = 31

Pearson's chi square value=12.95, df=4, p=0.01<0.05

Distribution of classification, all males and females, estimated sex from the distal humerus.

		1=M, 3=Ambiguous, 5=F					Total
		1		3		5	
SEX	Male	**10 (91%)**		0 (0%)		1 (9%)	11
	Female	5 (25%)		0 (0%)		**15 (75%)**	20
Total		15		0		16	*N*= 31

Pearson's chi square value=12.344, df=1, p=0.00<0.05

APPENDIX L: statistical analyses of non-metric pelvic characteristics, intra-observer results.

Distribution of classification for all males and females, subpubic concavity.

		1=M, 2=Intermediate M. 3=Ambiguous, 4=Intermediate F, 5=F					Total
		1	2	3	4	5	
SEX	Male	6 (55%)	5 (45%)	0 (0%)	0 (%)	0 (0%)	11
	Female	0 (0%)	0 (0%)	2 (10%)	14 (70%)	4 (20%)	20
Total		6	5	2	14	4	*N*= 31

Pearson's chi square value = 31.000, df = 4, p= 0.00<0.05

Distribution of classification for all males and females, subpubic angle.

		1=M, 2=Intermediate M. 3=Ambiguous, 4=Intermediate F, 5=F					Total
		1	2	3	4	5	
SEX	Male	4 (36%)	3 (27%)	3 (27%)	1 (9%)	0 (0%)	11
	Female	0 (0%)	0 (0%)	0 (0%)	2 (10%)	18 (90%)	20
Total		4	3	3	3	18	*N*= 31

Pearson's chi square value = 28.088, df = 4, p= 0.00<0.05

Distribution of classification for all males and females, ischio-pubic ramus width.

		1=M, 2=Intermediate M. 3=Ambiguous, 4=Intermediate F, 5=F					Total
		1	2	3	4	5	
SEX	Male	7 (64%)	1 (9%)	1 (9%)	1 (9%)	1 (9%)	11
	Female	2 (10%)	2 (10%)	1 (5%)	5 (25%)	10 (50%)	20
Total		9	3	2	6	11	*N*= 31

Pearson's Chi Square value = 11.498, df = 4, p = 0.02<0.05

APPENDIX L (continued): statistical analyses of non-metric humerus characteristics, intra-observer results.

Distribution of classification for all males and females, greater sciatic notch width.

		1=M, 2=Intermediate M. 3=Ambiguous, 4=Intermediate F, 5=F					Total
		1	2	3	4	5	
SEX	Male	5 (46%)	4 (36%)	0 (0%)	1 (9%)	1 (9%)	11
	Female	0 (0%)	0 (0%)	1 (5%)	4 (20%)	15 (75%)	20
Total		5	4	1	5	16	*N*= 31

Pearson's Chi Square Value = 23.410, df = 4, p= 0.00<0.05

Distribution of classification for all males and females, estimated sex for the pelvis.

		1=M, 2=Intermediate M. 3=Ambiguous, 4=Intermediate F, 5=F					Total
		1		3		5	
SEX	Male	11 (100%)		0 (0%)		0 (0%)	11
	Female	0 (0%)		0 (0%)		20 (100%)	20
Total		11		0		20	*N*= 31

Pearson's Chi Square Value = 31.000, df = 1, p = 0.00<0.05